Surface movement in mechanically agitated gas-liquid reactors

Patel, Ashvin G.

Award date:
1989

Awarding institution:
University of Bath

SURFACE MOVEMENT
IN
MECHANICALLY AGITATED GAS-LIQUID REACTORS

Submitted by

Ashvin G. Patel.

for the degree of

Doctor of Philosophy (PhD)

The University of **BATH**

April 1989

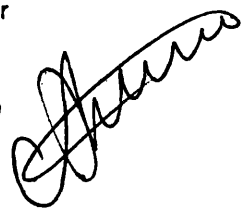

ProQuest LLC
789 East Eisenhower Parkway
P.O. Box 1346
Ann Arbor, MI 48106-1346

This work is dedicated

to

my parents

ABSTRACT

The physical phenomena affecting motion at the bulk gas-liquid surface in agitated mixing systems has been investigated experimentally. The experiments were performed in cylindrical vessels with diameters of 0.21, 0.75 & 1.0 m. Rushton turbines were employed with D/T ratios of 1/4, 1/3 and 1/2. A flat blade turbine with D/T = 1/3 was also used. For all the experiments, the impeller clearance was held constant at C/T = 0.25. The main measurements made were, the gassed impeller power, P_g, the overall gas holdup, E_G, and the point gas holdup, h_p, over a wide range of impeller speed, N and sparged gas flow rate, Q. Most of the experiments were made using air-water, which is a fast coalescing system. Additionally, some measurements using 'non-coalescing' NaCl solutions were carried out and the effect of the liquid height above the impeller was also investigated. The gassed impeller power, P_g and the total gas holdup, E_G have been correlated with the independent system variables, N, Q, D and T.

An automatic dispersion analyser (ADA) has been developed for measuring point gas holdup in the bulk mixing volume. This dispersion sampling technique and concurrent data analysis was automated and controlled by a microcomputer. The point gas holdup distributions in the 0.75 m. vessel are compared with values of total gas holdup.

The motion generated at the free liquid surface of the agitated vessel is related to the minimum impeller speed necessary for onset of gas recirculation, N_{CR} such that $N_R > N_{CR} > N_F$. N_{CR} is a measure of the recirculating gas-liquid flow at the free liquid surface. The values of N_{CR} for various operating conditions have been determined from point gas holdup distributions. This reveals that gas flow rates has no significant effect on either N_{CR} or N_R.

ACKNOWLEDGEMENTS

I would like to express my sincere appreciation to Dr. M. Greaves who contributed time and advice throughout the duration of this study.

The advice and help of the Department's technicians, especially of Mr. T. Walton, the Stores Technician is acknowledged. I express my appreciation to Mr. J. Bishop, the Electrical Technician for his assistance in instrumentation.

The CASE award from BP Chemicals and the SERC studentship are most gratefully acknowledged.

Finally, I want to thank my wife, Ila for encouragement during the write-up of this work. I would also like to thank her for her help in typing and preparation of Tables.

A. Patel

April 1989

CONTENTS

Chapter 1
INTRODUCTION

Mechanically agitated gas-liquid mixing vessels are widley used throughout the chemical, biochemical and pharmaceutical industries as mass transfer contactors and reactors. Such systems may also include a third solid particle phase (eg in oxidations, fermentations, hydrogenations, chlorinations, polymerisation and nitrations). Although the subject of extensive research, mixing in agitated vessels remain a complex and poorly understood process. The complex three-dimensional turbulent forces, with two or more phases, presents formidable problems in terms of understanding the fundamental fluid mechanics, interphase mass transfer and chemical reactions. However, sufficient progress has been made to unable a range of empirical relationships to be used for design purposes. Unfortunately, they are not consistant or reliable over a range of equipment sizes due to measurements on different equipment geometry. One area of the mixing vessel operation which has not been investigated to any detailed extent is the surface movement which in a gas-liquid stirred reactor occurs at the bulk gas-liquid interface. This motion is the result of gas-liquid flow transport to and from the impeller and the resulting interaction with the free-liquid boundary.

The movement generated at the free liquid surface can be an important factor in many different

mixing reactor operations. For example, re-incorporation of a light (refluxed) liquid from the surface is important in polymerisation reactor. The addition of solids fed onto the surface of a viscous liquid (eg in fermentation processes) is dependent on the surface movement. Knowledge of the surface movement processes is necessary to understand more fully how mixing reactors can be designed and operated more effectively.

Power requirements for the mechanical agitation of liquids, both aerated and unaerated have been investigated extensively, and is an important factor for scale-up. The majority of the gassed power correlations are, however, not directly predictive. Correlations based on the system independent variables, N, Q, D & T would provide a more useful basis for design.

In gas-liquid mass transfer and reacting systems fundamental knowledge of the interfacial surface area of the dispersion, gas holdup, mean bubble diameter and mass transfer rates are vitally important. The intensity of disturbances generated at the surface of the liquid is a result of complex interaction between agitator circulation and gas transport. At any operating condition ($N > N_{F=}$), dispersion and bulk circulation of gas are critically dependent on the agitator geometry.

Bubble size and gas holdup are also distributed non-uniformly throughout the mixing space due to the variation of mean circulation velocity and turbulence intensity. Therefore, a study of the gas holdup distribution in relation to agitator geometry can contribute to a deeper understanding of the surface movement phenomena. To date, however, a satisfactory technique for point gas holdup measurement in stirred reactors has not been available. The need for a measurement technique for a wide range of gas holdups with high accuracy, fast response, low construction costs and ease of application is most evident. To further this investigation, the ADA technique was developed in order to provide a reliable technique for fast, accurate measurement of gas holdup throughout the mixing volume.

The principal aim of this study was to relate the surface movement to agitator design. In addition, a study of the overall gas holdup in conjunction with the point gas holdup distributions was made. The effect of scale on surface movement was investigated in vessel sizes of up to 1.0 m. diameter. Two agitators, T_{100} & T_{21} were available. The third agitator, T_{75} was specifically constructed for this study. The aerated and unaerated impeller power consumption have also been investigated.

Each area of research is presented in separate chapters which include an introduction, literature review, results and discussion, and conclusion sections. Experimental equipment and measurement procedures are described separatly in Chapters 2 and 3 respectively. This was found necessary to simplify the presentation of the three vessels with differing measurement procedures. Impeller power consumption is studied in Chapter 4. The study of the total gas holdup is given in Chapter 5. Local gas holdup distributions are presented in Chapter 6 together with the technique developed for point gas holdup measurements. The study of 'surface movement' in agitated vessels is presented in Chapter 7. Recommendations for future work are given in Chapter 8.

Chapter 2
MIXING VESSELS

2.1 Introduction

The experimental equipment used in this study included three separate mixing vessels; namely of 1.0, 0.75 and 0.21 m. diameter. The 0.75 m. diameter vessel was specifically designed for this study. The 1.0, 0.75 and 0.21 m. diameter vessels are referred to as T_{100}, T_{75} and T_{21}, respectively, throughout this study . The impeller clearence from the base of the vessel was fixed for all vessels at C/T = 0.25.

Associated procedures for the measurement of power, impeller speed, overall and local gas holdups are described in Chapter 3. The technique used to measure the local gas holdup in the stirred vessels is described in detail in Chapter 6.

2.2 Mixing Vessel: T_{75}

2.2.1 General Description

A general view of the mixing vessel and the impeller shaft assemly is shown in Figure 2.1. The vessel is constructed of 316 stainless steel and has an

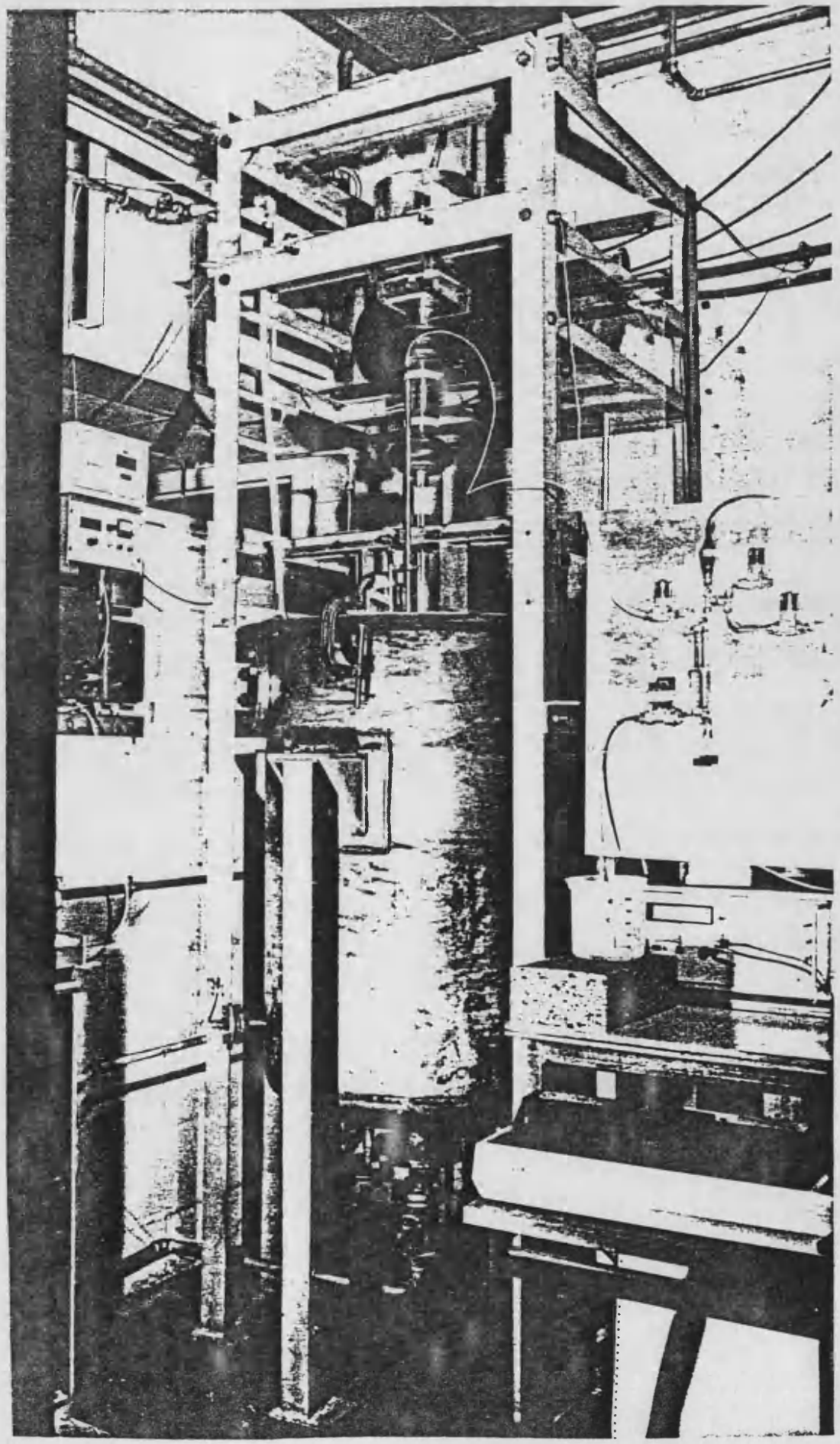

Figure 2.1 Mixing Vessel : T_{75}

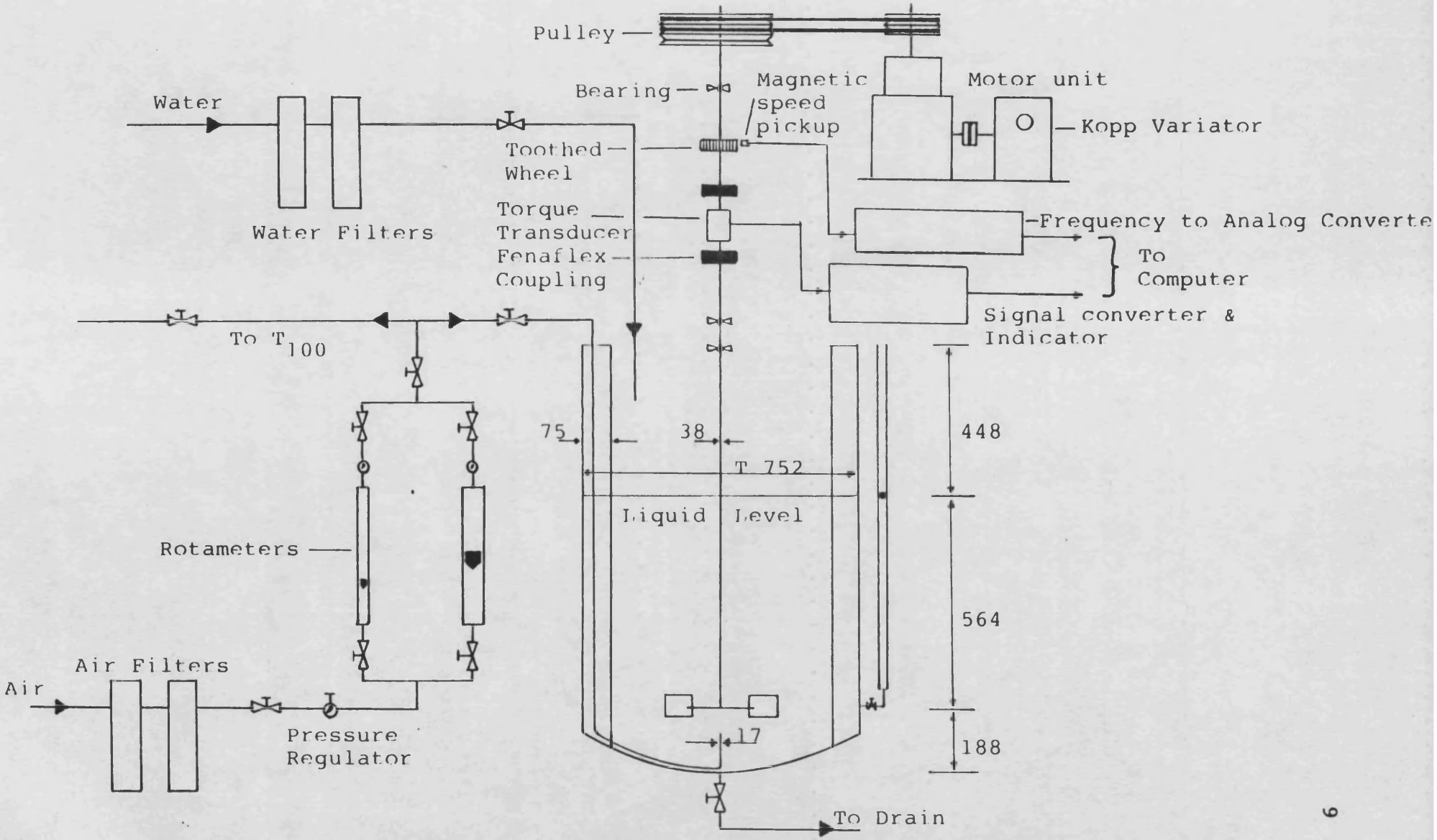

Figure 2.2 General Layout of the Mixing rig : T_{75} (Dimensions in mm.)

internal diameter of 0.752 m. and overall height of 1.2 m. The dished base of the vessel incorporated five flanged pipeline connections, with the central port being connected to the drain. The other four radial ports were blanked off and sealed with bungs in order to provide a flush internal diameter. A 5 mm. glass sight tube connected to the vessel via a 16 mm. pipe enabled accurate liquid level adjustment in the vessel. The top of the vessel was fitted with a M.O.D flange. Inside of the vessel wall was fitted with four vertical wall baffles, each one tenth the vessel internal diameter and extending the entire length of the vessel, Figure 2.2. The baffles were supported by, welded metal plates at the top flange and four equi-spaced circular 316 stainless steel rods (9 mm. diameter) fitted along the length of the baffles.

2.2.2 Drive Motor and Impeller Shaft Assembly

A 1.49 kW (2.00 hp), 3 phase motor located above the vessel was driven by a V-belt system and gearing on the motor was provided by a Kopp variator, as shown in Figure 2.2. The power to the shaft was delivered through a BHC torque transducer in line with the shaft between two bearings below the pulley system.

Shaft Sizing:

If T_c is the continuous rated torque on the impeller shaft [1],

Then $$T_C = \frac{P_O}{2\pi N} \quad \text{Nm} \qquad (2.1)$$

where,

P_O = power, watts
N = shaft speed, rps

Considering the largest impeller, D = 0.376 m. and N = 3.67 rps then P_o = 1483 watts and using Equation 2.1,

T_c = 64.4 Nm.

For a light mixing duty the shaft should be sufficiently strong to resist 1½ times the rated motor torque without the yield stress of the material being exceeded (or 0.002 per cent proof stress).
If T_m is the torque to be resisted under a stalled condition,

Then $T_m = 1.5*T_c = 96.6$ Nm.

This torque is to be resisted by a force F_m Newtons acting at a radius of 0.75r from the axis of the impeller shaft, and hence,

$$F_m = \frac{T_m}{0.75r} = 685 \text{ N} \qquad (2.2)$$

where r is the radius of the impeller.

The greatest bending moment M_m to be resisted by the impeller shaft occurs immediately below the bottom bearing, and

$$M_m = F_m * 1 = 691.9 \text{ Nm}$$

where, 1 is the distance from the bottom bearing to the mid-impeller plane.

Using the maximum elastic shear strain energy theory, the bending moment (M_{em}) equivalent to the combination of T_m and M_m is given by,

$$M_{em} = \sqrt{(M_m)^2 + 0.75\ (T_m)^2} \quad \text{Nm.}$$

$$= 696.9 \text{ Nm.}$$

Under these conditions the stress (f_y) in the impeller shaft is then given by:

$$f_y = \frac{32\ M_{em}}{\pi\ (d_t)^3} \quad Nm^{-2} \qquad (2.3)$$

where

d_t = diameter of shaft m.

For 316 stainless steel, $F_y = 230 * 10^6\ Nm^{-2}$.
From Equation (2.3)

$$d_t = \sqrt[3]{\frac{32\ M_{em}}{\pi\ (f_y)^3}} = 0.0314 \text{ m.} \qquad (2.4)$$

A 316 stainless steel shaft of 38 mm. diameter (supplied by BP Chemicals Ltd) was therfore adequate for this investigation.

The shaft system shown in Figure 2.2 incorporates three pillow block bearing units (RHP SL 1½"), with the top bearing unit supporting the shaft pulley. The strain gauge torque transducer for measuring shaft power was

connected to the shaft by means of two Fenaflex type couplings.

2.2.3 Impellers.

Rushton disc turbines and a flat blade turbine were used with T_{75}. Rushton et al [2] proposed the use of impeller ratios for D:L:W of 20:5:4 Figure 2.3. The dimensions are given in Table 2.1, and those for the flat blade turbine are given in Table 2.2.

2.2.4 Gas Sparging System.

The gas sparging system is shown in Figure 2.2. The compressed air is filtered by a set of purifying filters. The two in line rotameters (0 - 200 l/min. and 200-1000 l/min.) were calibrated at 3 bar. A series of ball and needle values allowed accurate metering of the air flow rate.

A simple orifice sparger located at the centre of the vessel below the impeller was selected for this study. Turbulent flow through the orifice is preferred but keeping orifice velocities below 100 m/s. to prevent excessive jetting [3]. The sparger consisted of a 10 mm.

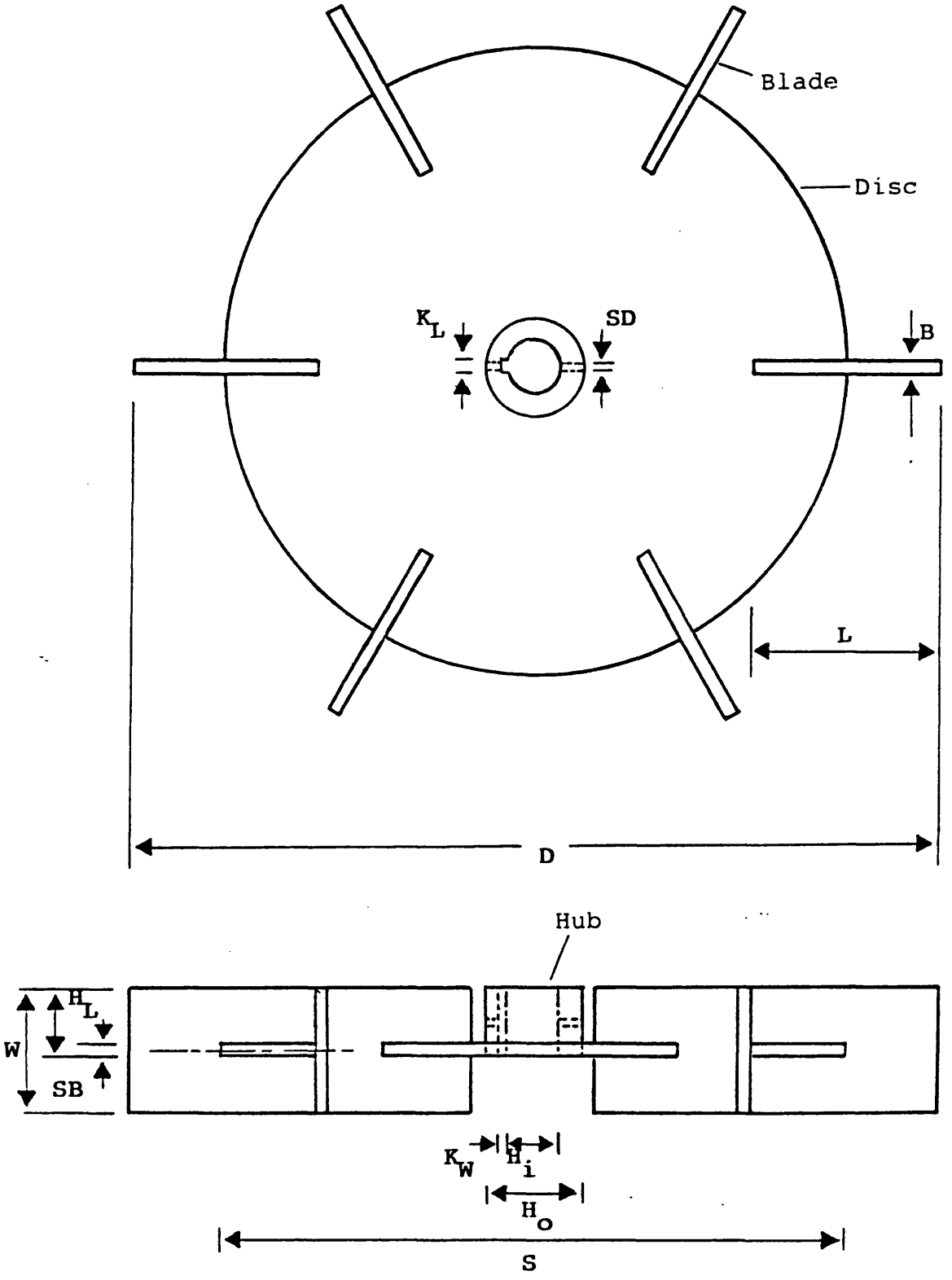

Figure 2.3 Rushton Disc Turbine

Table 2.1 : Disc Turbine Dimensions.

(All Dimensions are in mm.)

Mixing Tank	Impeller Diameter D	DISC		BLADE			HUB			Keyway		Set Screw SD
		Diameter S	Thickness SB	Width W	Length L	Thickness B	H_i	H_o	H_L	K_L	K_w	
T_{75}	376	282	2.0	75.2	94	2.0	38.2	58.2	8.0	9.5	6.3	M8
	250	187.5	2.0	50.0	62.5	2.0	38.2	58.2	8.0	9.5	6.3	M8
	188	141.0	2.0	47.6	37.6	2.0	38.2	58.2	8.0	9.5	6.3	M8
T_{100}	333	250	3.18	66.6	83.3	3.18	50.0	80.0	75.00	15.8	11.1	M12
T_{21}	67.5	50.8	1.6	13.5	16.9	1.6	9.52	19.05	7.94	-	-	2.00

Table 2.2 : 6 Flat Blade Turbine Dimensions.
(All Dimensions are in mm.)

Impeller	Diameter D	252
Blade	Length L	194
	Width W	50
Hub	H_i	38.2
	H_o	58.2
	H_L	80.0
Keyway	K_L	9.5
	K_w	6.3
Set screw	SD	M8

diameter tube to which was fitted a 30 mm. length of 17 mm. diameter tube at the point of discharge. The sparger tip was aligned directly into the centre of the impeller disc at the separation distance of 10 mm. In this investigation the maximum air flow rate that could be achieved was 6.87 * 10^{-3} m^3/s, limiting the specific flowrate in T_{100} and T_{75} to 0.52 and 0.93 vvm respectively.

2.2.5 Liquid Media.

Mains water, softened by a weak ion-exchange resin was fed through a set of particulate removing filters. Tap water was not used due to the excessive scaling deposition associated with it.

Table 2.3 Physical Properties at 293K

	Softened Water	Tap Water
Density kg/m^3	999	999
Viscosity Nsm^{-2}	$1.0*10^{-3}$	$1.0*10^{-3}$
Surface Tension N/m	$70.99*10^{-3}$	$72.7*10^{-3}$

Interestingly, the surface tension of the softened water is slightly below that of tap water. This is attributed to some surface active effect of the ion exchange resin but was not expected to seriously change the fast coalescing state compared with tap water. To stimulate a non-coalescing system, solutions of sodium chloride (commercial granular salt grade 2) were used. Table 2.4 shows the physical properties of the solutions used in this study.

Table 2.4 Physical properties of Sodium Chloride solutions

solute weight/100g solution	Density kg/m^3 at 293K	Absolute Viscosity $\frac{\text{of solution}}{\text{Viscosity of water}}$
1.0	1005.5	1.032
2.0	1012.9	1.063

Temperature control in T_{75} was not required since the stainless steel tank provided sufficient surface area for heat transfer to cool the dispersion.

The temperature of the dispersion was monitored for 8 hour runs and the temperature fluctuation was maintained in the range ± 1 °C.

2.3 Mixing Tank : T_{100}

The mixing vessel was a 1.0 m. diameter by 1.5 m. high. It was constructed of 8 mm. perspex plate. The vessel had a flat bottom and was fully baffled (0.1*T m.) with stainless steel plates equi-spaced projecting radially inward from the wall. The mixing vessel was installed inside a square-sectioned perspex water jacket which allowed the temperature of the dispersion to be controlled. Design details of T_{100} can be found elsewhere [5].

The impeller was driven by a 5.5 kW DC geared motor having adjustable speed over a 21:1 range (0.42-8.77 rev/s). The impeller shaft and the impeller were constructed of 316 stainless steel. The shaft diameter was 50 mm. A D/T ratio of 1/3 was employed for this study. Dimensions of the disc turbine are given in Table 2.1.

Compressed air is fed at the centre of the tank base below the impeller through a stainless steel tube

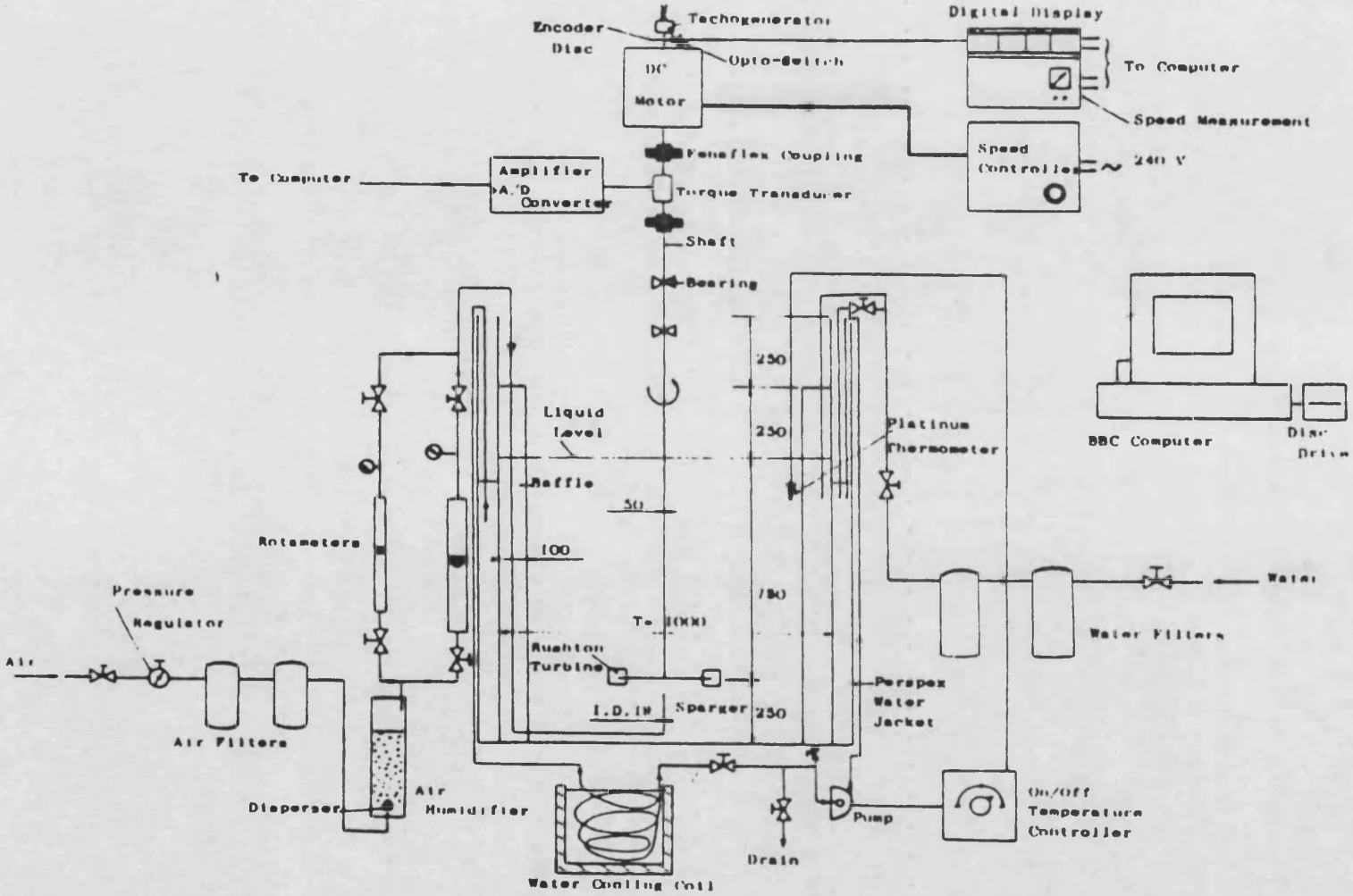

Figure 2.4 General Layout of the mixing rig: T_{100} (Dimensions in mm.)

with an orifice of 19 mm. diameter. This was rigidly supported by attaching it to one baffle. The purifying filters are common to both T_{75} and T_{100} as shown in Figure 2.2. The general layout of T_{100} is shown in Figure 2.4 (courtsey of M Barigou [5]).

2.4 Mixing Tank : T_{21}

The general layout of T_{21} is shown in Figure 2.5. The mixing vessel was a fully baffled 0.21 m. diameter 316 stainless steel tank with a flat base. Design details can be found elsewhere [6] and [7].

A 0.18 kW DC shunt motor was used to drive the impeller shaft. The power was transmitted from the motor to the shaft through a strain guage torque sensor. The impeller shaft was a 316 stainless steel rod of 9.52 mm. diameter. A standard 6 blade disc turbine of 0.0675 m. diameter (D/T = 0.32) was used for agitation. The impeller was of chromium plated brass construction. Dimensions of the impeller are given in Table 2.1. The sparger was a 6 mm. diameter stainless steel tube located immediately below the impeller.

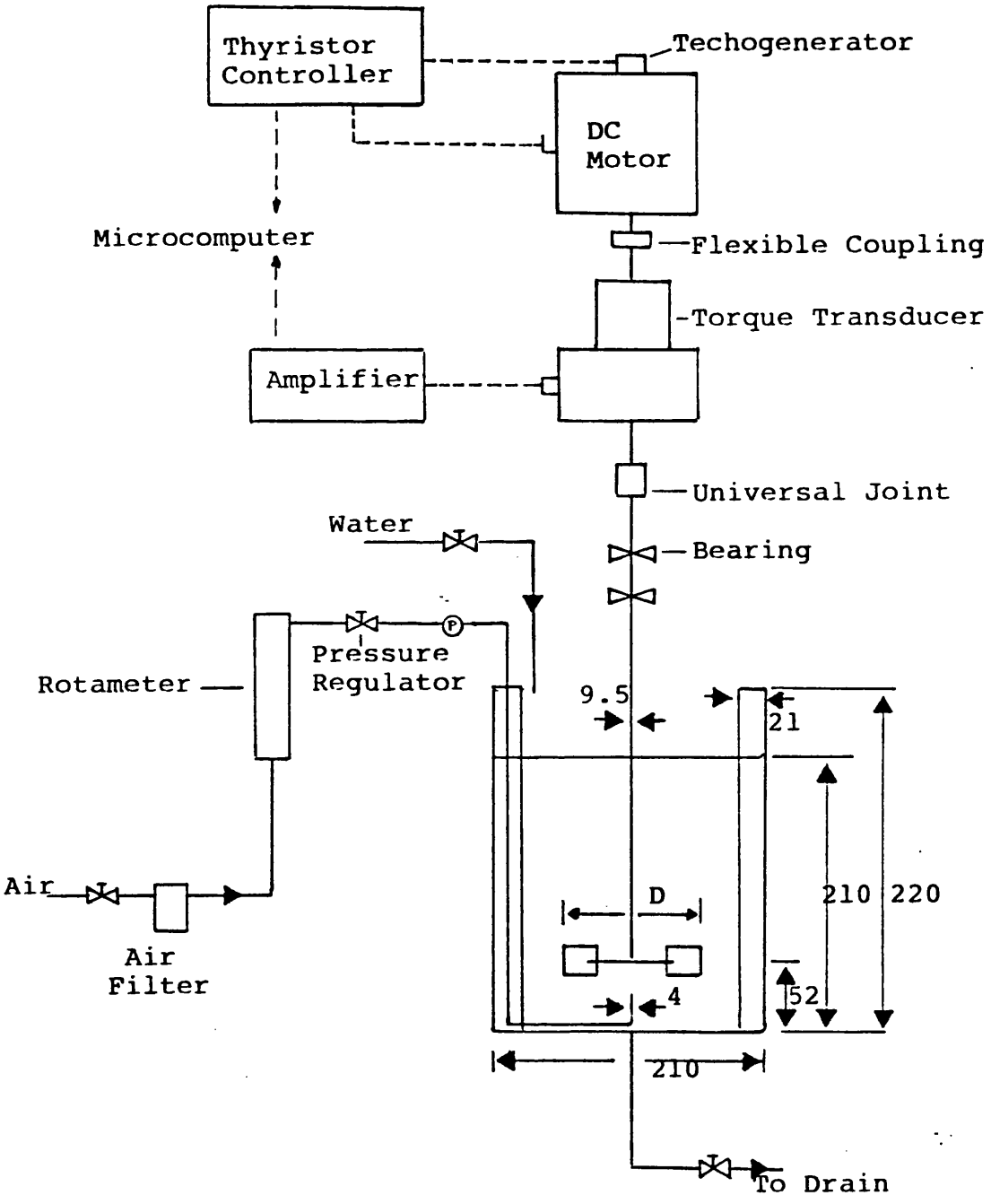

Figure 2.5 General Layout of T_{21} (Dimensions in mm.)

Chapter 3
EXPERIMENTAL PROCEDURE

3.1 Introduction

A MACYSM II microcomputer system (Analog Devices Ltd.) was used for data acquisition, control and analysis. The details of this are described in section 3.2.

The main parameters measured were impeller speed and torque, gassed power, local and overall gas holdup. The same techniques for measuring the local and the overall gas holdup were employed in all three mixing rigs. The different methods of measuring the torque and the impeller speed for the three mixing rigs are described separately.

3.2 Analysis and Data Acquisition

The MACYSM II microcomputer uses a programming language called MACBASIC. This is a high level interactive programming language based on Standard Dartmouth Basic, which is optimised for measurement and control applications. The various statements and the computer programmes developed are given in Appendix II. Figure 3.1 illustrates the control and data acquisition system used.

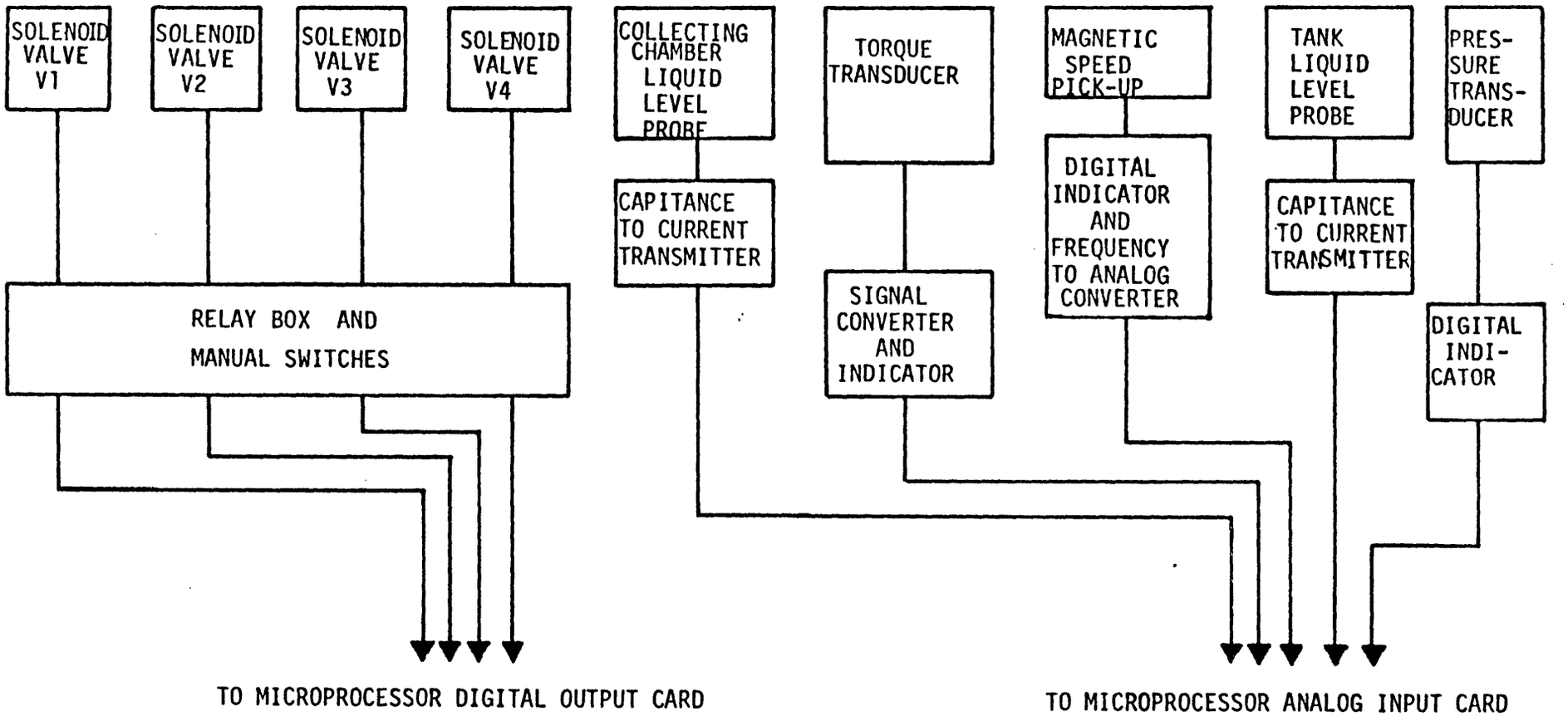

Figure 3.1 : Control and Data Acquisition System.

3.3 Mixing Tank: T_{75}

3.3.1 Impeller Speed

A magnetic speed pick-up obtains a signal from the 60-toothed wheel fitted to the impeller shaft as shown previously in Figure 2.2. The signal is fed to a frequency to analog converter which is calibrated to give an accuracy of ± 1 rpm. The analog signal is then fed to the microcomputer interface for measurement. A digital impeller speed indicator is also provided to monitor and set the impeller speed to the required value.

3.3.2 Impeller Torque

A strain gauge torque transducer (British Hovercraft made) with a range of 0 - 135 Nm was used to measure the torque exerted on the impeller. The torque transducer had a high sensitivity and accuracy ± 0.2% (other details are given in Appendix I).

The transducer measures the torque transmitted between the motor (via the pulley system) and the impeller shaft and is given by:

$$T_m = T_r + T_t \qquad (3.1)$$

where,

T_m = torque measured by the impeller

T_f = friction torque

T_t = torque exerted on the impeller

The accuracy of the torque exerted on the impeller, and hence the impeller power, depends on the accuracy with which the friction torque can be measured. The friction torque was measured with the impeller rotating in air. Figure 3.2 shows the friction torque of the three disc turbines and the flat blade turbine, over the full range of impeller speeds. The reproducibility of these results was ± 10%. The ratio of the friction to measured torque (ungassed) was generally a small fraction, as shown in Figure 3.3. Generally this ratio is higher for low impeller speeds, but under actual actual operating conditions, the friction torque was always less than 5 % of the ungassed torque. The impeller torque was reproducible to within ± 5 %.

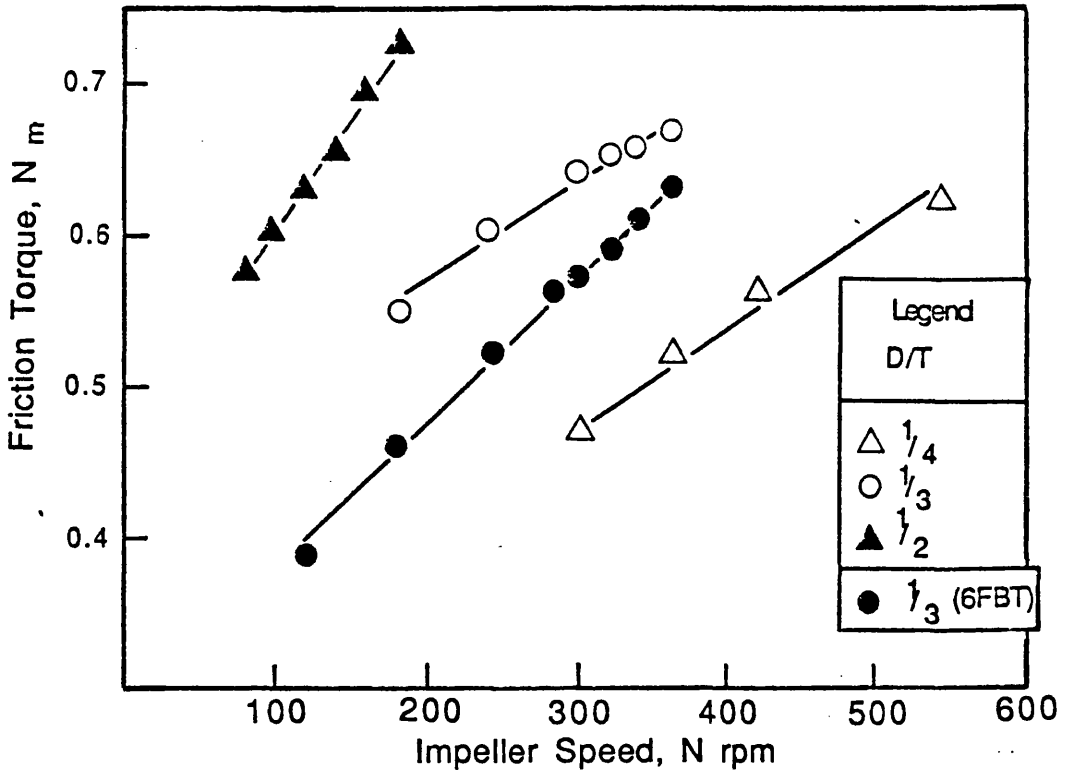

Figure 3.2 : Friction Torque V_s. Impeller Speed, T_{75}

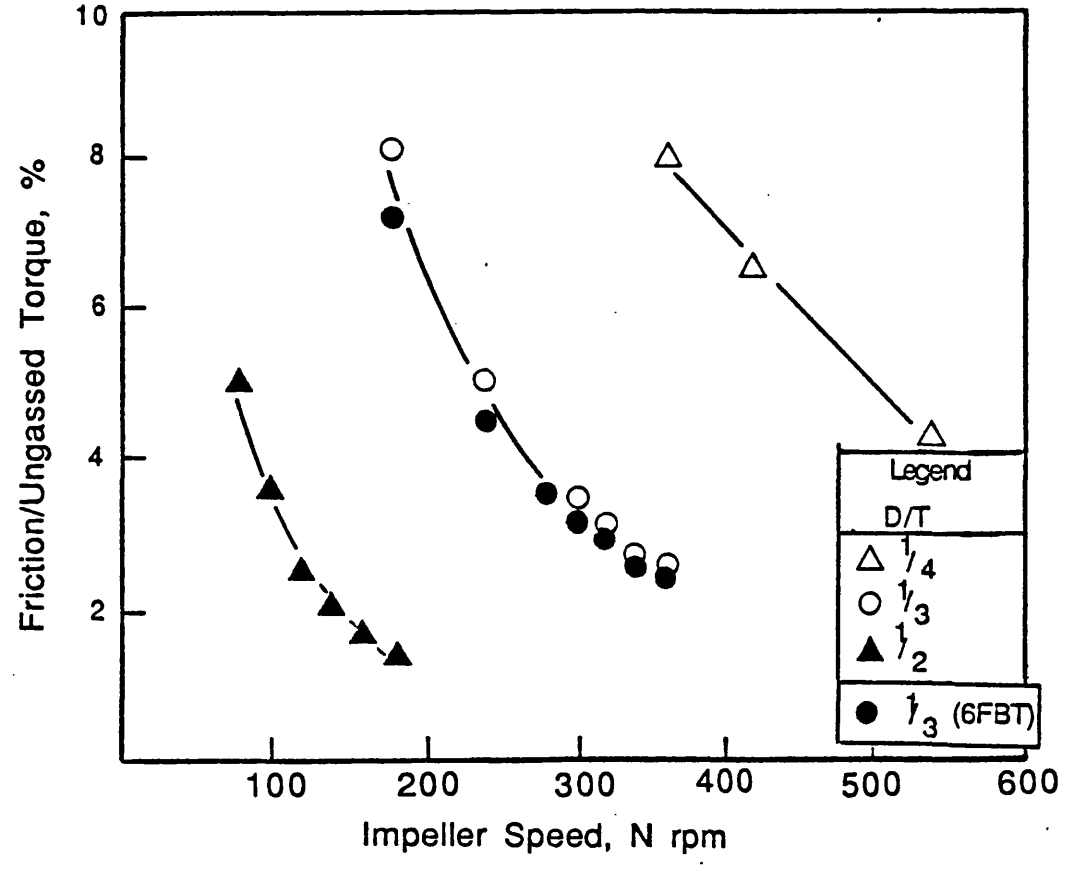

Figure 3.3 : Percentage Friction/Ungassed Torque V_s. Impeller Speed, T_7

3.4 Mixing Tank : T_{100}

The reader should refer to reference [5] for full details of this particular equipment. A summary of the main technical details is given below.

Impeller Speed :

A tachogenerator connected to the motor shaft provides a feedback of the shaft speed. The speed measurement is provided by an optical transducer incorporated between the motor and the tachogenerator. An optical switch assembly fitted to the motor body detects the passage of the 120 slots on the Nickel encoder disc. Pulses from the transducer are counted over a fixed period and displayed by the indicator in rpm.

Impeller Torque :

A strain gauge transducer mounted between the motor and the impeller shaft is used to measure the exerted torque on the impeller. The transducer is of the same make as the one fitted on T_{75} but with a range of 0 - 270 Nm. Torque exerted on the impeller is calculated from Equation 3.1. The reproducibility of the friction and the measured torque was $\pm$ 8 % and less than 5 %, respectively.

3.5 Mixing Tank : T_{21}

The reader is referred to references [6, 7] for the full specifications. A summary of the main technical details is given below.

Impeller Speed :

A tachogenerator fitted to the rotor of the DC motor generates a DC signal which is fed to the thyristor controller as the feedback signal of the speed control loop. An optical isolator is used to isolate this signal before it is fed to the microcomputer interface for measurement. The output signal from the isolator was averaged by the microcomputer, by sampling 5000 readings over 5 seconds. The accuracy of the impeller speed measurement was $\pm$ 0.5 %.

Impeller Torque :

A strain gauge torque transducer was used to measure the torque exerted on the impeller. The impeller torque was calculated from Equation 3.1. The friction torque was measured to within $\pm$ 10 %. The reproducibility of the impeller torque in the speed range investigated was better than $\pm$ 5 %.

3.6 Overall Gas Holdup Measurement

The equipment and the technique employed for the overall gas holdup measurement in this study is described here and further discussed in Chapter 5.

The overall gas holdup, E_g, is determined from the increase in the surface level of the dispersion in the tank compared with the initial level without agitation or sparging.

$$E_g = (h_g - h) / h_g \qquad (3.3)$$

where,

h_g = height of the aerated liquid

h = height of the unagitated level

In a flat based vessel (T_{100} & T_{21}), the change in the liquid level is related to the distance between the base of the vessel and the free liquid surface since the cross-sectional area of the vessel is constant. However, for the dish-based tank, T_{75}, the cross-sectional area of the tank is not constant over the height of the liquid. It is therefore necessary to relate the change in volume of dispersion in order to

determine the overall gas holdup in T75. The volume of the tank up to H = 0.75 m. was therefore accurately determined taking tank internals (i.e. shaft, impeller and baffles) into account.

The dispersion level was measured using a capacitance sensing probe. The level probe was made of 3.18 mm. diameter brass rod (254 mm. long), insulated with 1.59 mm. thick PTFE sheath. The electrode forms a capacitance between itself and the surrounding material. The capacitance changes with the level of the tank contents. A capacitance to current transmitter to produce a standard 4-20 mA DC current output signal that is directly proportional to the input capacitance of the probe was used. To calibrate the probe, known volumes of water were added to a vessel and from the corresponding changes in the output signal of the level transmitter, a linear relationship between the liquid level and the measured signal was obtained. The very low wettability of the electrode insulation coupled with the rapid response of the transmitter (0.1 sec.) provided a fast and accurate method of level measurement. However, under agitated conditions, fluctuations in the surface level caused the output signal to vary. This was therefore averaged by the MACYSM II microcomputer which sampled 1000 readings over a period of 5 seconds. Positioning of the probe is discussed in Chapter 5. Reproducibility of the overall gas holdup values was better than 5 %.

3.7 Local Gas Holdup Measurement

A fully automated system of sampling and analysis of the dispersion anywhere within the vessel was developed. The MACYSM II microcomputer is incorporated in the system to control the sampling of the dispersion, data acquisition and analysis. The technique is fully described in Chapter 5.

Chapter 4
AGITATION POWER REQUIREMENTS

4.1 Introduction

The gassed power of the agitator is an important design parameter and hence a reliable prediction method is required. Power requirements both aerated and unaerated have been extensively investigated, with respect to gas holdup and mass transfer performance. Flat-blade disc turbine impeller systems have received most attention in recent studies, but the literature review also includes a comprehensive study of gassed power correlations for other types of impeller configuration.

4.2 Literature Review

4.2.1 Agitator Power of ungassed systems

Earlier, original studies on the subject of single phase liquid mixing in stirred vessels was carried out by Rushton et al [2], Holland and Chapman [8], Uhl and Gray [9], and Nagata [10]. The equation for agitator power derived from dimensionless analysis represents the Power Number N_p as follows:

$$N_p = P_o / \rho N^3 D^5 \qquad (4.1)$$

where,

P_o = unaerated power consumption Watts

N = impeller speed

D = impeller diameter

ρ = density

If the vessel is not provided with baffles, a vortex occurs at the surface. For Re greater than approximately 300, the Froude Number Fr must be introduced.

4.2.2 Agitation Power : Gassed Systems

The introduction of gas in a mechanically agitated contactor reduces the power consumed by an impeller. This was originally thought to be mainly due to the reduction in the local density of the dispersion compared to that of pure liquid, Calderbank [11]. Van't

Reit et al [12],[13],[14] however identified the formation of stable gas cavity behind the impeller blades. These act to reduce the form drag and hence the power consumption.

Several investigators have attempted to correlate the reduction in power consumption with such parameters as, impeller diameter, speed, volumetric gas flow rate and in some cases the physical properties of the gas-liquid system. These correlations are summarised in Table 4.1.

In 1962, Michel-Miller [15] proposed the following correlation:

$$P_g = C\left(\frac{P_o^2 N D^3}{Q^{0.56}}\right)^{0.45} \qquad (4.2)$$

where the constant C = 0.71 when
the units are watts, r.p.s, m, $m^3 s^{-1}$.

The empirical correlation cannot be reliably applied to the scaleup design of large equipment.

Table 4.1 : Correlations for Gassed Power Requirement

Reference	Correlation	Liquids	Range of Physical Properties	Agitator Type	Experimental Conditions			$M = \frac{P_o^2 N D^3}{Q^{0.56}}$ (s.I)	Constant C in Correlation ( )	Exponent Of M	Remarks
					T	D/T	V_s mms^{-1} or Q m^{3}s^{-1}				
Calderbank [11] 1958	For Fl < 0.035: $\frac{P_g}{P_o} = 1 - 1.26 \frac{Q_G}{ND^3}$ For Fl > 0.035: $\frac{P_g}{P_o} = 0.62 - 1.85 \frac{Q_G}{ND^3}$	Water	P_c = (0.79-1.6) x 10^3 kgm^{-3} σ = (73.5 - 21.7) x 10^{-3} Nm^{-1} μ_c = (0.5 - 28.0) x 10^{-3} Pas	6 bladed turbine	0.5	0.33	Q < 8 x 10^{-5} to flooding	-	-	-	-
					0.184	0.33					

Table 4.1 : (cont) Correlations for Gassed Power Requirement

Reference	Correlation	Liquids	Range of Physical Properties	Agitator Type	Experimental Conditions			$M = \frac{P_o^2 N D^3}{Q^{0.56}}$ (s.I)	Constant C in Correlation ( )	Exponent Of M	Remarks
					T	D/T	V_s mms^{-1} or Q m^{3}s^{-1}				
Michel and Miller [15] 1962	$\frac{P_g}{P_o} = C\left(\frac{P_o^2 N D^3}{Q^{0.56}}\right)^{0.45}$	CCl_4 Al_2O_3 Glycerol	P_c = 800 to 1650 kgm^{-3} σ = (72 - 27)$_1$ x 10^{-3} Nm^{-1} μ_c = (0.9 - 100) x 10^{-3} Pas	6 bladed turbine (Rushton)	0.165	0.46	V_s 0.44 to 10.4	150-3500	0.63	0.42	
						0.25		100-3100	1.19	0.42	
					0.305	0.33	< 0.72	19-38000	0.95	0.43	
Clark and Vermeulen [19] 1963	$\frac{P_g}{P_o} = f\left\{E_G We^{\frac{1}{4}}\left(\frac{T^2 H}{D^2 W}\right)^{\frac{1}{2}}\right\}$	Glycerol Al cohol Isopropanol CCl_4	P = (0.79-1.6) x 10^3 kgm^{-3} σ = (21.5 - 72) x 10^{-3} Nm^{-1} μ = (1.0 - 13) x 10^{-3} Pas	4 blade paddle	0.254	0.5 0.6 0.5 0.3	V_s 3.2 - 22.4	0.4-1840 14-37000 3-15000 0.15-40	1.20 2.33 1.2	0.38 0.33 0.38	

Table 4.1 : (cont) Correlations for Gassed Power Requirement

Reference	Correlation	Liquids	Range of Physical Properties	Agitator Type	Experimental Conditions			$M = \frac{P_o^2 N D^3}{Q^{0.56}}$ (s.I)	Constant C in Correlation ( )	Exponent Of M	Remarks
					T	D/T	V_s mms^{-1} or Q m^{3}s^{-1}				
Phara-mond et al [22] 1975	$\frac{P_g}{P_o} = 1 - 1.6 \left(\frac{Q_G}{V}\right) D^{0.63}$ For $(Q_G/V)\ D^{0.63} < 3$ P_g/P_o = 0.5 to 0.55 For $(Q_G/V)\ D^{0.63} > 3$	Water	Properties of air-water system	6 bladed turbine (Rushton)	0.29 0.48 1.0	0.33	V_s 0.84 - 5.0 1.5 - 6.1 0.88 - 14.1	100-63000 900-24000 3000-10^7	0.93	0.75	These results are for impeller clearence of H/3
Hassan and Robinson [20] 1977	$\frac{P_g}{P_o} = C\left(\frac{PN^2D^3}{\sigma}\right)^m \left(\frac{Q}{ND^3}\right)^n \left(\frac{P_o}{P_g}\right)$ The Constant C depends upon geometry and varies with ionic strength. n = 0.38 m = 0.22 for 4 Bladed paddle m = 0.25 for 6 Bladed turbine	Aqueous Solutions	P = 1000 to 1100 kgm^{-3} σ = $(74 - 44)_1$ x 10^{-3} Nm μ_c = (0.8 - 3.0) x 10^{-2} Pas	4 to 6 blade paddle/ turbine	0.152 0.291	1/3 & 2/3	V_s 3.5 - 68 5 - 22.1	-	-	-	

Table 4.1 : (cont) Correlations for Gassed Power Requirement

Reference	Correlation	Liquids	Range of Physical Properties	Agitator Type	Experimental Conditions			$M = \frac{P_o^2 N D^3}{Q^{0.56}}$ (s.I)	Constant C in Correlation ( )	Exponent Of M	Remarks
					T	D/T	V_s mms^{-1} or Q m^{3}s^{-1}				
Loiseau et al [17] 1979	$P_g = C\left\{\frac{Po^2 ND^3}{Q^{0.56}}\right\}^{exp}$ (Accuracy ± 20%)	Glycerol Ethenol Water+ HCl+CuCl Aq. sodium Sulphite Acetic Acid Propenold-hyde water + sugar	Non-foaming P = (0.803-1.278) x 10^{3}kgm^{-3} σ = (61 - 23)$_1$ x 10^3 Nm μ = (1 - 48.5) x 10^3 Pas Foaming: P = 1085 to 1158 x 10^{3}kgm^{-3} σ = (56 - 54)$_1$ x 10^3 Nm μ = (1.5 - 5.4) x 10^3 Pas	6 flat blade turbine (Rushton)	0.225 0.19	0.33	V_s 0.75 - 85	1-200000 if M < 2 * 10^3 M > 2 * 10^3	0.83 0.64 1.88	0.45 0.45 0.31	Correlation modified for foaming system

Table 4.1 : (cont) Correlations for Gassed Power Requirement

Reference	Correlation	Liquids	Range of Physical Properties	Agitator Type	Experimental Conditions			$M = \frac{P_o^2 N D^3}{Q^{0.56}}$ (s.I)	Constant C in Correlation ( )	Exponent Of M	Remarks
					T	D/T	V_s mms^{-1} or Q m^{3}s^{-1}				
Luong and volesky [23] 1979	$\frac{P_g}{P_o} = C\left\{\frac{N^2 D^3 \rho}{\sigma}\right\}^m \left\{\frac{Q}{ND^3}\right\}^n$ $n = -0.38$ a) For Newtonian $m = -0.18$, $C = 0.49$ b) For non-Newtonian $m = -0.194$, $C = 0.514$	Glycol (8%wt) n CMC Sol (0.2;0.4; 0.67 %wt) Glycerol (40%wt) Methanol (10%vol)	ρ = 983-1100kgm^{-3} σ = (72 - 55) x 10^{-3} Nm^{-1} μ = (0.85 - 3.0) x 10^{-3} Pas	6 flat bladed turbine	0.22	0.33		-	-	-	
Yung et al [87] 1979	$P_g = C\left\{\frac{P_o^2 N D^3}{Q^{0.56}}\right\}^{exp}$ (Accuracy ± 20%)	Water Glycol (15% 30%) vol Acetone (30%vol) NaCl sol^n (0.2&0.4M) Na_2SO_4 Sol^n (0.03,-312M)	ρ = 960 to 1047 kgm^{-3} σ = (38.29 to 72.74) x 10^{-3} Nm^{-1} μ = (0.8 - 2.1) x 10^{-3} Pas	6 bladed turbine and 4 bladed paddle	0.4 0.4 hemi	0.225 0.325 0.45	Q 1.22 x 10^{-4} 27.2 x 10^{-4}	N r/s 3.33-23.3	0.812 0.829	0.45 0.45	

Table 4.1 : (cont) Correlations for Gassed Power Requirement

Reference	Correlation	Liquids	Range of Physical Properties	Agitator Type	Experimental Conditions			$M = \frac{P_o^2 N D^3}{Q^{0.56}}$ (s.I)	Constant C in Correlation ( )	Exponent Of M	Remarks
					T	D/T	V_s mms^{-1} or Q m^{3}s^{-1}				
Kobbacy [7] 1981	$P_g = 1007\left\{\frac{N^{3.33} D^{6.33}}{(nQ)^{0.4}}\right\}$	Water	Properties of air-water system	6 bladed turbine (Rushton)	0.2	0.25 0.33 0.625	V_s 2.6 - 12.31	N r/s 5-20	-	-	n is the dispersion effeiciency factor dependent upon regime of mixing
Barigou [5] 1987	$Pg = CN^a Q^b \left[\frac{D}{T}\right]^c$ Votex - clinging cavity Regime C = 441.4, a = 3.13, b = -0.5, c = 5.82 Large Cavity: C = 1737.1 a = 2.99 b = -0.31 c = 5.98	Water 0.15M NaCl^n sol	Properties of air-water system	6 bladed turbine (Rushton)	1.0	0.25 0.33 0.5	Q: 1.64 x 10^{-3} to 8.33 x 10^{-3}				

It also fails at extreme values of gas rate; as Q -> 0, P_g should approach P_o and as Q becomes very large, P_g should approach the value required by the impeller rotating in gas phase only. Michel - Millier did not find any dependence of the interfacial tension on the impeller power. The correlation was also found to hold for liquids containing up to 5% of suspended solids.

Recently, Mann[16] reorganised Miller's correlation in the form presented by most workers, showing the aeration number to be the dominating group:

$$P_g / P_o = \text{Constant} * Q^{0.2} (Q / ND^3)^{-0.45} \qquad (4.3)$$

Equation 4.2 was later verified by, Loiseau et al [17] and by Yung et al [18]. Correlations proposed by these workers (Table 4.1) differs only in the values of the constant and magnitude of the exponent and is mainly attributable to the difference in the physical properties of the liquid media employed. Loiseau's et al [17] and Yung's et al [18] correlations are in good agreement (within experimental error) for nonfoaming liquids. Yung et al found a slight increase in holdup with increase in elctrolyte concentration due to foam formation. Their investigations, however, were restricted to only slight or non-foaming solutions and

observed no effect of physico-chemical properties or ionic strength on the power requirements. Investigations with foaming solutions by Loiseau et al [17] showed a significant increase in gas holdup with a reduction in power compared to that for nonfoaming liquid in the same size tank and under the same agitation rate conditions. The constant and the exponent in the correlation are significantly different compared with those for nonfoaming solutions reported by the same authors. The correlation of Loiseau at el [17] covers the widest range of variables investigated and thus for pure liquids, nonfoaming ionic, and non-ionic solutions, or liquids containing a surface active agent, the correlation can be used to predict the gassed power with reasonable accuracy for vessel diameters up to 1.0 m.

Clark and Vermeulen [19] used the Weber Number to correlate the power of agitiation. They incorporated a perforated plate covering the bottom of the vessel, thus considerably modifying the behaviour of the dispersion with respect to flooding and recirculation. They proposed the following correlation:

$$\frac{P_g}{P_o} = f\left[E_G We^{0.25}\left(\frac{T^2 H}{D^2 W}\right)^{0.5}\right] \qquad (4.4)$$

In 1977, Hassan and Robinson [20] proposed a correlation which also involves the Weber Number.

$$P_g / P_o = C We^{l} N_A^{-.038} \qquad (4.5)$$

where the constant C depends on the dimension of the vessel and the ionic strength of the solution. The exponent l varies with the type of impeller. Equation 4.4 does not directly involve the gas flow Q_G whose influence is included in the hold-up term, while equation 4.5 provides $P_g/P_o \sim Q_G^{-0.38}$. The difference arises from the mode of distribution of the gas, which has a considerable influence on the dispersion if the distributor is near to the agitator.

Hughmark [21] made a statistical analysis of all the reported data and found that the coefficient for Weber Number (which involves surface tension) was not statiscally significant. Further, he found that the use of the liquid volume in the place of D^3 in the aeration number, and the use of a modified Froude Number, reduced the averge absolute deviation by 50% or more when correlating the data of Michel and Miller [15],

Pharamond et al [22], Luong and Volesky [23] and Bimbinet et al [24]. The correlation obtained is:

$$\frac{P_g}{P_o} = 0.1 \left(\frac{NV}{Q_G}\right)^{0.25} \left(\frac{N^2 D^4}{gWV^{2/3}}\right)^{-1/5} \qquad (4.6)$$

where,

V	= liquid volume	m^3
g	= acceleration due to gravity	ms_1
W	= impeller blade width	m
Q_G	= gas rate	m^3s^{-1}

Equation 4.6 covers the widest range of variables and is dimensionless. However, it fails at extreme values of gas flow rates.

Nagase et al [25] proposed an empirical relation for power consumption in connection with the circulation flow rate in agitated vessels as :

$$\frac{P_g}{\rho N^3 D^5} = C_R \left(\frac{D}{T}\right)^2 \left(\frac{Q}{ND^3}\right)^2 \qquad (4.7)$$

where C_R = 8.1 for turbine impeller

Bruijn et al [12] in an attempt to correlate the reduction in the power consumption with the number and the shape of cavities behind the impeller blades, found that surface tension was not important regarding the mechanism of cavity formation and shape of cavities. However, liquid viscosity was shown to influence the stability of the cavity but this effect could not be quantified.

Yamaguchi et al [26] correlated gassed power as:

$$\log\left(\frac{P_g}{P_o}\right) = -192\left(\frac{D}{T}\right)^{4.38}\left(\frac{ND^2}{\nu}\right)^{0.115}\left(\frac{N^2D}{g}\right)^{1.96(D/T)}\left(\frac{Q}{ND^3}\right) \qquad (4.8)$$

A more recent power correlation by Gray et al [27] takes the form of:

$$\left(\frac{P_T g_c}{N^3 D^5 \rho_L}\right) = 0.75\left(\frac{CTg^2}{(U_s/E_G)^2 N^2 D^2}\right)^{0.25} \qquad (4.9)$$

where,

P_T is the total power input in gas-liquid dispersion, Watts.

The authors claim an accuracy of ±20%.

Calderbank [11] proposed the following equations:

$$P_g/P_o = 1 - 1.26N_A \quad \text{for} \quad N_A < 0.035 \qquad (4.10)$$

and

$$P_g/P_o = 0.62 - 1.85N_A \quad \text{for} \quad N_A > 0.035 \qquad (4.11)$$

where,

N_A is the aeration number, Q/ND^3

These equations represent the form of the curves observed experimentally.

Nienow and Wisdon [28] expressed their results with:

$$P_g / P_o = 1 - 8.5\left(\frac{Q}{ND^3}\right) \quad \text{for } N_F \leq N \leq N_R \qquad (4.12)$$

In practice, these are 'average' relationships which do not consider the phenomena of recirculation. They are not well adapted for scale-up to large-sized equipment. Equation 4.12 does not hold for high gas flows.

Kobbacy [7] proposed Equation 4.13 which incorporates an impeller efficiency defined as the ratio of the rate of gas coalescence with its impeller cavities to the rate of gas sparging.

$$P_g = 1007\left(\frac{N^{3.33} D^{6.33}}{(\eta Q)^{0.404}}\right) \qquad (4.13)$$

where,

η = impeller efficiency.

$\eta = 1$ Efficient mixing region for $N_F \leq N \leq N_R$

$\eta_F = \eta < 1$ Flooding region for $N < N_F$

$\eta_R = \eta > 1$ Recirculation region for $N > N_R$

where,

$$\eta_R = 4.13 \left(\frac{N^{2.53} D^{5.93}}{T^{2.45} Q^{0.33}} \right) \qquad (4.14)$$

and $\eta_F = 0.45$ for $A \ll 1$

$$\eta_F = 0.25 + 0.26A \quad \text{for } A > 1$$

$$A = \left[\frac{N^{2.53} D^{4.44}}{T^{0.5} Q^{0.73}} \right] \qquad (4.15)$$

Recently Barigou [5] proposed correlations for the gassed power according to the vortex, clinging or large cavity regimes.

(i). Vortex cavity regime:

$$P_g = 441.4\, N^{3.13} Q^{-0.5} [D/T]^{5.82} \qquad (4.16)$$

(ii). Large cavity regime:

$$P_g = 1737.1\ N^{2.99}\ Q^{-0.31}\ [D/T]^{5.98} \qquad (4.17)$$

These correlations showed the gassed power to be more sensitive to the gas flow rate in the vortex - clinging cavity regime. The author claims an improvement of 40%, over the overall or combined correlation, Equation 4.18, in Equations 4.16 and 4.17. However, the use of Equations 4.16 and 4.17 requires the prior knowledge of the existing cavity regimes.

Overall correlation:

$$P_g = 706.3\ N^{3.01}\ Q^{-0.45}\ [D/T]^{5.38} \qquad (4.18)$$

4.3 Results and Discussion.

Gassed power measurements for T_{21}, T_{75} and T_{100} are presented in Figures 4.1 to 4.7 as gassed power number against flow number plots. These plots are very similar to those presented by Nienow et al [44], as shown in Figure 4.8. The minima in the curves (marked F) correspond well with the transition from Figure 7.3 (a to b) defined as the flooding point. The maxima on the curves (marked R) corresponds to gas recirculation back to the impeller and is discussed further in Chapter 7.

The effect of varying the liquid level from the standard configuration of H = T to H=1.2*T on the impeller power consumption was investigated in T_{75} for D/T = $^1/_3$. The negligible difference of the gassed power between the two systems was well within the experimental error range.

The air-salt solution was investigated in T_{75} for D/T = $^1/_2$ and Q = 1.76 x 10^{-3} m^3s^{-1}. Comparision of the impeller power consumption with the air-water system revealed no significant differences in the two systems. This is in agreement with other researchers [5, 15, 19, 35].

Figure 4.1 : Gassed Power Number Against Flow Number
Impeller Type : 6FBDT. Impeller Dia.: 0.188 m.
H=T= 0.75 m.

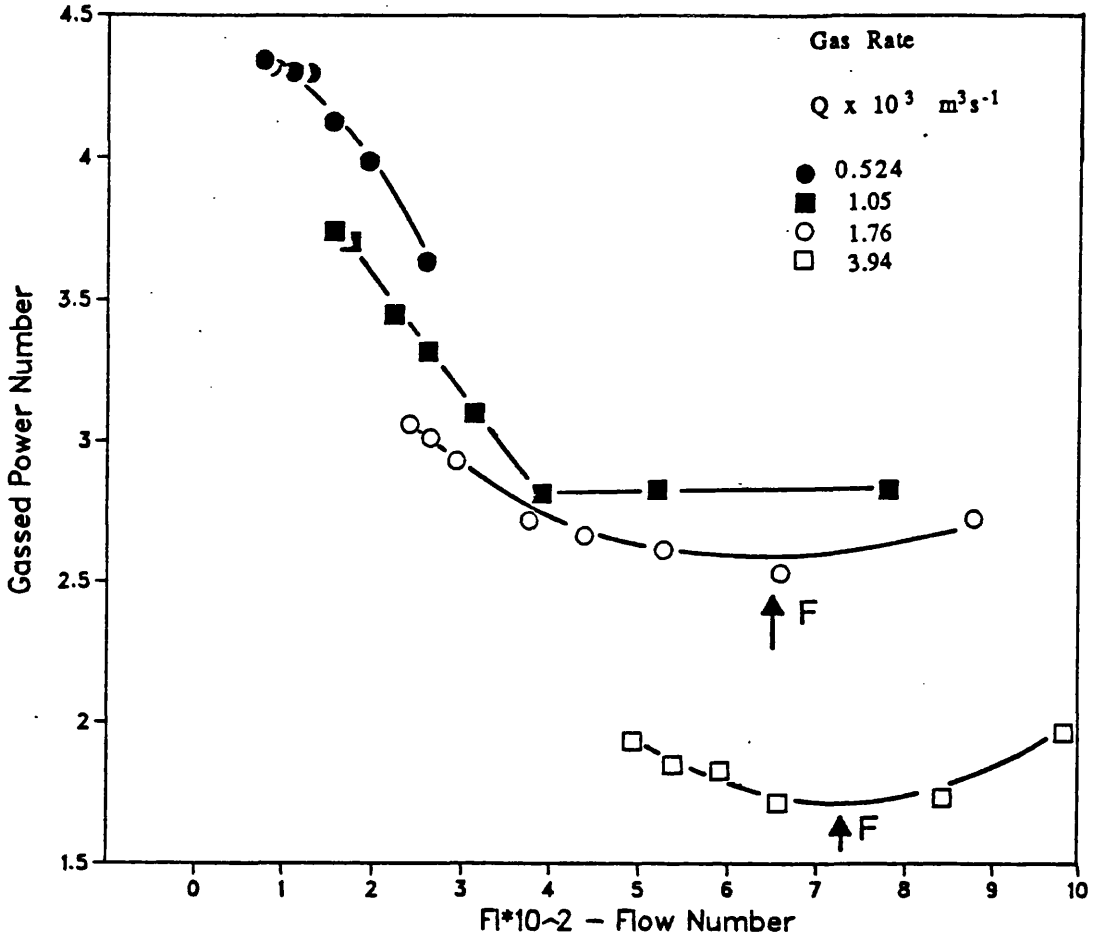

Figure 4.2 : Gassed Power Number Against Flow Number
Impeller Type : 6FBDT. Impeller Dia. : 0.25 m.
H=T= 0.75 m.

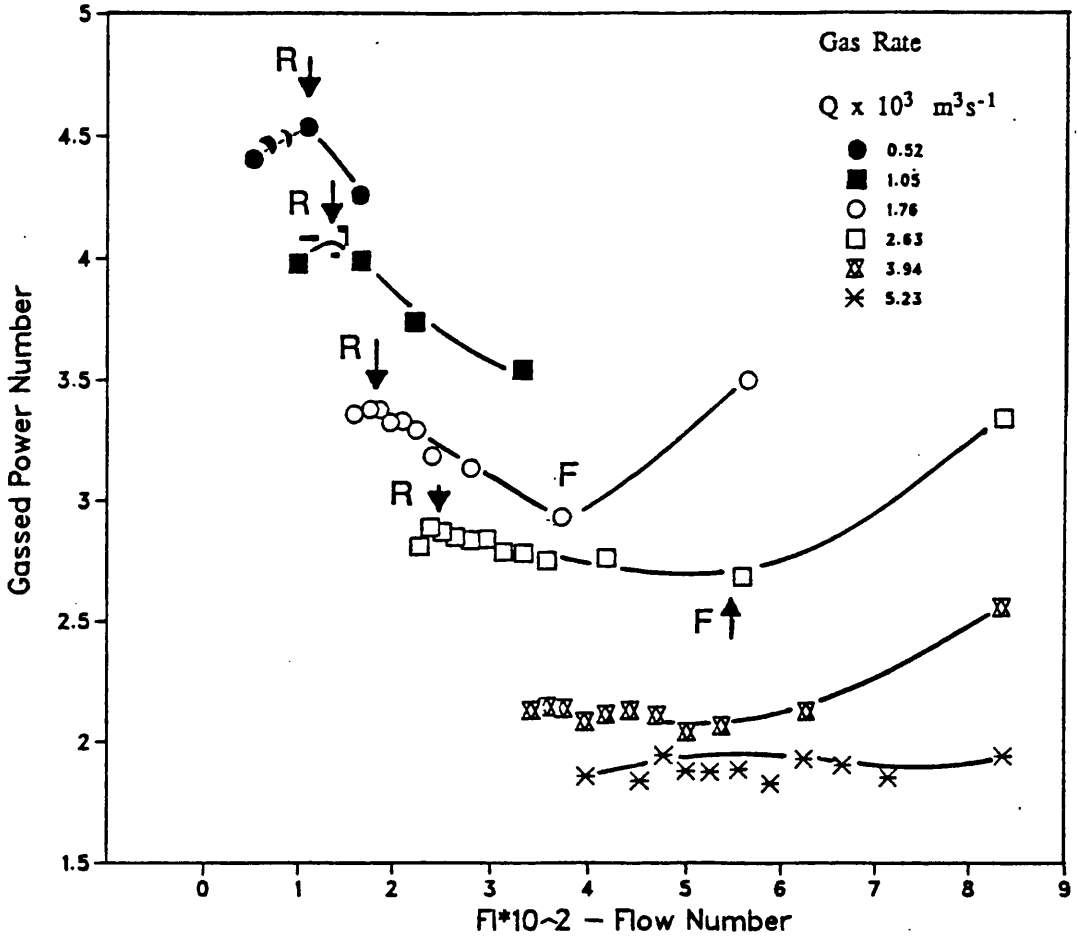

Figure 4.3 : Gassed Power Number Against Flow Number
Impeller Type : 6FBDT. Impeller Dia.: 0.376 m.
H=T= 0.75 m.

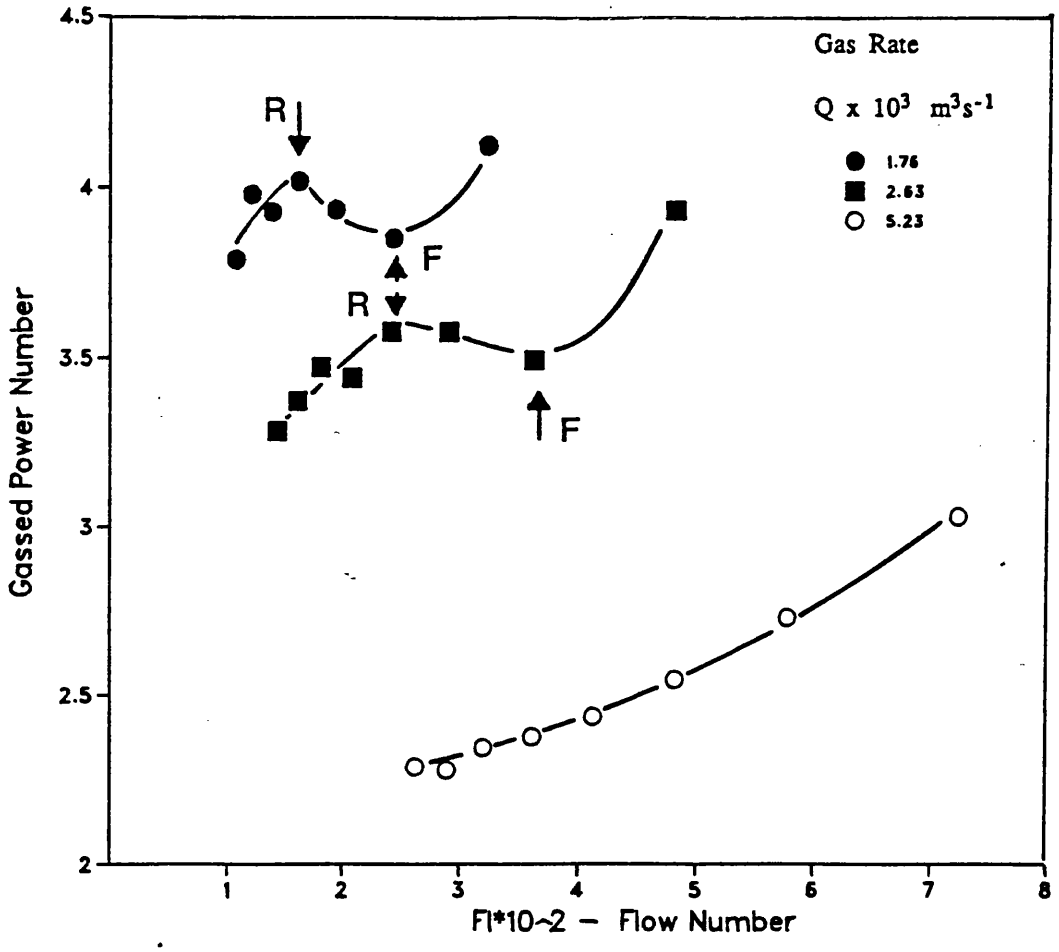

Figure 4.4 : Gassed Power Number Against Flow Number
Impeller Type : 6FBT. Impeller Dia. : 0.252 m.
H=T= 0.75 m.

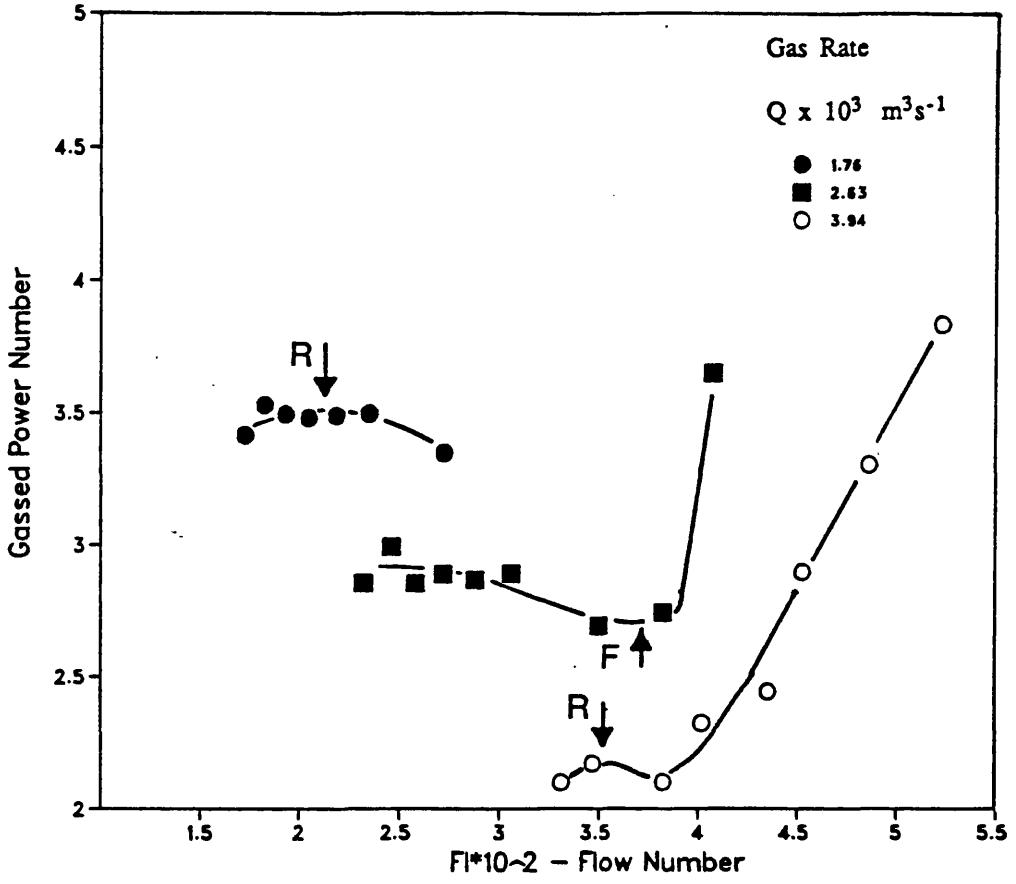

Figure 4.5 : Gassed Power Number Against Flow Number
Impeller Type : 6FBDT. Impeller Dia. : 0.0675 m.
T = H = 0.21 m.

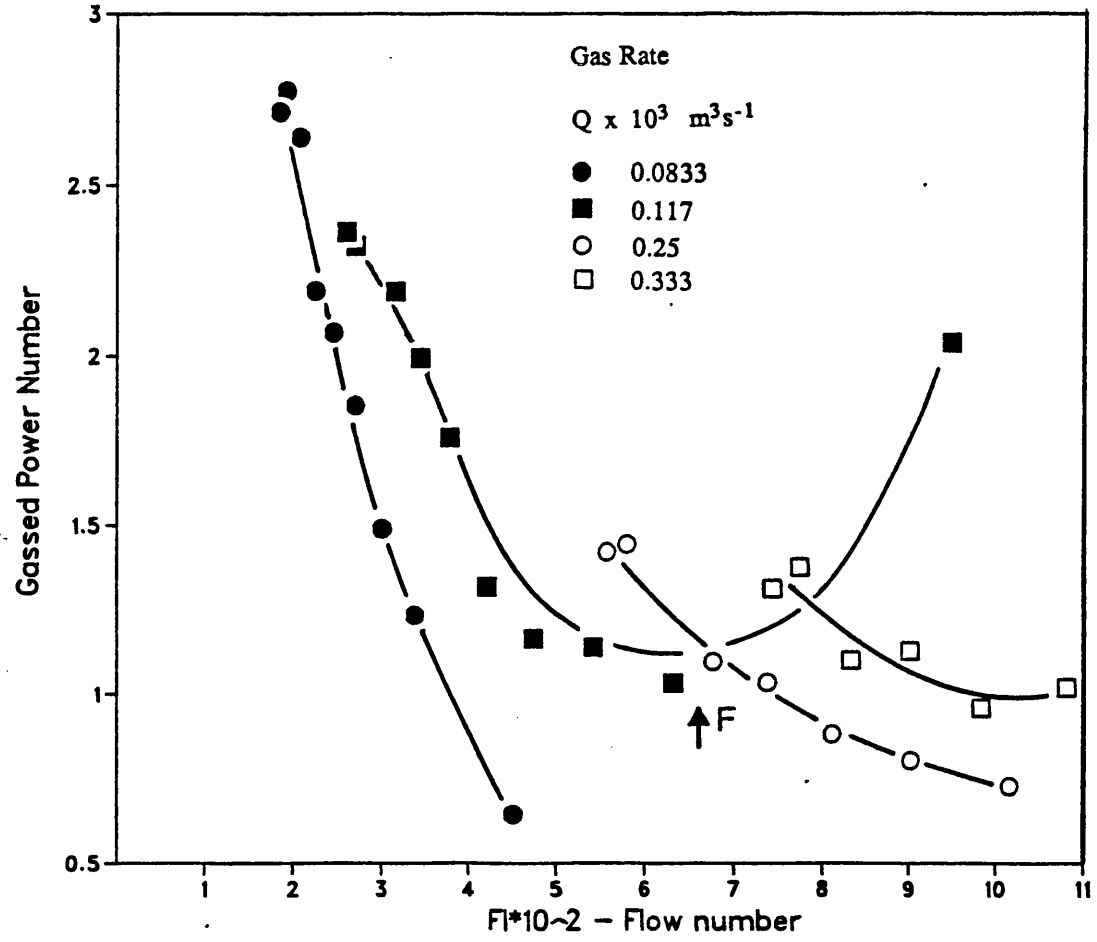

Figure 4.6 : Gassed Power Number Against Flow Number
Impeller Type : 6FBDT. Impeller Dia. : 0.333 m.
H = T = 1.00 m.

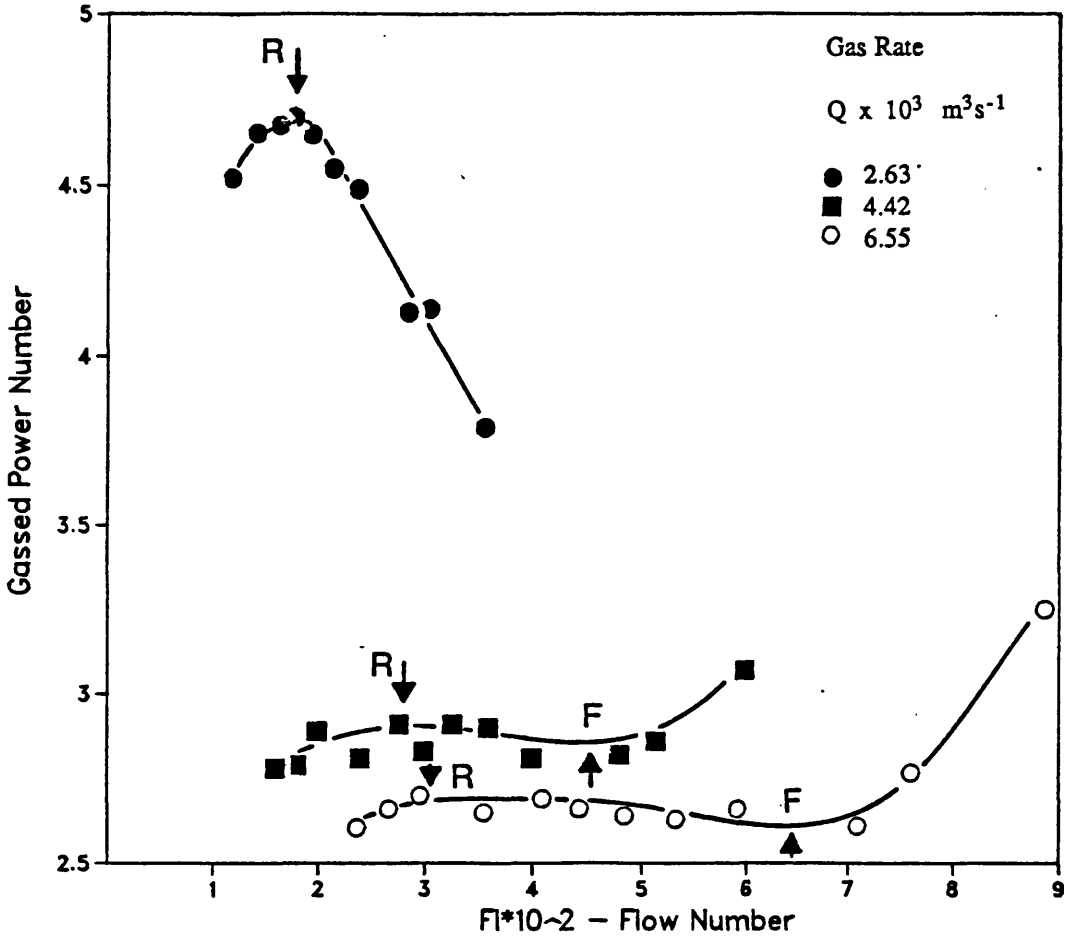

Figure 4.7 : Gassed Power Number Against Flow Number
Impeller Type : 6FBDT. Impeller Dia. : 0.25 m.
T= 0.75 m. H=1.2*T

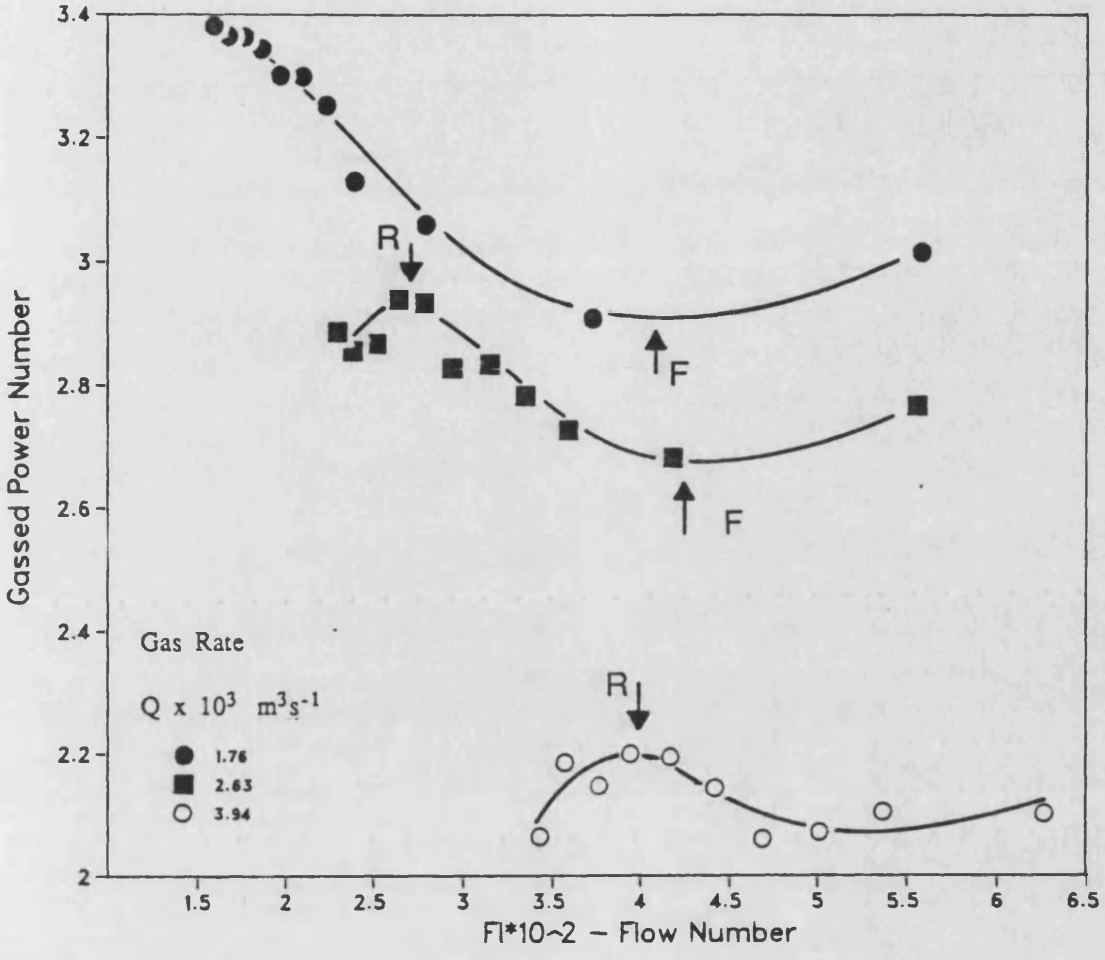

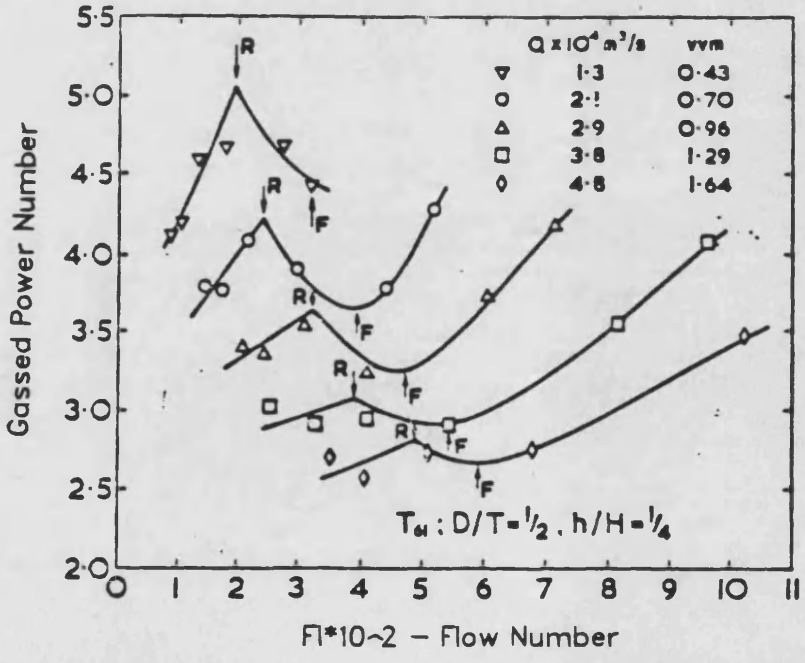

Figure 4.8: Gassed Power Data from Nienow et al [44]

All of the gassed power data representing 284 measurements was therefore correlated together. Only the independent variables D, T, Q and N were used to correlate the gassed impeller power consumption P_g:

$$P_g = 837.1 \frac{N^{2.96} D^{6.35}}{Q^{0.38} [D/T]^{0.797}} \qquad (4.19)$$

and on re-arranging

$$P_g = 837.1 \frac{N^{2.96} D^{5.55} T^{0.797}}{Q^{0.38}} \qquad (4.20)$$

where s = 0.18 and R-sq = .993

This correlation is plotted in Figure 4.9.

The data scatter of ±10% is well within the experimental range.

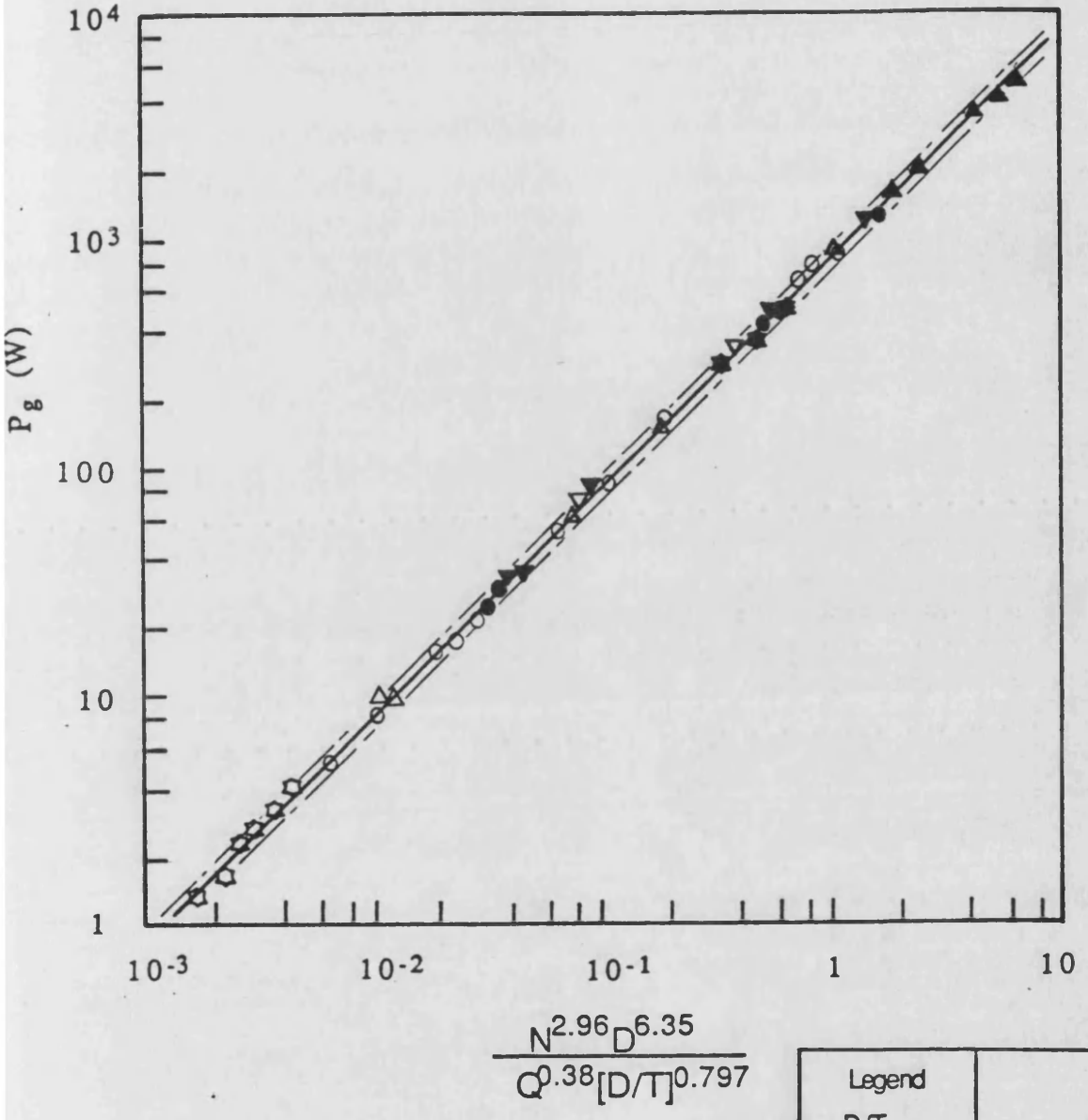

Legend D/T	
○ 1/4 ● 1/3 △ 1/2	T_{75}
▲ 1/3	T_{100}
✡ 0.32	T_{21}
✸ 1/3	T_{75} (6FBT)
▼ 1/3 ▽ 1/2	T_{75} H - 1.2 * T T_{75} Air/salt
———	Correlation
— - - —	± 10%

Figure 4.9: Gassed Power

4.3.1 Comparision with literature

Kobbacy [7] derived Equation (4.13) from measurements in T_{21} only. Substituting n = 1 in Equation (4.13) i.e the efficient mixing region, the exponents of the independent variables N, Q and D compare well with the respective exponents of Equation (4.19) which correlates measurements in three vessel sizes namely T_{21}, T_{75} and T_{100}.

The correlations proposed by Barigou [5] relate to measurements in T_{100} alone. The exponents for N, Q and D, of the 'large cavity regime' correlation, Equation (4.17), compares well with the respective exponents of Equation (4.20). The exponent of T in his correlation is -5.98 compared with +0.797 in the present study. The author's measurements were made in T_{100} where T = 1.0 m. Equation (4.17) should therefore actually contain the term $D^{5.97}$ rather than $(D/T)^{5.97}$. The correlations (Equation 4.16 - 4.18) are therefore misleading with respect to the true significance of the tank diameter, T on the gassed power, P_g. It is not recommended to use Equations (4.16 to 4.18) for T # 1. Figure 4.10 shows the gassed power data of Barrigou [5] plotted against the proposed correlation of Equation 4.19. The scatter about the correlation is ±10% compared with the ±15% scatter for Equations 4.16 & 4.17.

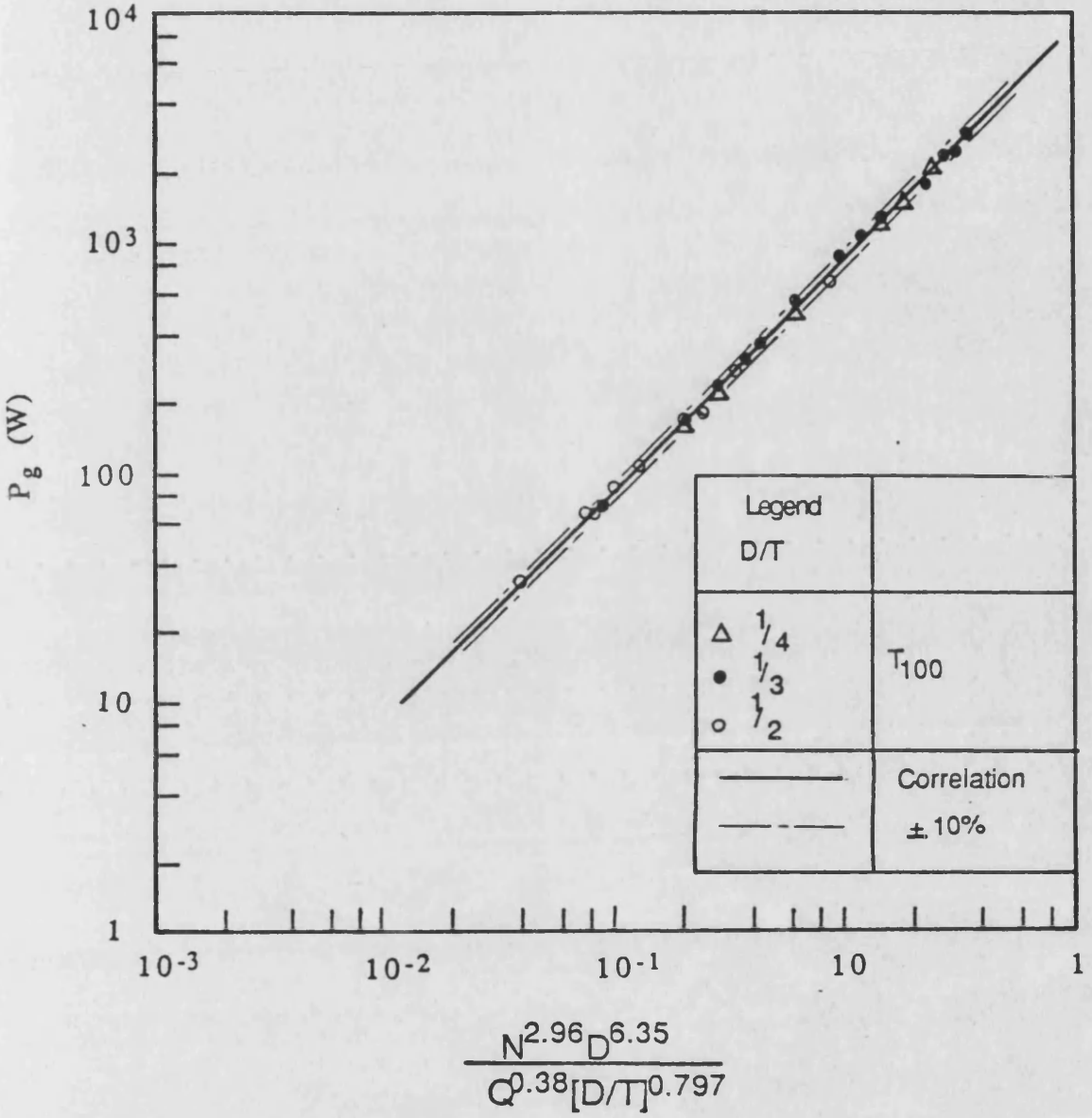

Figure 4.10: Gassed Power Data of Barrigou [5]

This represents an improvement of over 30%.

4.4 Conclusions.

- The effect of varying the liquid level from the standard configuration of H = T to H = 1.2 * T on the gassed impeller power consumption is not significant.

- Similarily there is negligible effect on the gassed impeller power consumption when using an air-salt solution compared with the air/water system.

- The gassed power consumption has been correlated in terms of the independent variables N, Q, D and T. The correlation is accurate to within ±10% for measured data obtained from vessels of 0.2 to 1.0 m. diameter.

Chapter 5
TOTAL GAS HOLDUP

5.1 Introduction

Gas-liquid mass transfer is important in many reactions such as oxidations, fermentations, hydrogenations, polymerisation, chlorinations and nitrations. Knowledge of the surface area of gas-liquid dispersions, gas holdup, and mean bubble diameter, as well as mass transfer rates are of fundamental importance. Interfacial area is related to gas holdup and mean bubble size by:

$$a = \frac{6\,E_G}{D_{BM}} \qquad (5.1)$$

where,

D_{BM} is the sauter mean, or surface volume mean diameter defined as :

$$D_{BM} = \frac{\sum_1^n n D^3}{\sum_1^n n D^2} = \frac{6\,E_G}{a} \qquad (5.2)$$

where, E_G = total gas holdup.

Bubble size and its distribution in an agitated vessel is not within the scope of the present study. The reader is referred to the research by Barigou [5] and Kobbacy [7], who provide information on bubble size and distribution in agitated vessels.

A study of the total gas holdup was conducted in connection with the local gas holdup distribution described in (Chapter 6) and 'surface movement' described in Chapter 7. The following review covers various measurement techniqes and proposed correlations for the total gas holdup.

5.2 Measurement techniques

Loiseau et al [17] measured total gas holdup by draining the liquid overflow . Clearly the method cannot give a complete picture of the mixing process and furthermore the technique is likely to greatly overestimate the gas holdup.

Sridhar and Potter [31], Calderbank [11], [29] and Yoshida et al [30] used various forms of manometry. Yoshida et al [30] measured the bulk density

of aerated liquid by means of two pressure taps located on the inside of the tank wall, at about midway between two adjacent baffles. One was located near the tank bottom and the other near the free liquid surface. In a mixing vessel, there is a wide spatial variation of local gas holdup so the density of the aerated liquid is not uniform. Their techniques do not account for this non-uniformity. Sridhar and Potter [31] corrected their manometer readings for dynamic pressure differences by measuring the pressure differential in the clear liquid and in the aerated liquid at the same impeller speed. Calderbank [11], [29] used a probe to measure the pressure at various depths of immersion. The free surface was determined by extrapolating the zero pressure differential. All of the techniques are time consuming and non of them accounts for the fluctuations of the free liquid surface.

Foust et al [33] and Rushton and Bimbenet [32], used a "level-taker" to measure liquid level. A number of holes were drilled on two concentric copper tubes with a loose packing of glass wool between the inner and outside tubes to obtain a quiescent liquid surface in the inner tube. The indicated level was read by an inclined gauge connected to the level-taker by a siphon.

Hassan and Robinson [20] measured the liquid level by a cathetometer directed at the impeller shaft region. This technique eliminates the fluctuations in the level that occur in the vicinity of the tank wall due to the baffles, but ignores the fluctuations in the level in the impeller shaft region.

Numerous investigators [5, 6, 7, 20, 34, 54, 62, 64 & 65] have used level probes to detect the increase in the level of the dispersion at a single position of the vessel cross-section. The main drawback of this technique is that fluctuations at the surface, particularily those in the vicinity of the baffles and impeller shaft are not accounted for. The ideal method for gas holdup measurement would need to define the complete surface under aeration conditions, taking into account the disturbances at the wall baffles. However, this necessitates measuring the liquid level at many points across the surface and would be extremely time consuming in practice.

Similar to other workers [5, 6, & 7] the level probe used in this study was positioned mid-way between two adjacent baffles and mid-way between the impeller shaft and the vessel wall. This position was selected to give the 'best' representation level of the dispersion in the vessel.

Gas bubbles are entrained at the liquid surface by surface aeration under ungassed conditions when the impeller speed exceeds a certain value. This provides an accompanying increase in the liquid level and further complicates the measurement of gas holdup. The ungassed liquid height h in Equation 3.3 was measured without agitation in this study. The measured total gas holdup data reported here is therefore due to the sparged gas and also gas entrained from the surface.

5.3 Correlations for Total Gas Holdup.

The overall holdup of dispersed gas is strongly influenced by the presence of dissolved inorganic salts [34]. Generally, the solutes which modify the behaviour of the gas-liquid interface inhibit bubble coalescence which in turn, affects the gas holdup. Therefore, separate correlations of E_G for pure liquids and ionic solutions are required.

The majority of the correlation for gas hold up (Table 5.1) are based on power per unit volume, P/V and the superficial gas velocity U_s. The exponents of P/V range from 0.25 and 0.5 with a value of 0.4 being the most common.

Table 5.1 : Correlations for Gas Holdup

Reference	Correlation	Method	SYSTEM		Agitator Type	Sparger	Experimental Conditions				Remarks
			Liquid	Gas			V_s cms^{-1}	T cm	D/T	N rpm	
Foust et al [33] 1944	$E_G \propto \left(P_g/V\right)^{0.47} V_s$	Level detector	Water	Air	Arrowhead Turbine (6-10 bladdes)	4 Orifices	0.51 to 2.54	30.2 to 2450	0.33 to 0.2	85 to 854	
Calder-bank [11] 1958	$E_G = [A] + [B\ C\ D]$ $A = \left\{\frac{V_s\ E_G}{U_T}\right\}^{0.5}$ $B = 2.16 \times 10^{-2}$ $C = \left\{\frac{(P_g/V)^{0.4}\ \rho^{0.2}}{\sigma^{0.6}}\right\}$ $D = \left\{\frac{V_s}{U_T}\right\}^{0.5}$	Inclined Mano-meter	Water, EtOH, CCl_4, Toluene, Nitro-benzene	Air	6 blade Turbine	1 Orifice ϕ = 3.18×10^{-3} m	0.30 to 1.83	20.1 to 51.2	0.33		At high rates of power dissipation the correlation reduces to: $E_G \propto (P_g/V)^{0.4} V_s^{0.5}$ i.e similar to Foust et al

Table 5.1 : (cont) Correlations for Gas Holdup

Reference	Correlation	Method	SYSTEM		Agitator Type	Sparger	Experimental Conditions				Remarks
			Liquid	Gas			V_s cms^{-1}	T cm	D/T	N rpm	
Yoshida & Miura [30] 1963	$E_G \propto N^{0.8} D^{1.2} V_s^{0.75}$ For glycerol	Inclined mano-meter	NaOH, Water, Glycerol	CO_2	Winged disc turbine 12-16 blades	1 orifice, ϕ = 4-8-12 x 10^{-3} m	0.17 to 0.76	25.2 39.4 58.8	0.4	60 to 350	For NaOH and water systems the exponent of V_s was between 0.49-0.61 and for N - 0.8-0.6
Rushton and Bimbinet [32] 1968	$\frac{E_G}{1 - E_G} = C_1 \left\{\frac{P_{gt}}{V}\right\}^{C_2} V_s^{0.6}$ where C_1 & C_2 depend on D & T	Level detector	Water Water + syrup	Air	6 blade turbine		0 - 3	22.9, 30.5, 45.7, 61.0, 91.4	0.177 to 0.53		

Table 5.1 : (cont) Correlations for Gas Holdup

Reference	Correlation	Method	SYSTEM		Agitator Type	Sparger	Experimental Conditions				Remarks
			Liquid	Gas			V_s cms^{-1}	T cm	D/T	N rpm	
Van Dieren-donck [54] 1968	$E_G = [A\,B] + \frac{[C]}{2.3}$ $A = 0.31\left\{\frac{\mu V_s}{\sigma}\right\}$ $B = \left\{\frac{\rho\sigma}{g\mu^4}\right\}^{1/6}$ $C = \frac{0.45(N-N^*)\,D^2}{T(gT)^{0.5}}$	Liquid Level	Water, EtOH, cyclo-hexane, salt sol^{ns} in organic liquids	Air N_2 H_2	6 blade turbine		0.8 - 5	17 to 45	0.31 to 0.55	2440	
Miller [62] 1974	$E_G = A + [B\,C\,D]$ $A = \left\{\frac{V_s E_G}{V_s + U_t}\right\}^{0.5}$ $B = 2.16 \times 10^{4}$ $C = \left\{\frac{P_{gt}/V)^{0.4}\rho^{0.2}}{\sigma^{0.6}}\right\}$ $D = \left\{\frac{V_s}{V_s + U_t}\right\}^{0.5}$	Liquid level	Water	Air	4 flat blades	Variable	0.76 to 2.54	.1524m 0.305m 0.686m	0.67	170 to 420 103 to 420 25 to 168	Modification of Calderbank's correlation for high gas sparging rates.

Table 5.1 : (cont) Correlations for Gas Holdup

Reference	Correlation	Method	SYSTEM		Agitator Type	Sparger	Experimental Conditions				Remarks
			Liquid	Gas			V_s cms^{-1}	T cm	D/T	N rpm	
Hassan & Robinson [20] 1977	$E_G = C_3\left\{\frac{QN^2}{g}\right\}^{C_4}$ C_3 & C_4 depend on impeller type and the nature of the aqueous electrolyte.	Liquid Level	Water, ethylene glycol, glycerol, and solutions of Na_2SO_4	Air	Flat blade turbine 4 - 6 blades	2 Orifices 3.17 x 10^{-3} m 5.95 x 10^{-3} m	0.35 to 6.8 0.5 to 2.21	0.152m 0.291m	1/3 and 2/3	5 - 35	
Machon et al [34] 1977	$E_G = [A\ B\ C\ D]$ $A = 1.34 \times 10^{-4}$ $B = \left\{\frac{N^2 D^3 \rho}{\sigma}\right\}^{0.86}$ $C = \left\{\frac{Q}{ND^3}\right\}$ $D = \left\{2 - \exp(-\psi/\psi_{int})\right\}^{0.56}$ where ψ = coalescence rate charactistic defined by Lee & Meyrick [35]	Liquid Level	ionic solutions	Air	6 blade turbine	1 Orifice 4 x 10^{-3} m dia.	0.18 to 0.53	0.29m	0.26	350 450 550	

Table 5.1 : (cont) Correlations for Gas Holdup

Reference	Correlation	Method	SYSTEM		Agitator Type	Sparger	Experimental Conditions				Remarks
			Liquid	Gas			V_s cms^{-1}	T cm	D/T	N rpm	
Loiseau et al [17] 1977	$E_G = [A\ B\ C]^{0.36}$ $A = 0.011\left\{\frac{V_s}{g}\right\}$ $B = \left\{\frac{1}{\mu^{0.056}}\right\}$ $C = \left\{\frac{P_{gt}}{V_L}\right\}^{0.27}$	Liquid overflow	Water, EtOH, glycol, sugar sol^n, sodium sulphate	Air	2 turbines 6 blades	Open tube (.8cm dia.) perforated ring (30 holes @ 0.1 cm) porous ring (6 cm dia.)	0.74 to 1.98	0.22m	0.33	300 700	
Roustan [63] 1978	$\frac{E_G}{1 - E_G} = A + [B]$ $A = 4.0\,V_s^{0.72}$ $B = 1.75\,Q^{0.6}\left\{\frac{D}{T}\right\}(N - N_R)$		Water	Air	turbines 6 -12 blades	dia. 1×10^{-3} m	0.5 - 2.4	1.0m	0.4	240 to 1400	

Table 5.1 : (cont) Correlations for Gas Holdup

Reference	Correlation	Method	SYSTEM		Agitator Type	Sparger	Experimental Conditions				Remarks
			Liquid	Gas			V_s cms^{-1}	T cm	D/T	N rpm	
Figuereido & Calderbank [29] 1978	$E_G = [A\ B]$ $A = 0.23 \left\{\frac{P_{gt}}{V}\right\}^{0.26}$ $B = V_s^{0.68}$	Inclined manometer	Water	Air	6 blade turbine		0.63 to 1.27	0.915	0.3		
Yung et al [18] 1979	$E_G = [A\ B]$ $A = 0.0052 \left\{\frac{Q}{ND^3}\right\}^{0.5}$ $B = We^{0.65} \left\{\frac{D}{T}\right\}^{1.4}$	Inclined manometer	Water, glycol, ethylene, toluene	Air	6 blade turbine			0.4			
Bottom et at [64] 1980	$E_G = \left\{\frac{V_p}{V_{pf}}\right\}^{C_5}$ where V_p = Tip velocity of stirrer C_5 depends on the ratio of V_s / V_{sf} where V_{sf} is a fictitious value of V_s at E_G = 1.0	Liquid level	Water water+ Glycol (50% wt)	Air	6 bladed turbine (Rushton)	Perforated with a diameter of 0.2T. Diameter of holes 1,2 & 2.5mm depending on T.	< 10.0	0.085 0.12 0.25 0.6	0.5 0.3		Impeller clearence : T/3

Table 5.1 : (cont) Correlations for Gas Holdup

Reference	Correlation	Method	SYSTEM		Agitator Type	Sparger	Experimental Conditions				Remarks
			Liquid	Gas			V_s cms^{-1}	T cm	D/T	N rpm	
Sridhar and Potter [40] 1980	$E_G = [A] + [B\ A\ D\ C]$ $A = \left\{\frac{V_s}{U_T}\right\}^{1/2}$ $B = 0.0216\left\{\frac{(P_g/V)^{0.4}\rho^{0.2}}{\sigma^{0.6}}\right\}$ $C = \left\{\frac{P_{gt}}{P_g}\right\}$ $D = \left\{\frac{\rho_g}{\rho_a}\right\}^{0.16}$	Mano-meter	Cyclo-hexane	Air	6 bladed turbine	Single Orifice 6mm ø	< 3.2	0.13	0.3	1250 to 1450	
Econo-mides [6] 1981	$E_G = 6.6\left\{\frac{P}{V}\right\}^{0.4} Q^{0.58}$	Liquid level	Water	Air	6 bladed turbines (Rushton)	10 orifices on $\frac{1}{8}$" O.D. tube. ø of holes = 0.5mm	.274 to 2.5	0.2	0.25 0.33 0.625	240 to 550	Impeller clearance ratio $C/H = 1/3$

Table 5.1 : (cont) Correlations for Gas Holdup

Reference	Correlation	Method	SYSTEM		Agitator Type	Sparger	Experimental Conditions				Remarks
			Liquid	Gas			V_s cms^{-1}	T cm	D/T	N rpm	
Sridhar and Potter [40] 1980	$E_G = [A] + [B\ A\ D\ C]$ $A = \left\{\frac{V_s}{U_T}\right\}^{1/2}$ $B = 0.0216\left\{\frac{(P_g/V)^{0.4}\rho^{0.2}}{\sigma^{0.6}}\right\}$ $C = \left\{\frac{P_{gt}}{P_g}\right\}$ $D = \left\{\frac{\rho_g}{\rho_a}\right\}^{0.16}$	Mano-meter	Cyclo-hexane	Air	6 bladed turbine	Single Orifice 6mm ø	< 3.2	0.13	0.3	1250 to 1450	
Econo-mides [6] 1981	$E_G = 6.6\left\{\frac{P}{V}\right\}^{0.4} Q^{0.58}$	Liquid level	Water	Air	6 bladed turbines (Rushton)	10 orifices on $\frac{1}{8}$" O.D. tube. ø of holes = 0.5mm	.274 to 2.5	0.2	0.25 0.33 0.625	240 to 550	Impeller clearance ratio $C/H = \frac{1}{3}$

Table 5.1 : (cont) Correlations for Gas Holdup

Reference	Correlation	Method	SYSTEM		Agitator Type	Sparger	Experimental Conditions				Remarks
			Liquid	Gas			V_s cms^{-1}	T cm	D/T	N rpm	
Chapman [65] 1981	$E_G = 17.9 \left\{\frac{P}{V}\right\}^{0.31} V_s^{0.67}$	Liquid level measured mid-way between two baffles	Water	Air	6 blade disc turbine 4 angled blade disc turbine 4 MFD, 6 MFD 3 blade marine propeller	Single Orifice	0.25 to 1 vvm	0.29 0.3 0.91 1.83 0.56	0.25 0.5 0.33 * used in T = 0.56m	< 960*	Impeller clearance ratio $C/_H = 1/_4$ * Most results obtained in T = 0.56m
Kobbacy [7] 1981	$E_G = [A\ B\ C]$ $A = 0.051\left\{\frac{P_{gt}}{V}\right\}^{0.36}$ $B = V_s^{0.27}\left\{\frac{D}{T}\right\}^{0.85}$ $C = \left\{\frac{P}{P_a}\right\}^{0.15}$	Liquid level	Water 0.11M potass-ium sulphate sol^n	Air	6 blade turbines (Rushton)	5 orifices in $1/_8$" dia. tube. ϕ of holes = 1.2mm	0.26 to 1.231	0.2	0.25 0.33 0.625	60 to 1200	Incorporates the effects of vessel pressure. Impeller clearacne ratio $C/_H = 1/_4$

Table 5.1 : (cont) Correlations for Gas Holdup

Reference	Correlation	Method	SYSTEM		Agitator Type	Sparger	Experimental Conditions				Remarks
			Liquid	Gas			V_s cms^{-1}	T cm	D/T	N rpm	
Barigou [5] 1987	$E_G = [A\,B]$ $A = 4.07N^{0.62}$ $B = Q^{0.64}\left[\frac{D}{T}\right]^{1.39}$ $A = 4.20N^{0.79}$ $B = Q^{0.52}\left[\frac{D}{T}\right]^{1.92}$	Liquid level	Air - Water Air - NaCl		6 blade turbines (Rushton)	Single orifice	0.21 to 1.06	1.0	0.25 0.33 0.5	40 to 500	

The exponent of U_{∞} ranges from 0.27 and 0.68, and commonly is about 0.5.

Lee and Mayrick [35] have shown that in electrolytic solutions, a new quantity can be introduced:

$$\Psi = c\left(\frac{d\sigma}{dc}\right)\phi \qquad (5.3)$$

where, c is the molar concentration and ϕ is defined as

$$\phi = \left(1 + \frac{d\ln f}{d\ln c}\right)^{-1} \qquad (5.4)$$

where, f is the activity coefficient.

Machon et al [34] correlated the gas holdup with the quantity Ψ in Equation 5.3, the gas flow and the Weber number, yielding a dimensionless equation with constants depending on the geometry of the apparatus. Machon et at [34] measured the gas holdup in various

electrolytes for a number of concentrations and a range of impeller speeds and gas flow rates. They found that with increasing value of the quantity Ψ, the gas holdup increased up to a certain value and then remained constant. The critical value of Ψ_{cr} was estimated to be 3×10^{-6} $kg^2 kmol^{-1} m^3 s^{-4}$.

Sridhar and Potter [31] studied the effect of vessel pressure on gas holdup and expressed the effect of pressure at high power inputs as:

$$E_G \propto (P / P_A)^{0.16} \qquad (5.5)$$

where P = vessel pressure

P_A = atmosheric pressure

Loiseau et al [17] found a dependence of viscosity on gas holdup, however, most other workers report a negligible effect up to a viscosity of 100 cp.

Hassan and Robinson [20] found that the exponent and the constant in their correlation depended on the type of the impeller and the nature of the aqueous electrolyte.

Results of Clark and Vermeulen [19] give the influence of a distributor covering the agitator. For a perforated plate covering the total cross section of the vessel, they proposed the relatively complex correlation:

$$\frac{E_G}{1 - E_G} = \left\{\frac{E_G}{1 - E_G}\right\}_O + \Delta\left\{\frac{E_G}{1 - E_G}\right\} \qquad (5.6)$$

where the increment Δ due to agitation is a function of U_m, We, P_g/P_o and the geometric factor.

Many investigators [5, 18, 20, 30, 34, 54 & 63] have correlated the total gas holdup with independent variables and the physical properties of the gas-liquid systems. The exponents of the independent variables, N, Q, D & T are given in Table 5.2.

$$E_G \propto N^a Q^b D^c T^d \qquad (5.7)$$

The most consistant factor among these correlations in Table 5.2 is the exponent on Q, which ranges from 0.5 to 0.75 for air-water systems and 0.36 to 0.52 for ionic solutions. The wide spread disagreement amongst these correlations, (Table 5.2) may be the result of the

Table 5.2 : Exponents of Equation 5.7

Author	a	b	c	d	
Yoshida & Miura [30]	0.8	0.75	-0.3	-	AIR WATER
Hassan & Robinson [20]	1.14	0.57	-	-	
Yung et al [18]	1.8	0.5	1.85	-1.4	
Barigou [5]	0.62	0.64	1.39	-1.39	
Machon et al [34]	1.64	0.36	1.2	-	IONIC SOLUTIONS
Hassan & Robinson [20]	0.88	0.44	-	-	
Yung et al [18]	0.8	0.5	1.4	-	
Barigou [5]	0.79	0.52	1.92	1.92	

differing techniques of gas holdup measurement and also different vessel and impeller configurations employed.

5.4 Results and Discussion

Total gas holdup measurements for T_{21}, T_{75}, and T_{100} are given in Figures 5.1 to 5.7. Each plot illustrates the effect of increasing the impeller speed and the sparged gas flow rate, Q.

The effect of varying the liquid level from a value of H = T to H = 1.2*T on the total gas holdup was investigated in T_{75} for D/T = 0.333, as shown in Figures 5.2 and 5.3. For a particular gas flow rate at low impeller speeds, the total gas holdup is higher for H = 1.2*T than H = T. However, for higher impeller speeds the total gas holdup is lower for H = 1.2*T compared with H = T. This can be explained by surface aeration effect. Greaves & Kobbacy [68], Clark & Vermeulen [66] and Sawant & Joshi [67] have found that the critical impeller speed for the onset of surface aeration is dependent on the liquid height above the impeller. Thus, surface aeration at higher impeller speeds is more

Figure 5.1 : Gas Holdup Against Impeller Speed
Impeller Type : 6FBDT. Impeller Dia. : 0.188 m.
H = T = 0.75 m.

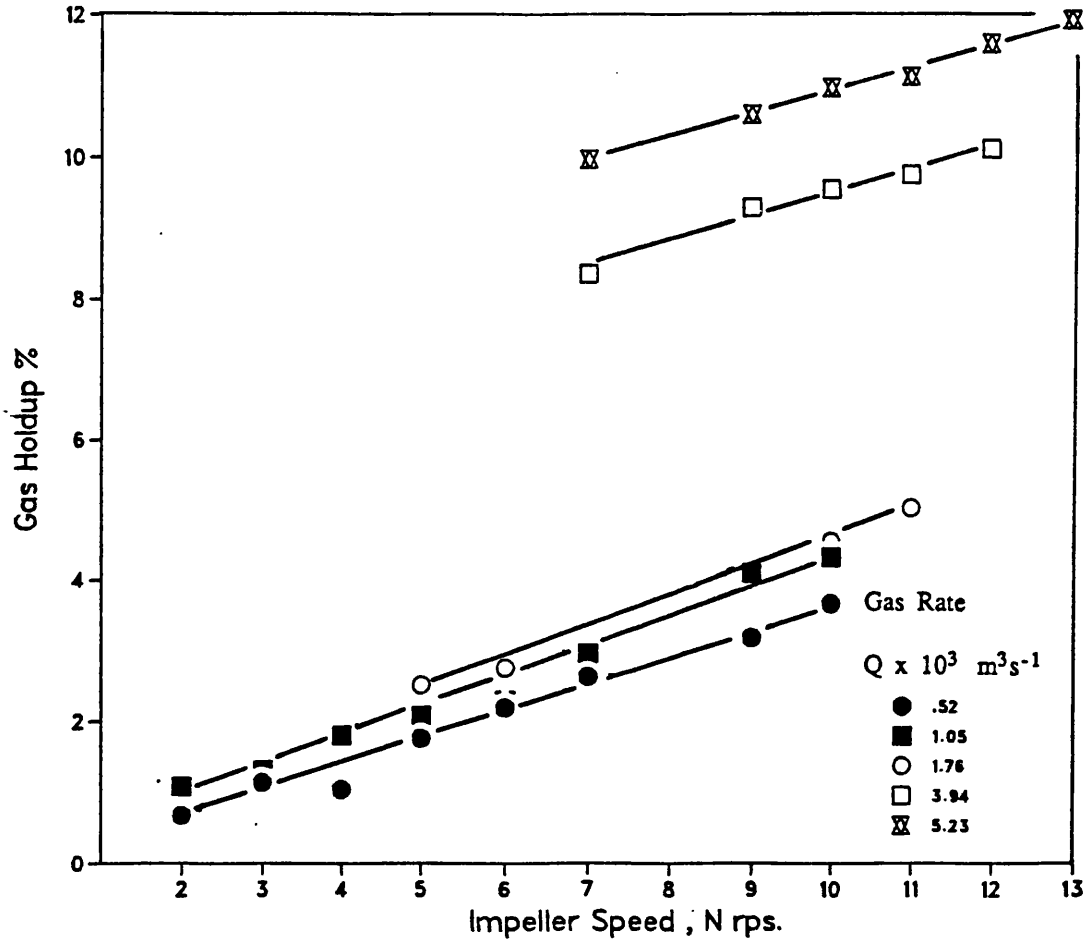

Figure 5.2 : Gas Holdup Against Impeller Speed
Impeller Type : 6FBDT. Impeller Dia. : 0.25 m.
H = T = 0.75 m.

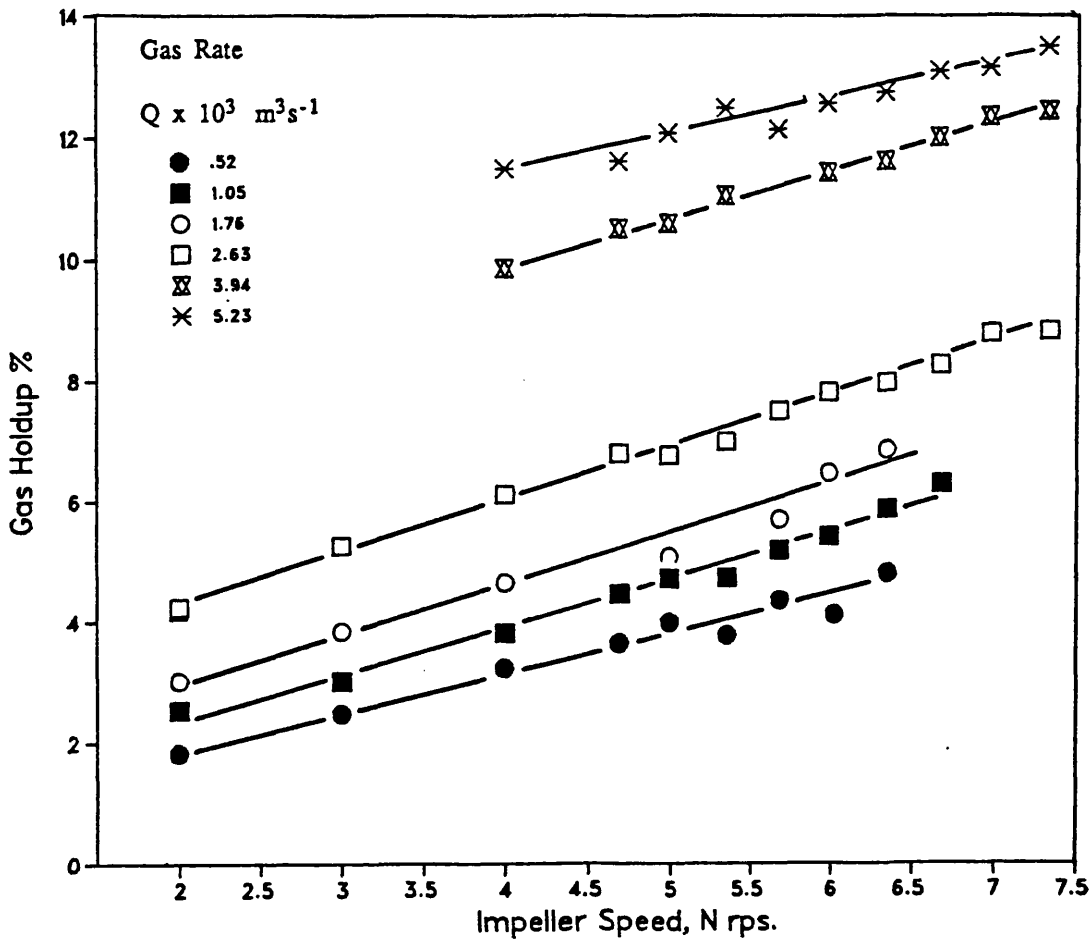

Figure 5.3 : Gas Holdup Against Impeller Speed
Impeller Type : 6FBDT. Impeller Dia. : 0.25 m.
T = 0.75 m. H = 1.2*T

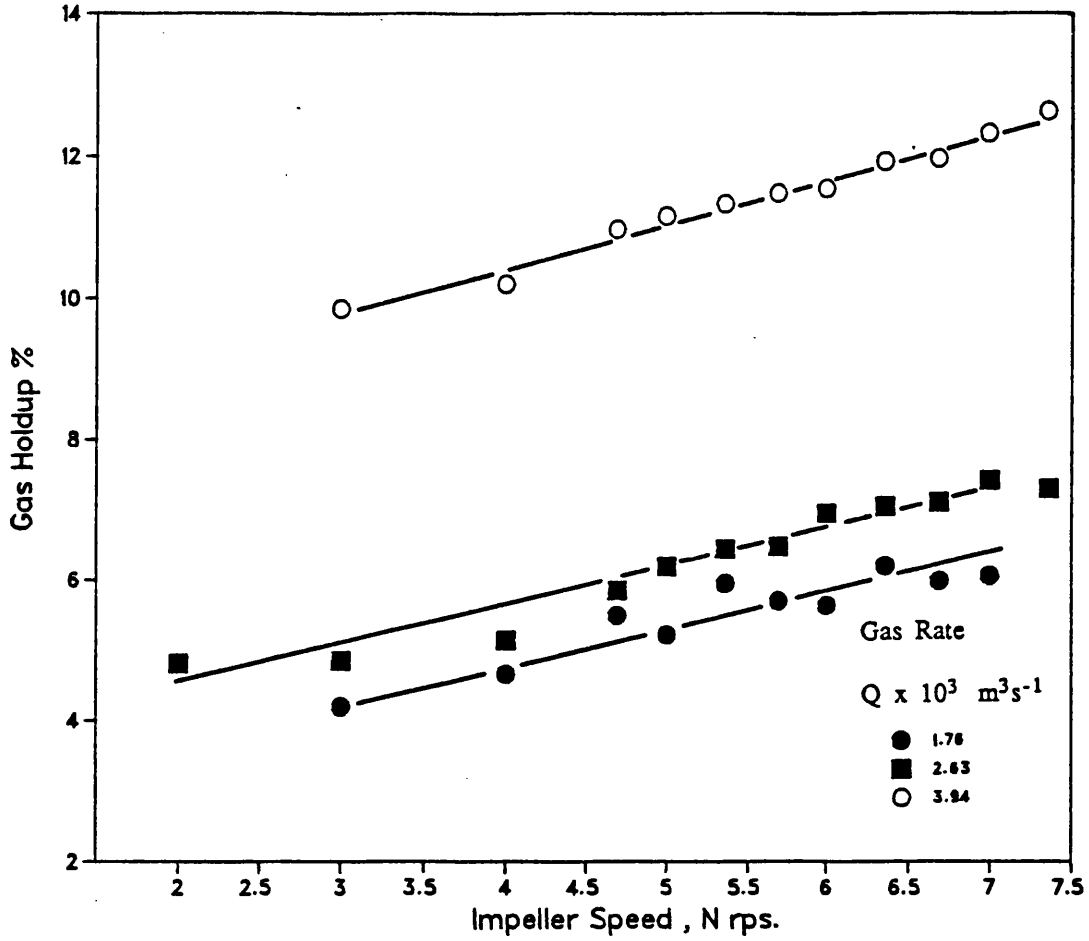

Figure 5.4 : Gas Holdup Against Impeller Speed
Impeller Type : 6FBDT. Impeller Dia. : 0.376 m.
H = T = 0.75 m.

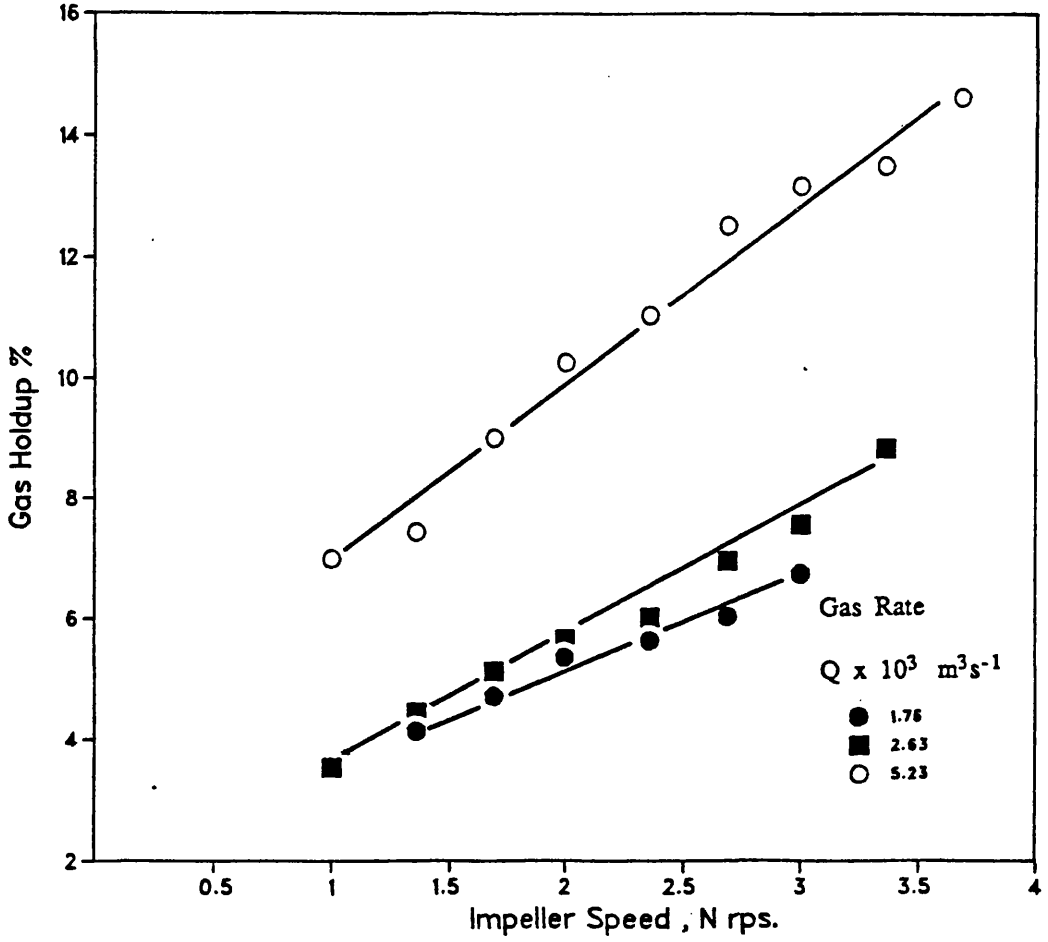

Figure 5.5 : Gas Holdup Against Impeller Speed
Impeller Type : 6FBT. Impeller Dia. : 0.252 m.
H = T = 0.75 m.

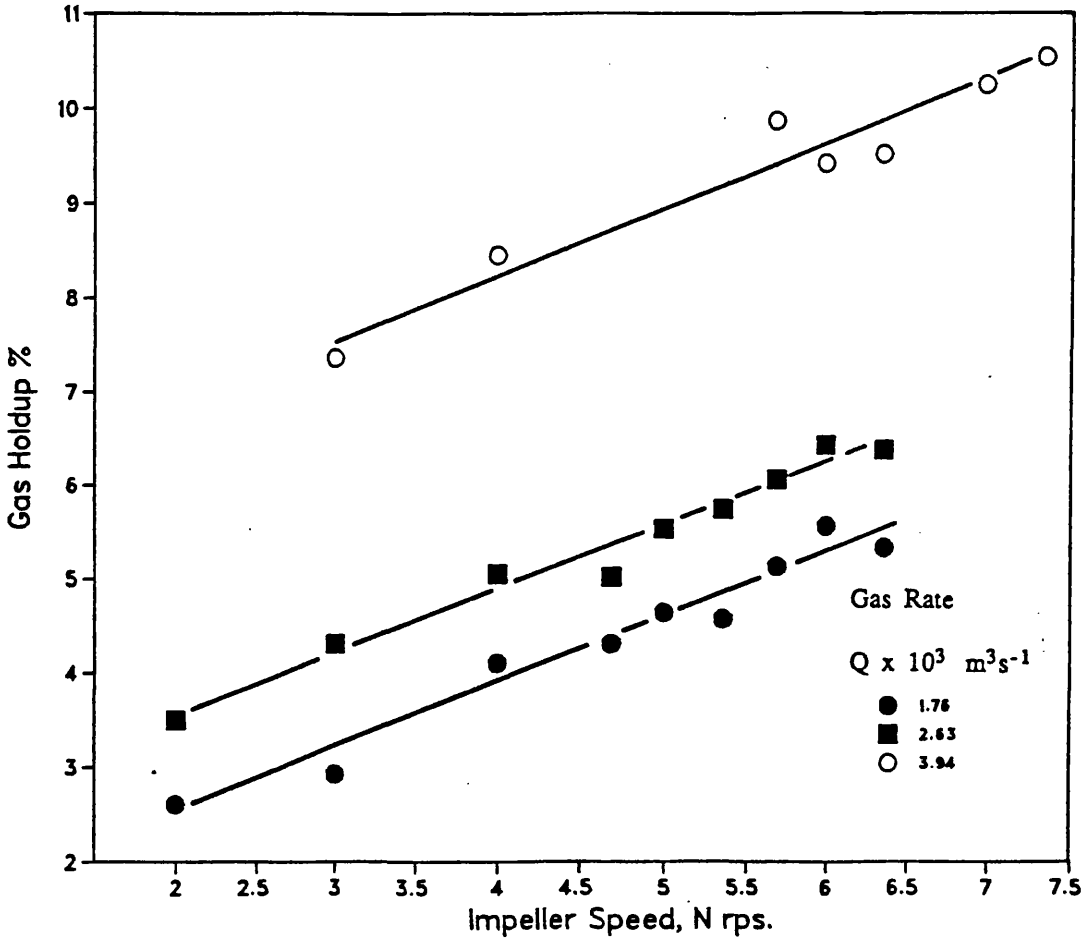

Figure 5.6 : Gas Holdup Against Impeller Speed
Impeller Type : 6FBDT. Impeller Dia. : 0.333 m.
H = T = 1.00 m.

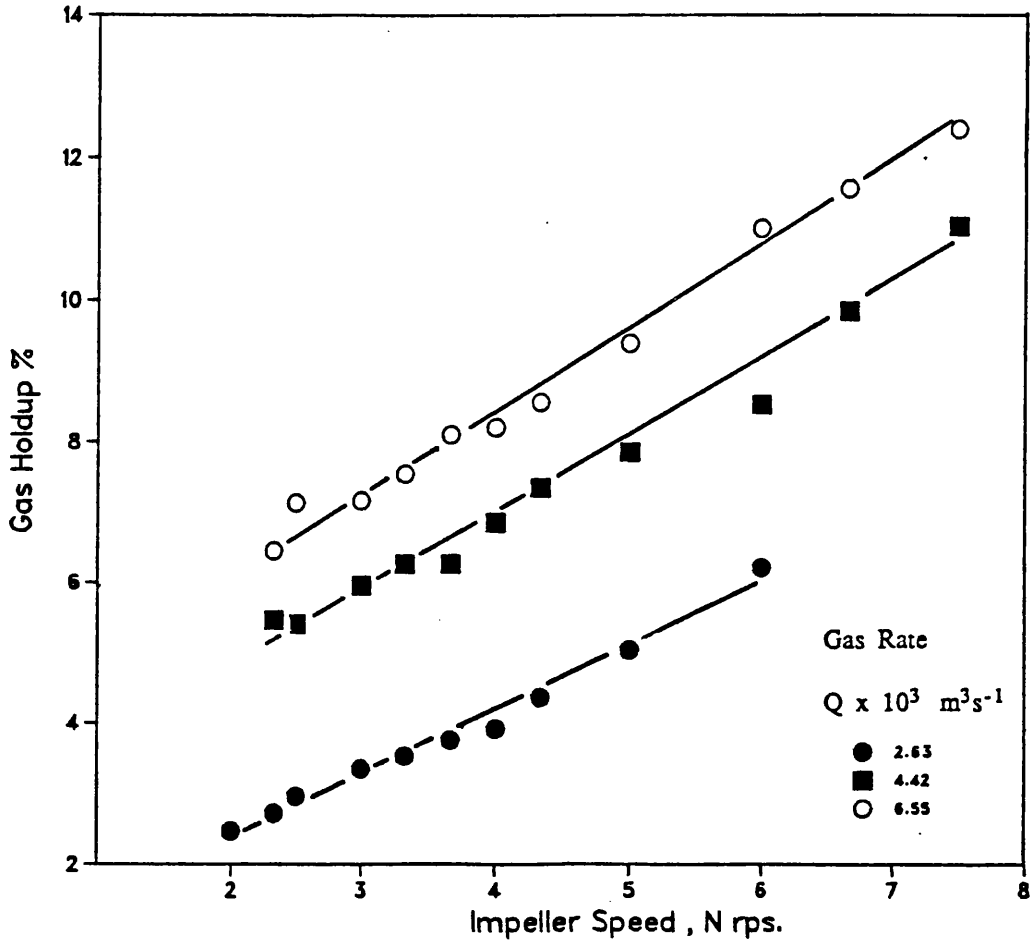

Figure 5.7 : Gas Holdup Against Impeller Speed
Impeller Type : 6FBDT. Impeller Dia. : 0.0675 m.
H = T = 0.21 m.

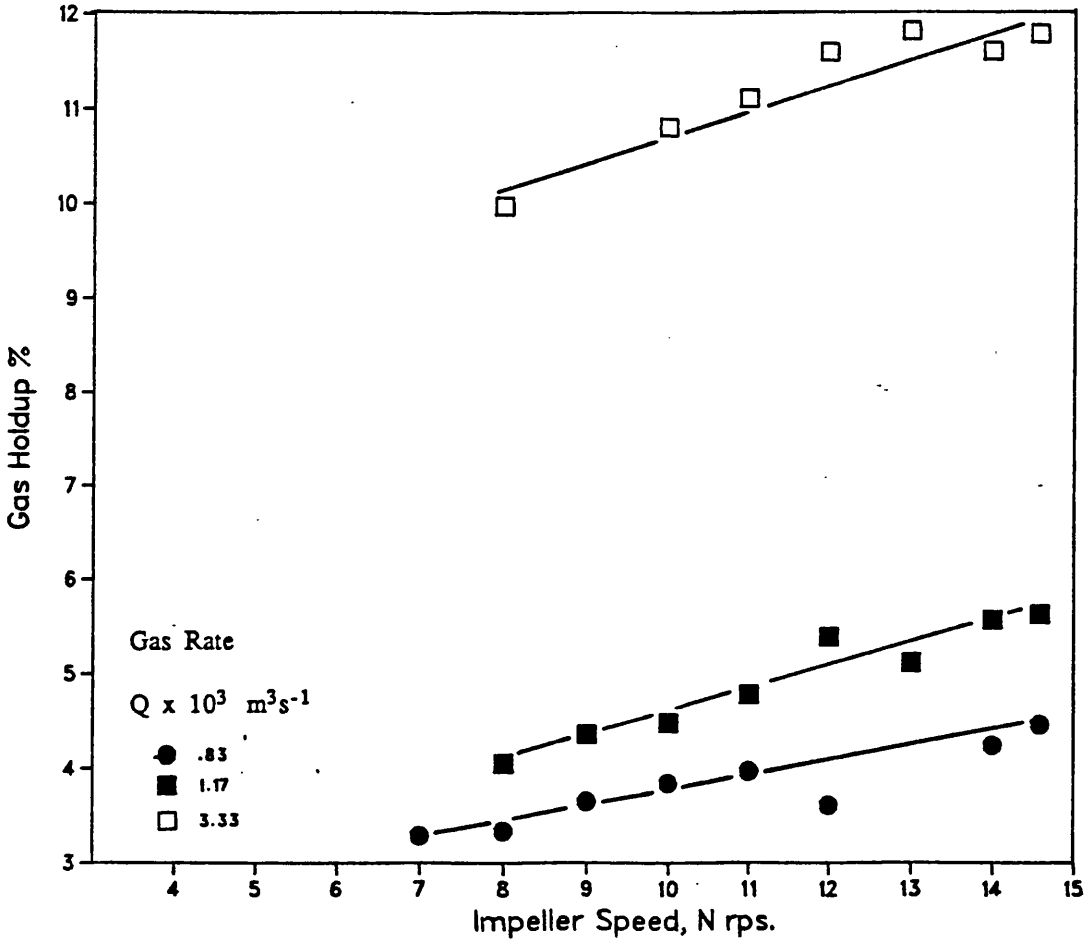

significant for H = T than for H = 1.2*T, resulting in a higher gas holdup for H = T. However, at the highest gas flow rate investigated, Q = 0.00394 m^3s^{-1}, the total gas holdup was almost the same when high impeller speeds were used. Nienow et al [47] have reported that surface aeration decreases very rapidly with increase in gas flow rate. The effect of the liquid height above the impeller is therefore diminished at high gas flow rate. The present results confirm the findings of these investigators [47, 66, 67 & 68].

The effect of impeller type on the total gas holdup was investigated in T7S using a standard Rushton turbine (6FBDT, D = 0.25 m.) and a 6-flat blade paddle (6FBT, D = 0.252 m.). The results are shown in Figures 5.2 and 5.5 respectively. The total gas holdup for the 6FBT is lower compared with the results for 6FBDT. The 6-flat blade paddle therefore has a much lower gas handling capacity than the standard Rushton turbine.

Plots of total gas holdup against the Flow Number in Figures 5.8 to 5.14 show that the total gas holdup increases more rapidly with increase in the impeller speed below a certain Flow Number. This may well be the result of gas recirculation and is discussed in detail in Chapter 7.

Figure 5.8 : Gas Holdup Against Flow Number
Impeller Type : 6FBDT. Impeller Dia. : 0.188 m.
H = T = 0.75 m.

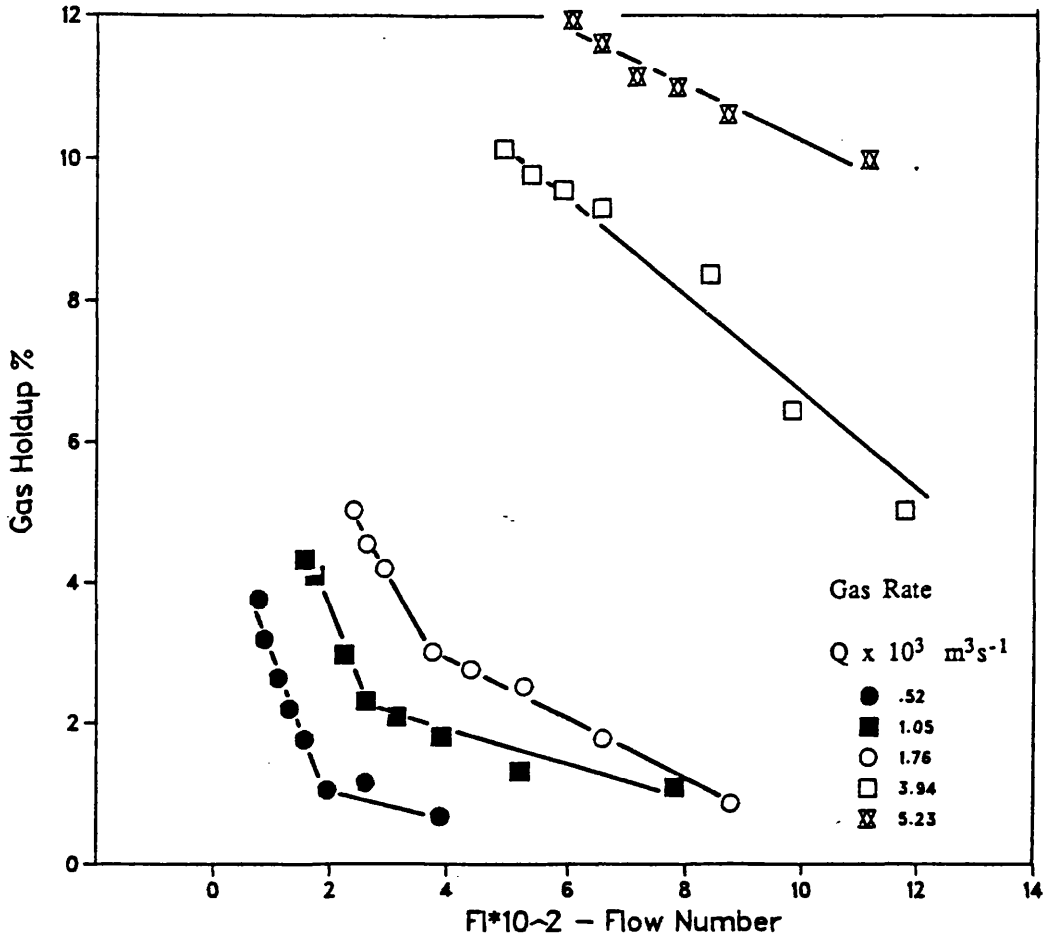

Figure 5.9 : Gas Holdup Against Flow Number
Impeller Type : 6FBDT. Impeller Dia. : 0.25 m.
H = T = 0.75 m.

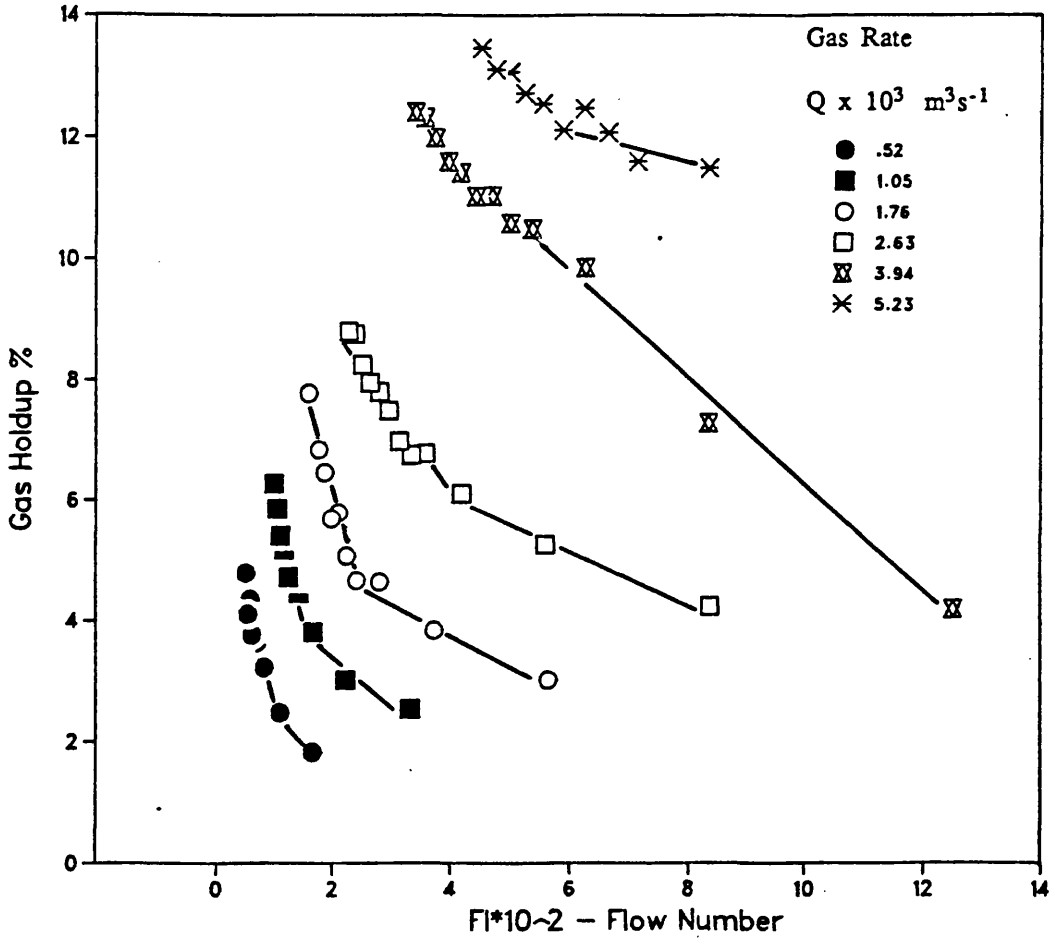

Figure 5.10 : Gas Holdup Against Flow Number
Impeller Type : 6FBDT. Impeller Dia. : 0.376 m.
H = T = 0.75 m.

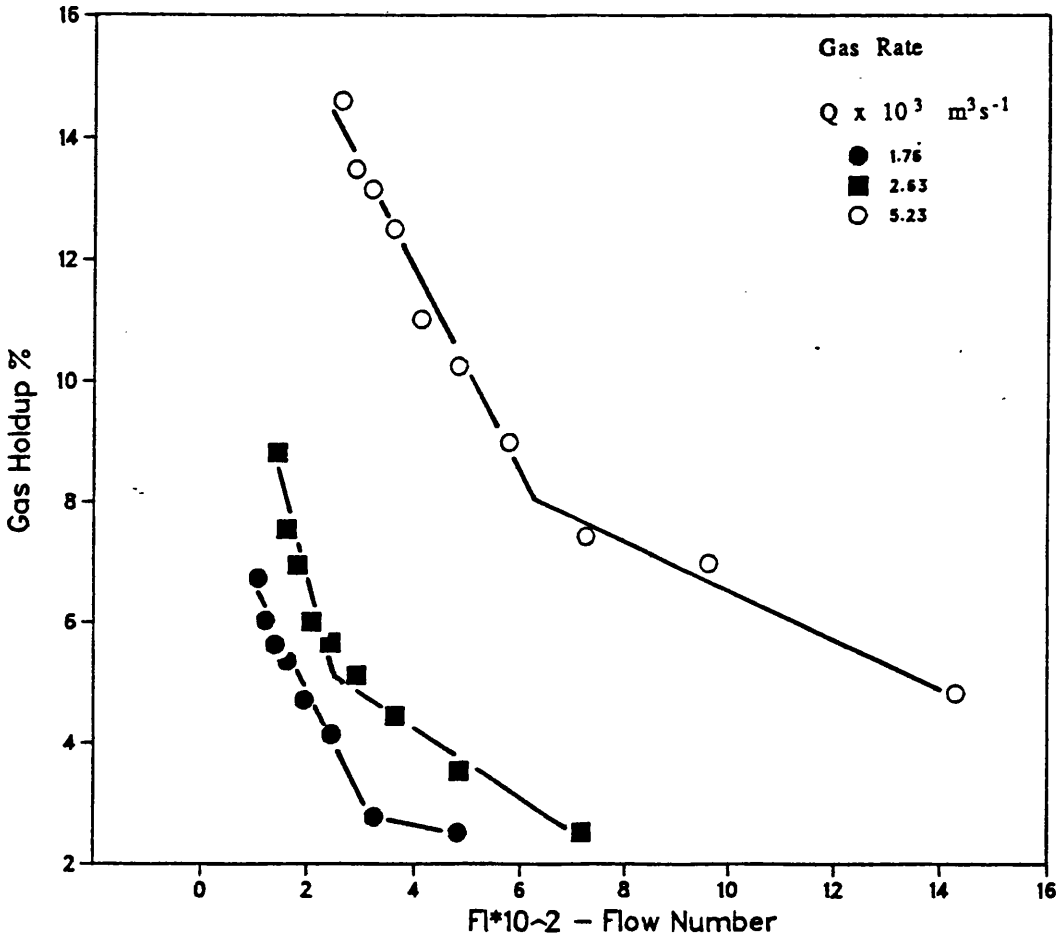

Figure 5.11 : Gas Holdup Against Flow Number
Impeller Type : 6FBT. Impeller Dia. : 0.252 m.
H = T = 0.75 m.

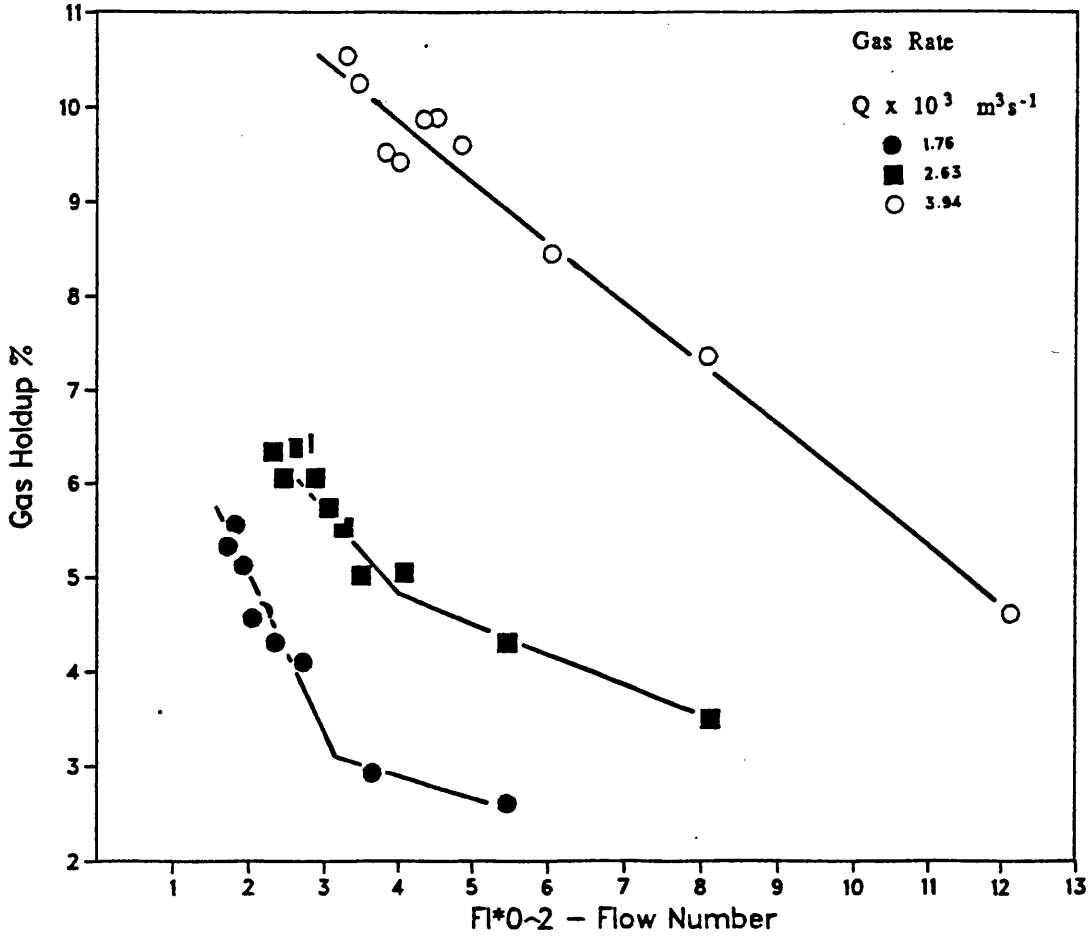

Figure 5.12 : Gas Holdup Against Impeller Speed
Impeller Type : 6FBDT. Impeller Dia. : 0.25 m.
T = 0.75 m. H = 1.2*T

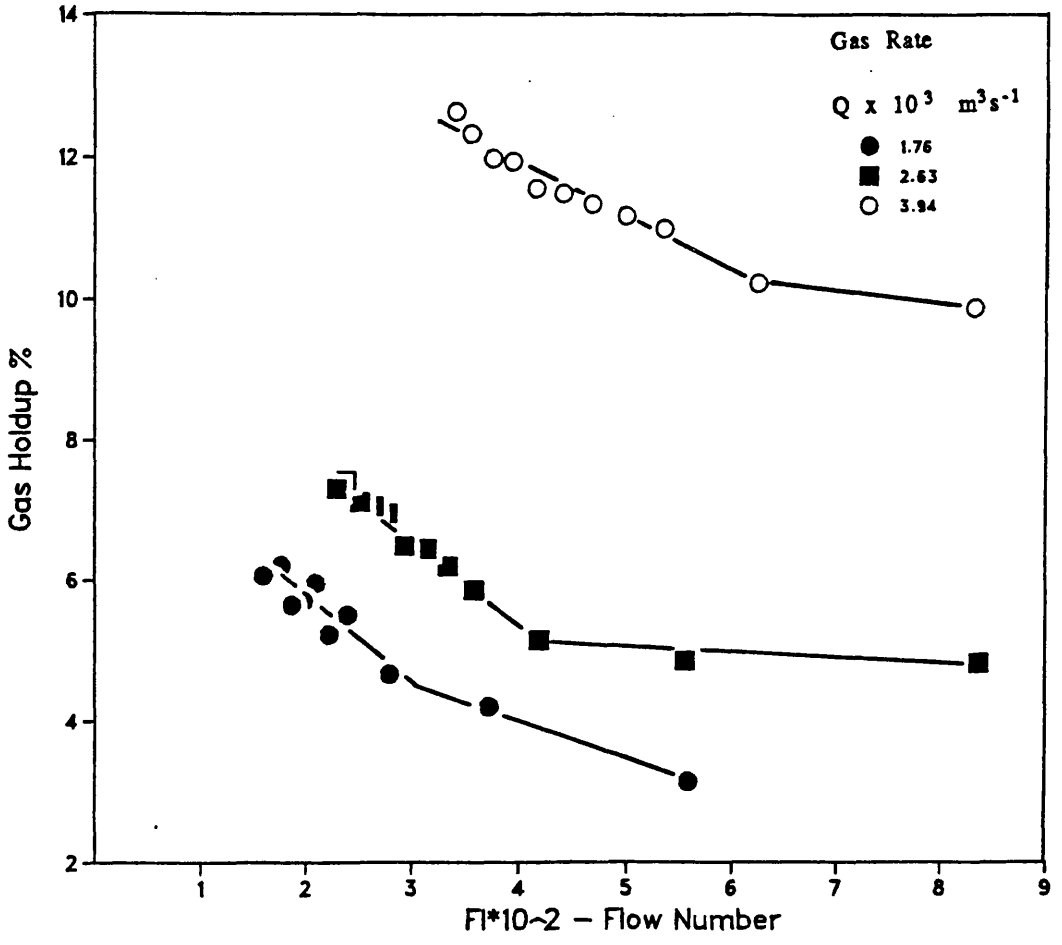

Figure 5.13 : Gas Holdup Against Flow Number
Impeller Type : 6FBDT. Impeller Dia. : 0.333 m.
H = T = 1.00 m.

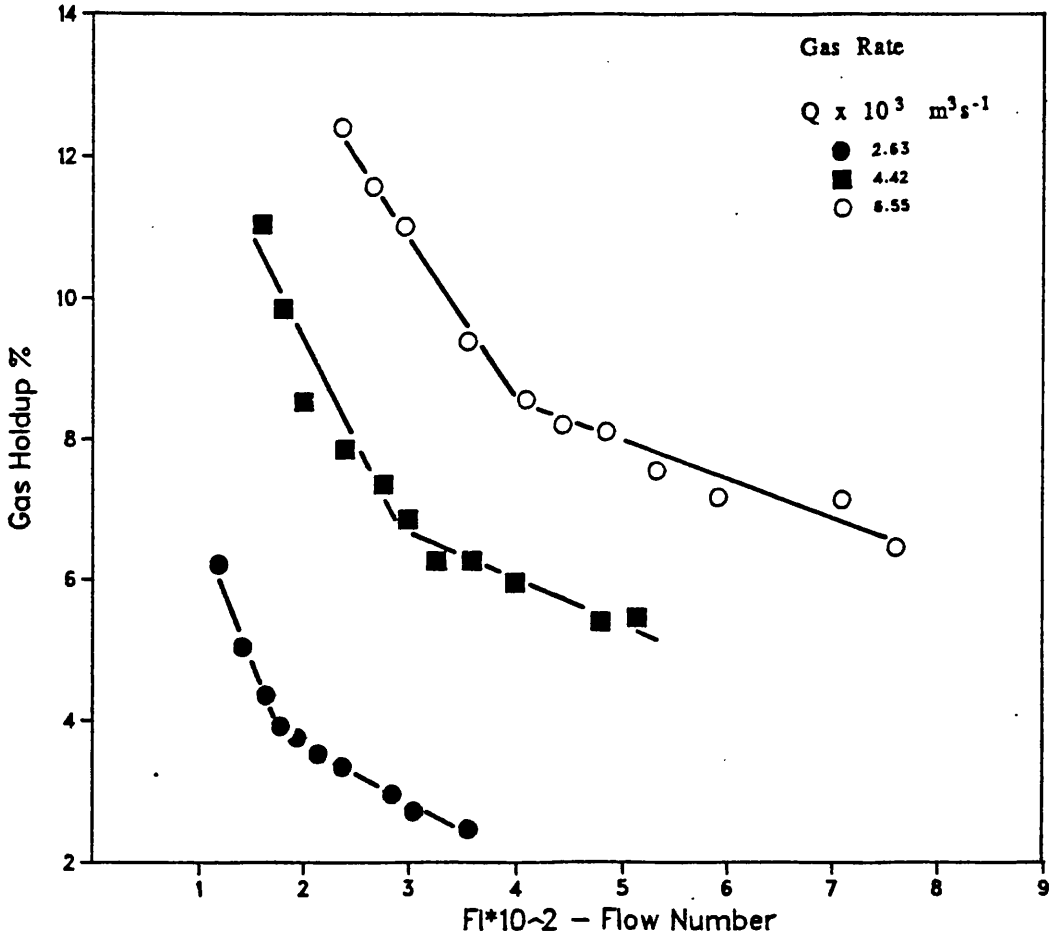

Figure 5.14 : Gas Holdup Against Flow Number
Impeller Type : 6FBDT. Impeller Dia.: 0.0675 m.
H = T = 0.21 m.

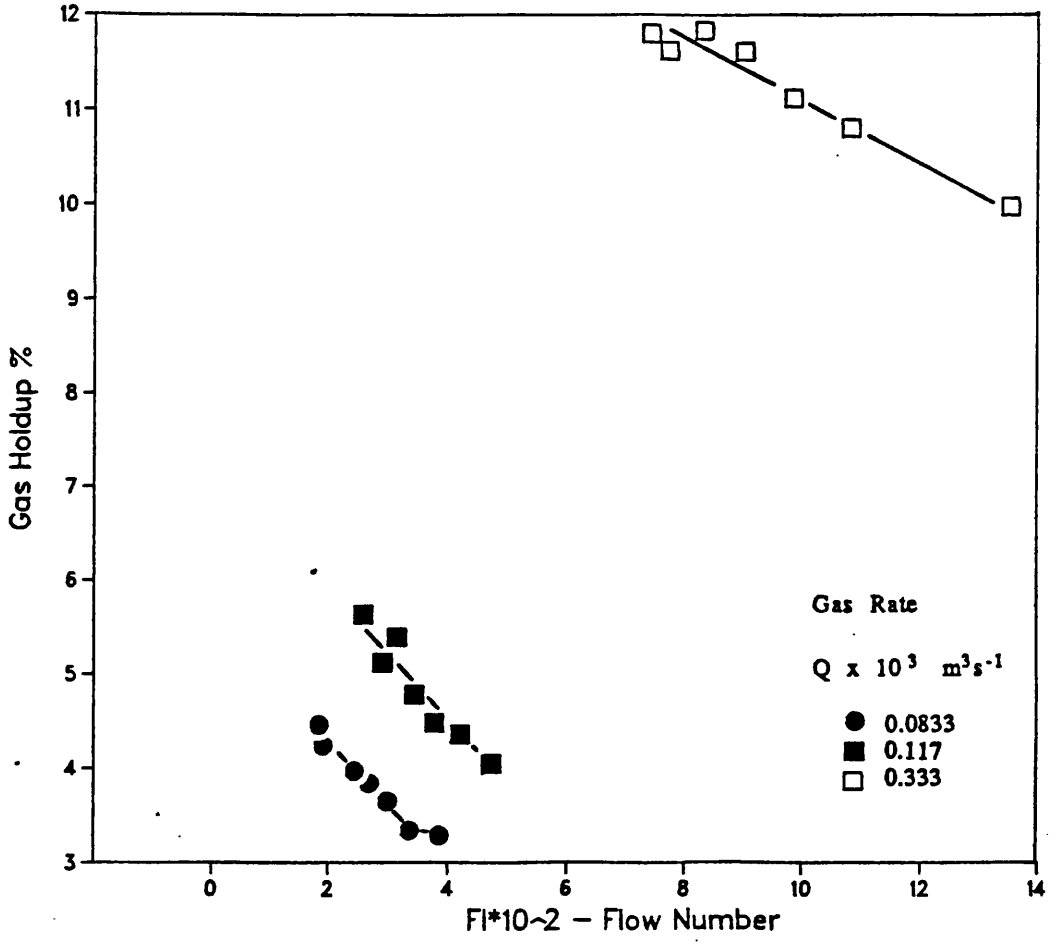

Total gas holdup measurements for the air-water system in T_{21}, T_{75} & T_{100} were correlated with the independent variables, N, Q, D and T, representing 240 measurements. Data for H = 1.2 * T were not included in the correlation due to the deviation from the standard configuration. Equation 5.8 was obtained using non-linear least square regression analysis. All the variables are highly significant.

$$E_G = \frac{290\, N^{0.76}\, Q^{0.53}\, [D/T]^{2.55}}{D^{0.7}} \qquad (5.8)$$

where, the coefficient of determination, r = 0.97

the standard deviation, s = 0.21

The correlation of Equation (5.8) is plotted on Figure 5.15. The data scatter is ± 20% which is within the acceptable range.

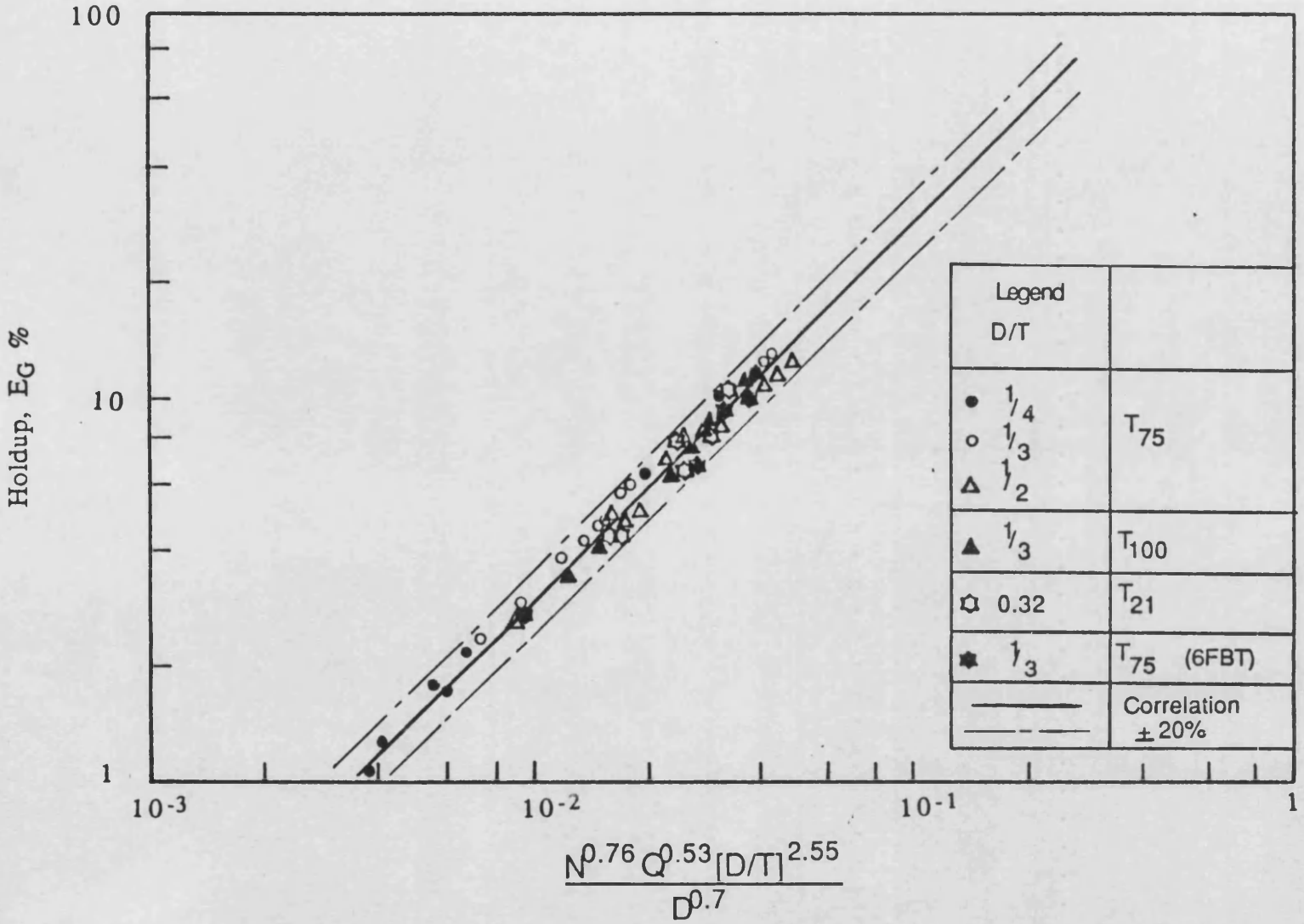

Figure 5.15: Total Gas Holdup : Air-Water System

The correlation proposed by Yoshida & Miura [30] was obtained using curved disc turbines with 12 and 16 blades. Their exponents on N and Q (0.8 & 0.75) compare well with the respective exponents obtained in this study (0.76 & 0.53). However, the exponent value on the impeller diameter, D in their correlation is significantly different compared with Equation 5.8. It has already been pointed out that the type of impeller used affects the total gas holdup (Figures 5.2 & 5.5).

The exponent on Q, 0.57 in Hassan & Robinson's [20] correlation (Table 5.1 & 5.2) for air-water is very close to the one obtained here, 0.53 (Equation 5.8). Their data was obtained with vessels smaller than 0.3 m. diameter. This may well explain the higher significance of N in their equation.

Similarily, Yung et al [18] show a higher significance of N in their equation (Table 5.2) compared with Equation 5.8. Their exponents of Q and D (0.5 & 1.85) are almost identical to the present values (0.53 & 1.85). However, there is a significant difference in the exponents of T of the two studies. Since their measurements were obtained with a single vessel size, the significance of T in their equation is questionable.

Equation 5.8 is in reasonably good agreement with the overall correlation of Barrgou [5] (Table 5.1 & 5.2) with the exception of the significance of the vessel diameter, T. His measurements were obtained using a single vessel, where T = 1.0 m. and consequently his correlation does not reflect the true significance of the tank diameter, T. Barrigou [5] further classified the total gas holdup correlation according to the cavity regime; namely, vortex-clinging and large cavity regime. However, the classified correlations are of little practical value as they require prior knowledge of the existing cavity regimes which is not presently quantified.

5.5 Conclusions.

- The effect of varying the liquid level, from the standard configuration of H = T to H = 1.2 * T, on the total gas holdup is complex due to the surface aeration effect.

- The total gas holdup is dependent on the type of impeller used, so that a 6 flat blade paddle (6FBT), which has a lower gas handling compacity, than a standard Rushton turbine (6FBDT), generates lower gas holdup.

- The effect of increasing N and Q is to increase the total gas holdup.

- Total gas holdup has been correlated in terms of the independent variables N, Q, D & T. The correlation is accurate to within ±20%.

Chapter 6

LOCAL GAS HOLDUP DISTRIBUTION

6.1 Introduction

Knowledge of bubble size and gas holdup distribution in agitated vessels is important for understanding the mechanisms involved in gas phase dispersion processes. The theory of interdispersion of immiscible fluids by turbulent forces has been given by Hinze [36] and Calderbank [37]. Calderbank presented equations for the two cases where the dispersive forces of turbulence are restricted by viscous and surface tension forces. It was further shown that viscous forces may be ignored in the dispersion of gasses in liquids under most conditions. Thus generally, the size of gas bubbles produced and the gas holdup in gas-liquid dispersions are determined by the balance between surface tension forces and those due to turbulent fluctuations.

This chapter deals with the local gas holdup distribution in mechanically stirred vessels. The literature review identifies the need to develop a technique for local gas holdup measurements. The automated technique described in Section 6.3 was developed for measuring point gas holdup in stirred vessels. An extensive study of the local gas holdup distribution in stirred vessels has been made.

6.2 Literature review - Measurement Methods.

6.2.1 Electrical Contact Methods.

When a bubble impinges on an electrically charged wire, there is an instantaneous withdrawal of charge from the surface of the wire which can be recorded electronically. There have been many attempts to make this method work, of which the most successful reported is that of Gardiner [38]. For most systems, it is difficult to avoid the occurence of spurious signals. An electric circuit is closed over a conducting liquid between the needle-probe, which is insulated apart from its tip, and an electrode, sufficiently large not to be affected by gas bubbles. The electric circuit is broken if a gas bubble strikes the tip. The time intervals during which the probe tip is surrounded by gas bubbles are summed up enabling the resultant mean value of the local gas holdup to be determined. Linneweber and Blass [39] used a combination of needle and impedence probes for measurement of the local gas and solids holdup in three phase bubble columns. They reported a measurement error of not less than 17.5 %. The sources of errors, which could not be estimated were:

(a) due to very small bubbles which did not strike the tip of the needle probe and

(b) because only bubbles striking the tip at narrow angles were detected, causing a significant underestimation of the actual gas holdup.

A similar probe was used by Burgess and Calderbank [40] and Figueiredo [41]. The probe only accepts bubbles whose central axis is coincident with the vertical central probe. The local gas holdups were therefore again underestimated. Although they were able to measure single bubbles rising in isolation accurately, such ideal conditions do not exist in agitated vessels, making the application of the probe unsuitable for agitated vessels.

More recently Barigou [5] used an improved conductivity probe tip to measure local gas holdup in a stirred vessel. He reported an error of up to 21 % due to the difficulties associated with this technique.

6.2.2 Photoelectric Probes.

A sterilizable photoelectric probe was developed by Weiland et al [42] for use in fermentation media. A small sample from the dispersion was sucked through a transparent capillary tube in which the

bubbles are transformed to slugs. The length of these slugs is determined by means of two light sensors on the basis of different light absorption in gas and liquid. The length of the slugs are proportional to their volume and hence the length of the slugs can be determined from the time intervals measured by the sensors.

Kobbacy [7] investigated the complex flow pattern of gas slugs travelling in short capillaries and also the effect of the liquid film surrounding the gas bubbles. These effects were not considered by Weiland et al [42]. However, since he used only one sensor to detect the bubbles, errors due to bubble interaction and breakage inside the capillary tube particularly at high bubble concentrations are expected to be significant. Investigation by Barrigou [5] with this method produced very high estimates of gas holdup due to the 'blocking effect' by the gas slug at the capillary probe entrance, i.e. the volume of liquid sampled is reduced.

6.2.3 Other Methods.

Wisdom [43] and Nienow et al [44] measured local gas holdups by withdrawing samples through a capillary tube using a variable speed peristaltic pump.

The amount of liquid in the dispersion was measured after the gas had disengaged

Calderbank [11] measured local gas holdup by withdrawing samples from the dispersion. He used a 6.35 mm. diameter probe. The probe was attached to an evacuated 500 ml. glass bulb sealed with a gas burette. Sampling was performed by operating the stopcock on the glass bulb, the vacuum in the glass bulb providing the suction for withdrawing the dispersion. With the probe removed, the glass bulb was shaken to resaturate the water with air. The volume of the gas in the burette was read at atmospheric pressure.

Clark and Vermeulen [19] measured local gas holdup with a similar technique as the one employed by Calderbank [11] but using a smaller sample of dispersion (30 ml.).

Although these methods are simple to use, they all suffer from certain drawbacks:

(a) they are tedious and time consuming
(b) require continuous sampling [43 &44]
(c) substantial quantities of dispersion are required for volumetric analysis.

Moreover, the local gas holdup is expected to fluctuate about some mean value due to the variation of the mean circulating velocity and the turbulence intensity. This factor was not allowed for in the above investigations [11,19,43 &44].

6.3 Auto - Dispersion Analyser (ADA).

The Auto Dispersion Analyser, referred to as ADA was developed to measure the local gas holdup distribution in a stirred vessel. In contrast to direct volumetric measurement of the gas [11,19,43 & 44], the ADA technique is based on pressure changes, which occur when the dispersion sample is trapped in an isolated chamber. This only requires a small volume of dispersion (of approximately 6 to 7 ml.) to be withdrawn from the stirred vessel. The whole process of sampling and measurement was automated to provide for a rapid method of analysis.

6.3.1 Theory.

The introduction of a sample of gas-liquid dispersion into an isolated collecting chamber (initially at pressure P_1 and volume V_2) causes an increase in the pressure, Figure 6.1. The increase in pressure arises from two causes:

(i) the volume of air in the collected sample and
(ii) the compression effect due to the liquid in the sample. This sequence of effects is illustrated in Figure 6.1.

The following equations can be written from basic thermodynamic principles. At isothermal conditions, the final volume of liquid in the sample collecting chamber is the sum of the initial volume V_{L1} (at pressure P_1) and the liquid in the sample of dispersion, V_{L2} collected at pressure P_2.

$$V_{L1} + V_{L2} = V_{L3} \qquad (6.1)$$

For ideal gas law behaviour:

$$P_1 V_1 + P_2 V_2 = P_3 V_3 \qquad (6.2)$$

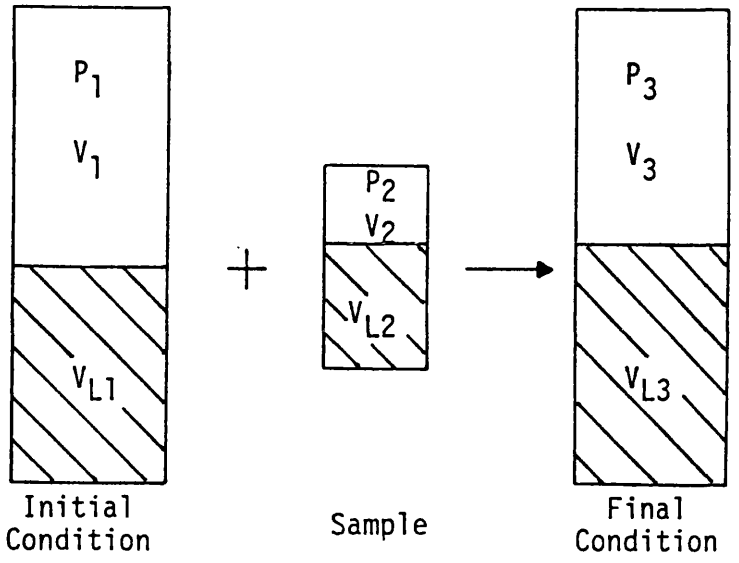

Figure 6.1 Sampling Process

From equation (6.2), the volume of air in the sample is given by:

$$V_2 = (P_3V_3 - P_1 V_1)/ P_2 \qquad (6.3)$$

The volume of water in the sample is determined from Equation (6.1). The pressure of the air in the collected sample, (P_2) can be determined from thermodynamic considerations. Applying the Helmholtz free energy concept, Mori et al [45] derived the

following relationship for the pressure in an air bubble.

$$P_2 = P_s + 2\sigma/r \qquad (6.4)$$

where P_{ss} is the pressure in the liquid phase, equal to the atmospheric pressure, plus the hydrostatic head of the dispersion above the sampling position, r is the radius of the bubble, and σ is the surface tension.

Since $P_{ss} >> 2o / r$, the latter term in Equation (6.4) can be neglected. The point gas holdup is then given by:

$$h_p = V_2 / (V_2 + V_{L2}) \qquad (6.5)$$

6.3.2 Degassing Effect

The solubility of gases in liquids is proportional to their partial pressure in the vapour phase. The coefficient of Henry's Law is not sufficiently affected below normal atmospheric pressure.

$$P_A + HX_A \qquad (6.6)$$

However, reduction in P_A will cause a decrease in X_A, the mole fraction of air in the liquid phase. Using ADA, the dispersion sample is subjected to a vacuum in the isolated collecting chamber. The sampling system (Section 6.3.3) was designed to minimise mass transfer or temperature effects [46], so that degassing of the collected dispersion sample could be neglected. Furthermore, any increase in the collecting chamber pressure due to the introduction of water alone was accounted for by the reduction of the free gas space only (Appendix III, p 234).

6.3.3 Measurement System

The ADA system developed for measuring the sample volumes of gas and liquid is shown in Figure 6.2. A glass tube (1.5 mm. i.d.) supported by a stainless steel tube, Figure 6.3B was used to withdraw samples of gas-liquid dispersion from the stirred vessel. The probe was connected to the calibrated 'collecting chamber' at the solenoid valve V1, Figure 6.3 by means of a flexible nylon tube (3.1 mm. o.d.). A series of four 2-way solenoid valves (V1-V4) were used to control the sequence of sampling, which was performed automatically using an Analog Devices Macysm II microcomputer. The valves could also be operated manually.

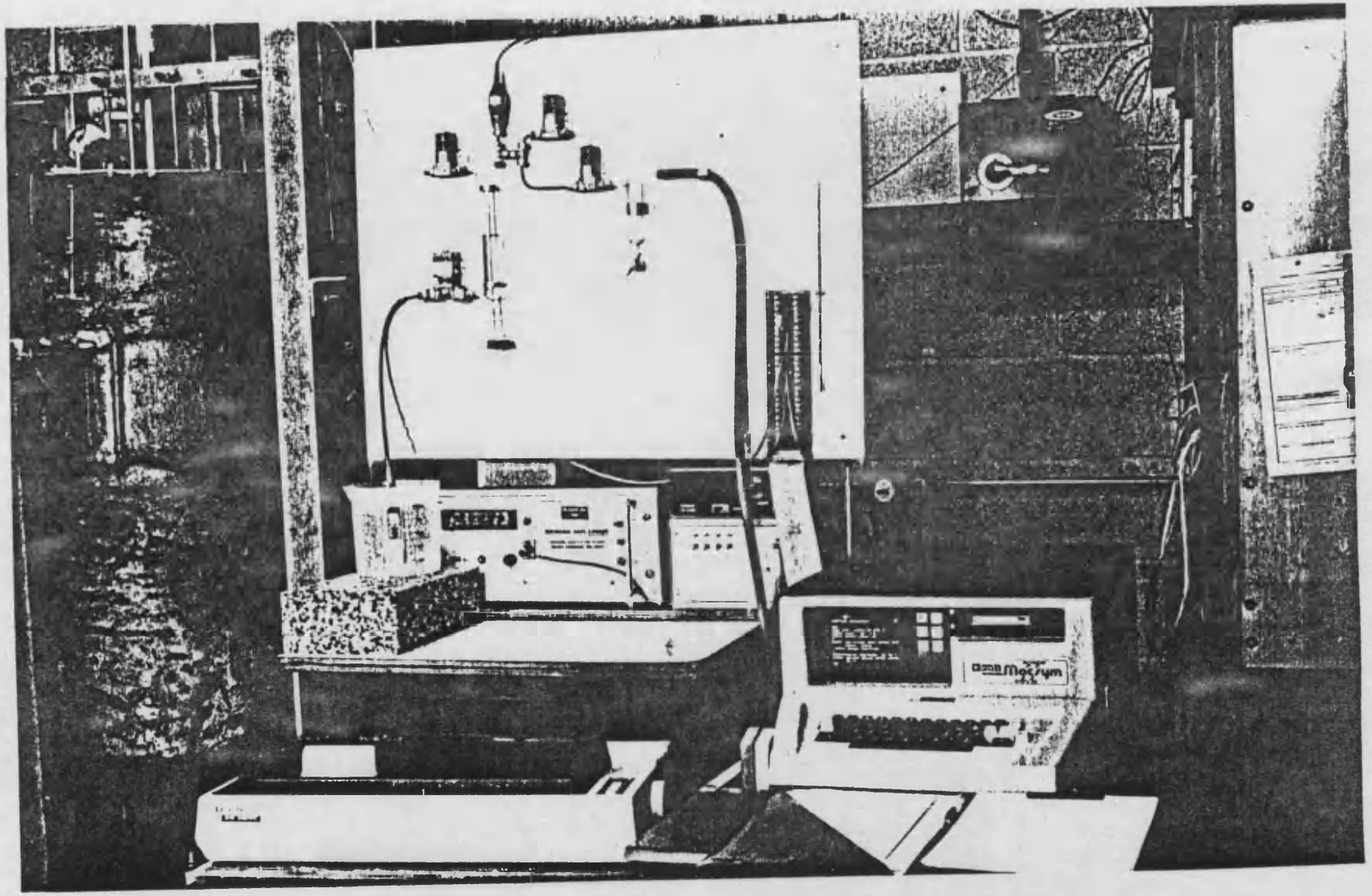

Figure 6.2 ADA Measurement System

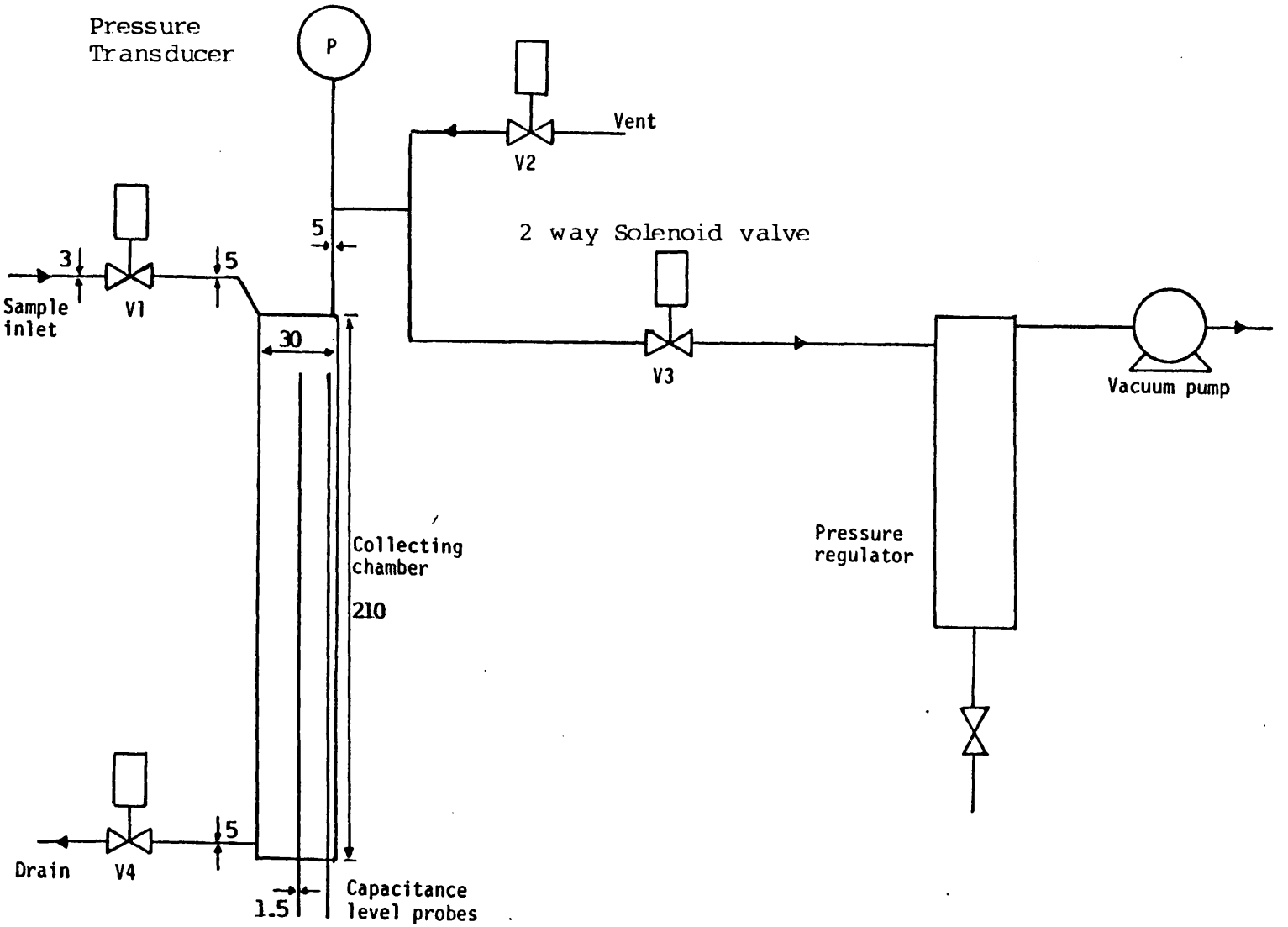

Figure 6.3 Schematic Illustration of Auto Dispersion Analyser (Dimensions in mm.)

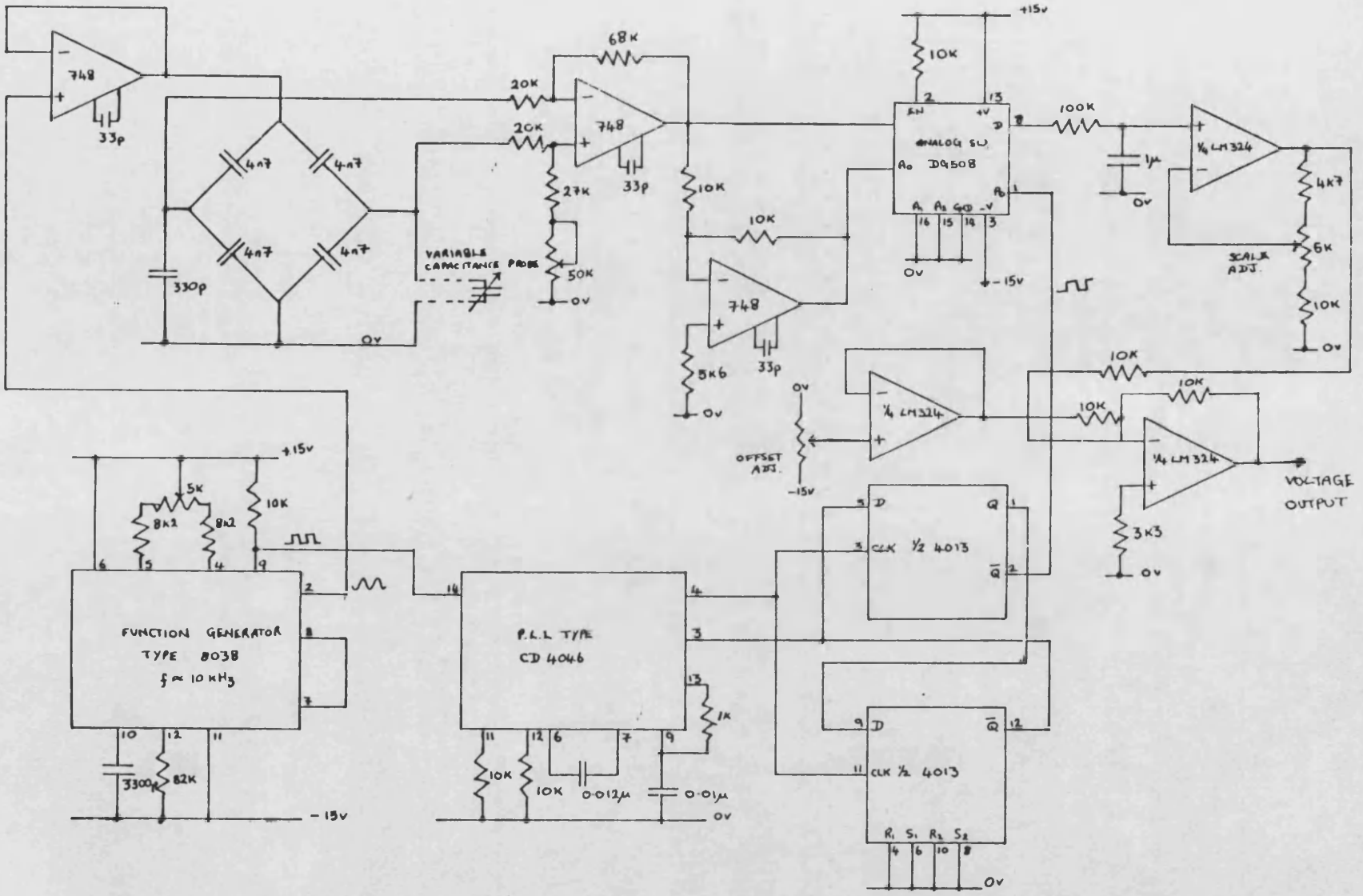

Figure 6.3A Variable Capacitance Probe Circuit

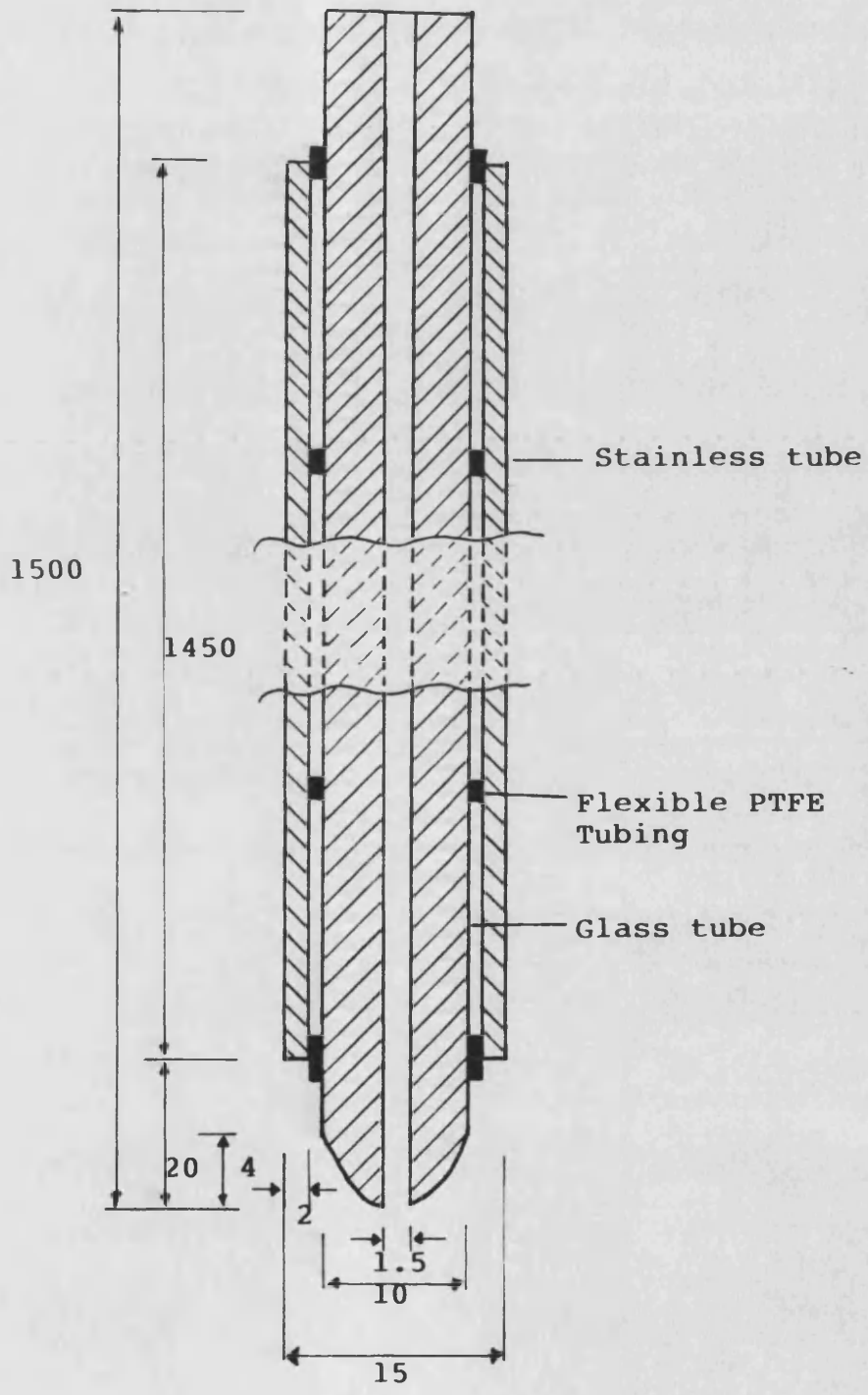

Figure 6.3B Sampling Probe
(Dimensions in mm.)

A high performance thin film strain gauge pressure transducer (0-1 bar absolute) was used to measure pressure changes in the collecting chamber. Capacitance level probes were used to control and measure the liquid level in the chamber. The probes were made from 1.5 mm. diameter pure copper wire coated with 0.043 mm. thick Polyurethane layer. The probes were sealed with a PTFE spray to prevent adhesion of gas bubbles.

The variable capacitor probe is connected in parallel with one arm of an A.C. capacitor bridge, which is arranged to be balanced when the probe is half immersed in water as shown in Figure 6.3A. The output of the bridge is amplified using a differential amplifier, and an inverted version of the amplifier output is obtained using an inverting amplifier. The two signals are applied to two inputs of a DG 508 analog switch which serves as a phase-sensitive detector (psd). The output of the psd is filtered and buffered to provide a voltage output proportional to water level. Scaling and offset are also provided.

6.3.4 Sampling Procedure

The collecting chamber was evacuated to a low preset pressure (50 mm. Hg. absolute) by opening valve

V3. V1 was then opened for a specific period (see Section 6.3.6) to withdraw a sample from the vessel into the chamber. The initial and final readings of pressure and the liquid in the chamber were monitored by the computer, allowing the gas-liquid volume fractions of the sample to be evaluated from Equations 6.1 and 6.2. The initial conditions (pressure and liquid level) in the collecting chamber were re-established for each successive sample collection. The number of samples required for a point gas holdup measurement was determined experimentally (Section 6.3.6) in order to ensure an acceptable level of reproducibility. Control of the sampling time, sample size and the initial conditions in the chamber were sequenced automatically by the computer. The computer program is given in Appendix II. The control and data acquisition system has been illustrated in Figure 3.1, (Chapter 3).The initial chamber pressure determines the sampling rate but by keeping this below 50 mm.Hg absolute, there is no effect on the measured gas holdup.

6.3.5 Probe Selection

The sampling and measurement technique consists of three main operations:

(i) sample withdrawal
(ii) measurement and analysis
(iii) re-establishment of initial conditions in the collecting chamber.

A number of different probe tip geometries were investigated to evaluate their performance. Observations made in a glass tank showed that during periods (ii) and (iii), i.e. when a sample is not being withdrawn, air bubbles tended to collect at the tip when a funnel shaped entrance was used. This had the effect of displacing the resident water from the tip, thereby causing the point gas holdup to be artificially high. This effect was eliminated by using a probe with a contoured outer surface, i.e. receding away from the tip entrance, Figure 6.3B.

The effect of varying the internal diameter of the probe was investigated by measuring the gas holdup under identical conditions in T_{75} and T_{21}. Four sizes of probe (1.5, 2.5, 3.0, & 4.0 mm. i.d.) were

studied, using a sample size of 30 and a sample time of 2 seconds. The results are given in Appendix III (Tables A1 & A3). Comparision of the means at the 5 % confidence level showed that the larger 4 mm. i.d. probe gave significantly different results compared with the other probes. However, there was essentially no difference between the other three probes. The larger entrance of the 4 mm. i.d. probe in effect tends to exhibit similar characteristics to those found previously with the funnel-shaped probe tip. Accordingly, the 4 mm. i.d. probe was rejected and the final selection was based on a study of the sampling time for the other three probe sizes ($P_{1.5}$, $P_{2.5}$, & $P_{3.0}$).

6.3.6 Sampling Time

The effect of varying the sampling time was investigated in T_{75} for probes $P_{1.5}$, $P_{2.5}$ and $P_{3.0}$ (subscripts refer to the internal diameter of probes in mm.). The test results are given in Appendix III, (Table A2). Variance analysis at the 5 % confidence level shows that for a particular probe size, the sampling time has no significant effect. Therefore, the selection of an appropriate probe size is based on the degree of reproducibility achieved, commensurate with

the sample time being at an acceptable level so as to minimize the total experimental time. The best reproducibility, with an accuracy better than ±5 % was achieved with the 1.5 mm. i.d. probe and a sampling time of 6 seconds.

6.3.7 Sample Size

The effect of sample size on the reproducibility of the point gas holdup values is given in Appendix III (Table A4). It is evident that a sample time of 6 seconds and a sample size of 30 represents the optimum condition with respect to the total experimental time and accuracy. This combinatiion requires 7 minutes for a single point gas holdup measurement. This combination of sample time and sample size was used throughout the study of point gas holdups. The reproducibility of the results obtained is better than 5 %. Additional advantages of the ADA method are that it is relatively simple to use and it is also inexpensive.

Figure 6.4: 0.1 x 0.1D Matrix, Showing Sampling Position Numbers

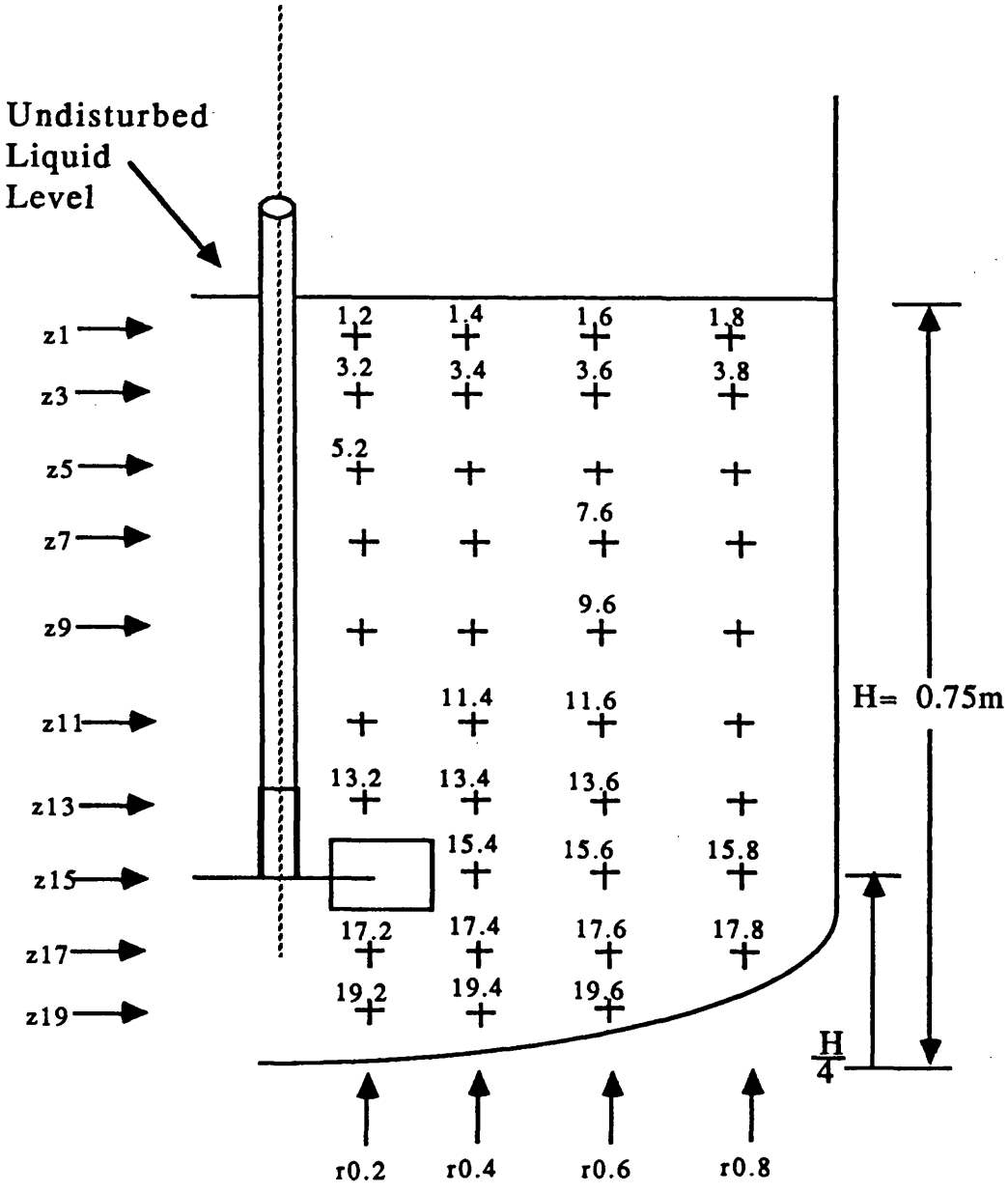

6.3.8 Sampling Positions

The plane midway between two baffles was selected for study. This position avoids the turbulent fluctuations occuring near the baffles. Most other investigations [5, 11 & 44] have also been made in this plane. The midplane was divided into a 0.1D * 0.1D matrix and the assigned position numbers are shown in Figure 6.4. This matrix and the position numbers being common to all the three vessels (T_{21}, T_{75} & T_{100}) was used.

6.3.9 Estimation of Overall Gas Holdup from Point Gas Holdup

Comparision of the overall gas holdup with the estimates from the point values is presented in Table 6.1. The integral means in Table 6.1 are the weighted values based on radial position of the sampling point. For the lowest combinations of Q and N investigated, the estimates from point values deviate significantly from the overall gas holdup, where the point gas holdup values are less than 1.0 %. The ADA technique is therefore not recommended for measuring very low gas holdups.

Table 6.1: Comparison of Overall gas holdup with estimates from point values T_{75} D/T = $^1/_3$

Experimental conditions		Overall gas holdup E_G%	Estimates from point gas holdup %		Deviation of $\bar{h}p$ from E_G %
Q vvm	Ns^{-1}		Simple mean $\bar{h}p$	Integral mean	
0.1	1.75	1.29	0.12	0.1	90.7
	2.17	1.4	0.08	0.05	94
	3.73	2.57	1.38	1.4	46
	5.18	3.53	1.86	2.14	47
0.2	2.43	1.99	1.44	1.42	27
	3.37	2.70	2.73	2.53	1.1
	5.18	3.91	4.74	4.89	21
0.336	2.43	3.17	2.77	2.86	12.6
	3.37	4.74	5.17	5.19	9.1
	5.18	5.58	7.15	7.19	28

Please see corrected integral mean values on p235

However, for moderate to high combinations of Q & N the estimates from point values are in reasonable agreement with the overall gas holdup. These estimates could be significantly improved if the number of sampling points in the measurement grid were increased. Secondly, sampling was only performed in one 2-Dimensional plane whereas the reality is 3-Dimensional. Finally, the region under the impeller was not accessible for point gas holdup measurements resulting in over or under estimations of overall gas holdup from point values, depending on the absence or presence of gas circulation below the impeller plane.

6.3.10 Results and Discussion

The point gas holdup measurements for the air-water system are shown in Figures 6.5 to 6.8. The results show a non-uniform spatial distribution of gas in the stirred vessel. The gas-liquid flow pattern is divided into circulation loops above and below the impeller plane. The circulation above the impeller plane is more easily established at low to moderate agitation rates due to the natural rise of the gas bubbles under buoyancy forces. However, circulation below the impeller requires much higher agitation rates.

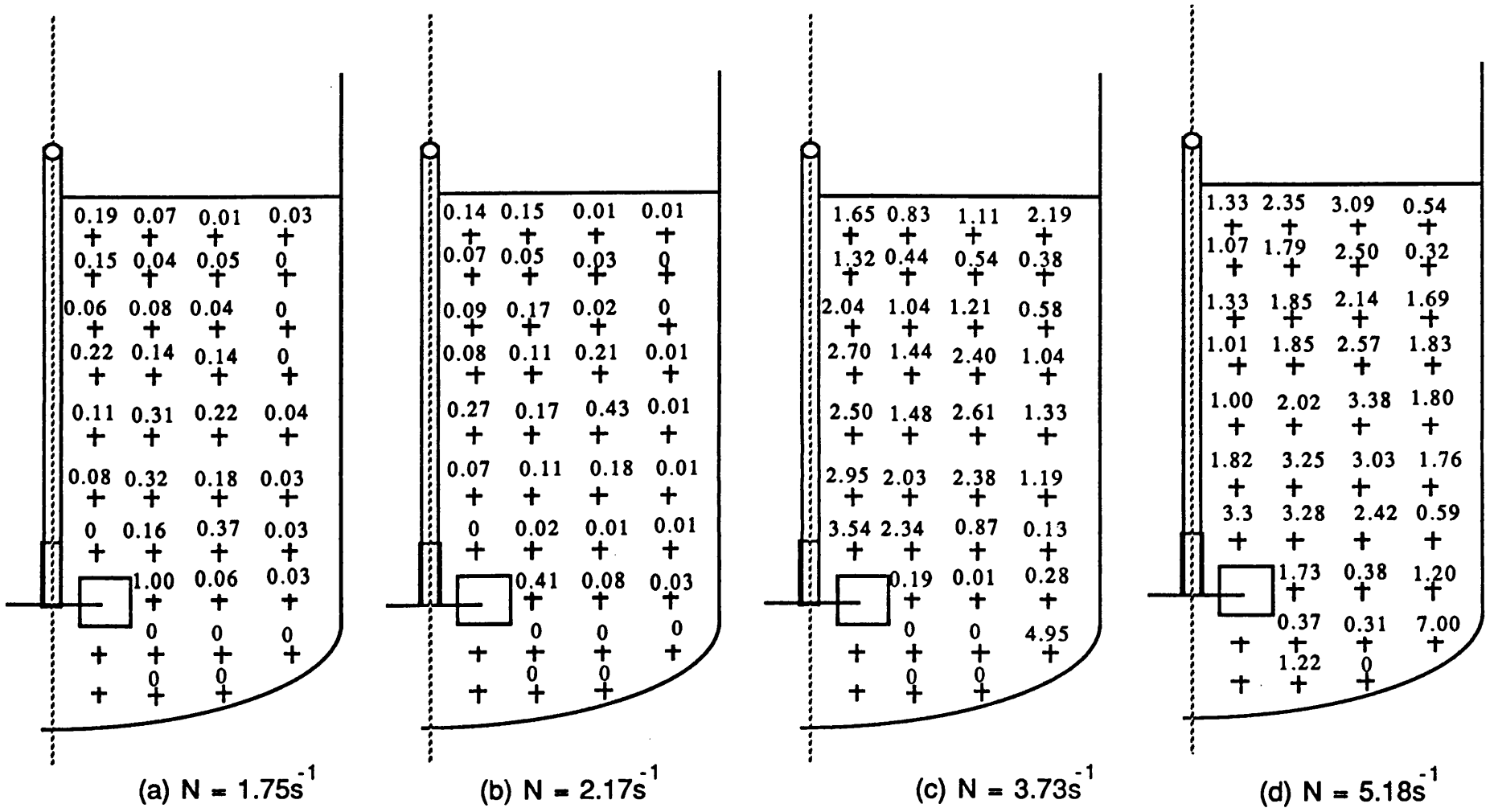

Figure 6.5 : Point Gas Holdup Distribution (%) T_{75}

$Q = 5.207 \times 10^{-4}$ m^3/s $H = T = 0.75m$

$D = 0.25m$ $D/T = 1/3$ $N_R = 3.03s^{-1}$

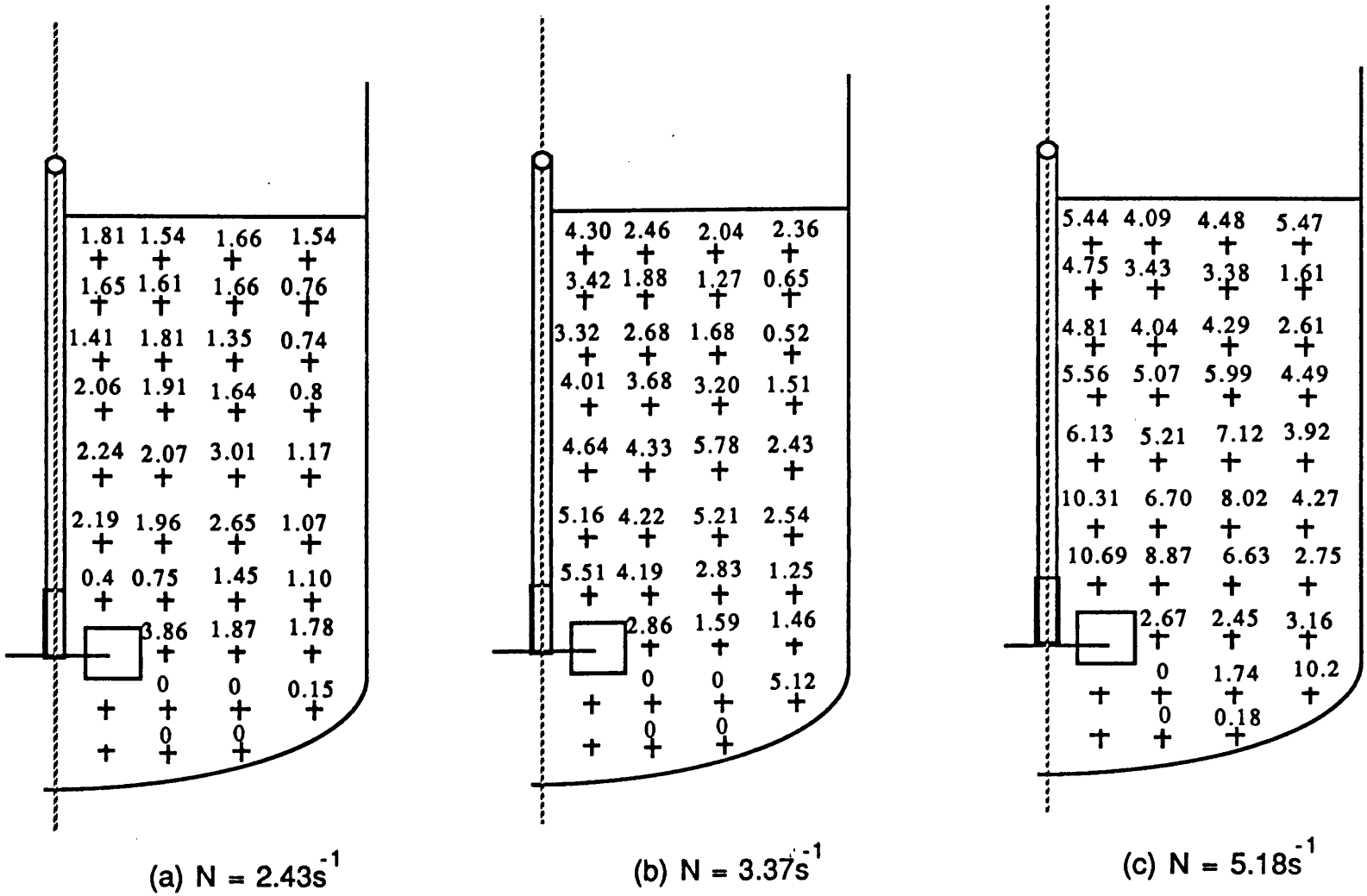

(a) N = 2.43s^{-1} (b) N = 3.37s^{-1} (c) N = 5.18s^{-1}

Figure 6.6 : Point Gas Holdup Distribution (%) T_{75}

Q = 1.04 x 10^{-3} m^3/s H = T = 0.75m

D = 0.25m D/T = 1/3 N_R = 5.15s^{-1}

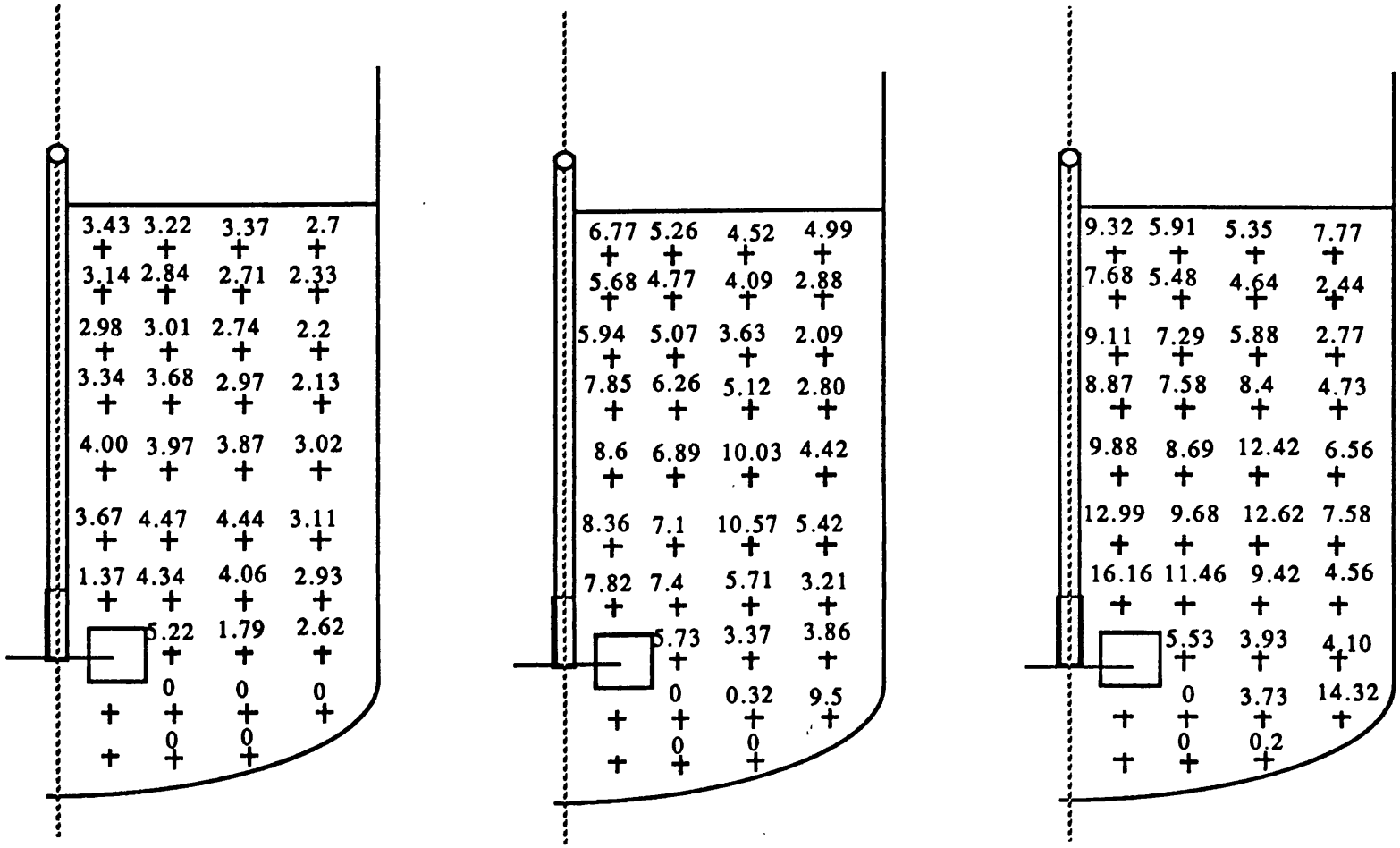

(a) $N = 2.43s^{-1}$ (b) $N = 3.73s^{-1}$ (c) $N = 5.18s^{-1}$

Figure 6.7 : Point Gas Holdup Distribution (%) T_{75}

$Q = 1.76 \times 10^{3}$ m^3/s $H = T = 0.75m$

$D = 0.25m$ $D/T = 1/3$ $N_R = 6.09s^{-1}$

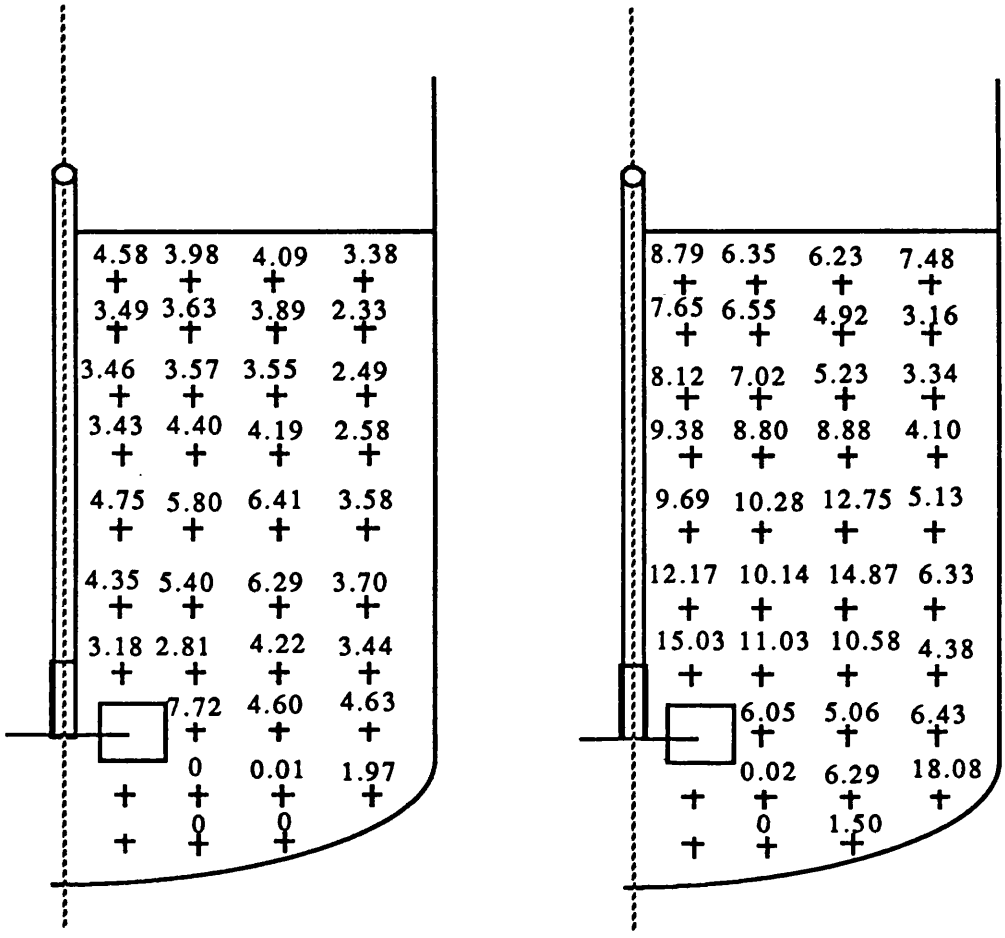

(a) $N = 5s^{-1}$ (b) $N = 10s^{-1}$

Figure 6.8: Point Holdup Distribution (%) T_{75}
$Q = 1.76 \times 10^{-3}$ m^3/s $H = T = 0.75m$
$D = 0.1875m$ $D/T = 1/4$

Under all the conditions investigated in T_{75}, circulation of gas bubbles in the central region below the impeller plane was very limited. Much higher agitation rates were not possible due to the limits imposed by the motor drive.

The two most noticable features of the point holdup distributions in Figures 6.5 to 6.8 are the high values in the central region above the impeller, midway between the impeller shaft and the vessel wall, and also the region below the impeller plane near the vessel boundary. These effects are further highlighted by the vertical and radial profiles plotted in Figures 6.9 to 6.16.

The gas-liquid flow patterns exhibited by the point gas holdup distributions show good agreement with those reported by Nienow et al [44], shown in Figure 7.1. At low impeller speeds, Figures 6.5 (a & b), 6.6 (a) and 6.7 (a), the vessel behaves as a bubble column. In Figures 6.5 (c & d), 6.6 (b & c) and 6.7 (b & c) increased circulation of the gas is evident in the lower part of the vessel as the impeller speed increases. Above the impeller plane, where the gas-liquid flow is well established, there is a general decrease radially towards the vessel wall except for high holdups near the centre of the vessel (Positions 9.6 & 11.6).

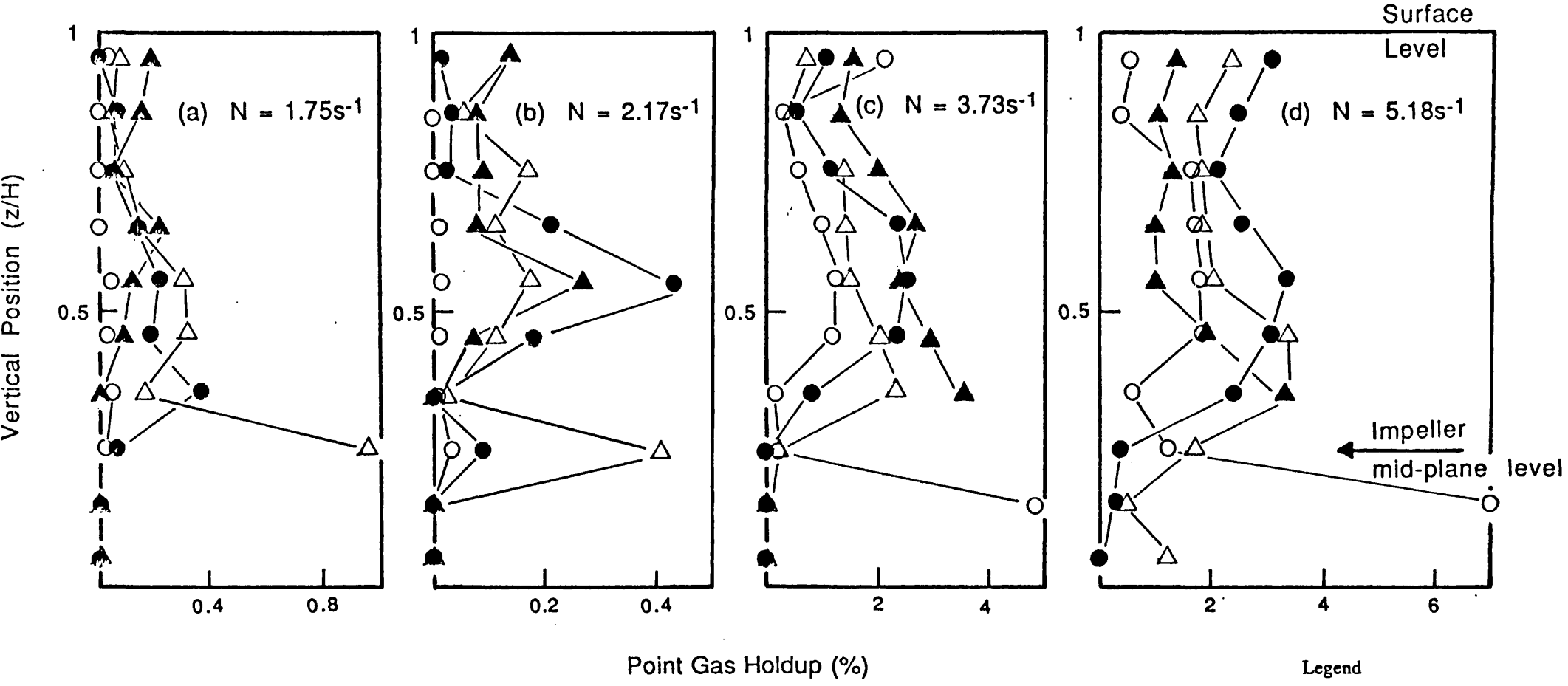

Figure 6.9 : Vertical Gas Holdup Distribution T_{75}

$Q = 5.207 \times 10^{-4} m^3/s$ H = T=0.75m

D = 0.25m D/T = $^1/_3$

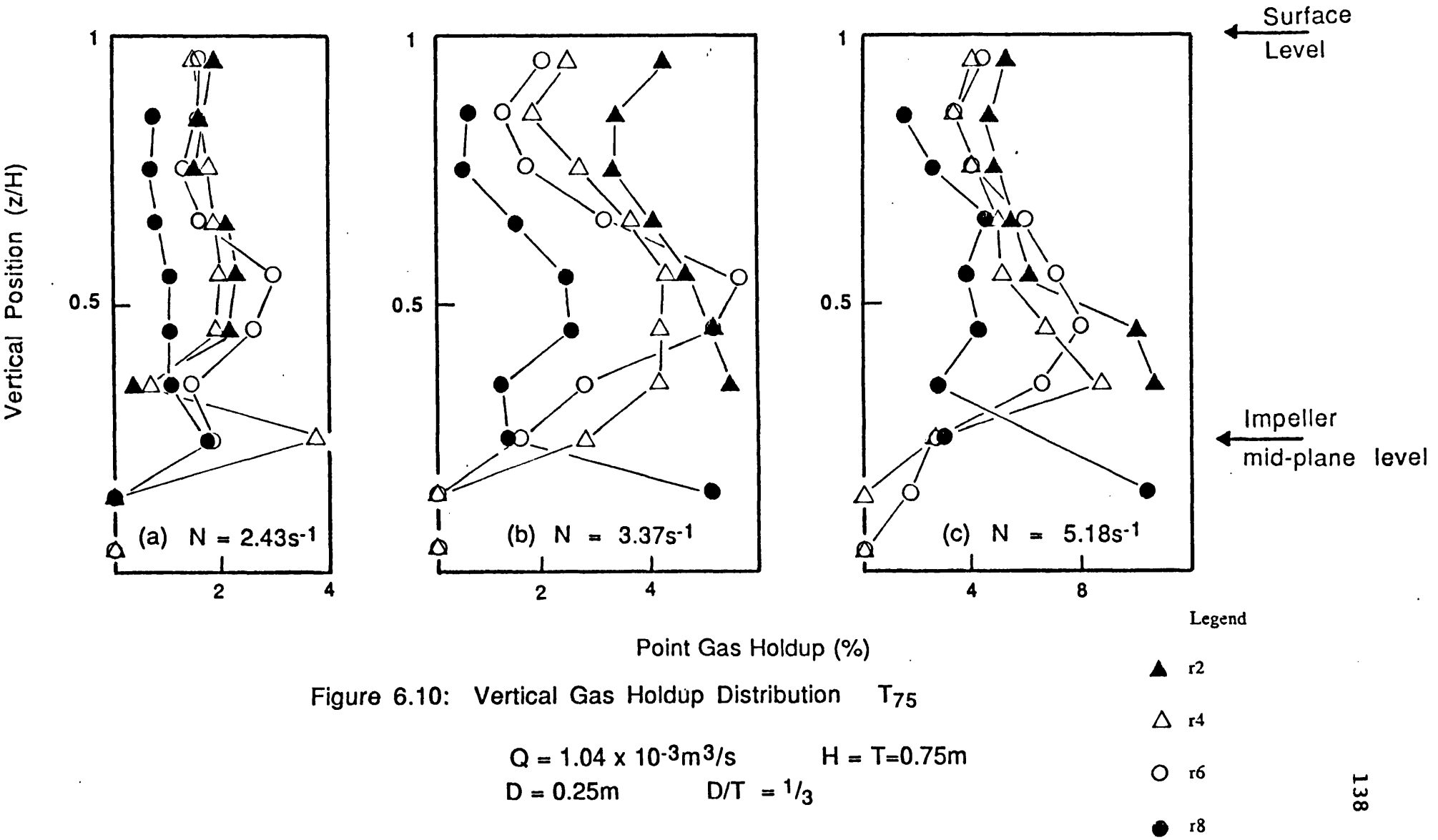

Figure 6.10: Vertical Gas Holdup Distribution T_{75}

$Q = 1.04 \times 10^{-3} m^3/s$ $H = T = 0.75m$

$D = 0.25m$ $D/T = 1/3$

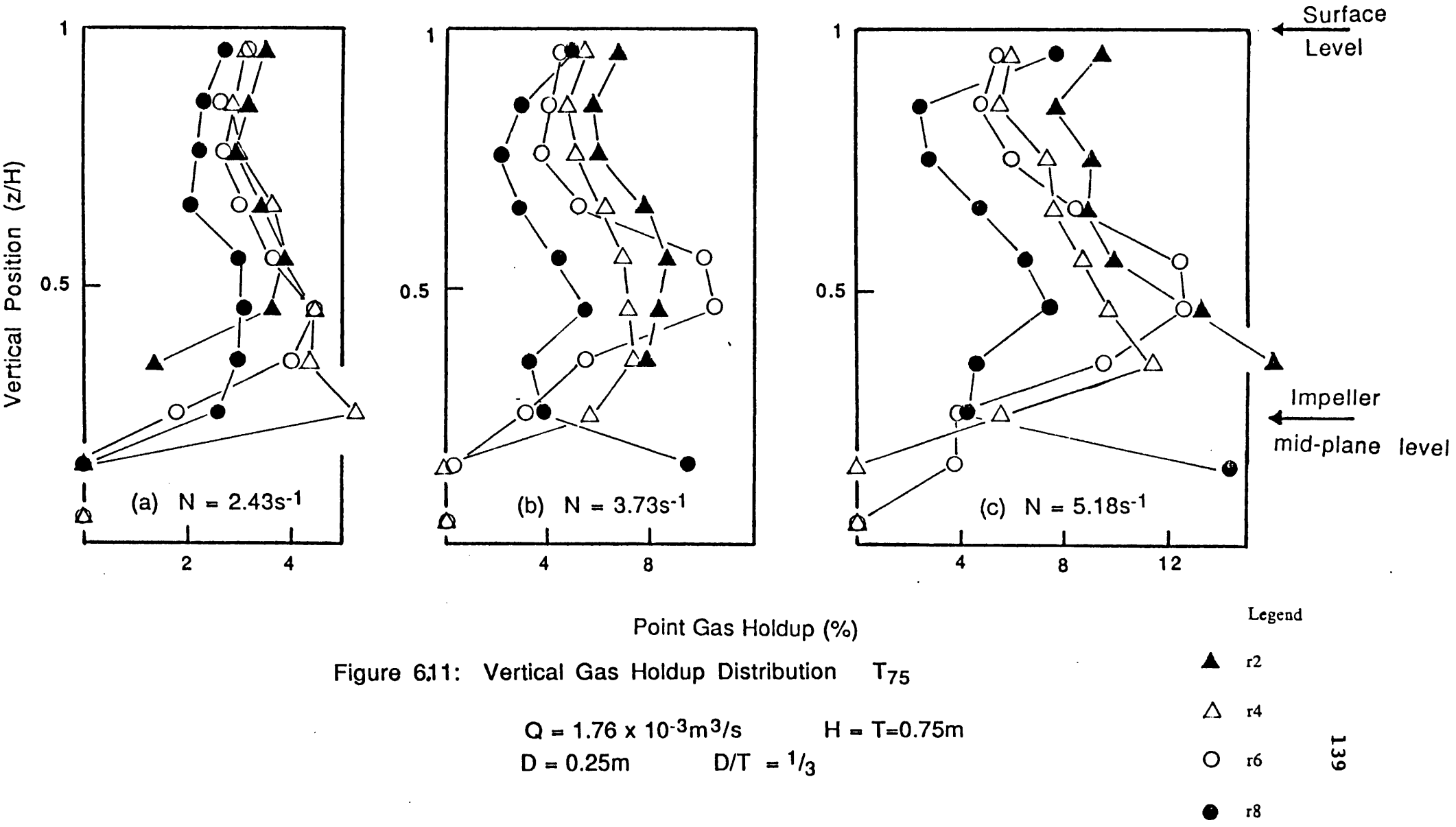

Figure 6.11: Vertical Gas Holdup Distribution T_{75}

$Q = 1.76 \times 10^{-3} m^3/s$ H = T=0.75m

D = 0.25m D/T = $^1/_3$

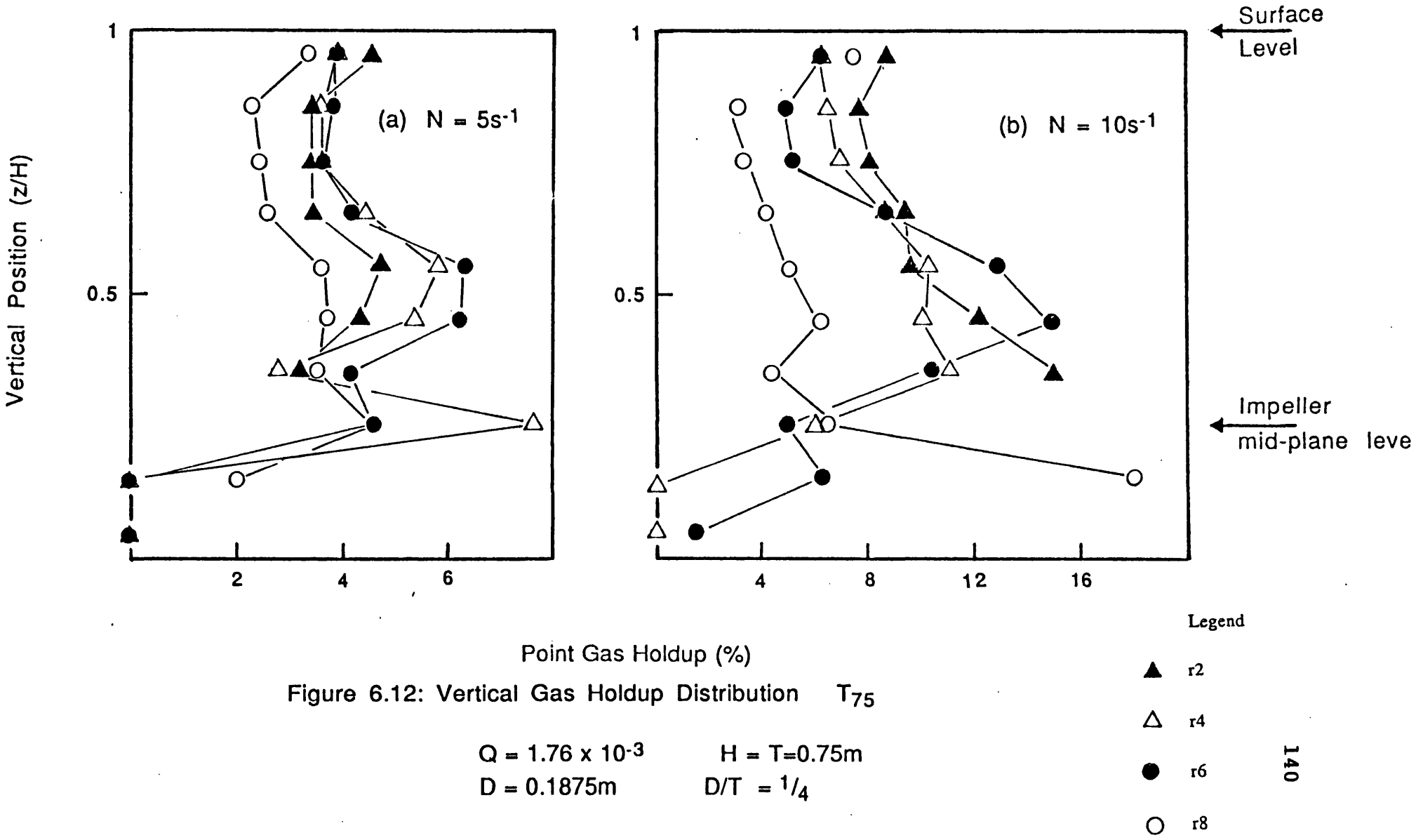

Figure 6.12: Vertical Gas Holdup Distribution T_{75}

$Q = 1.76 \times 10^{-3}$ H = T=0.75m

D = 0.1875m D/T = $^1/_4$

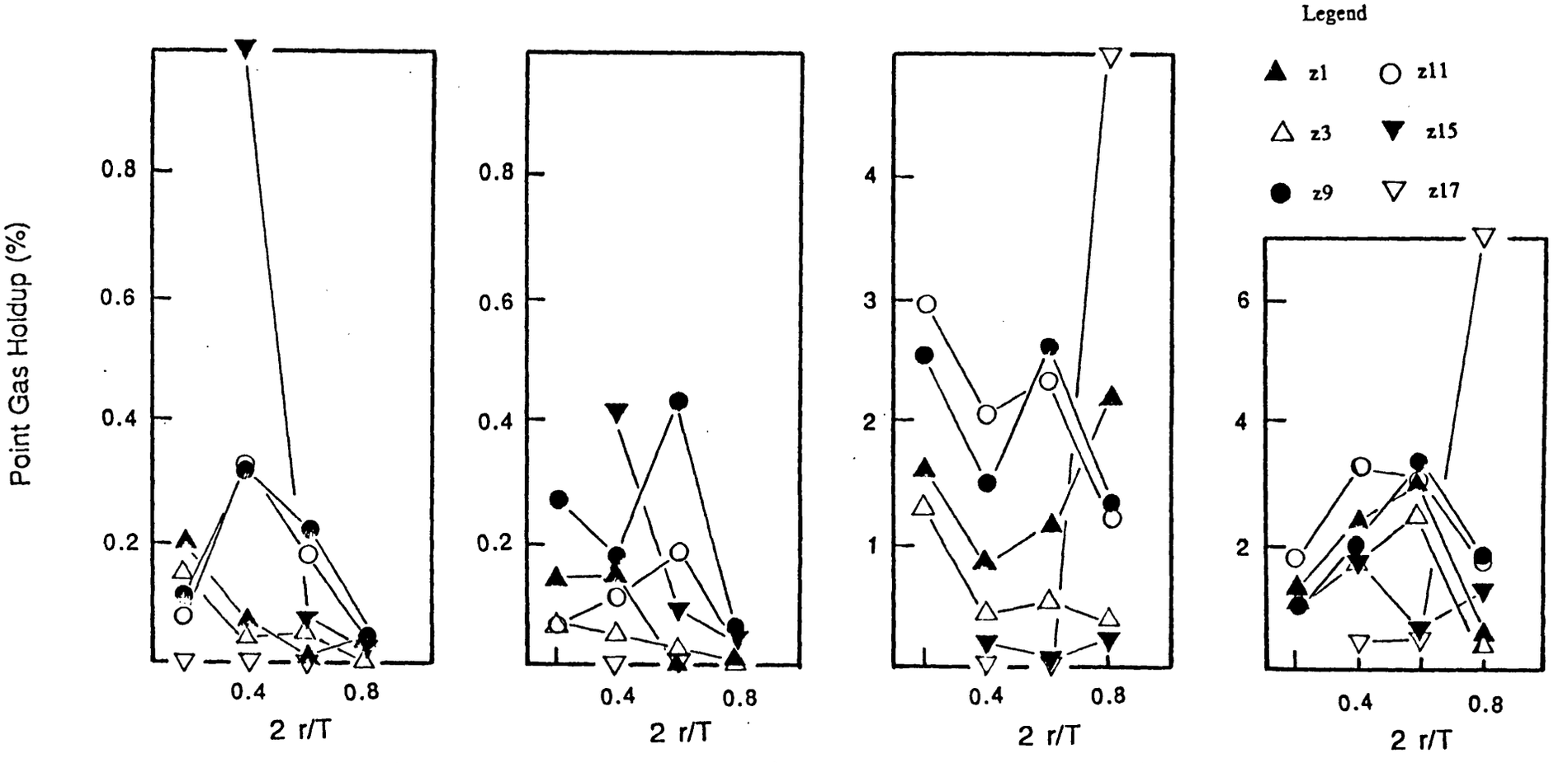

Figure 6.13: Radial Gas Holdup Distribution T_{75}

$Q = 5.207 \times 10^{-4} m^3/s$ H = T=0.75m

D = 0.25m D/T = $^1/_3$

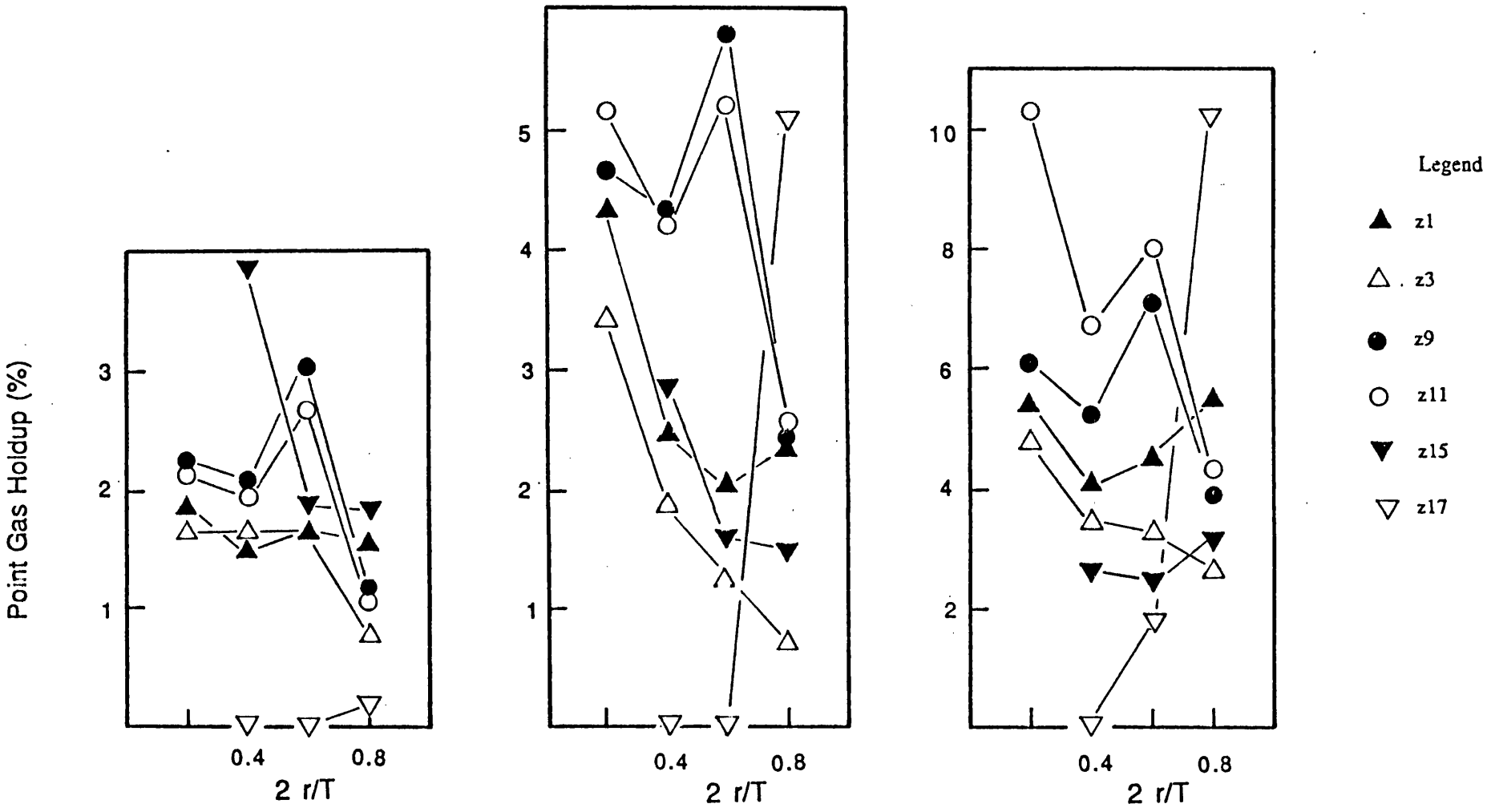

Figure 6.14: Radial Gas Holdup Distribution T_{75}

$Q = 1.04 \times 10^{-3} m^3/s$ H = T=0.75m

D = 0.25m D/T = 1/3

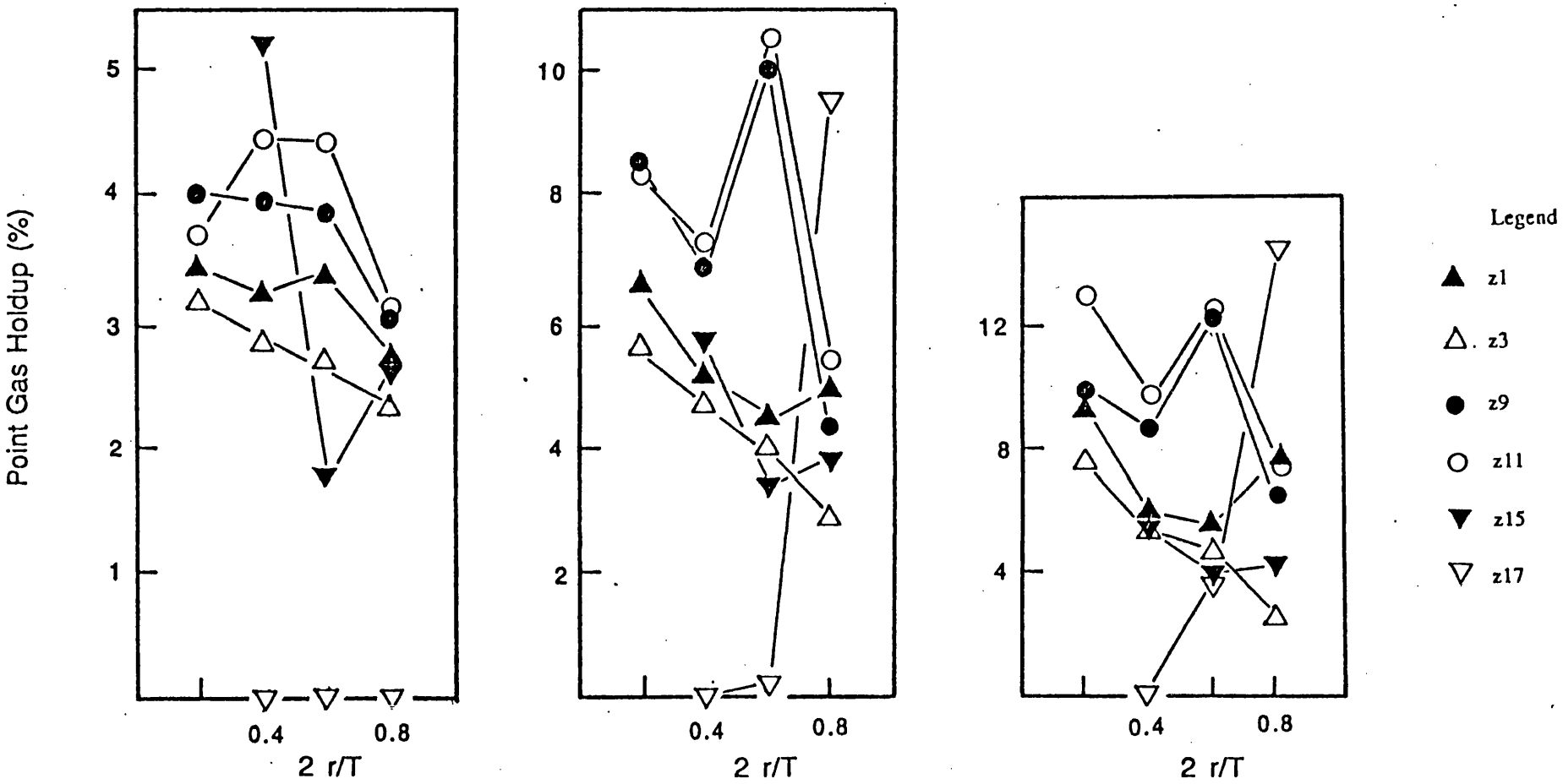

(a) $N = 2.43s^{-1}$ (b) $N = 3.73s^{-1}$ (c) $N = 5.18s^{-1}$

Figure 6.15: Radial Gas Holdup Distribution T_{75}

$Q = 1.76 \times 10^{-3} m^3/s$ $H = T = 0.75m$

$D = 0.25m$ $D/T = 1/3$

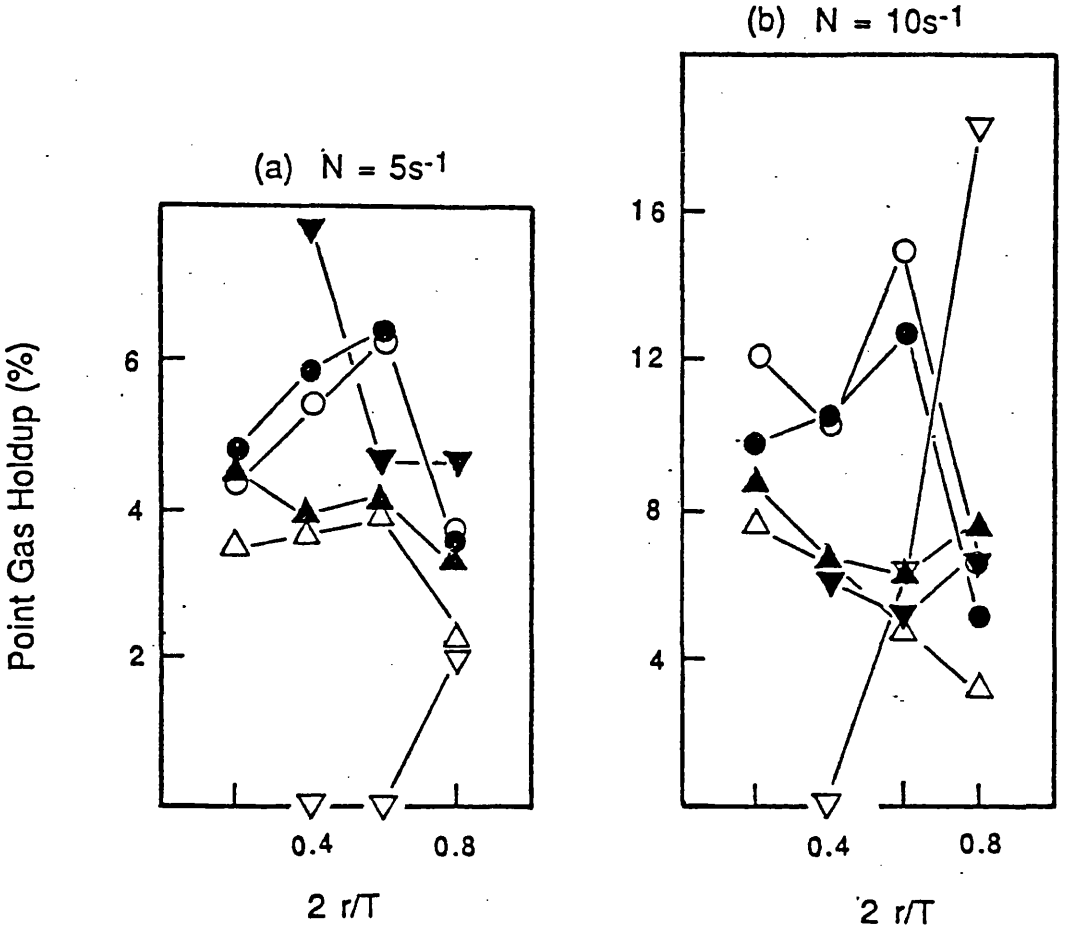

Figure 6.16: Radial Gas Holdup Distribution T_{75}

$Q = 1.76 \times 10^{-3} m^3/s$ H = T=0.75m

D = 0.1875m D/T = $^1/_4$

Legend

▲ z1

△ z3

● z9

○ z11

▼ z15

▽ z17

This is associated with recirculation of the dispersion into the central region. In the region just above the impeller blade (Position 13.2) near the shaft, there is a significant increase in h_p with increase in N. Concurrently with this is the occurence of circulation of gas below the impeller plane, (Position 17.8). A detailed study of these positions is given in Chapter 7.

Increasing the impeller speed causes an increase in h_p at every point in the vessel except in the impeller plane. This is in good agreement with the findings of Nienow et al [44], shown in Figure 6.18A. However, the results of Barigou [5], shown in Figure 6.18C indicate an increase in h_p with increase in N at every point in the vessel including the impeller plane. The effect of the impeller speed, N on the radial mean gas holdup is shown in Figure 6.17. The radial mean gas holdup values are the radial arithmetic mean of the point gas holdups.

The effect of the gas rate, Q on the radial mean gas holdup is shown in Figure 6.18. For a particular N, increasing the gas rate increases the radial mean gas holdup in the whole vessel. The point gas holdup (Figures 6.5d, 6.6c & 6.7c) above the impeller plane increases with Q but shows both increasing and decreasing trends below the impeller

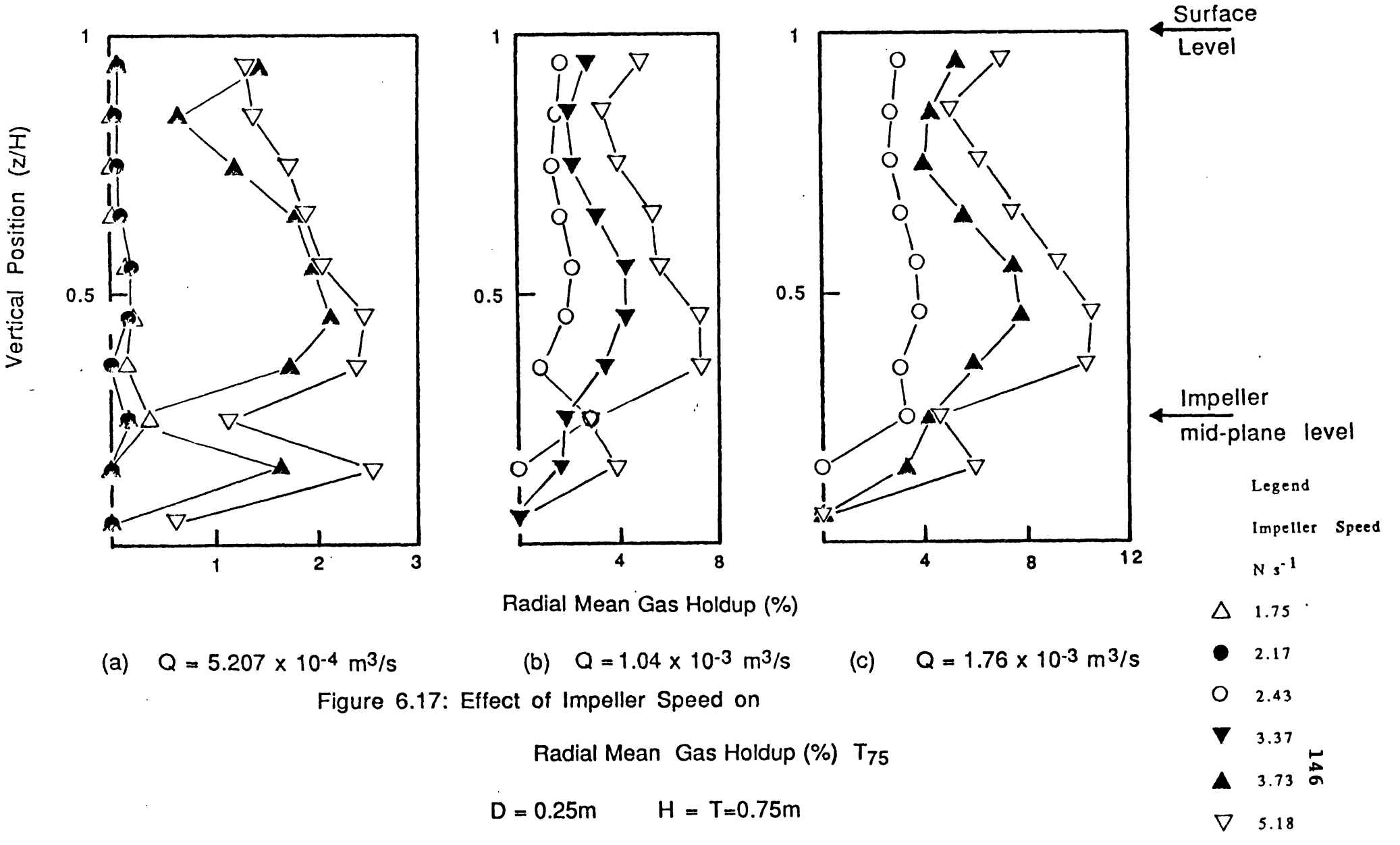

(a) $Q = 5.207 \times 10^{-4}$ m^3/s (b) $Q = 1.04 \times 10^{-3}$ m^3/s (c) $Q = 1.76 \times 10^{-3}$ m^3/s

Figure 6.17: Effect of Impeller Speed on

Radial Mean Gas Holdup (%) T_{75}

D = 0.25m H = T=0.75m

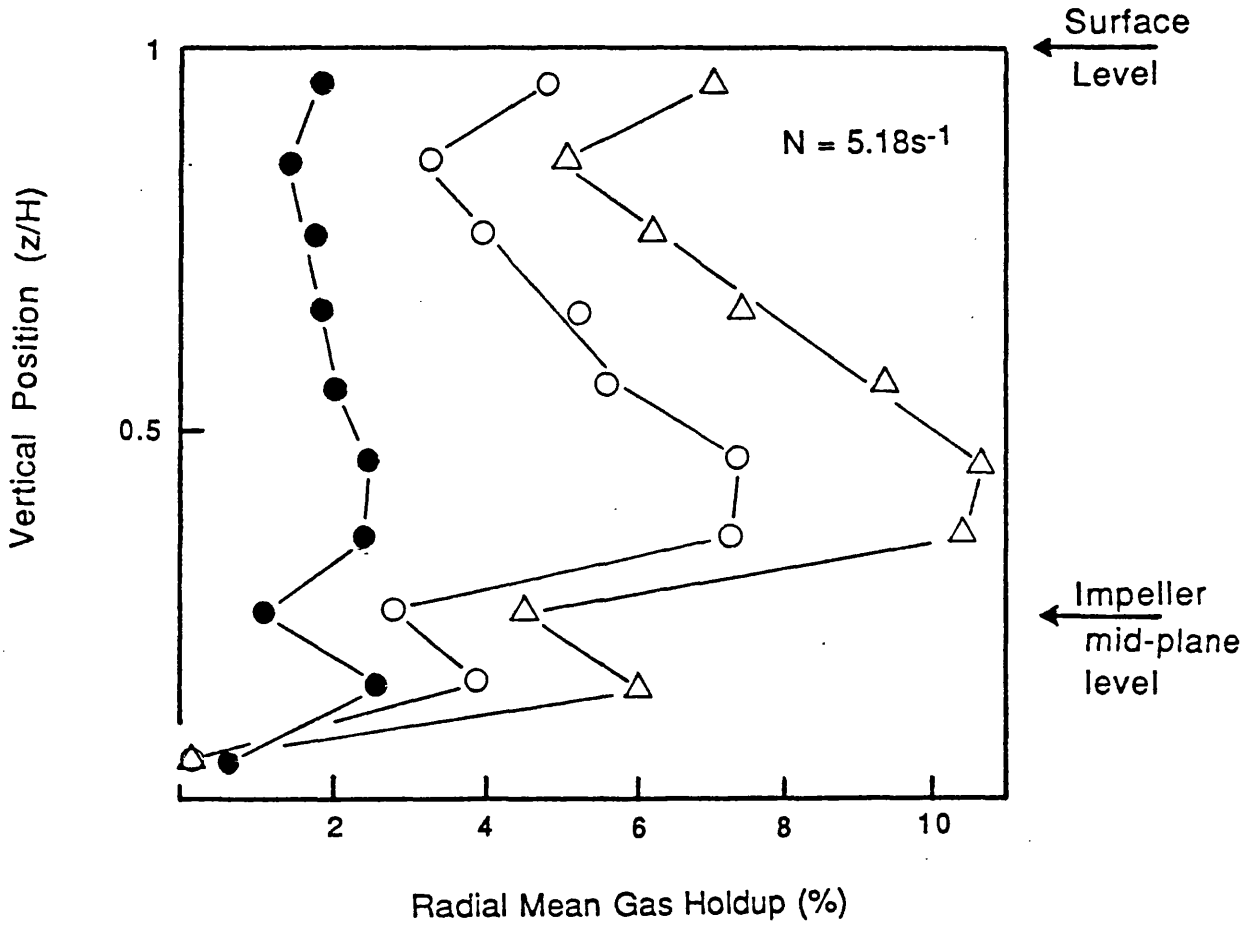

Figure 6.18: Effect of Gas Rate on

Radial Mean Gas Holdup (%) T_{75}

D = 0.25m H = T=0.75m

Legend

. Q m^3/s

● 5.2×10^{-4}

○ 1.04×10^{-3}

△ 1.76×10^{-3}

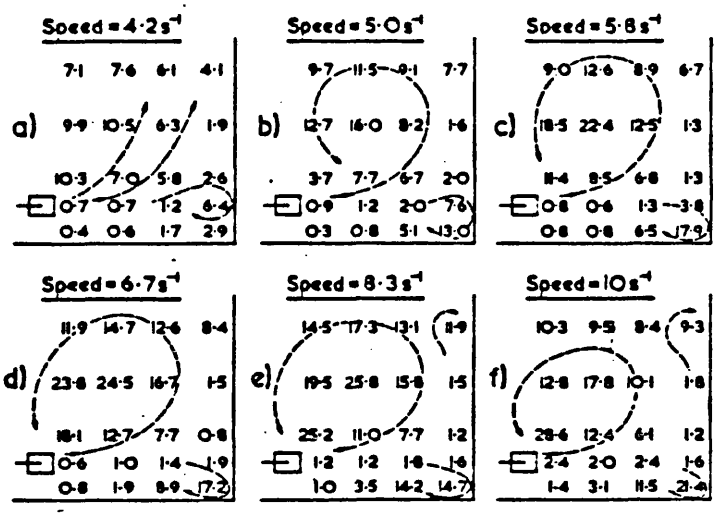

(i) Spatial distributions of gas holdup %

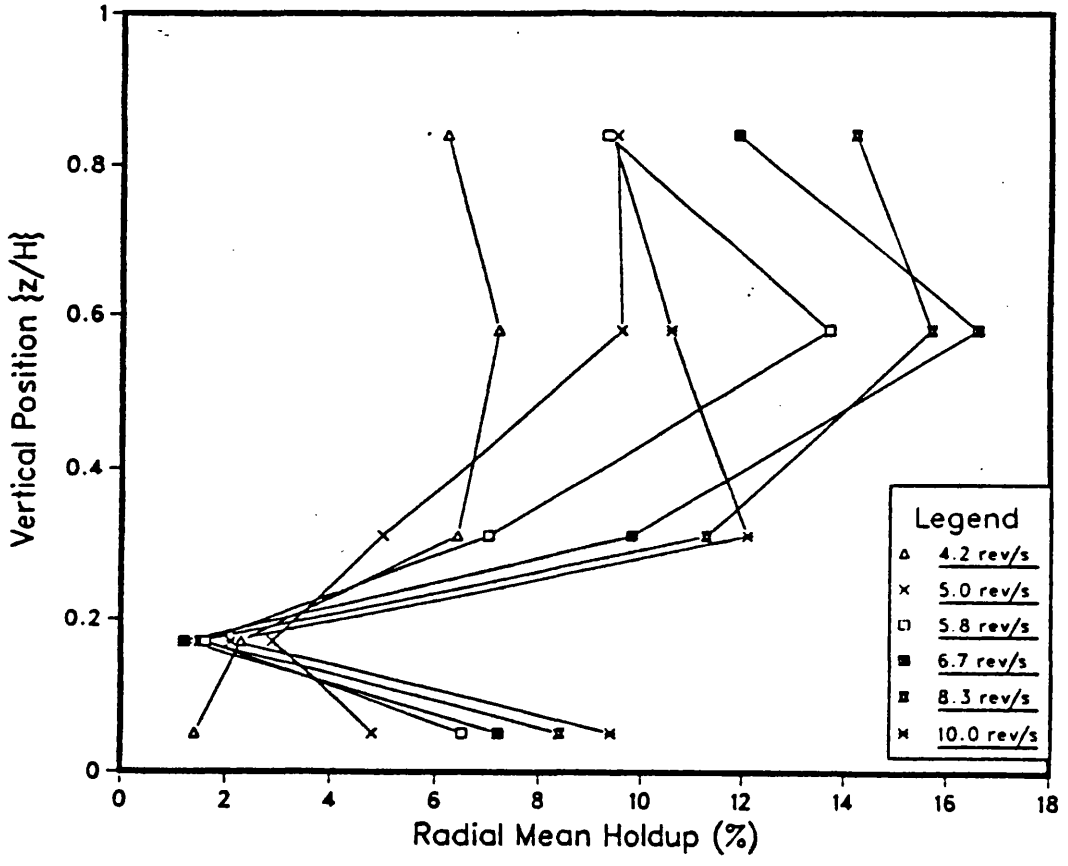

(ii) Vertical gas holdup distributions

Figure 6.18A: Point gas holdup data from Nienow et al [44]
T = 0.29m. D = 0.096m. Q = 1.14 x 10^{-4} m^3/s

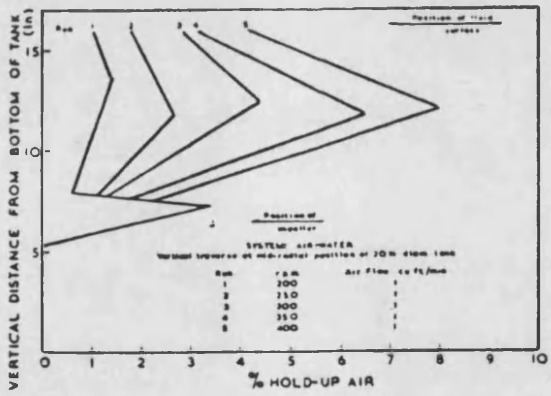

Figure 6.18B: Vertical gas holdup distributions from Calderbank [11]
T = 0.5m. D = 0.167m.

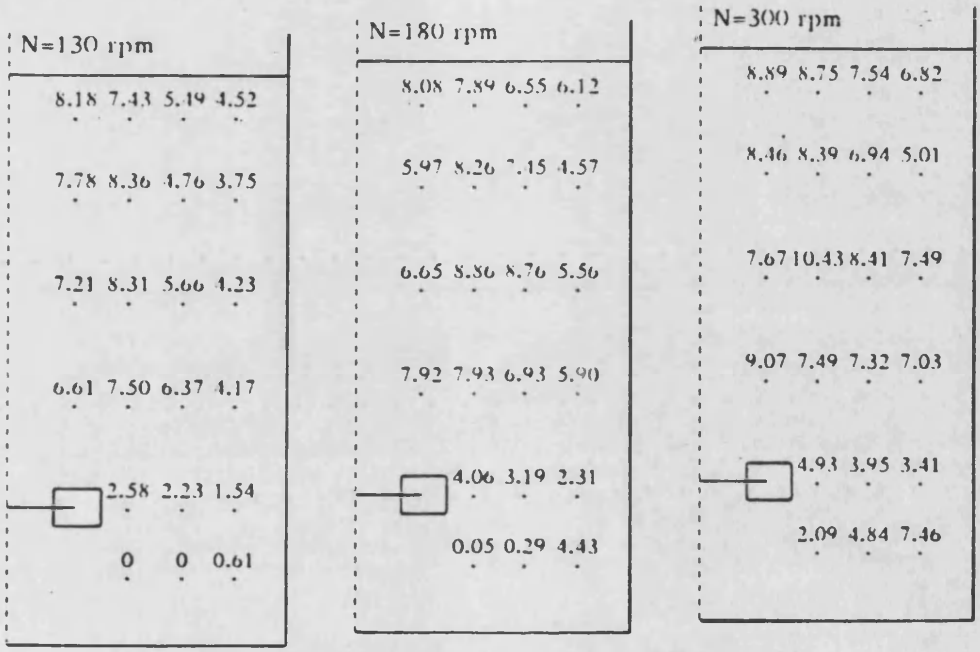

(i) Spatial distributions of gas holdup %

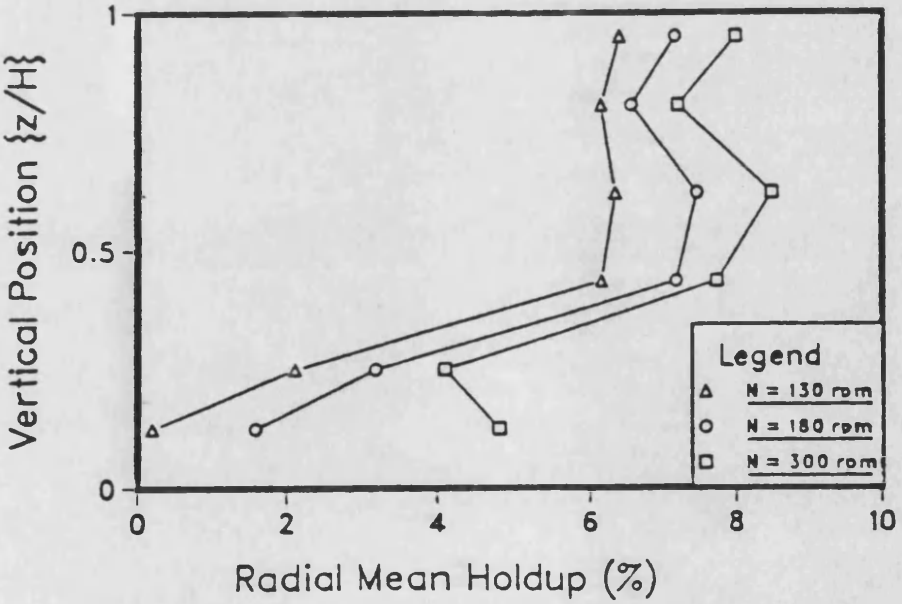

(ii) Vertical gas holdup distributions

Figure 6.18C: Point gas holdup data from Barrigou [5]
T = 1.0m. D = 0.33m. Q = 0.00438m^3 /s

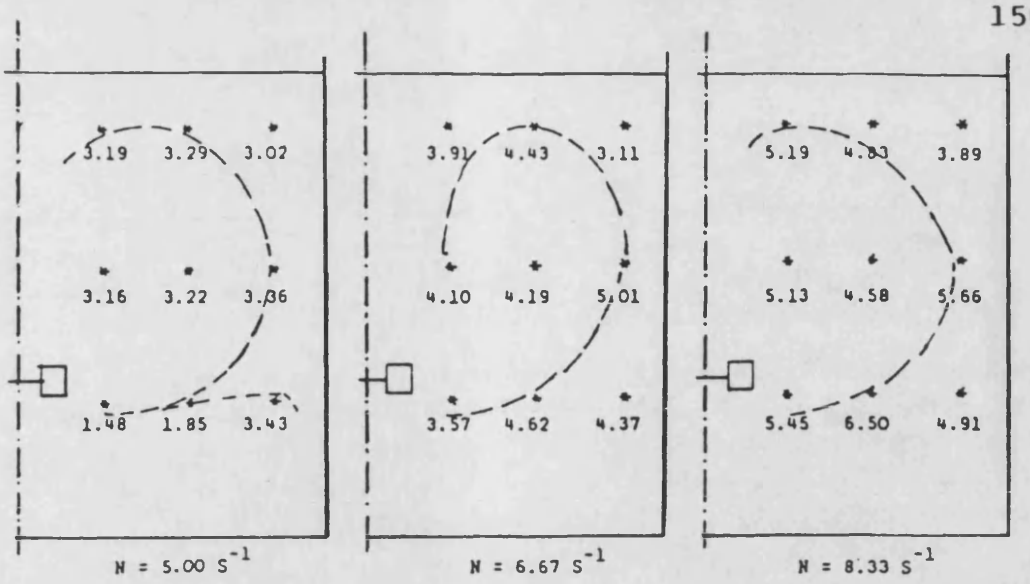

Figure 6.18D: Spatial distributions of gas holdup from Figueiredo [41]

$T = 0.91m.$ $D = 0.3m.$ $Q = 4.16 \times 10^{-3}\ m^3/s$

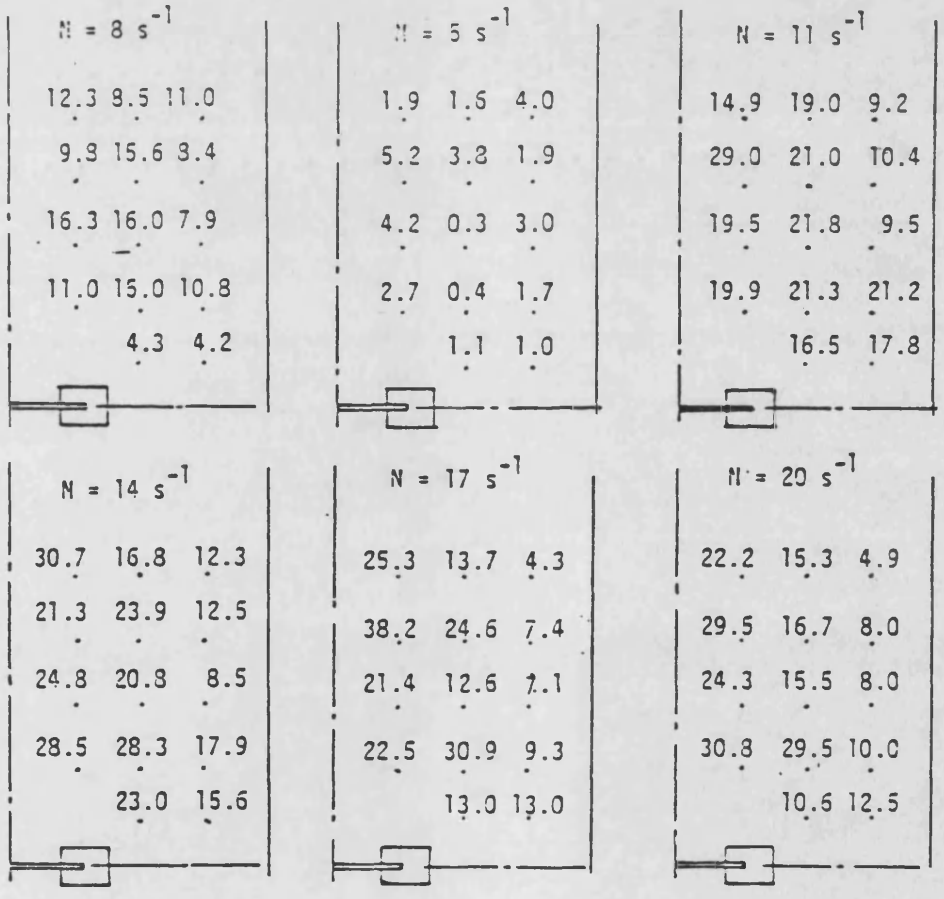

Figure 6.18E: Spatial distributions of gas holdup from Kobbacy [7]

$T = 0.21m.$ $D = 0.076m.$ $Q = 3.77 \times 10^{-4}\ m^3/s$

plane. This is not unexpected since increase in Q must be complimented by an increase in N to achieve gas-liquid circulation below the impeller plane.

The most persistent variation in the point gas holdups were found near the liquid surface, the sampling positions being on a plane just 3.8 cm. below the undisturbed liquid level. The liquid surface in an agitated vessel is never quiescent, but is in incessant motion. This 'turbulent' motion of the liquid surface is probably the main cause of this variation in h_p in the vicinity of the surface.

Calderbank [11] was the first to publish point gas holdup distributions for a stirred vessel. His measurements, Figure 6.18B made in a 0.5 m. vessel show excellent agreement with Figures 6.9 to 6.12. The distributions peak mid-way between the impeller plane and the liquid surface. Calderbank's results, Figure 6.18B show a second peak in the impeller plane at the lowest impeller speed investigated, which is consistent with this work, Figures 6.9 (a &b), 6.10 (a), 6.11 (a) and 6.12 (a).

Figueiredo [41] only made measurements for 9 positions in a 0.91 m. vessel, Figure 6.18D. These

results are not illustrated graphically due to the limited points available. Her results indicate a distinct variation near the liquid surface (16 cm. below the liquid level). Here the gas holdup was found to increase towards the centre of the vessel and then decrease towards the vessel wall. This trend is not evident in the present results but variation in point gas holdup radially towards the vessel wall and near the liquid surface are noticable.

Nienow et al [44], whose data, Figure 6.18A was obtained in a 0.29 m. vessel shows good agreement with the point gas holdup distributions of this work, Figures 6.17 & 6.18. In the region above the impeller, the gas holdup decreases radially towards the vessel wall with a peak midway between the impeller shaft and the vessel wall. However, they did not measure point gas holdup in the vicinity of the impeller shaft. They also found that h_p increased with N everywhere in the vessel except in the impeller plane, where initially they encountered a fall in h_p up to N_R and an increase in the gas holdup beyond N_R, in consistent with the present work, Figure 6.5. This fall in the point gas holdup in the impeller plane as N increases is associated with an increase in the liquid discharge from the impeller. However, beyond N_R, the point gas holdup in the discharge flow begins to increase due to the

recirculation of the gas from the upper circulation loop into the cavities behind the impeller blade.

Kobbacy [5] investigated h_p in a 0.21 m. vessel in the region above the impeller only, Figure 6.18E. In agreement with this study, he found the point gas holdup to increase in this region with increase in N. However, the peak in h_p in his case occurs in the vicinity of the impeller shaft, which contradicts all the investigations in the literature including the present study.

Barrigou [5] presented measurements for a 1.0 m. vessel. His distributions, Figure 6.18C above the impeller plane show a decrease in h_p radially towards the vessel wall with a peak in the mid-plane. The maximum point gas holdup was found in the central region between the impeller plane and the free liquid surface in agreement with this study. Similar to present investigations, significant gas circulation below the impeller plane was only achieved at the highest combination of agitation speed and gas flow rate. However, the effect of increasing N increases h_p in the impeller discharge which contradicts Nienow et al [44] and the present work where h_p in the impeller discharge decrease up to N_R and then increases beyond N_R. Barigou's data indicate increasing uniformity of h_p with

Figure 6.19: Coefficient of Variation with Impeller Speed, N.

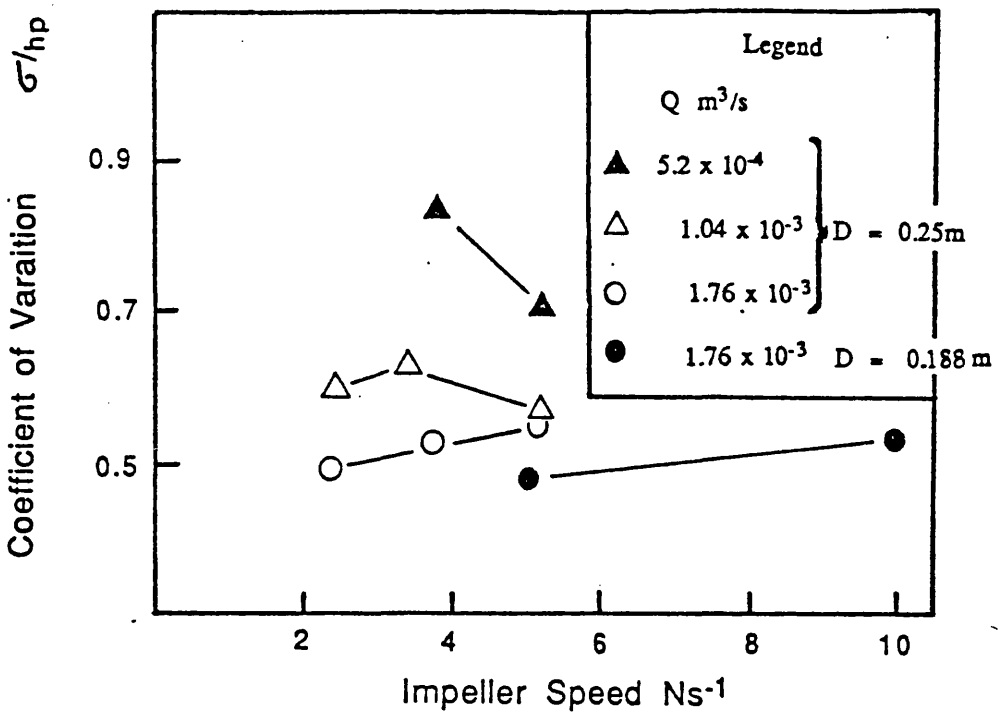

Figure 6.20: Coefficient of Variation with N.

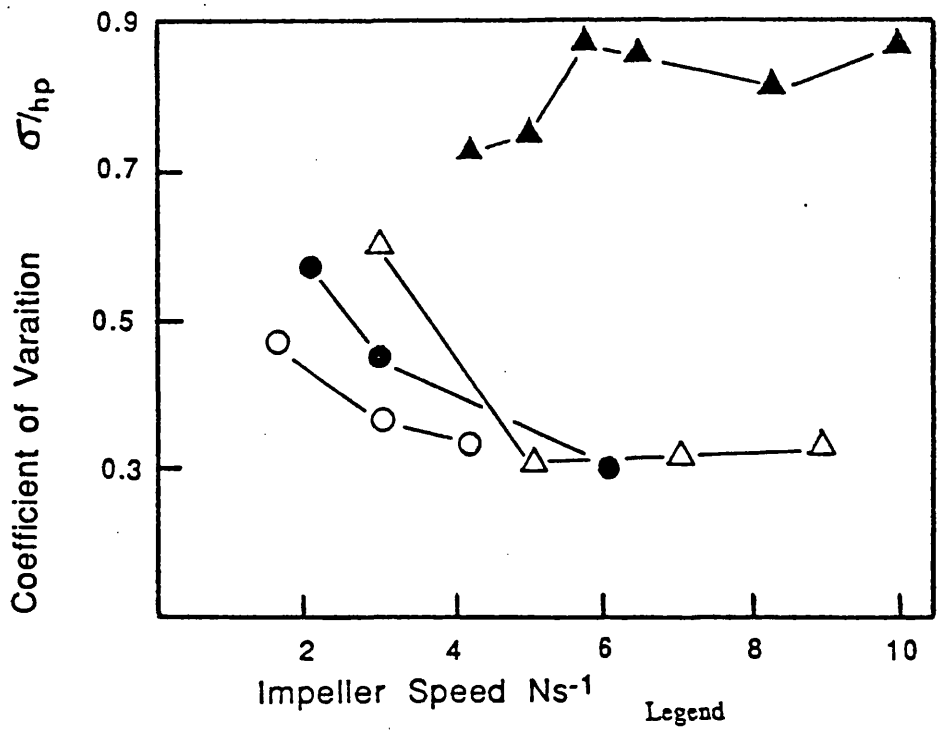

	Q m³/s	Tm	Dm	Reference
▲	1.15 x 10⁻⁴	0.29	0.097	Nienow et al [44]
●	4.38 x 10⁻³	1.00	0.333	Barigou [5]
○	1.64 x 10⁻³	1.0	0.333	Barigou [5]
△	3.62 x 10⁻⁴	0.21	.076	Kobbacy [7]

increasing N in the whole reactor under all conditions. This was shown by the decreasing values of the coefficients of variation of the spatial holdup distributions, Figure 6.20. Results of this study are given in Figure 6.19. Such deductions from the coefficient of variation of point gas holdup with N can not be made on the basis of these few investigations, Figures 6.19 & 6.20, which do not indicate any definite trends.

6.4 Conclusions

- Auto Dispersion Analyser, (ADA) has been developed to measure the local gas holdup distribution in a stirred vessel.

- The estimates of the overall gas holdup obtained from point values (h_p), generally shows good agreement with the overall gas holdup determined from the change in liquid level.

- The point gas holdups indicate a non-uniform spatial distribution of gas in the stirred vessel.

- The effect of increasing the impeller speed, N is to increase the point gas holdup at most positions in the vessel.

- At constant impeller speed, N increasing the gas sparge rate, Q causes an increase in the point gas holdups above the impeller plane with a reduction of gas circulation below the impeller plane.

Chapter 7
SURFACE MOVEMENT AND RECIRCULATION

7.1 Introduction

In a gas-liquid system, the intensity of the disturbances generated at the surface of the liquid is the result of complex interaction between agitator circulation and gas transport. At any operating condition ($N > N_F$), dispersion and bulk circulation of gas are critically dependent on the agitator geometry. Bubble size and gas holdup are also distributed non-uniformly (Chapter 6) through the mixing volume, due to the variation of mean circulating velocity and turbulence intensity.

In order to detect the gas transport arising from surface aeration and recirculation, the local gas holdup has been measured in two regions of the vessels (T_{100}, T_{75} & T_{21}); namely the region near to the liquid surface and also close to the impeller. In addition, gas holdup at a point below the impeller level was monitored to detect gas recirculation into the lower region of the vessel.

7.2 Surface Flow Pattern

Surface flow patterns generated at the free liquid surface in an agitated vessel can be important in many different reactor operations. For example, the re-incorporation of a lighter liquid which is added on to the surface, or solids that are fed directly into a viscous liquid from the surface, are both dependent on the surface movement. Further, since the bulk flow pattern (section 6.3.10) extends up to the free liquid surface causing surface renewal and/or recirculation into the bulk, examination of these characteristics for various combinations of N and Q should provide useful qualitative information regarding the mixing of materials added through the free liquid surface of the vessel.

For a given sparging rate Q, the state of the free liquid surface is described by the following categories, as the speed, N is increased:

(i) 'Spontaneous eruptions' or geysers on surface

(ii) Calm or slightly rippled.

(iii) Rotating vortices behind baffles (position marked by 'X' on Figure 7.2a) with surface bubble movement to and from the central impeller shaft.

(iv) Highly agitated ill-defined surface.

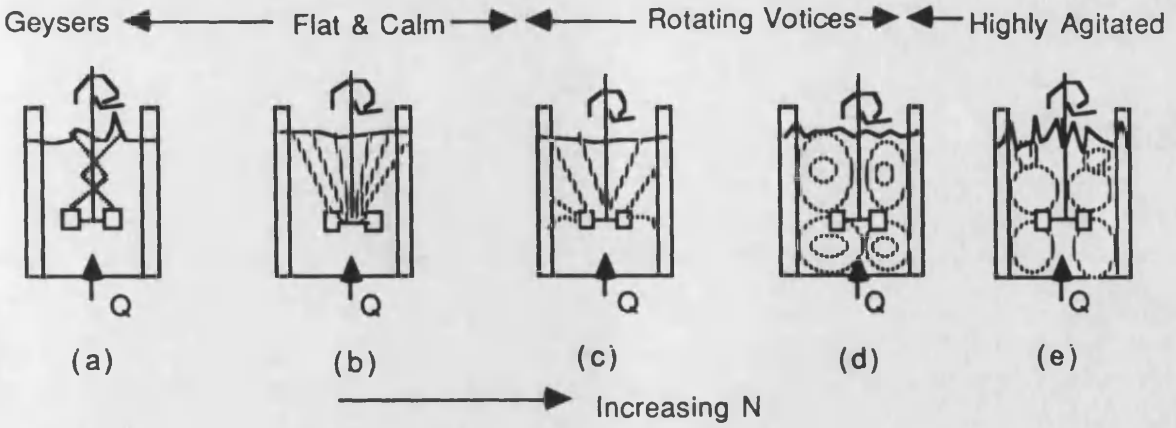

Figure 7.1 Bulk flow pattern at constant Q

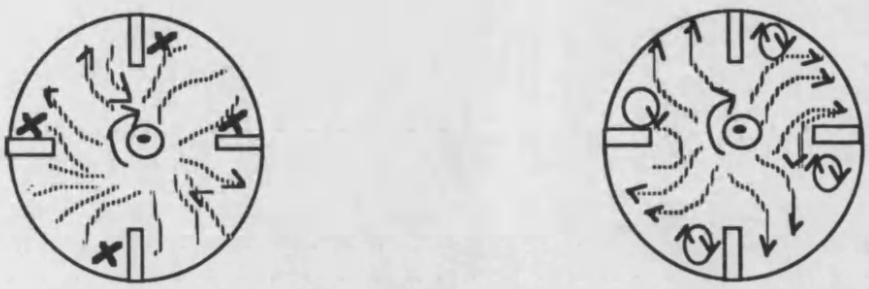

(a) Smooth and Calm

(b) Rotating vortices

Figure 7.2 Surface Flow Patterns

Transition refer to Fig 7.1	Definition of Transition	Authors
a → b	Flooding Point Flooding Point Minimum Agitation Rate Minimum Agitation Speed for Dispersion Impeller Flooding	Wiedmann [50] Pollard [51] Van Dierendonck [54] Westerterp [55] Warmoeskerken & Smith [48]
b → c	Flooding Point Impeller Loading	Ruston & Bimbenet [32] Warmoeskerken & Smith [48,56]
c → d	Onset of Flooding Disengagment or Loading Point Impeller Loading with Gas recirculation	Nienow & Wilson [28] Westerterp et al [55] Warmoeskerken & Smith [48,56]

Table 7.1 Definitions of Bulk Flow transitions

The abrupt change from (i) to (ii) corresponds to the change of bulk flow pattern in Figure 7.1 (a to b) and reflects the condition N_F, which is the impeller speed at which the vessel is just no longer flooded. However, the change from (ii) to (iv) is a gradual one. The explanation is apparent from Figure 7.1 (b to e). Although there is a considerable change in the bulk flow pattern in Figure 7.1 (b to e) with the introduction of gas below the impeller region, the free liquid surface is virtually unaffected until the upper circulation loops extend to the free liquid surface, Figure 7.1 (d & e).

In an unaerated vessel, rotating vortices form in the central area of the free liquid surface resulting in surface aeration. The mechanism of vortex formation on the free liquid surface in a fully baffled vessel has been described by Kobbacy [7]. Under aeration conditions however, the vortices are only noticable at the positions marked 'X' in Figure 7.2(a). This obviously represents a very small fraction of the surface compared with the central area available for surface aeration which therefore explains the sharp drop in surface aeration with sparging reported by Nienow et al [47].

At higher gas flow rates (generally above 0.5 vvm) for all geometries used, the large number of gas bubbles bursting through the free liquid surface results in a frothy surface condition.

The surface movement is clearly very dependent on the bulk flow pattern (Figure 7.1) for combinations of N and Q and a detailed discussion is given in the following section.

7.3 Bulk Flow Patterns

The stages of developing bulk flow patterns, illustrated in Figure 7.1 are summarised as follows:

(a) Negligible dispersion

(b) Gas dispersion in the upper part of the vessel without any radial dispersion in the impeller plane.

(c) Dispersion in the impeller plane reaches the vessel wall with some gas circulation below the impeller plane in the vicinity of the vessel wall.

(d) Extensive mixing in the bulk with gas recirculation back to the impeller.

(e) Secondary circulation loops near the free liquid surface.

These stages are by no means distinct in themselves since for a certain impeller speed between stages (c) and (d), gas recirculation, though not necessarily back to the impeller (see section 7.4.2), is evident. A further distinction for stage (d) can be made by considering the D/T ratio where, for a lower D/T ratio, gas recirculation in the lower part of the vessel maybe absent [48].

The most important transitions from the point of reactor design and operation are a->b, b->c and c->d. In spite of the importance of these transitions, there is great disparity concerning the definitions relating to them, (Table 7.1).

Rushton and Bimbenet [32] have defined the flooding point condition as the transition between Figures 7.1(c) and (b), which is the onset of gas circulation into the lower part of the vessel.

Nienow & Wisdom [28], however, considered the transition between (d) and (c) in Figure 7.1 as the onset of flooding i.e. the vessel is just no longer flooded when for a particular gas rate, the impeller speed is sufficient to bring the gas dispersion to all parts of the tank. The advantage of this definition is that it corresponds closely with the minimum on the N_{PG} versus Flow Number plot.

Oldshue and Connelly [49] refer to the transition between Figures 7.1 (a) and (b) in terms of gas controlled flow patterns and agitator controlled flow patterns and liquid surface movement (i.e the height of the geysers and the diameter of the swell created by a gas controlled flow pattern).

Wiedmann [50], Pollard [51], Roustan and Bruxelmaine [52] and Jiri et al [53] have defined the transition between Figures 7.1 (a) and (b) as the onset of flooding i.e when the stirrer is no longer capable of dispersing the gas.

Recently Warmoeskerken and Smith [48 & 56] have described the transition from Figure 7.1(a) to (b) as impeller flooding to impeller loading. They described Figure 7.1(d) as impeller loading with gas

recirculation. Their definition does not allow for gas recirculation in the upper part of the vessel between Figure 7.1 (c) and (d). They do, however, recogonise (as suggested by Nienow et al [28]) that gas recirculating in the upper part of the vessel may be the major form of recirculation.

The need to carefully define flow patterns in relation to the definitions adopted in this work is quite clear from the above discussion. This is illustrated in Figure 7.3 which includes the minimum impeller speed for gas recirculation, N_{CR} (Section 7.4.2), a transition previously not reported in literature.

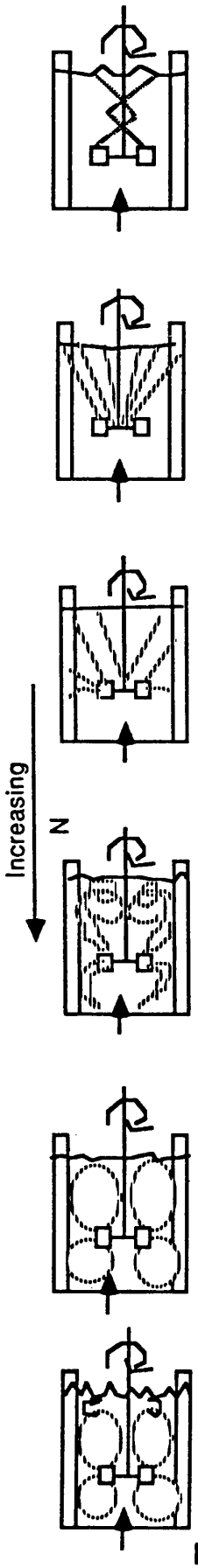

Impeller Flooding

(a)

N_F The transition a to b occurs when the impeller is just no longer flooded, reprsented by N_F which also corresponds to the minimum on the N_{pg} versus Flow number plot - Flooding Point.

(b) Vessel loading without radial flow in the impeller plane

(c) Vessel loading with radial flow in the impeller plane

N_{CR} Minimum impeller speed for gas recirculation (Gas is not recirculated back to the impeller)

(d) Vessel loading with no recirculating of gas back to the impeller

N_R Gas recirculating back to the impeller corresponding to the maximum on the N_{pg} versus Fl plot

(e) Vessel Flooding. Extensive back mixing. (For smaller D/T ratio gas recirculation below the impeller may be absent [48]

(f) Secondary gas circulation loops only possible at very high agitation rates

Figure 7.3 Bulk Flow pattern at constant Q

7.4 Recirculation

The recirculation of gas commences when the liquid velocity in the bulk of the tank is sufficiently high to carry gas bubbles back towards the impeller region. The impeller speed at which gas recirculation commences is referred to as N_{CR}. This increases the residence time of the gas bubbles and hence the gas holdup. Increasing the impeller speed beyond N_{CR} causes the gas recirculation loop to advance closer to the impeller. Eventually the recirculating gas flow reaches the trailing vortices behind the impeller blades and coalesces with it. The impeller speed corresponding to this condition has been defined as N_R, the impeller speed above which the sparged gas passing through the impeller is supplemented by gas from the bulk recirculation loops. This coincides with the maximum on the N_{PG} versus the Flow Number plot.

The transitions represented by N_{CR} and N_R (Figure 7.3) are of greatest importance in relation to surface movement. The main distinction between N_{CR} and N_R is that while N_R affects power consumption, N_{CR} has essentially no effect. This may explain why N_{CR} has previously been difficult to evaluate and consequently why it has not been reported in the literature.

7.4.1 Literature Review

Generally, industrial mixing operations are performed at impeller speeds greater than N_F. However the determination of N_F for reactor operation and design is most important. Numerous investigations have been made on the flooding point condition [7,28,32,44,48,50 to 59], N_F, or the minimum agitation speed (N_S) required for good dispersion as defined by Westerterp [60,61] and Van Dierendonck et al [54]. While they all refer to the same transition, Figure 7.3 a to b, the most significant difference between the correlations is the dependency, or not, of the transition point on the sparged gas flow rate, Q. There is, therfore, a need for more investigation of this transition point. However, this is not within the scope of this study and the reader should refer to the references given above.

In spite of the great importance of recirculation in mixing operations, very few investigations are reported in the literature.

Nienow et al [44] were the first to present a correlation for N_R, (Equaltion 7.1) the impeller speed for gas recirculation. N_R was evaluated from the peak on the N_{P_g} versus Flow Number plots at constant Q. Their

correlation was based on experiments carried out in a range of vessel sizes up to 1.83m diameter.

$$N_R = 1.5 \frac{Q^{0.2} T}{D^2} \qquad (7.1)$$

Kobbacy [7] working on a 0.21 m. diameter vessel presented Equation 7.2 for N_R.

$$N_R = 0.57 \frac{Q^{0.13} T^{0.97}}{D^{2.34}} \qquad (7.2)$$

where the constant is a function of the average bubble size. For a 0.1M K_2SO_4 solution the value of the constant was 0.48. This correlation is similar to that presented by Nienow et al (Equation 7.1). Apart from the constant being only third of the value in equation 7.1, Kobbacy's correlation indicates a weaker dependence of the sparged gas rate, Q on N_R.

7.4.2 Critical impeller speed for the onset of gas recirculation, N_{CR}

The gassed power number, N_{Pg} increases steadily with increasing impeller speed, from N_F to N_R, representing the minimum and the maximum, respectively, on the N_{Pg} versus the Flow Number plot, at constant Q. Since N_{CR} lies between N_F and N_R, its evaluation is not possible from gassed power measurements. However, there should be a marked increase in the local gas holdups for impeller speeds greater than N_{CR} due to the increased residence time of gas bubbles in the bulk.

Due to the nature of the bulk flow pattern there are necessarily exceptions in certain regions of the mixing vessel where this sudden increase in the local gas holdup will not be evident. The region of the impeller plane is one such case where the local gas holdup increase at N_{CR} is difficult to establish (see section 6.3.10) due to the high flow velocities in this region. Gas circulation in the region below the impeller plane is generally absent before N_R (Figure 7.3) and therefore N_{CR} is not applicable in this region.

Point gas holdups were measured for constant Q with increasing impeller speeds. A number of positions

in two regions of the mixing vessels, the region near the impeller and also near to the free liquid surface were selected. The measurements were made in three mixing vessels (T_{21}, T_{75} & T_{100}) for gas rates of 0.2 - 0.75 vvm.

7.4.2.1 Results and Discussion.

Point gas holdups are plotted against the Flow Number for a range of constant sparged gas rates, Figures 7.4 to 7.27. Generally, for all geometries and combinations of Q and N, the data show a pronounced increase in the local gas holdup below a certain Flow Number. The corresponding impeller speed was found to lie between N_R and N_F determined from N_{Pg} versus Fl number plots at constant Q. The sudden increase in the local gas holdup can only be due to gas recirculation locally. The impeller speed identified by the break point in these curves (Figures 7.4 to 7.27) is referred to as N_{CR} and is defined here as the critical (or minimum) impeller speed for onset of gas recirculation.

Under certain conditions, however, no pronounced increase in the point gas holdups was observed. This was especially the case for the highest sparged gas rates used for T_{75} and T_{100}.

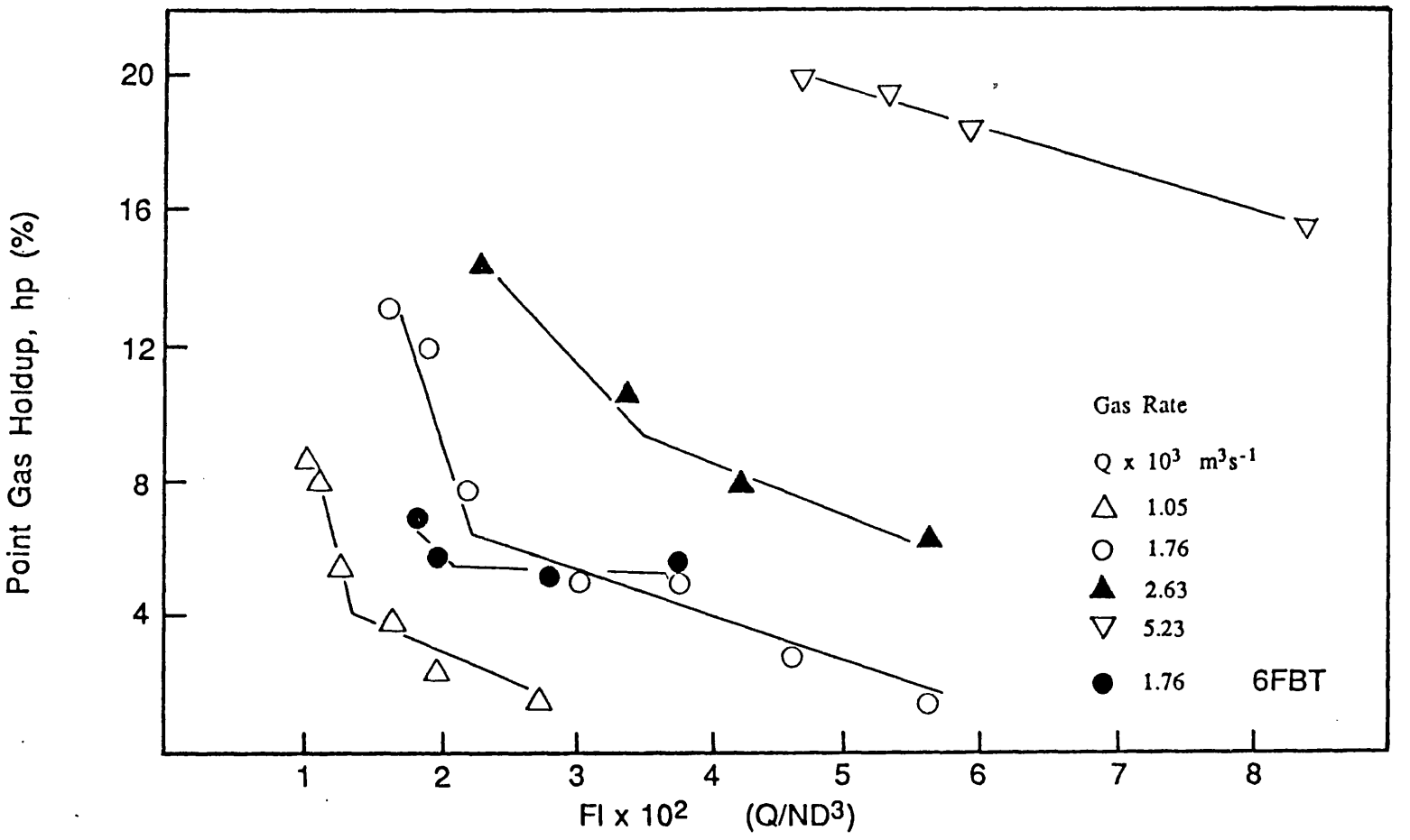

Figure 7.4: Point Gas Holdup Against Flow Number for Position 1.8

T_{75} D/T = 1/3 H = T

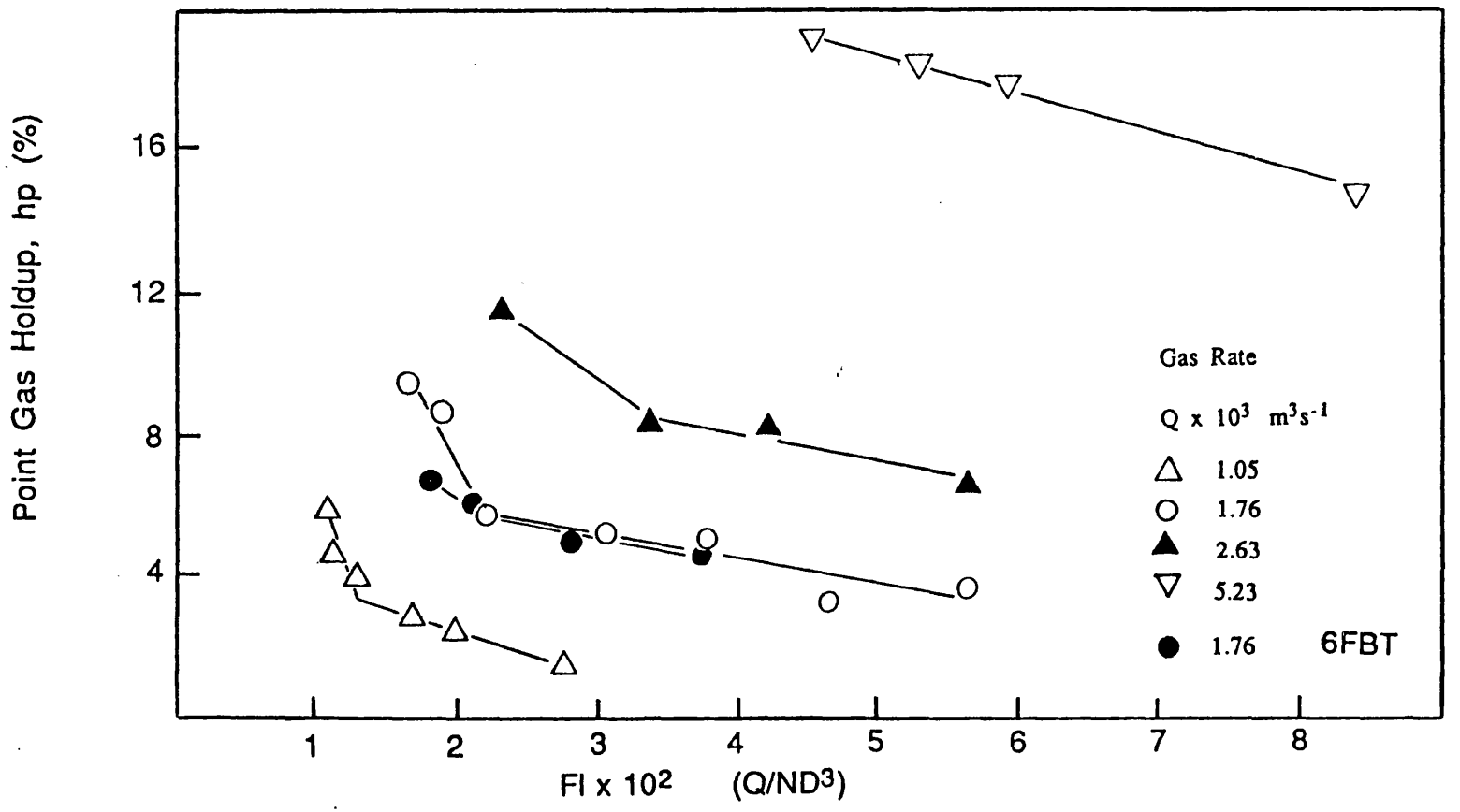

Figure 7.5: Point Gas Holdup Against Flow Number for Position 1.4

T_{75} D/T = 1/3 H = T 6FBDT

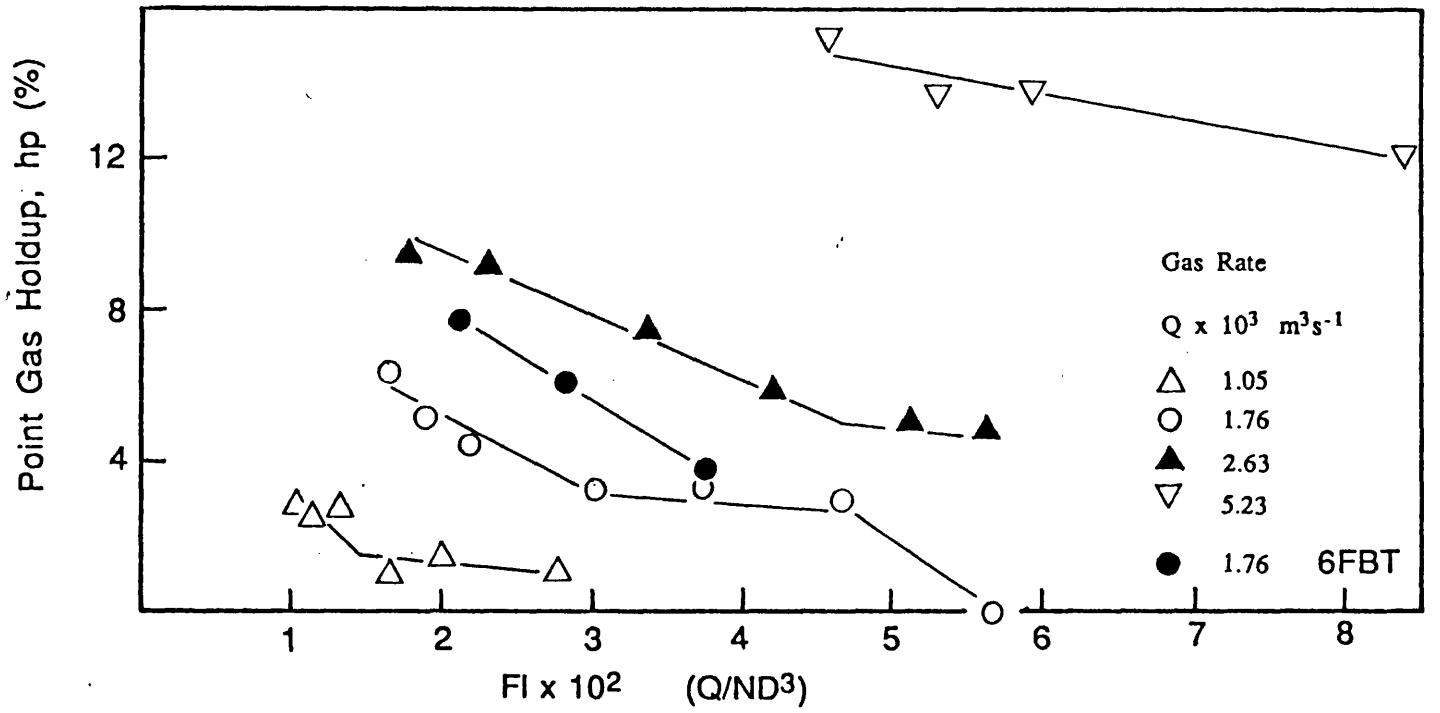

Figure 7.6: Point Gas Holdup Against Flow Number for Position 13.8

T_{75} D/T = 1/3 H = T

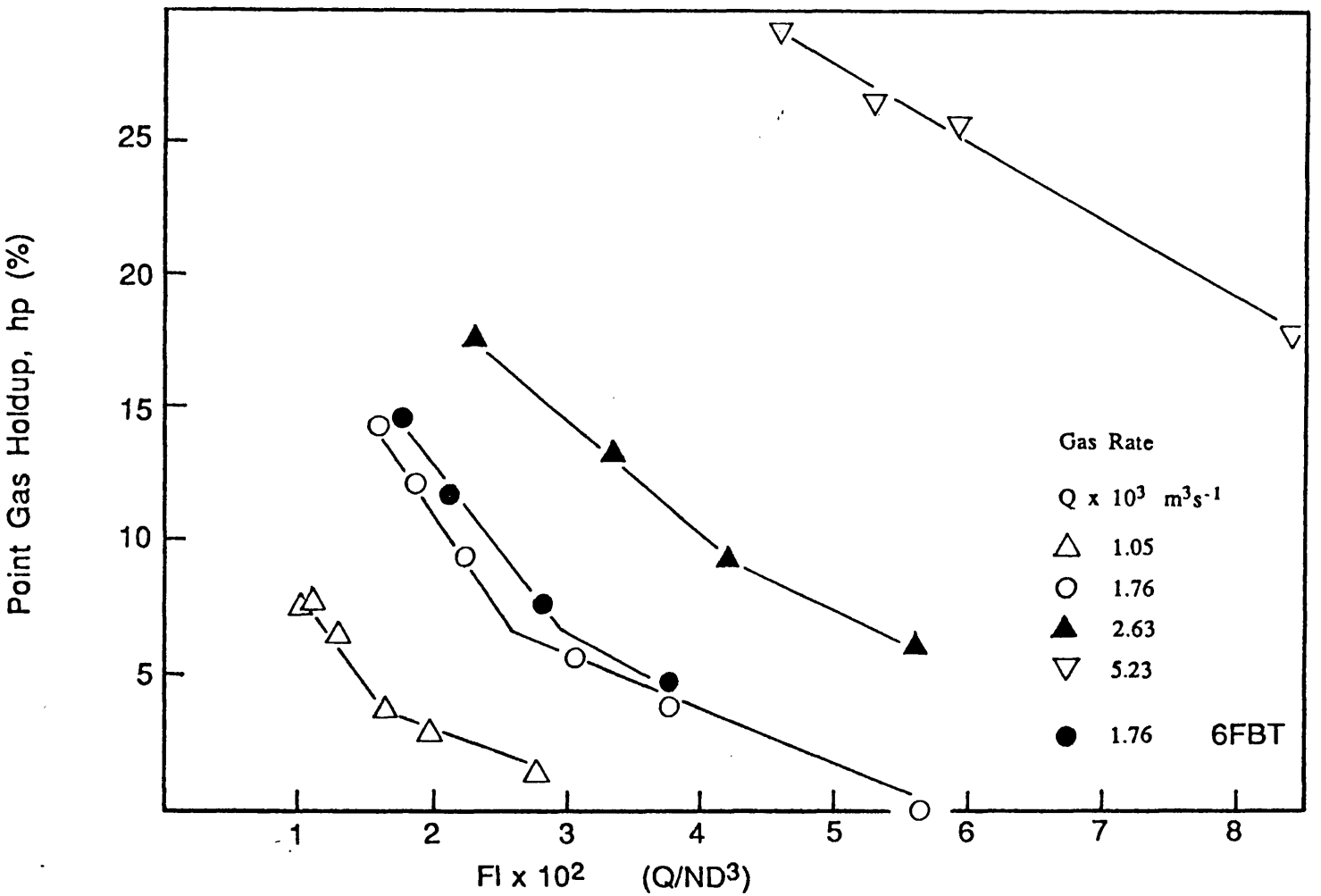

Figure 7.7: Point Gas Holdup Against Flow Number for Position 13.6

T_{75} D/T = 1/3 H = T

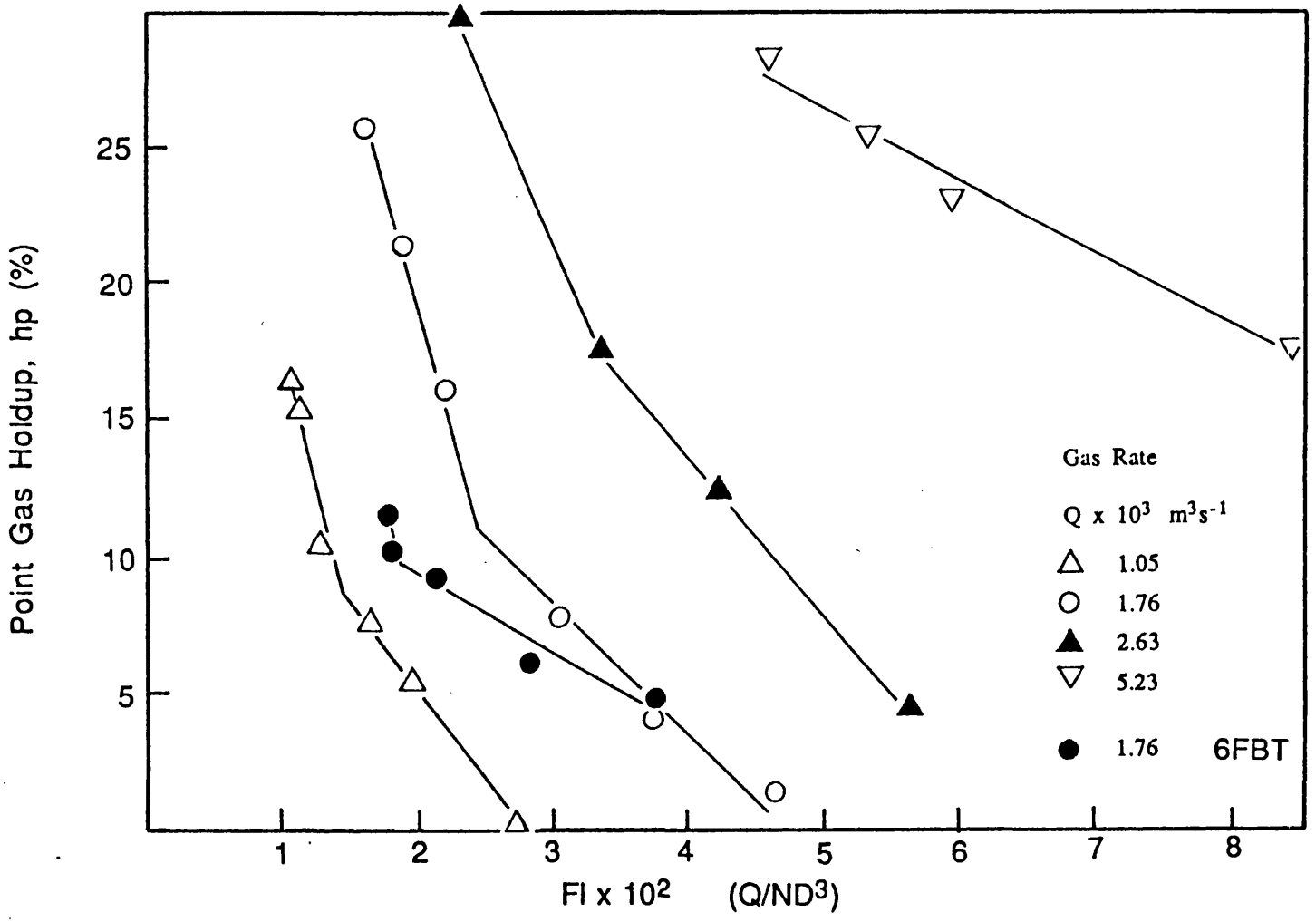

Figure 7.8: Point Gas Holdup Against Flow Number for Position 13.2
T_{75} D/T = 1/3 H = T

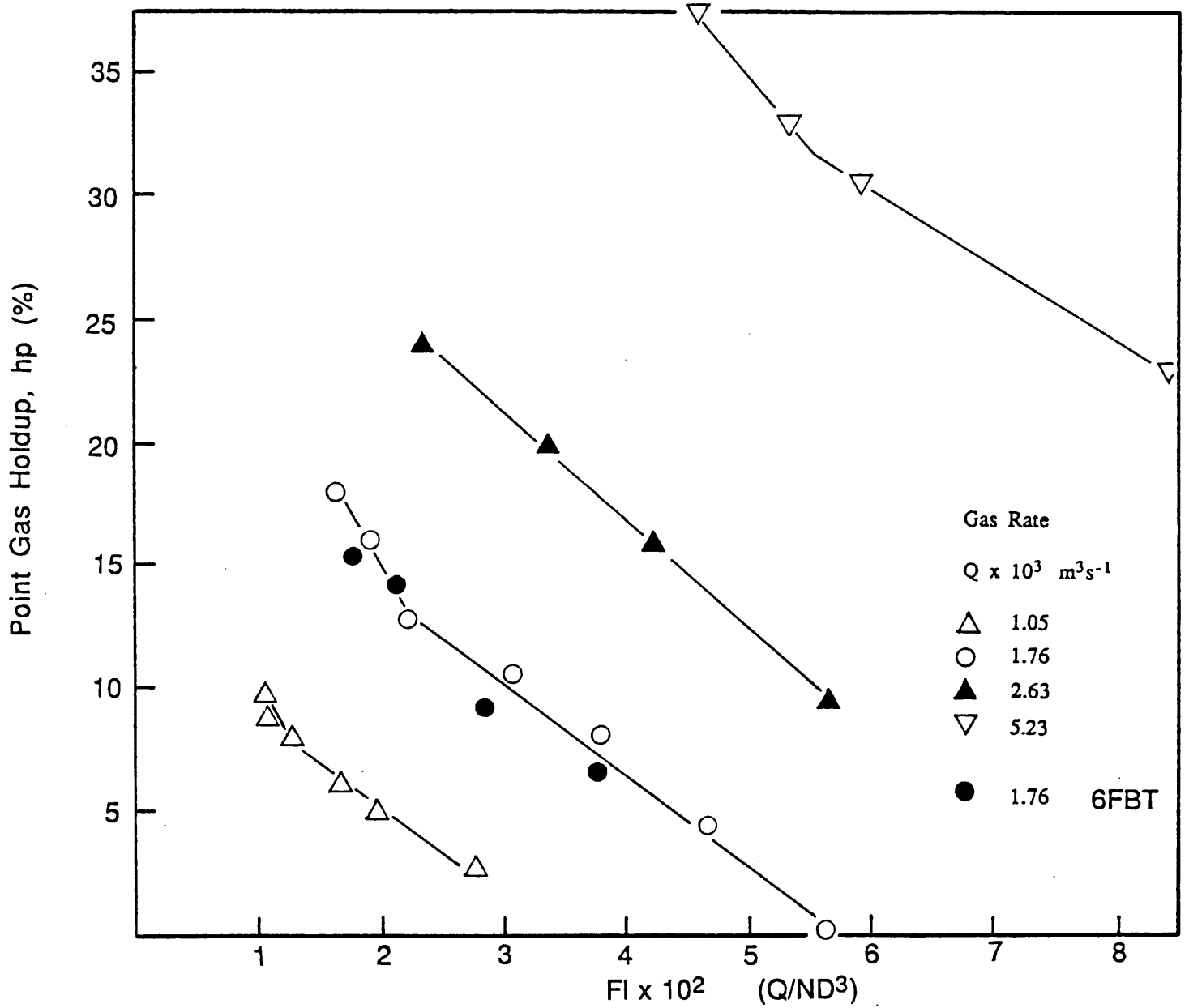

Figure 7.9: Point Gas Holdup Against Flow Number for Position 11.6

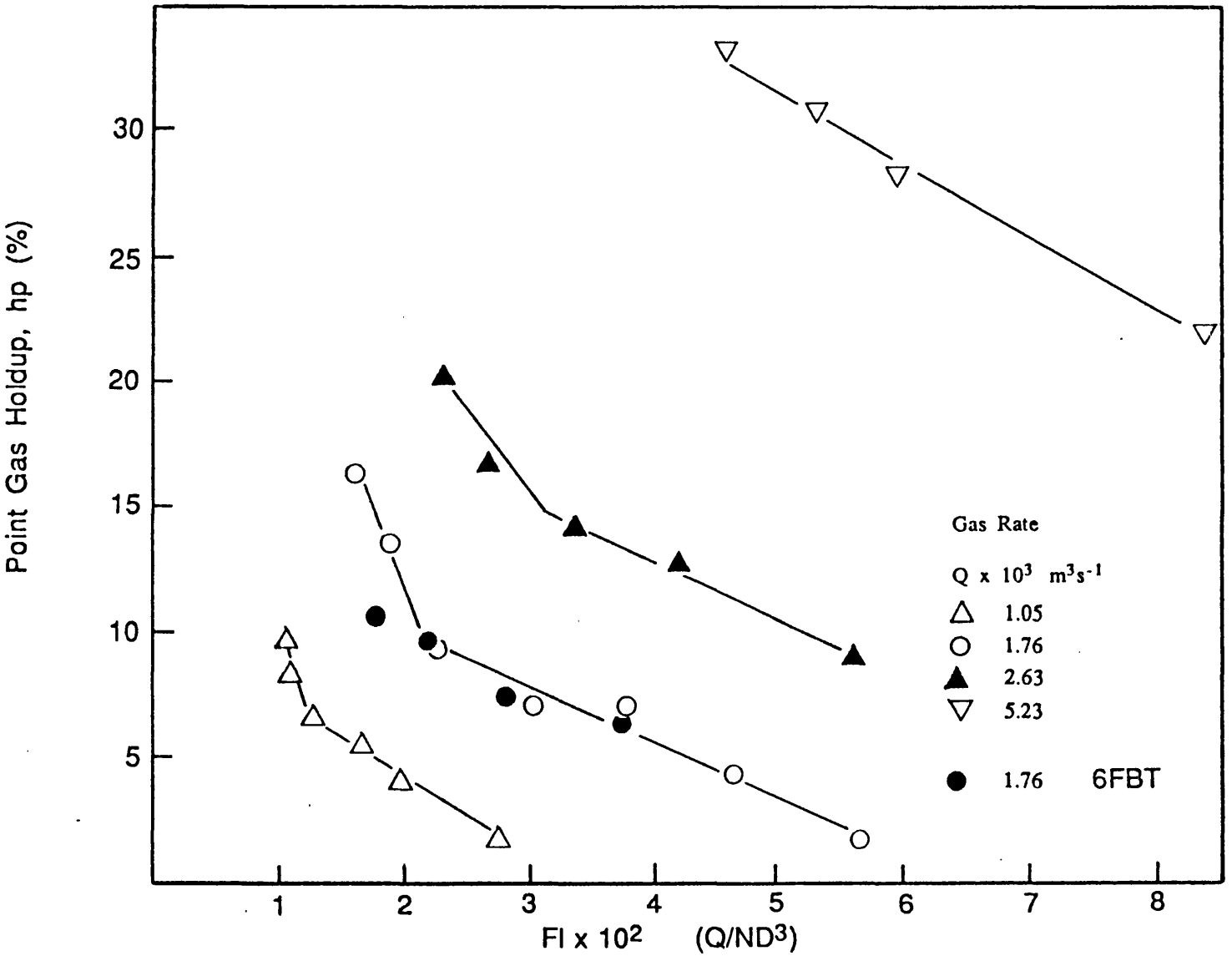

Figure 7.10: Point Gas Holdup Against Flow Number for Position 11.4

T_{75} D/T = 1/3 H = T

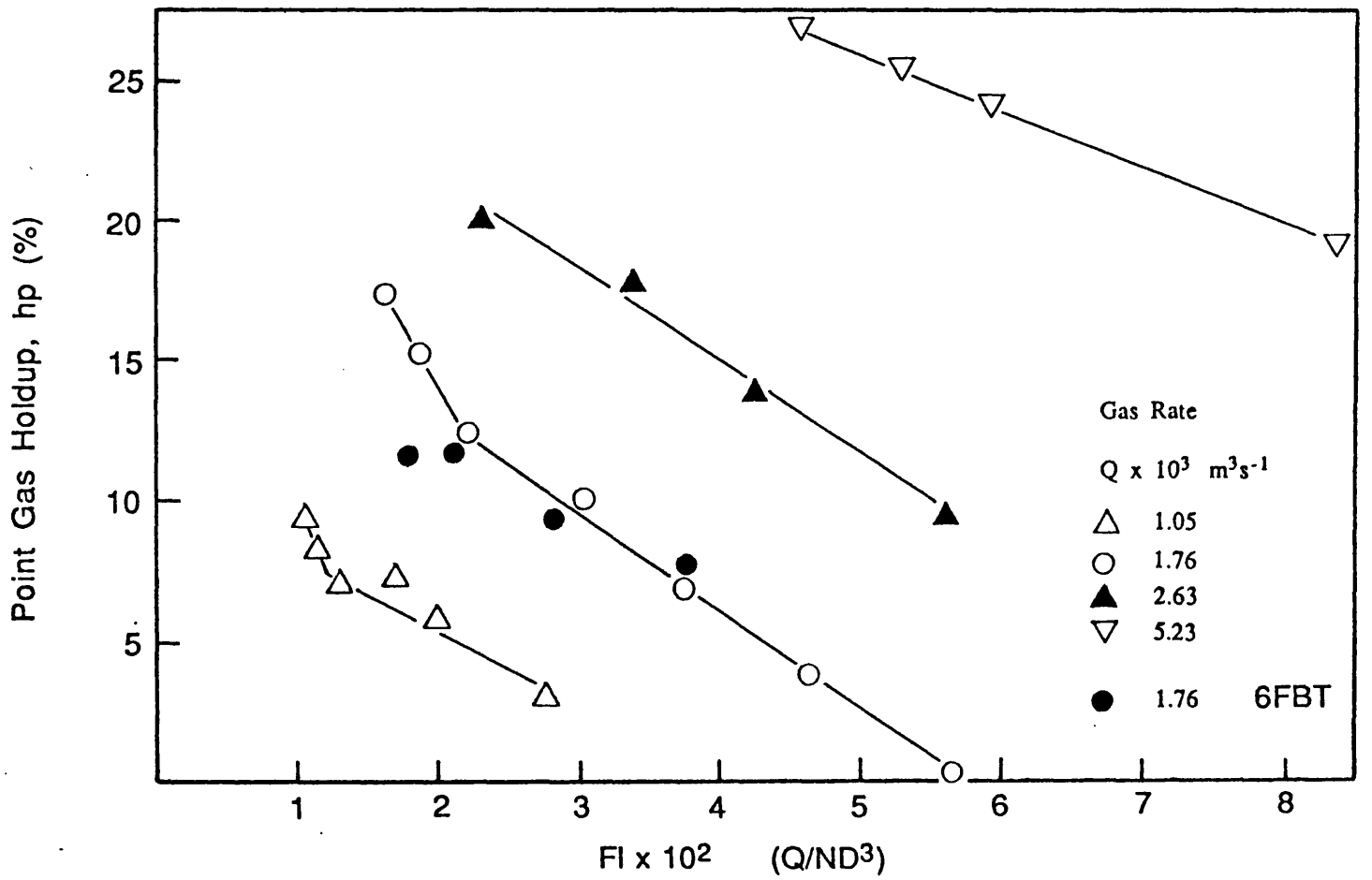

Figure 7.11: Point Gas Holdup Against Flow Number for Position 9.6

T_{75} D/T = 1/3 H = T

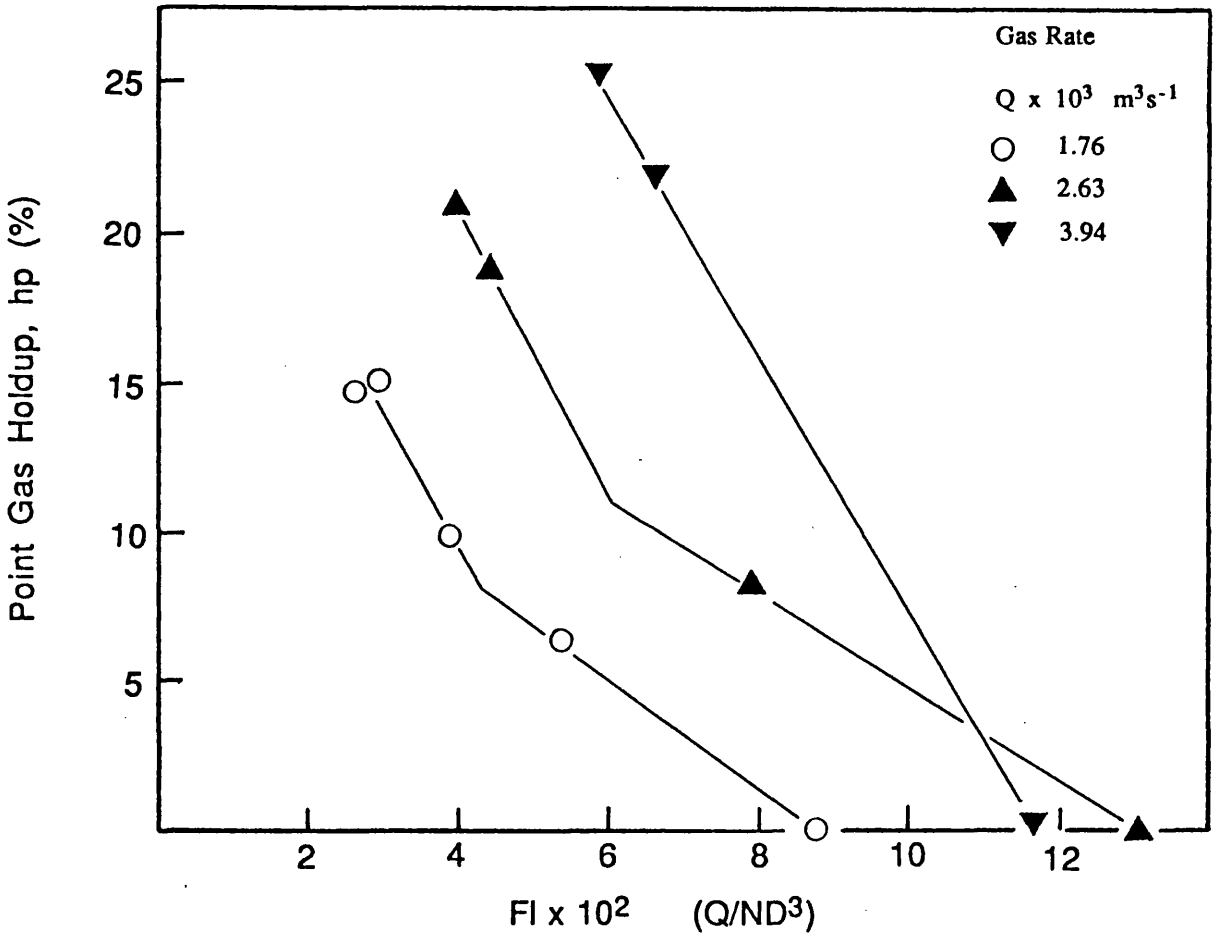

Figure 7.12: Point Gas Holdup Against Flow Number for Position 11.6

T_{75} D/T = 1/4 H = T

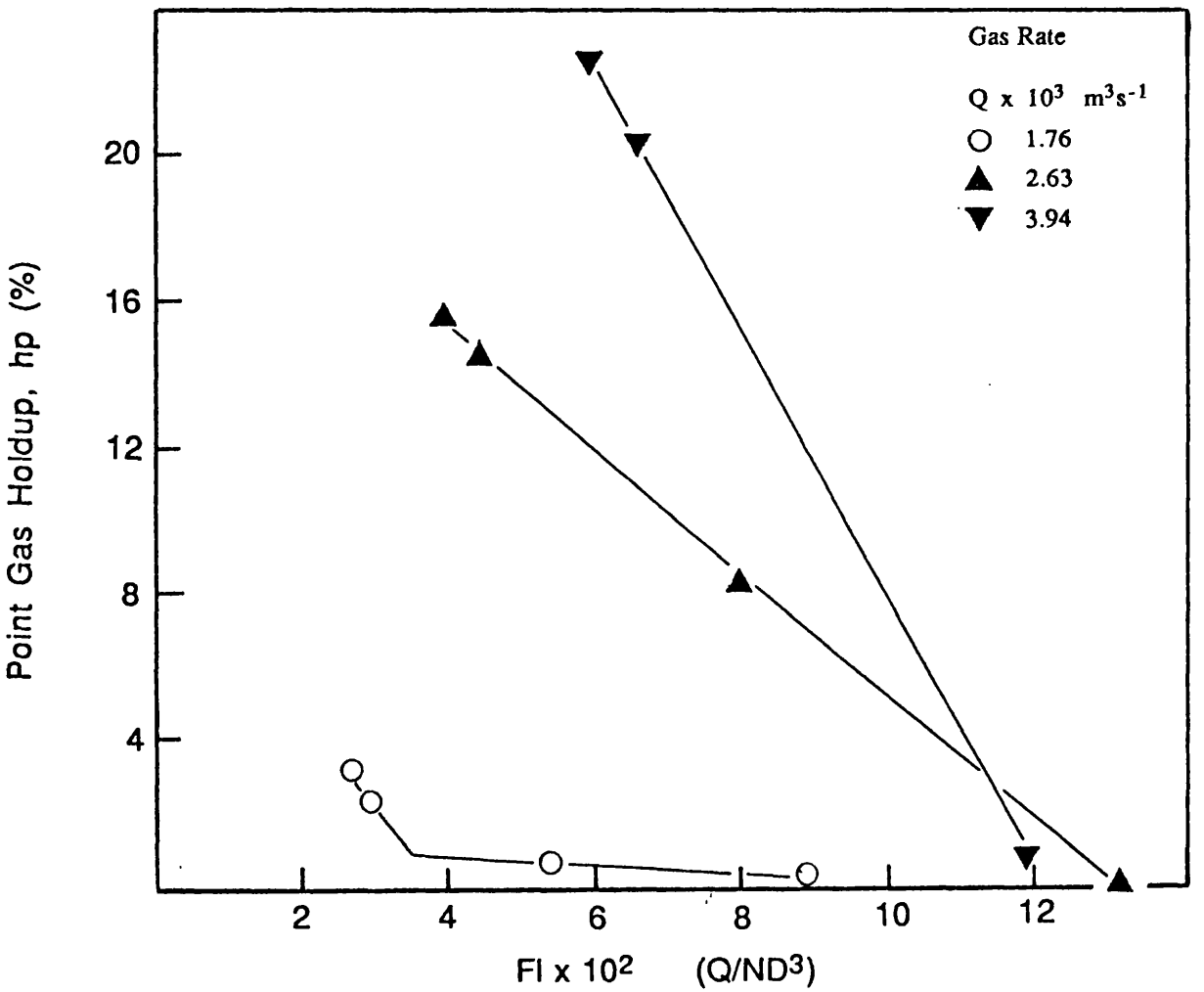

Figure 7.13: Point Gas Holdup Against Flow Number for Position 11.4
T_{75} D/T = 1/4 H = T

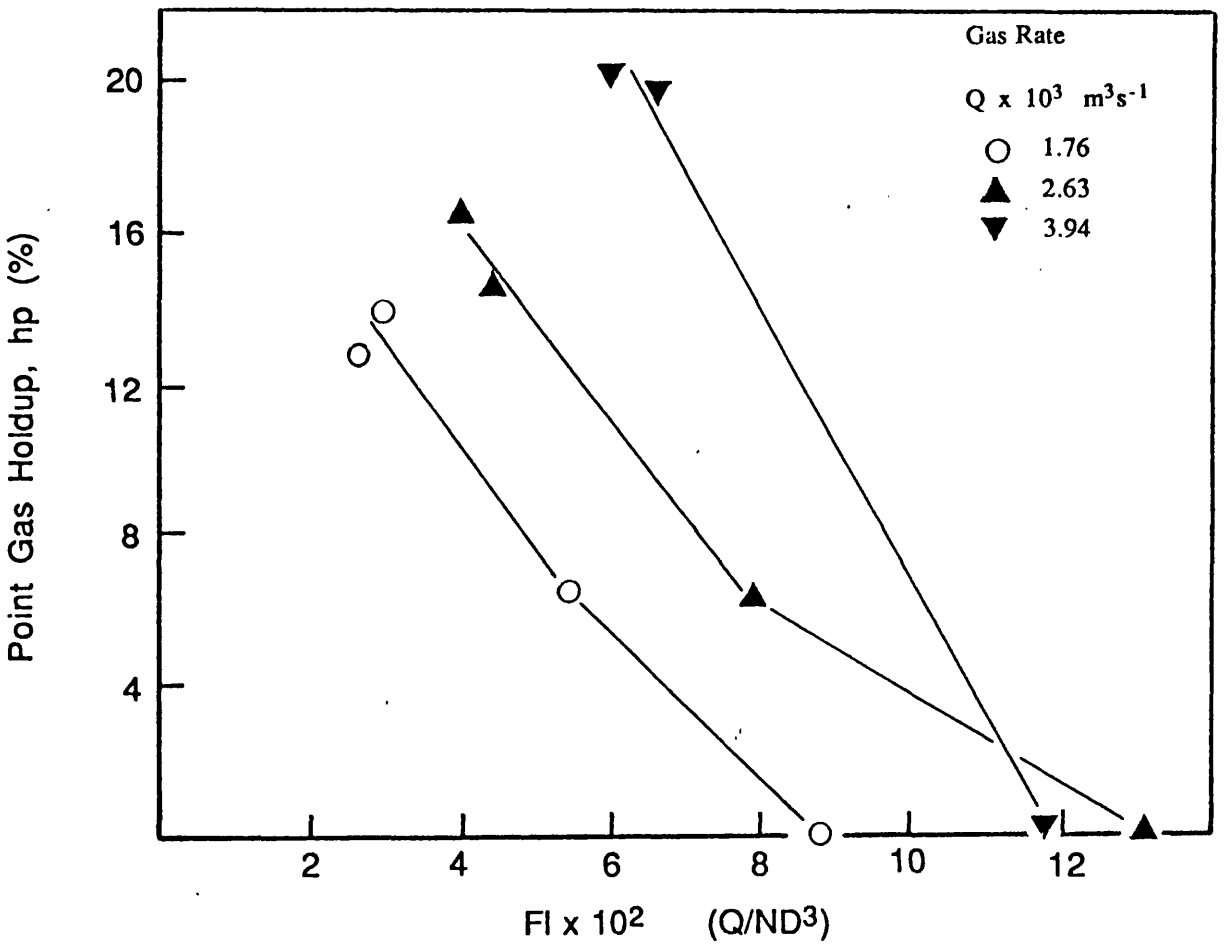

Figure 7.14: Point Gas Holdup Against Flow Number for Position 9.6

T_{75} D/T = 1/4 H = T

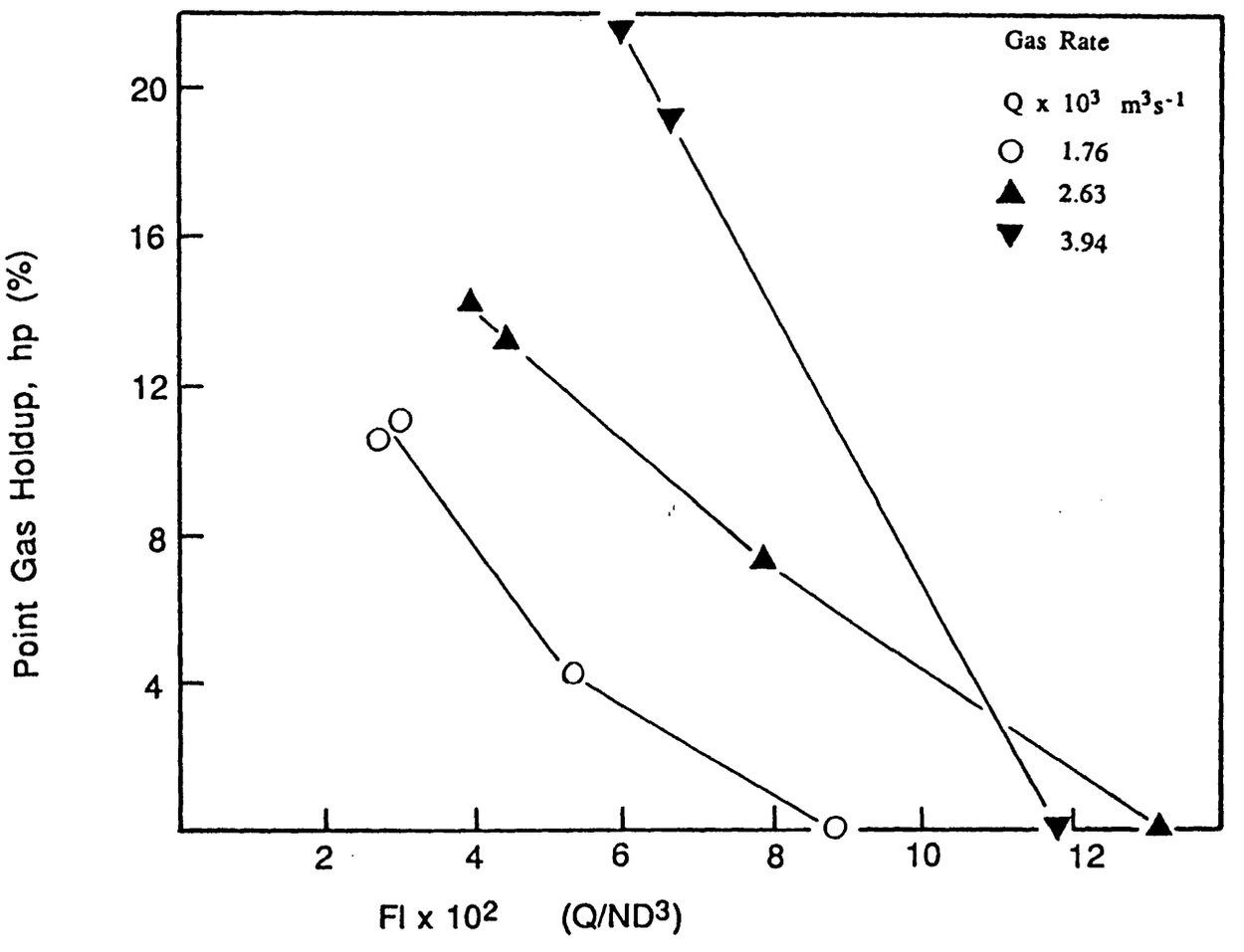

Figure 7.15: Point Gas Holdup Against Flow Number for Position 13.6
T_{75} D/T = 1/4 H = T

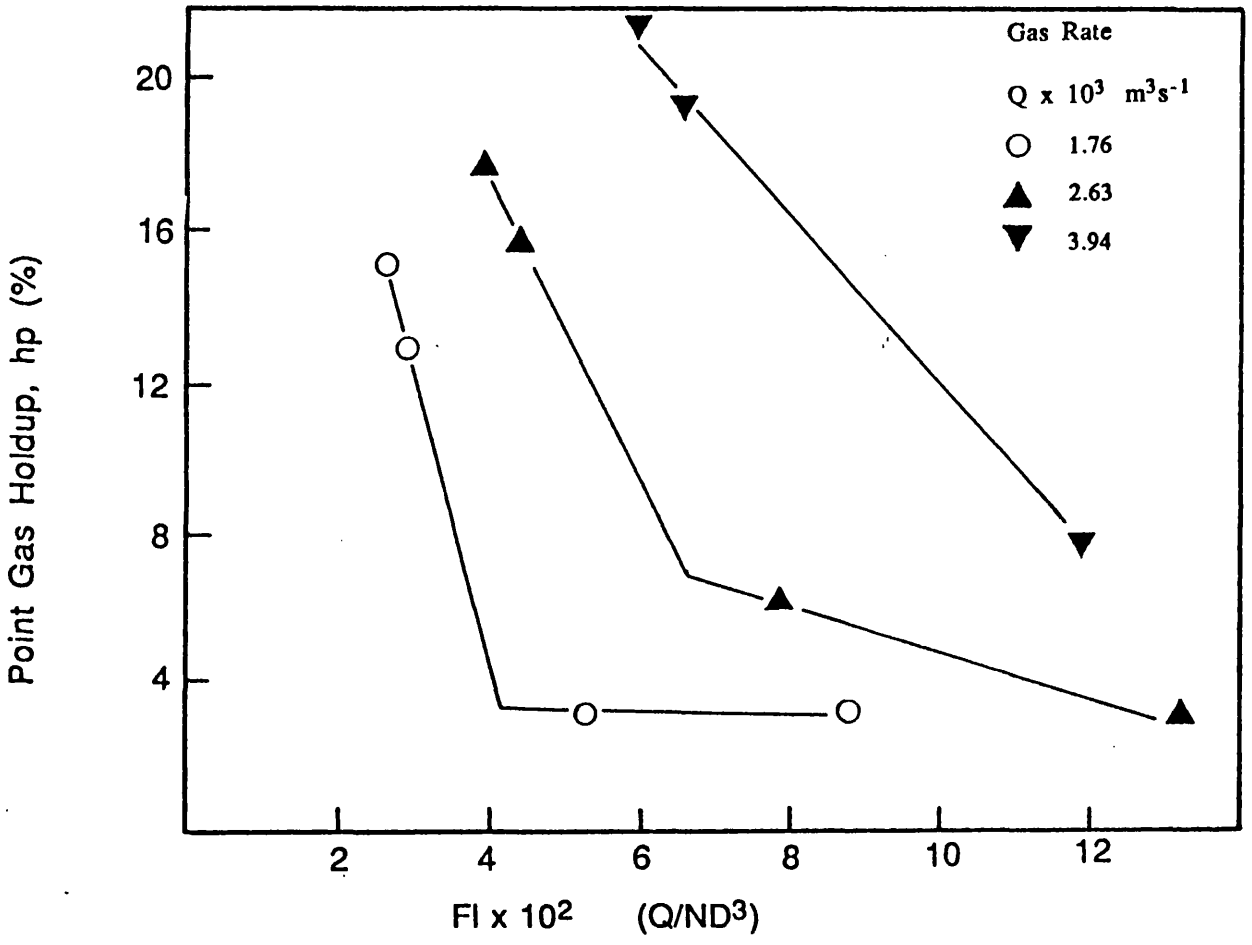

Figure 7.16: Point Gas Holdup Against Flow Number for Position 13.2
T_{75} D/T = 1/4 H = T

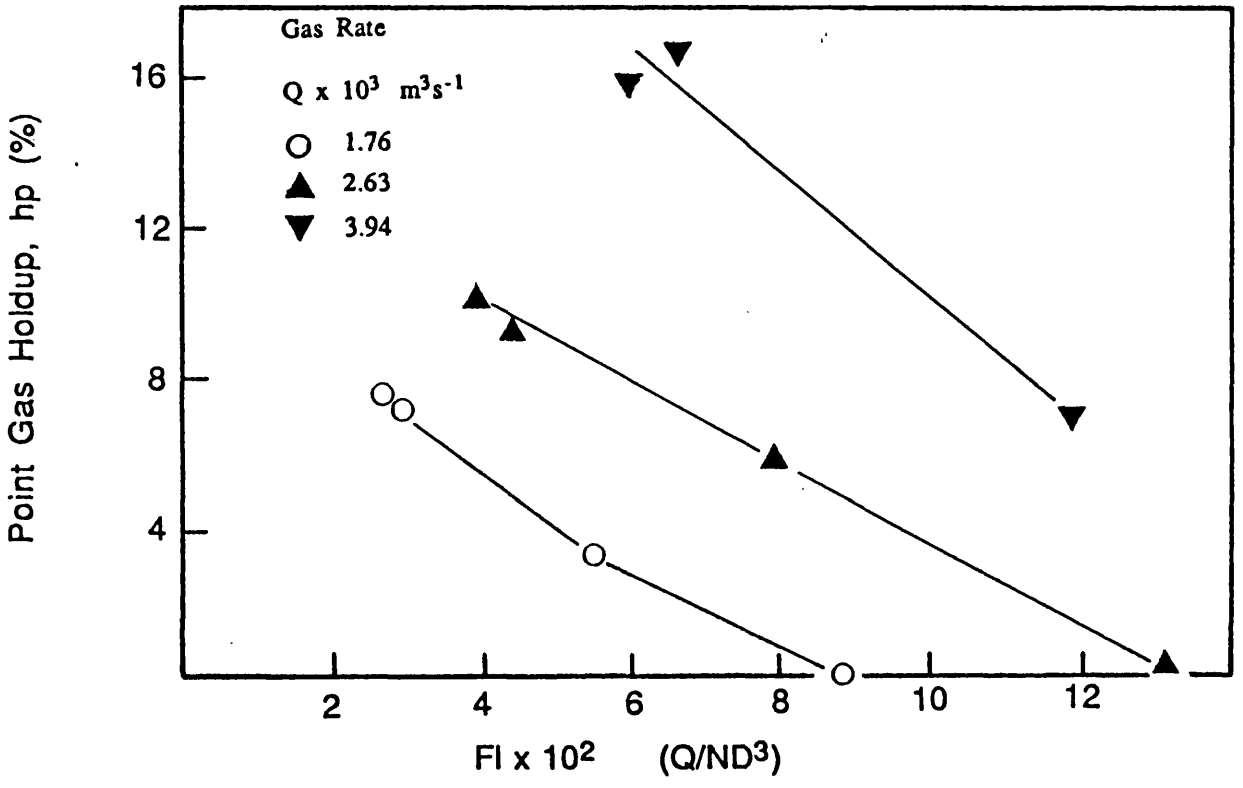

Figure 7.17: Point Gas Holdup Against Flow Number for Position 1.8

T_{75} D/T = 1/4 H = T

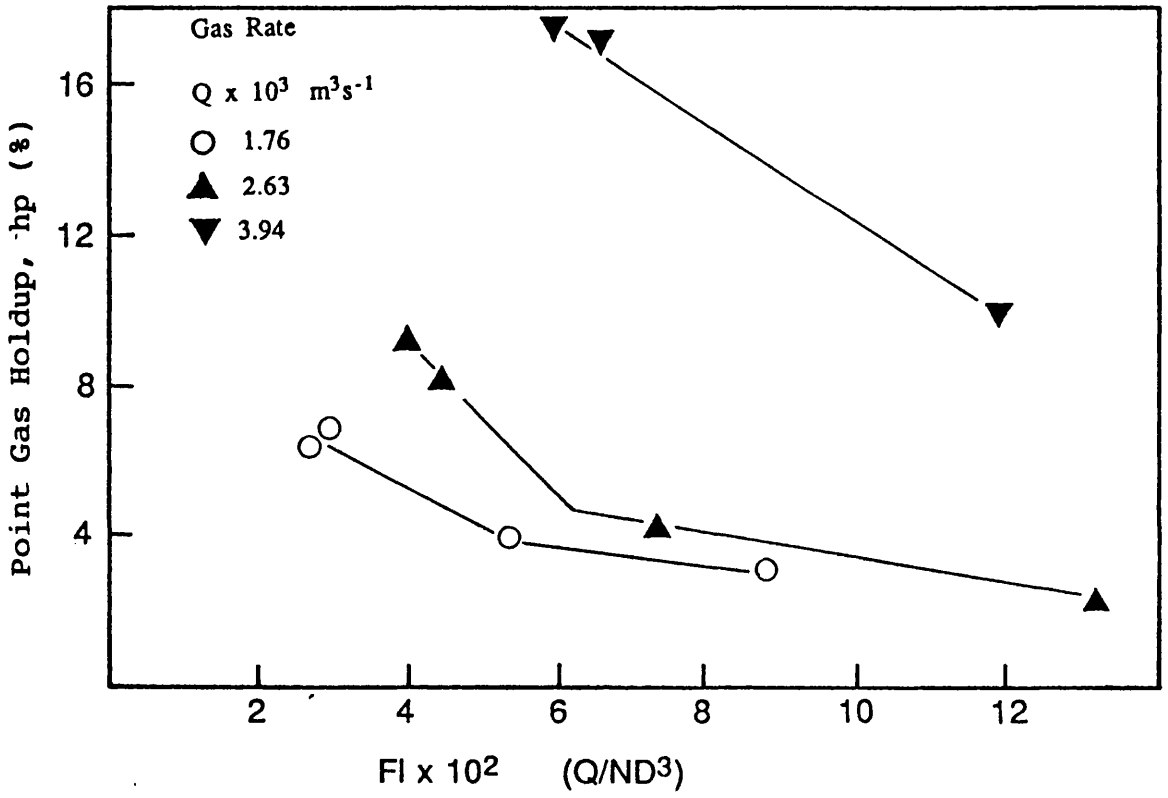

Figure 7.18: Point Gas Holdup Against Flow Number for Position 1.4

T_{75} D/T = 1/4 H = T 6FBDT

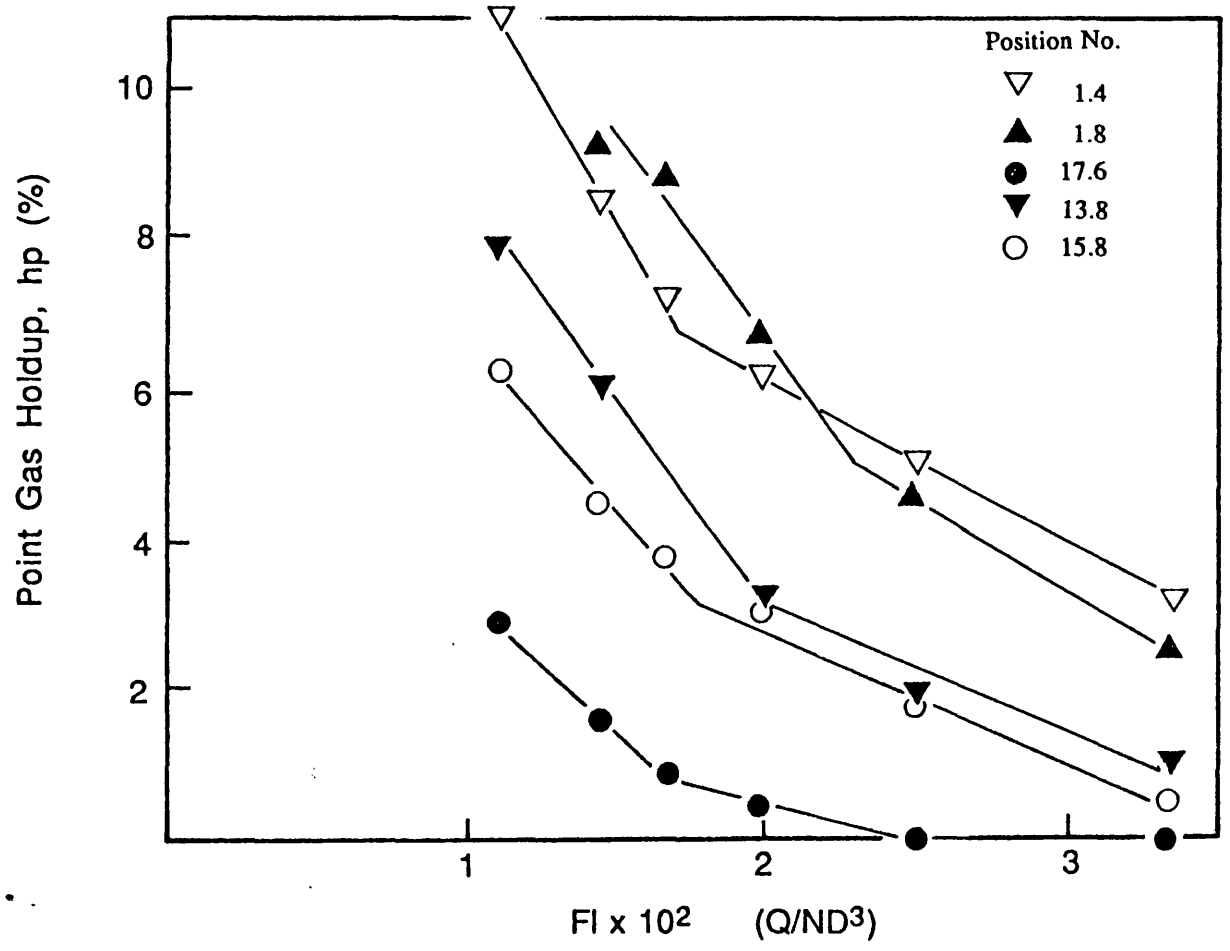

Figure 7.19: Point Gas Holdup Against Flow Number

T_{75} D/T = $^1/_2$ H = T Q = 1.76 x $10^3 m^3/s$ (0.336 vvm)

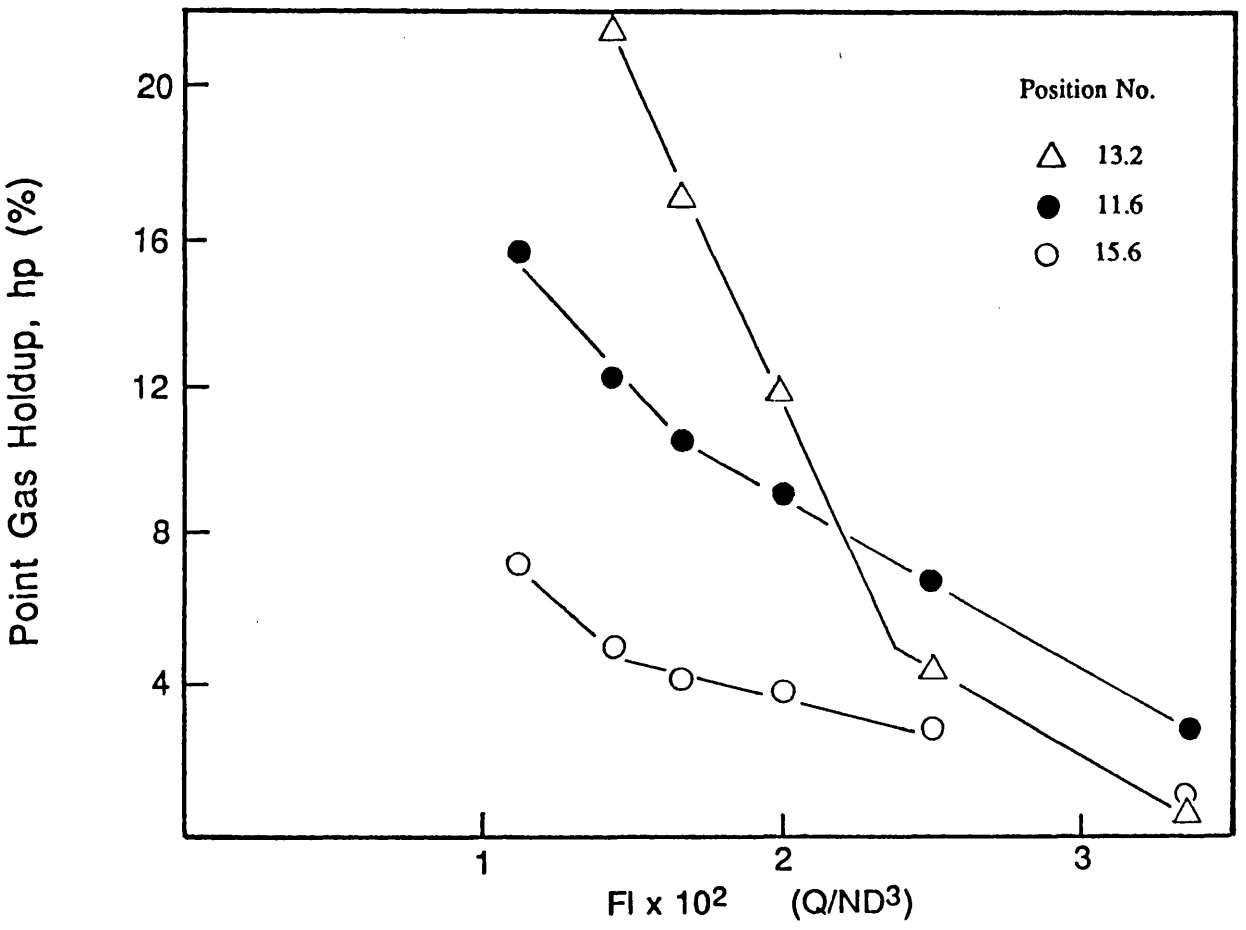

Figure 7.20: Point Gas Holdup Against Flow Number

T_{75} D/T = $^1/_2$ H = T Q = 1.76 x $10^3 m^3/s$ (0.336 vvm)

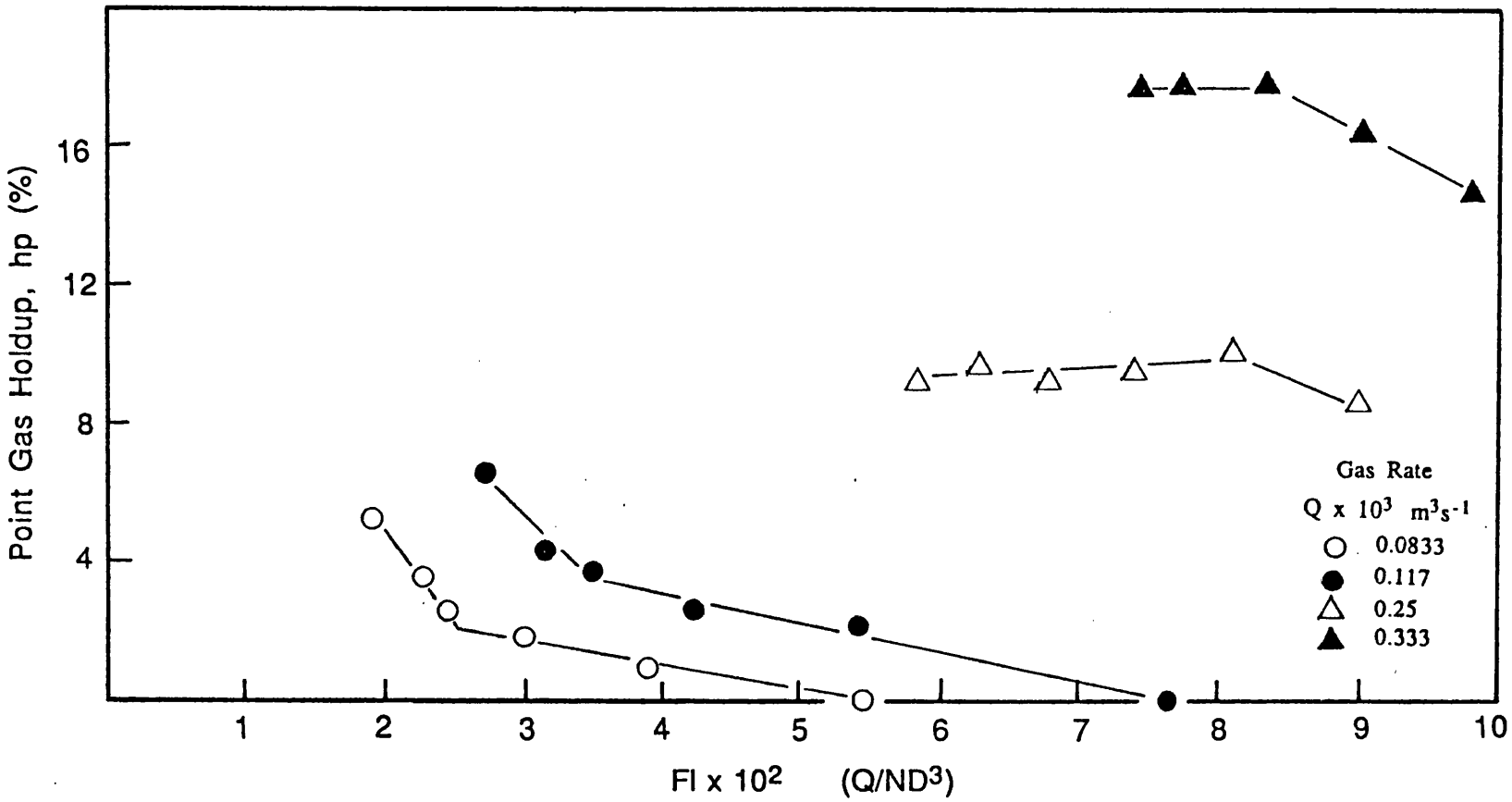

Figure 7.21: Point Gas Holdup Against Flow Number for Position 13.8

T_{21} D/T = 0.32 H = T

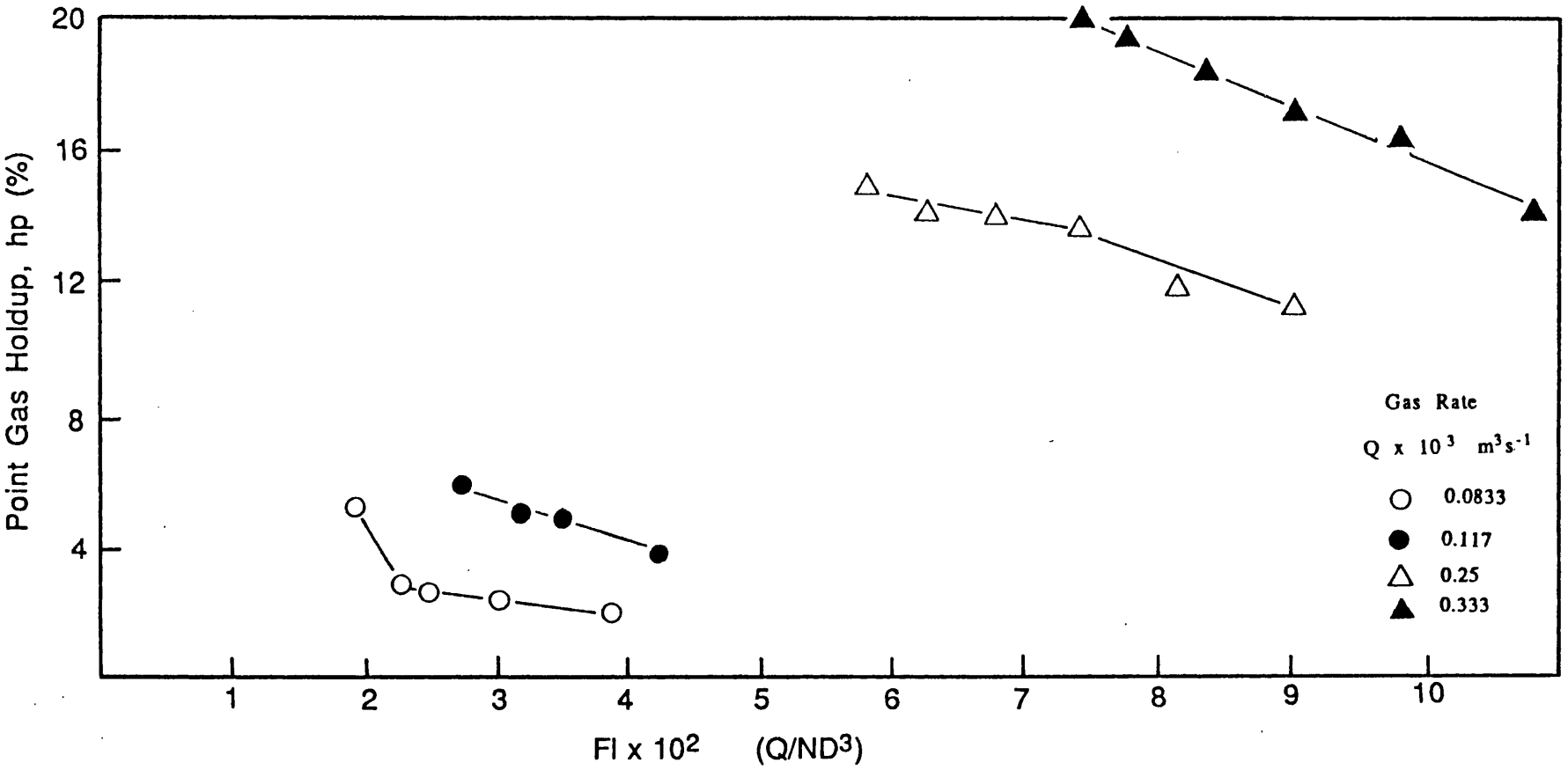

Figure 7.22: Point Gas Holdup Against Flow Number for Position 1.4

T_{21} D/T = 0.32 H = T

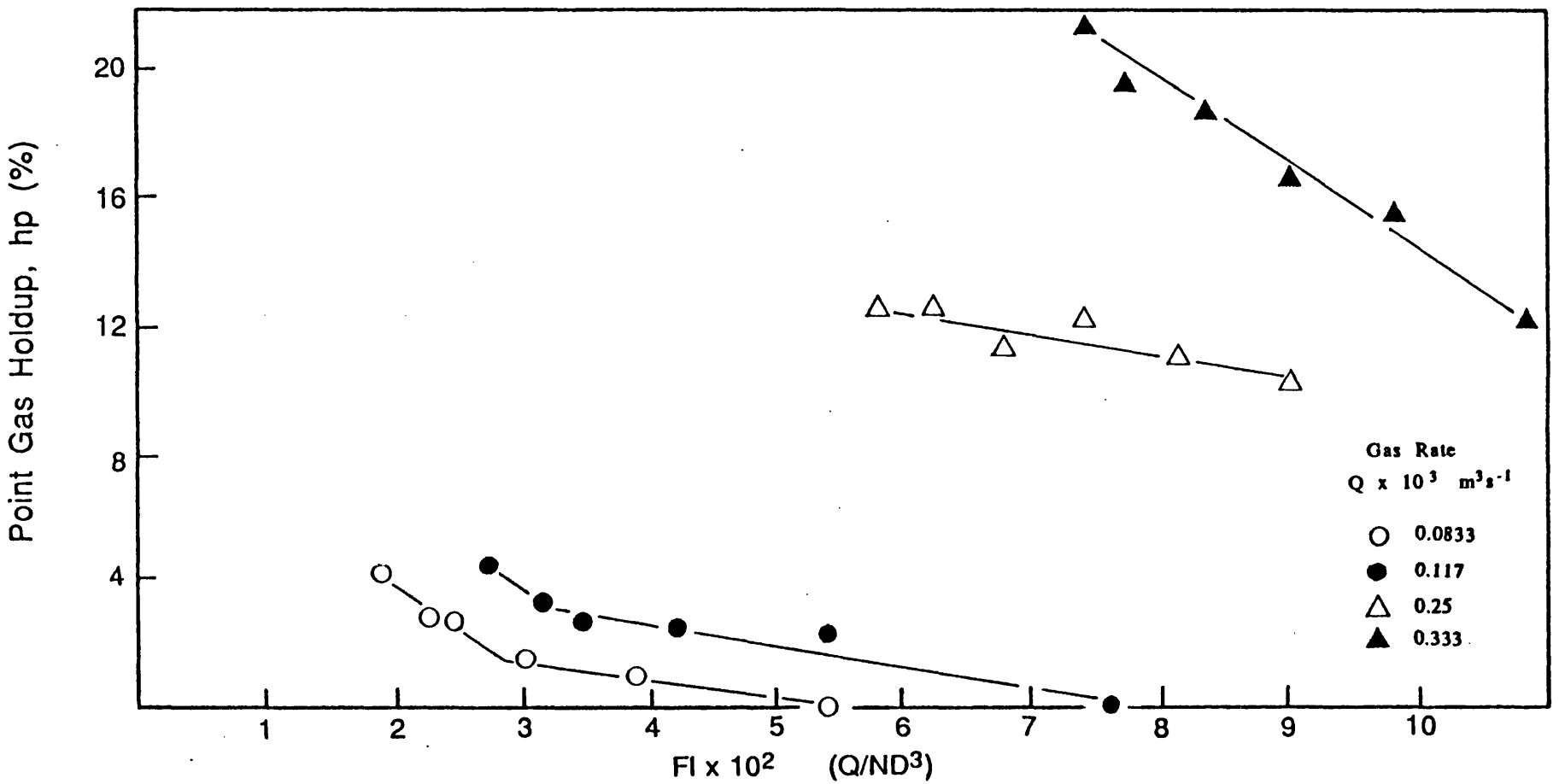

Figure 7.23: Point Gas Holdup Against Flow Number for Position 1.8
T_{21} D/T = 0.32 H = T

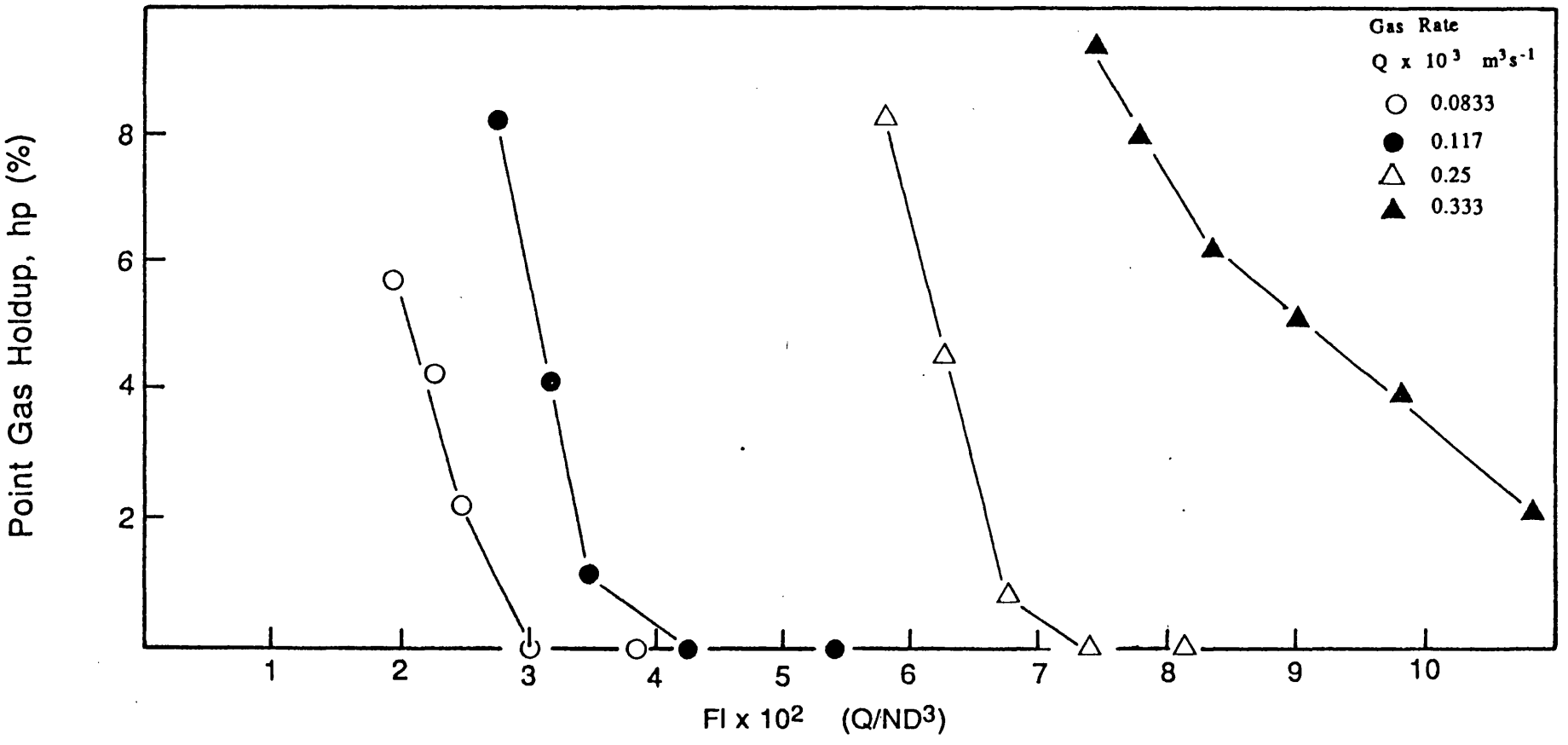

Figure 7.24: Point Gas Holdup Against Flow Number for Position 13.2

T_{21} D/T = 0.32 H = T

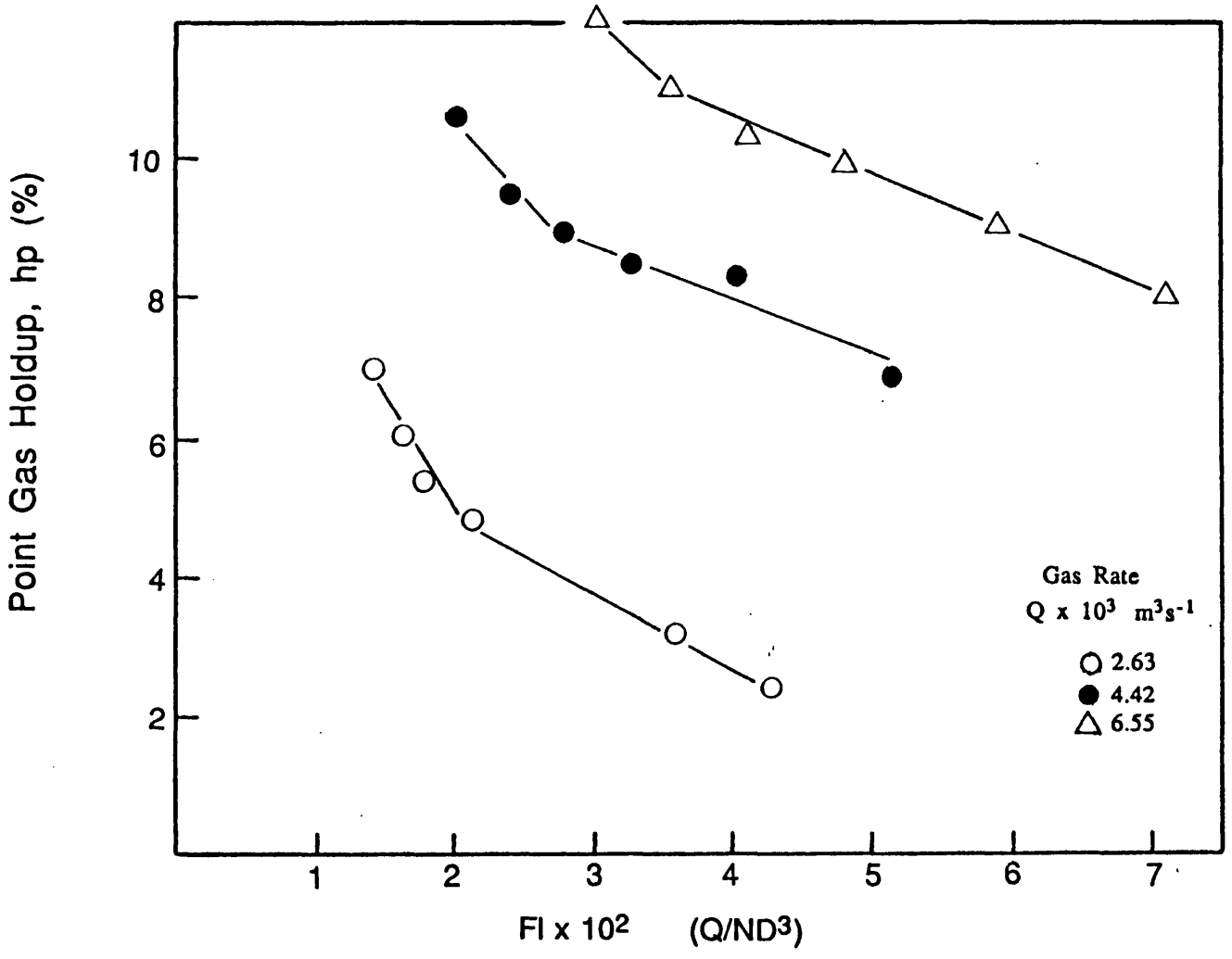

Figure 7.25: Point Gas Holdup Against Flow Number for Position 1.6
T_{100} D/T = 1/3 H = T

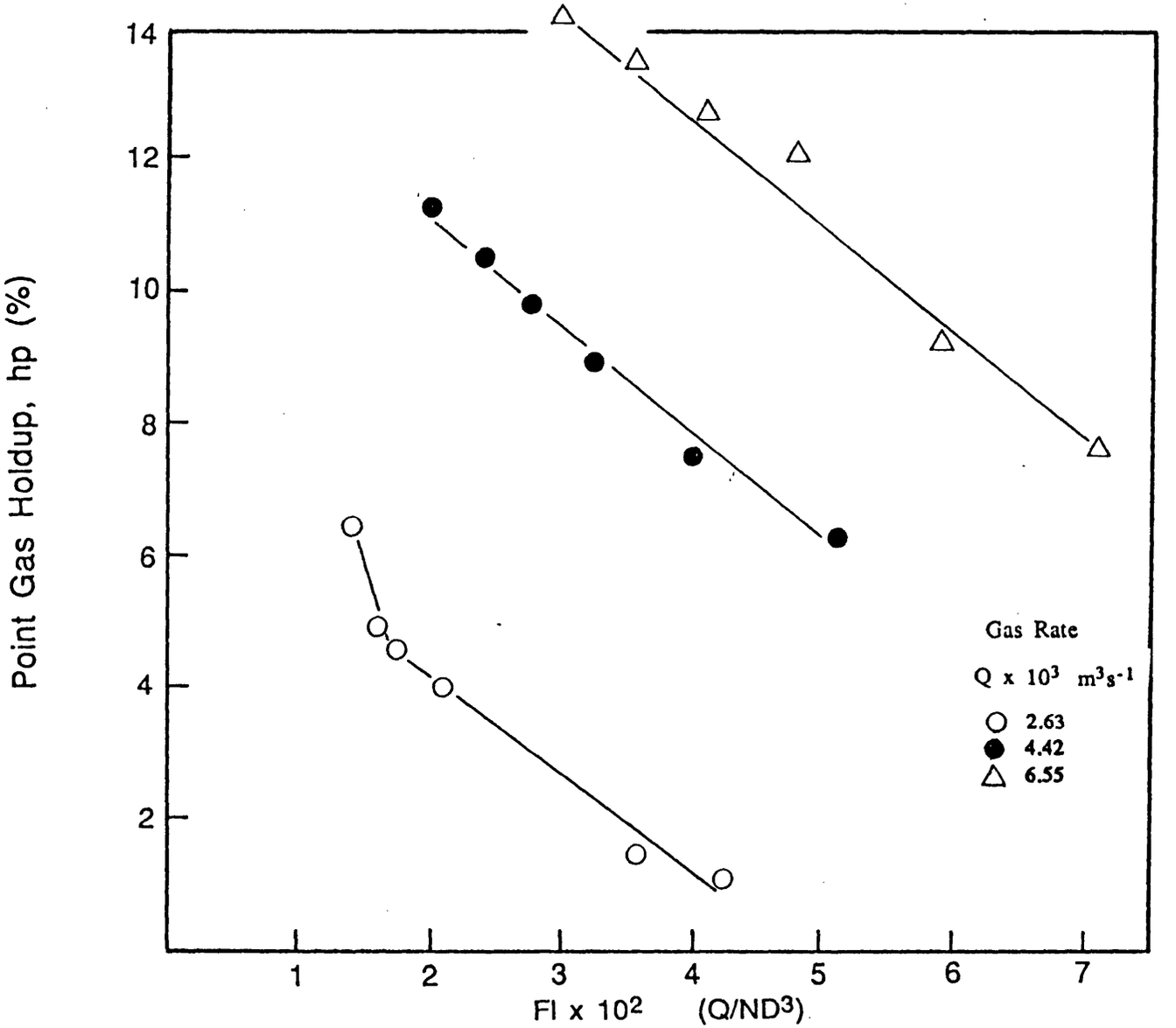

Figure 7.26: Point Gas Holdup Against Flow Number for Position 1.8
T_{100} $D/T = 1/3$ $H = T$

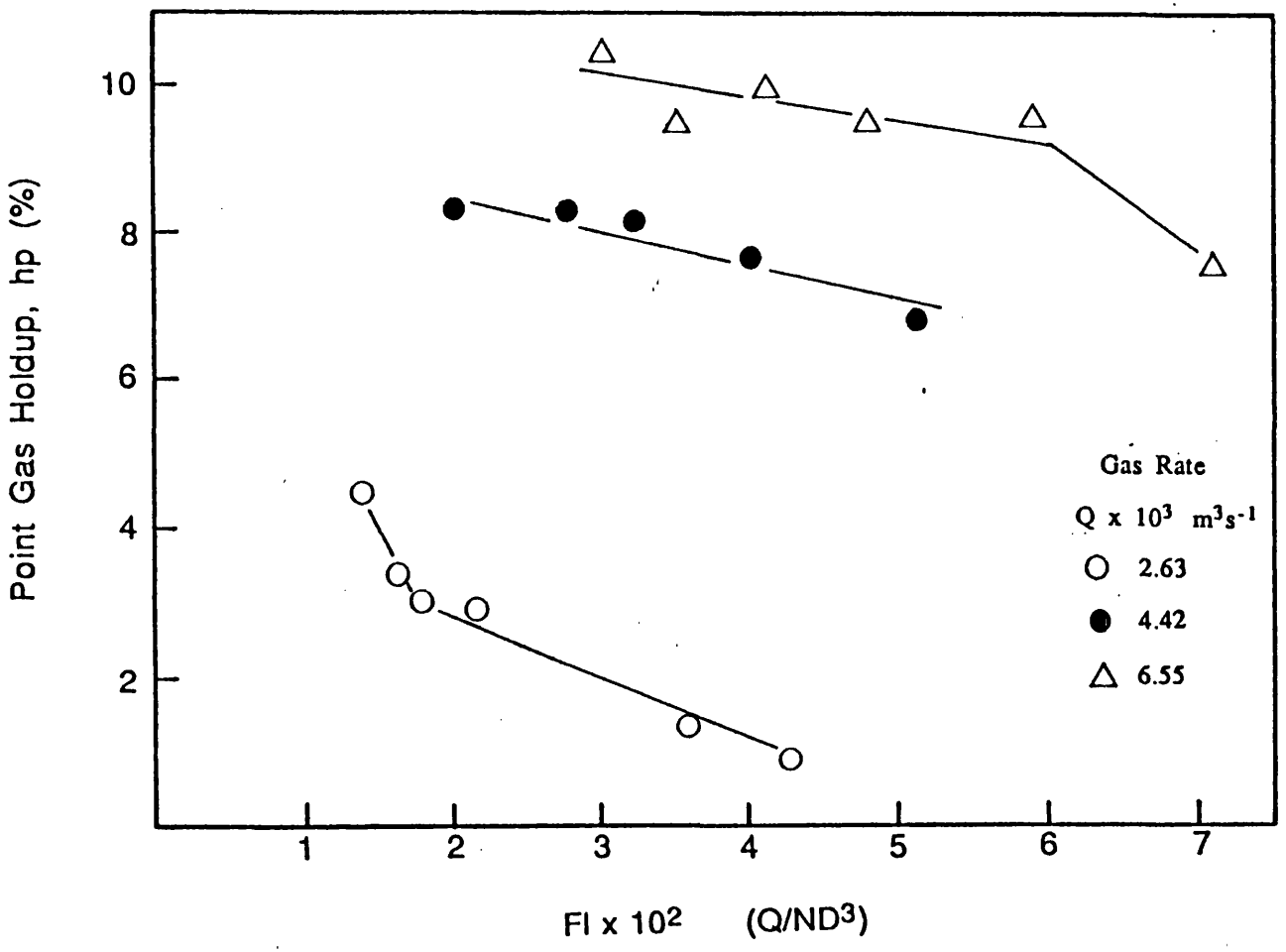

Figure 7.27: Point Gas Holdup Against Flow Number for Position 13.2

T_{100} D/T = 1/3 H = T

It is difficult to explain this trend without investigating even higher combinations of sparged gas rates and impeller speeds. Due to the limitations imposed by the experimental equipment used in this study, this was not possible.

Correlation of N_{CR}:

Correlating N_{CR} with all of the independent variables (Q, D/T, and T) provide the following relationship:

$$N_{CR} = 0.375\ Q^{-0.045}\ (D/T)^{-1.73}\ T^{-0.66} \qquad (7.3)$$

where s = 0.083 R-sq = .896

Table 7.2 Statistics of Equation 7.3

Predictor	Coefficient	St.dev	t-ratio
Constant	0.375	0.198	-2.19
log Q	-0.045	0.0664	-0.68
log (D/T)	-1.73	0.1558	-11.11
log T	-0.662	0,137	-4.8

The low t-ratio for Q (Table 7.2) shows that the sparged gas rate, Q, is not a significant correlating variable. Therefore Equation 7.3 is reduced to:

$$N_{CR} = 0.497 \left(\frac{D}{T}\right)^{-1.72} T^{-0.75} \qquad (7.4)$$

where s = 0.083 R-sq = .895

i.e the accuracy of the correlation is un affected.

Table 7.3 Statistics of Equation 7.4

Predictor	Coefficient	St.dev.	t-ratio
Constant	0.497	0.076	-3.98
log (D/T)	-1.7165	0.153	-11.18
log T	-0.749	0.049	-15.22

The elimination of Q from the correlation greatly improves the significance of the other variables (see t-ratios in Table 7.3) especially that of the vessel diameter T.

As regards surface movement and the mixing of materials added at the surface of the liquid, knowledge of N_{CR} should be useful for reactor design and operation.

7.4.3 Recirculation of gas back to the impeller, N_R

Gas recirculation back to the impeller, represented by the transition in Figure 7.3 d to e, coincides with the maximum observed on the N_{PG} versus Flow Number plots. The corresponding impeller speed is designated N_R.

Where possible, N_R was determined from the maximum on the N_{PG} versus Flow Number plots (Chapter 4). N_R was correlated with the independent variables Q, D/T, and T, Equation 7.5.

$$N_R = 0.648\, Q^{-0.15} \left(\frac{D}{T}\right)^{-2.55} T^{-0.9} \qquad (7.5)$$

where s = 0.061 R-sq = .971

Table 7.4 Statistics of Equation 7.5

Predictor	Coefficient	St.dev.	t-ratio
Constant	0.648	0.32	-0.57
log Q	0.146	0.124	1.18
log (D/T)	-2.55	0.274	-9.3
log T	-0.899	0.218	-4.12

re-arranging Equation 7.5 gives

$$N_R = \frac{0.648\, Q^{0.15}\, T^{1.65}}{D^{2.55}} \qquad (7.6)$$

This correlation is similar to that proposed by Nienow et al [44], Equation 7.1. Their exponents on D and T (2 and 1 respectively) are lower compared with the present findings. The exponent of Q, however, compares well with present results.

Kobbacy's [7] correlation compares well with Equation 7.6 except that there is a greater dependence on T in our case.

Neither Nienow et al or Kobbacy have stated the significance of the correlating variables. The t-ratio for Q (Table 7.4) in Equation 7.6 indicates that it is not a highly significant correlating variable. Eliminating Q from the correlation yields:

$$N_R = 0.28 \left(\frac{D}{T}\right)^{-2.56} T^{-0.66} \qquad (7.7)$$

or

$$N_R = 2.8 \frac{T^{1.9}}{D^{2.56}}$$

where $s = 0.063$ $R\text{-sq} = .965$

Table 7.5 Statistics of Equation 7.7

Predictor	Coefficient	St.dev.	t-ratio
Constant	0.28	0.12	-4.43
log (D/T)	-2.556	0.282	-9.07
log T	-0.659	0.083	-7.93

The correlation of Equation 7.7 is almost unaffected with the standard deviation and R-sq values of 0.063 and 0.965 respectively compared with the values obtained with Equation 7.5. However, the omission of Q from the correlation greatly improves the significance of the remaining variables as shown by the t-ratio values in Table 7.5.

Van Dierendonck [54] and Westerterp [55] presented correlations for the minimum agitation speed for dispersion, or N_F. Although investigating a different transition, their correlations were shown to be independent of the sparged gas flow rate Q which agrees with the present investigation.

7.5 Conclusions

- Surface movement is related to the bulk flow pattern.

- Description of the bulk flow patterns with related definitions of the transitions have been proposed in a modified form.

- A new transition N_{CR} is proposed. This is defined as the minimum impeller speed for gas recirculation.

- N_{CR} has been correlated with the independent variables, Q, D, and T and is shown to be independent of the sparged gas flow rate, Q.

- N_R the impeller speed at which gas recirculates back to the impeller has been correlated with the independent variables, Q, D & T. The sparged gas flow rate, Q is not a significant correlating variable.

- Where materials are added at the surface of the liquid, the agitator should be operated when $N > N_{CR}$.

Chapter 8
RECOMMENDATIONS FOR FURTHER WORK

(1) In the present studies, the range of gas rates used was limited to less than 1.0 vvm in T_{75} & T_{100} (V_m = 1.18 & 0.83 cm/s respectively). However in large scale industrial processes Q can be much higher than this and further work should explore Q up to say 3.0 vvm.

(2) 'Real' liquid systems includes surfactants, suspended solids, higher ionic concentrations and a light 'refluxed' liquid as a second liquid phase. Further work should include such 'real' liquid systems.

(3) The effect of particle size and concentration in three phase solid-liquid-gas systems should be investigated with extension to four phase systems.

(4) Photographic observation of the surface state to study amplitude and frequency of surface turbulence should be made.

Nomenclature

(unless otherwise stated in the text)

a	specific interfacial area	m^2m^{-3}.
C	impeller clearance	m.
D	impeller diameter	m.
d_t	shaft diameter	m.
E_g	overall gas holdup	%.
g	acceleration due to gravity	ms^{-2}.
H, h	height of the unagitated liquid level	m.
hg	height of the aerated liquid	m.
hp	point gas holdup	m.
H	Henry's constant	-
L	length of the impeller blade	m.
N	impeller speed	rps.
P	pressure	Nm^{-2}.
P_{gt}	total power supplied by the impeller plus gas stream	watts.
P_g	gassed power consumption	watts.
P_o	unaerated power consumption	watts.
Q	sparged gas flow rate	m^3s^{-1}.
T	vessel diameter	m.
T_f	friction torque	Nm.
T_t	torque exerted on the impeller	Nm.
T_m	measured torque	Nm.
U_T	bubble terminal velocity	ms^{-1}.
U_s, V_s	superficial gas velocity	ms^{-1}.
V	liquid volume	m^3.
W	width of impeller blade	m.
	density	kgm^{-3}.
	surface tension	Nm^{-1}.
	viscosity of the liquid	Nsm^{-2}.

Subscripts:

g	aerated
o	unaerated
L, l	liquid
CR	critical
F	flooding
R	recirculation

Dimensionless groups:

Fr	Froude Number
N_A	Aeration/Flow Number
N_P	Power Number
N_{Pg}	Gassed Power Number
Re	Reynolds Number
We	Weber Number

REFERENCES

1) EEUA Hanbook No 9, 'Agitator Selection and Design', (1962) Pub. Constable & Co. Ltd.

2) Ruston, J. H., Costich, E.W., and Evert, HJ., Chem. Eng. Prog., 46, Part I p395, Part II p467, (1950)

3) Barona, N., Hydrocarbon Proc., 180, (July 1979)

4) CRC Handbook of Chemistry & Physics. Editor Weast, R.C., 54th Edition (1973)

5) Barigou, M., Bubble size, Gas Holdup and Interfacial area Distributions in Mechanically Agitated Gas-Liquid Reactors, PhD thesis, University of Bath, (1987)

6) Economides, C.A., 'Gas Liquid Mixing in an Agitated vessel', PhD Thesis, University of Bath, (1981)

7) Kobbacy, K.A.H., 'Power consumption and gas dispersion in agitated vessels', PhD Thesis, University of Bath, (1981)

8) Holland, F.A., and Chapman, F.S., Liquid mixing in stirred tanks, Van. N. Reinhold, N.Y., p16.

9) Uhl, V.W., Gray, J.B., 'Mixing, Theory and Practice', Vol 1, Academic Press (1966) N.Y.

10) Nagata, S., 'Mixing - Principles & Applications', Halstead Press, Tokyo, (1975)

11) Calderbank, P.H., 'Physical Rate Processes in Industrial Fermentation', Trans. Inst. Chem. Eng., 36, p443-449 (1958)

12) Riet, K. Van't., Bruijn, W., and Smith, J.M., 'Power consumption with aerated Rushton Turbines', Trans. Inst. Chem. Eng., 52, p88-104, (1974)

13) Riet, K. Van't., and Smith, J.M.," The Behaviour of gas-liquid mixtures near Rushton turbine blades", Chem. Eng. Sci., 28, p1031-1037, (1973)

14) Reit, K. Van't., Boom, J.M., and Smith, J.M., 'Power consumption, Impeller coalescence and Recirculation in Agitated vessels', Trans. Ist. Chem. Engrs., 54, p124-131, (1976)

15) Michel, B.J., and Miller, S.A., 'Power Requirements of Gas-Liquid agitated systems',A.I.Ch.E. Journal, 8, No2, p262-266, (May 1962)

16) Mann, R., Mavros, P., and Middleton, S.C., Fluid Mixing, I. Chem.E.Symp. Ser. 64, pG1, (1981)

17) Loiseau, B., Midoux, N., and Charpenter, J.C., 'Some hydrodynamics and Power Input Data in Mechanically agitated gas-Liquid contactors' A.I.Ch.E. Journal, 23, p931-935, (Nov. 1977)

18) Yung, C.N., Wang, C.W., abd Chang, C.L., Can. J. Chem.Eng., 57, p672, (1979)

19) Clark, M.W., and Vermeulen, T., 'Power requirements for mixing of gas-liquid systems', UCRL - 10996, University of Califonia, Berkeley, (1963)

20) Hassan, I.T.M., and Robinson, C.W., 'Stirred-tank mechanical power requirement and gas holdup in aerated aqueous phases', A.I.Ch.E. Journal, 23, p48, (1977)

21) Hughmark, G.A., 'Power requirements and Interfacial area in Gas-Liquid Turbine Agitated systems', Ind. Engng. Chem. Proc. Des. Dev., 19, p638, (1980)

22) Pharamond, J.C., Roustan, M., and Roques. H., 'Determination de la puissance consomme' dans usse cuve aeree et agitee', Chem.Eng.Sci., 30, p907-912, (August 1975).

23) Luong, H.T., and Volesky, B.,'Mechanical power requirements of Gas-Liquid agitated systems', A.I.Ch.E. Journal, 25, No5, p893, (Sept 1979)

24) Bimbinet, J.J., M.S. Thesis, purdue University, Lafayette, Indiana (1959)

25) Nagase, Y., and Kikuchi, M., 'An empirical formula of power consumption in relation to circulation flow rate in agitated vessels', Journal of Chem. Eng., Japan, 10(2), p164-166, (April 1977)

26) Yamoguchi, I., et al., 'Power consumption of turbine impellers in gas-liquid mixing vessels', Kagaku, 31,10, p1016-1019, 1967

27) Gray, D.J., Treybal, R.E., and Barnett, S.M., 'Mixing of single and two phase systems: Power consumption of impellers.', A.I.Ch.E. Journal, 28, No2, p195-199, (March 1982).

28) Nienow, A.W., and Wisdom, D.J., Inst. Chem. Engrs., 3rd Annual. Res. Meeting, Salford, (1976)

29) Calderbank, P.H., and Figuereido, M., Inst. Symp., Mixing, Mons., C3, (1978)

30) Yoshida, F., and Miura, Y., 'Gas absorption in agitated gas-liquid contactors', Ind. Eng. Chem. Process. Des. Dev. Vol 2, No4, p263-268, (1963)

31) Sridhar, T., and Potter, D.E., Ind.Eng.Chem. Fundam., 19,No1,p21, (1980)

32) Rushton, J.H., and Bimbinet, J.J., 'Holdup and flooding in air-liquid mixing', Canadian Journal of Chem.Eng., 46, p16-21, (1968)

33) Foust, H.C., Mack, D.E., and Rushton, J.H., 'Gas-Liquid contacting by mixers', Ind.Eng.Chem., 36 p517, (1944)

34) Machon. V., Vleck, J., Nienow, A.W., and Solomon, J., 'Some effects of Pseudoplasticity on Holdup in aerated vessels., Chem.Eng., J., 19, p67-74, (1980)

35) Lee, J.C., and Meyrick, D.L., Trans. Inst. Chem. Engrs., 48, pT37, (1970)

36) Hienze, J.O., A.I.Ch.E. Journal, 1, No3, p289, (1955)

37) Calderbank, P.H., British Chem. Eng., 1, 206, (1951)

38) Gardinar, J.A., Instrum. Practice, 18, p353-356, (1964)

39) Linneweber, K.W. and Blass, E., Ger. Chem.Eng. Vol 6, No1, p28-33, (1983)

40) Burgess, J.M., and Calderbank, P.H., Chem.Eng.Sci., 30, p743, (1975)

41) de Figueredo, M.M.L., Phd Thesis, University of Edinburgh (UK), (1978)

42) Weiland, P., Brentrup, L. and Onken, U., Ger. Chem.Eng., 3, p296, (1980)

43) Wisdom, D.S., PhD Thesis, University of London (UK), (1974)

44) Nienow, A.W., Wisdom, D.J. and Middleton, J.E., 2nd Eur. Conf. on Mixing,Cambridge, (1977)

45) Mori, Y., Hijikata, K., and Nagatani, T., Int. J. Heat Mass Transfer, Vol 20, p41-50, (1977)

46) Thompson, P.W., Symposium on Degassing, London, p111-120, BHRA Fluid Engineering, (1978)

47) Nienow, A.W., and Chapman, C.M., 'Gas Recirculation rate through Impeller Cavity and Surface aeration in sparged agitated vessels', The Chem.Eng. Journal, 17, p111-118, 1979

48) Warmoeskerken, M.M.C.G., and Smith, J.M., 'Flooding of Disc Turbines in Gas Liquid Dispersions, Chem.Eng.Sci., Vol 40, No11, pp 2063-2071, 1985

49) Oldshue, J.Y., and Connelly, F.L., 'Gas-Liquid contacting with Impeller Mixers', Chem.Eng. Prog., pp85-89, March 1977

50) Wiedmann, J.A., 'The Flooding behaviour of 2 and 3 phase stirred reactors', Int. Chem. Engineering, Vol 26, No. 2, p189-203, April 1986

51) Pollard, G.J., 'Flooding & Aeration Efficiency in standard stirred vessels', Int. Symp. on Mixing, Paper C4, p1-16, 1978

52) Roustan, M. and Bruxelmaine, M., 'Loading & Flooding points in Turbine Agitated Gas Liquid Dispersion', pp D3.3, CHISA 1981

53) Jiri, V., Ivan, F., Vludmir, K., Vlastimil, H., and Antonin, 'Determination of Power Input and Flooding Point in High Capacity Industrial Aerated stirred reactor pB3.6, CHISA 1981

54) Van Dierendonck, L.L., Fortuin, J.M.H., and Venderbos, D., 'The specific contact area in gas-liquid reactors', Proc. 4th European Symp. on Chem. Reaction Engineering, Brussel, p205-213, 1968

55) Westerterp, K.R., Van Dierendonck, L.L., Kraa, J.A., Chem. Eng. Sci. 18, 157, 1963

56) Warmoeskerken, M.M.C.G., and Smith, J.M., 'The Flooding transition with gassed Rushton turbines', Inst. of Chem. Eng. Symp. Series No 89, p59-67, 1984

57) Chapman, C.M., Nienow, A.W., Cooke, M. and Middleton, J.C., 'Part II : Gas Liquid Mixing', Chem. Eng. Res. Des., Vol 61, March 1983

58) Midoux, N., and Charpentier, J.C., 'Mechanically agitated gas-liquid reactors: Part I. Hydrodynamics', Int. Chem. Eng., Vol 24, No.2, p249-286, April 1984.

59) Nienow, A.W., Warmoeskerken, M.M.C.G., Smith, J.M., and Konno, M., 5th European Conf. on Mixing, West Germany, paper 15, 1985

60) Westerterp, K.R., 'Design of agitators for gas-liquid contacting', Chem. Eng.Sci., Vol 18, p495-502, 1963

61) Westerterp, K.R., PhD Thesis, Technical University, Delft, Holland, 1962

62) Miller, D.N., A.I.Ch.E. Journal, Vol 20, No.3, p445, 1974

63) Roustan, M., Charles, J.M., and Martinet, J.P., Int. Symp. Mixing Mass., C1., 1978

64) Bottom, R., Cosserat, D., and Charpenter, J.C., Chem. Eng. Sci., 35, p82, 1980

65) Chapman, C.M., PhD Thesis, University of London, 1981

66) Clark, M.W., and Vermeulen, T., 'Incipient Vortex Formation in Baffled Agitated vessels', A.I.Ch.E. Journal, p420-422, May 1964

67) Sawant, S.B., and Joshi, J.B., 'Critical impeller speed for the onset of gas induction in gas-inducing types of agitated contactors', Chem. Eng. Journal, 18, 1, p89-91, August 1979

68) Greaves, M., and Kobbacy, K.A.H., 'Surface Aeration in Agitated vessels', IChemE Symposium Series No.64, pH1., 1981

69) Greaves, M. and Barigou, M., 'Estimation of gas holdup and impeller power in a stirred vessel reactor', Fluid Mixing III, I.Chem.E., p235-255, Bradford, Sept. 1987

70) Greaves,M. and Kobbacy,K.A.H.,"Power consumption and impeller dispersion efficiency in gas-liquid mixing", IChemE Symp. Series No. 64, L1-L33, 1981

71) Reith,T., and Beek,W.J.,'Bubble coalescence rates in a stirred tank contactor', Trans. Inst. Chem.Eng., 48, T63, 1970

72) Mann,R.,'Gas-Liquid contacting in mixing vessels', I.Chem.E Industrial Research Fellowship Report, Inst.Chem.Eng., 1983

73) Nienow,A.W., and Wisdom,D.J.,'Flow over disc turbine blades', Chem.Eng.Sci.,29,p1997-1999, 1974

Appendix I
Equipment Specifications

A The Microcomputer

Make	Analog Devices Ltd.
Model	MACYSM II

Adio Controller:

Analog/Digital Converter	
Non-linearity Error	± ½ lsb
Gain Temperature	± 15 ppm °C max
A/D Conversion Time	25 u.sec max

Central Processor Unit (CPU):

Word Length	16 bit
Memory	64 K words
Execution speed	
Arithmetic/Logic Instructions	1.2 u.s.
Memory reference Instructions	1.8 u.s.

Analog Input Card (MUX):

Number of Inputs	32 single ended or 16 true differential
Gain	1. 16, 256
Gain Accuracy	± 0.02 %
Gain/Temp. Coefficient	± 30 ppm/°C
Linearity	± 0.001 %
Settling Time	25 u.sec. G = 1, 16 50 u.sec. G = 256

Pacer Clock Card:

It allows a programmable number of A/D measurements to be made at accurately controlled time intervals.

Time Interval	20 u.sec - 42949 sec in 10 u.sec steps
Delay Time	20 u.sec - 0.655 sec

	in 10 u.sec steps
Accuracy	± 30 u.sec. max

B Torque Transducer

Make	British Hovercraft
Type	TT2.4.CA
Serial Number	S2.E.15887
Sensitivity	2.277 mV/V.
Range	0 - 135 Nm.
Max. Load	270 Nm.
Max. Axial Load	13.5 Nm.
Max. Misalingment	± 0.004"

C Torque Transmitter

Make	EEL Limited, Isle of Wight.
Model No.	TM43
Type	MTL 400A
Serial No.	1096

D Pressure Transducer

Make	CEC Instrumentation
Type	BHL 4200-00-04Mo
Serial Number	222399
Range	0-1 Bar Absolute
Temp. Range	-54 to +120 °C
Span	29.54 mV
Zero Shift	+ 0.004 %Span/°C
Linearity	+ 0.08 %Span

Hysteresis	+ 0.14 %Span
Non-repeatibility	± 0.05 %Span
Electrical excitation	10 V D.C. rated.
Accuracy	± 0.5 %

E Level Transmitter

Make	Robertshaw Skil Ltd, Skelmersdale, Lancs.
Model	160
Output	4-20 mA DC
Linearity	± 0.25 % for 10 to 500 p.f. span
Temperature Effect	
Span	0.01 %/ F
Zero	0.01 %/ F
Max. Output Ripple	0.25 % peak to peak
Response Time	100 msec.
Stability	1 % max/30 days,

F Level Probe: Measurement of surface level in vessels.

Make	University of Bath
Electrode	Brass rod
Diameter	3.18 mm.
Length	254 mm.
Insulation	PTFE, 1.59mm. thick

Calibration

$$L = L_{\infty} + K(V - V_{\infty})$$

where,

L = level to be measured mm.

L_{∞} = datum level mm.

V = output voltage at measured level mm.

V_o = output voltage at datum level mm.

K = calibration constant

APPENDIX II
Computer Programs
and
MACYSM Statements

A MACSYM II Microprocessor (Analog Devices Ltd.,) was used for measurements and analysis of the experimental results. The programming language developed for the MACSYM II is MACBASIC. MACBASIC is a high level interactive programming language based on standard Dartmouth Basic, and optimised for measurements and control applications. Real time MACSYM statements are described below. The computer programs used in this study are also listed in this Appendix. For more details, the reader is referred to the MACSYM II SYSTEM MANUAL.

AIN (s, c, g, m)

This statement is used to measure analog input signal, where

s = 1 (the slot number in the I/O card cage where the card is physically located)

c is the card channel number. In the present work specific channel has been selected for the output signal of each measuring device such that

I/O Card Channel number	Measuring device
0	Collecting chamber Pressure
1	Impeller Speed, T_{21}
2	Torque, T_{21}
3	Liquid level: chamber
4	Liquid level: vessel
5	Torque, T_{75}
10	Impeller Speed, T_{75}

g is the gain code

when g = -1 auto ranging (default)
= 0 Gain = 1
= 1 Gain = 2
.
.
.
= 11 Gain = 2048

m = 1 (differential mode)

Example :

```
10        x = AIN (1, 5, 1)
20        PRINT X
```

This program when executed will measure the output signal of torque transducer (channel 5) in volts, and assign the value to variable X. This variable can be treated as any normal variable in computer program, eg, in statement 20 the value of X will be printed.

AVG (s, c, g, n, t)

This statement averages the value of measured analog signal over a period of time, where

s, c, g — as defined for AIN ( )
n = — number of readings to be acquired
t = — time (in seconds) between readings.

Example :

```
10        A = AVG (1, 2, 0, 1000,  0.01)
20        PRINT A
```

Statement 10 when executed will measure analog signal from channel 2 with gain = 1 (g=0) 1000 times with time period of 0.01 seconds between every two readings. The average value of these 1000 readings will be assigned to variable A.

The AVG statement has been used for measuring devices in the 'steady state' experiments. The averaging process with suitable sampling frequency has the advantage of eliminating any noise effect.

PROGRAM 1

Impeller Power Consumption & Overall Gas Holdup

```
 10 OPENW :2"$QTO:1"
 20 @ GASSED/UNGASSED POWER & TOTAL GAS HOLDUP MEASUREMENT
 30 @   O(J) : UNGASSED POWER, W.
 40 @   P(J) : UNGASSED POWER NO.
 50 @   R    : REYNOLDS NO.
 60 @   X    : FROUDE NO.
 70 @   W    : WEBER NO.
 80 @   S    : GASSED POWER, W.
 90 @   U    : GASSED POWER NO.
100 @   V    : POWER RATIO
110 @     F: FLOW NO. (Q/ND^3)
120 @     H3 : TOTAL HOLDUP %
130 DIM N(30),A(30),B(30),T(30),O(30),P(30),G(30),L(30)
140 DIM Z$(5),C(30)
142 Z5=AVG(0,5,2,1000,0.005)
144 PRINT " ZERO LOAD OUTPUT:",Z5
150 PRINT "FRICTION TORQUE MEASUREMENT. EMPTY TANK"
160 J=1
170 PRINT "PRESS ANY KEY WHEN READY"
180 INPUT Z2
190 N(J)=(AVG(0,10,0,1000,0.005))*86.8
200 N(J)=N(J)/60
210 PRINT N(J)
220 WAIT 5
230 A(J)=AVG(0,5,2,1000,0.005)
232 PRINT A(J)
240 PRINT "ANY MORE READINGS, Y/N"
250 INPUT Z$
260 IF Z$="Y" J=J+1 GOTO 170
270 D=0.188
280 PRINT "UNGASSED POWER, FILL TANK"
290 PRINT "UNDISTURBED LEVEL READING, RETURN WHEN READY"
300 INPUT Z1
310 M=AVG(0,3,0,1000,0.005)
320 PRINT :2"              ",PTIME :2
330 PRINT :2"       UNGASSED POWER MEASUREMENTS"
340 PRINT :2
350 PRINT :2
360 PRINT :2 TAB(5);"SPEED",TAB(15);"POWER",TAB(25);"NUMBER"
            ,TAB(35);"REYNOLDS",TAB(45);"FROUDE",TAB(55);"WEBER"
370 PRINT :2 TAB(5);"R.P.S.",TAB(15);"  W.",TAB(25);"  NP",
             TAB(35);"   NO.",TAB(45);"  NO.",TAB(55);" NO."
380 FOR J=1 TO J
390   PRINT "SET SPEED TO:",N(J)*60,"RPM"
400   PRINT "PRESS RETURN WHEN READY"
410   INPUT Z
420   B(J)=AVG(0,5,2,1000,0.005)
430   C(J)=AVG(0,3,0,1000,0.005)
440   T(J)=(B(J)-A(J))*67.79
450   O(J)=6.283*N(J)*T(J)
460   P(J)=O(J)/(998*(N(J))^3*D^5)
470   R=0.998*N(J)*D^2
480   X=(N(J))^2*D/9.8
490   W=(998*(N(J))^2*D^3)/0.072
492   PRINT B(J),C(J)
500   PRINT :2 TAB(5);N(J),TAB(15);O(J),TAB(25);P(J),TAB(35)
              ;R,TAB(45);X,TAB(55);W
```

```
510 NEXT J
520 PRINT :2
530 PRINT :2
540 PRINT "INPUT FLOWRATE & PRESSURE"
550 INPUT Q0,R2
560 Q=Q0*1E-3*(SQR((R2/43.53))/60)
570 Q1=Q*60/0.314
580 PRINT :2 PRINT :2
590 PRINT :2"     GASSED POWER"
600 PRINT :2
610 PRINT :2 PRINT :2
620 PRINT :2 TAB(20);"Q=",Q,"CU.M./S","(",Q1,"VVM.)"
630 PRINT "NO.OF FIRST READING"
640 INPUT K
650 PRINT :2 PRINT :2 PRINT :2
660 PRINT :2 TAB(5);"SPEED",TAB(15);"POWER",TAB(25);"POWER",
          TAB(35);"POWER",TAB(45);"AERATION",TAB(55);"TOTAL GAS"
670 PRINT :2 TAB(5);"R.P.S.",TAB(15);"  W.",TAB(25);" NO.",
          TAB(35);"RATIO",TAB(45);"  NO.",TAB(64);"HOLDUP %"
680 FOR J=K TO J-1
690   PRINT "SET SPEED TO :",N(J)*60,"RPM & RETURN"
700   INPUT Z2
710   G(J)=AVG(0,5,2,1000,0.005)
720   L(J)=AVG(0,3,0,1000,0.005)
730   H2=25.115*(L(J)-M)/1.1
740   H3=100*H2/(H2+314)
750   H=(G(J)-A(J))*67.79
760   S=6.283*N(J)*H
770   U=S/(998*(N(J))^3*D^5)
780   V=S/O(J)
790   F=Q/(N(J)*D^3)
792   PRINT G(J),L(J)
800   PRINT :2 TAB(5);N(J),TAB(15);S,TAB(25);U,TAB(35);V,TAB
            (47);F,TAB(64);H3
810 NEXT J
820 GOTO 520
```

PROGRAM 2

Point Gas Holdup Measurement using ADA

```
 10 OPENW 12"$STD:1"
 20 ZERO TIMER
 30 PRINT "TANK DIA.,IMPELLER DIA.?"
 40 INPUT R1,I1
 50 PRINT "PROBE SIZE ?,MM, I.D."
 60 INPUT C4
 70 DIM A$(5) DIM B$(5)
 71 DIM A5$(3)
 80 DIM A1$(3) DIM A2$(3)
 90 DIM Z(500)
100 U=0 I=1 D=1 S=0
101 D0=0
102 REM CHAMBER LEVEL CALIBRATION
103 PRINT "INPUT WATER LEVEL,CM"
104 INPUT D5
105 C1=D5-(AVG(0,4,1,2000)*6.38)
110 PRINT "START AGITATION ONLY AFTER ATM. PRESS. INPUT"
120 PRINT " INPUT PROBE POSITION"
130 INPUT P0
140 L1=AVG(0,3,1,1000)
142 H5=6.5953+4.7217*L1
144 PRINT H5,"CM"
146 PRINT "TYPE Y IF LEVEL 20.0"
147 INPUT A5$
148 IF A5$="Y" THEN GOTO 150
149 GOTO 140
150 PRINT "ATMOSPHERIC PRESSURE, MM HG.?"
160 INPUT C
170 PRINT "PROBE HEIGHT BELOW WATER LEVEL, CM.?"
180 INPUT D
190 L=(D*0.7055)-2.2
200 L2=AVG(0,3,1,1000)
210 H0=100*(L2-L1)*4.7217/20.0
220 PRINT "INPUT FLOWMETER READING, L/MIN"
230 INPUT Q0
240 PRINT "INPUT AIR INLET PRESSURE(GAGE) P.S.I."
250 INPUT P2
260 Q=Q0*1E-3*(SQR((P2+14.388)/14.696))/60
270 Q1=Q*60/(3.67*1E-3)
280 REM SPEED & TORQUE MEASUREMENT
290 R=AVG(0,1,4,5000)
300 N=170.8+5515.3*R-13075*R^2+77238*R^3-78757*R^4
310 W=(AVG(0,2,2,1000))*0.7807
320 PTIME :2
330 PRINT :2
340 PRINT :2"EXPERIMENTAL CONDITIONS"
```

```
350 PRINT #2"-------------------------------------------------"
360 PRINT #2
370 PRINT #2"TANK DIA.=",R1,"M.","  IMPELLER DIA.= ",I1,"M."
380 PRINT #2
390 PRINT #2"IMPELLER SPEED= ",N," R.P.M.","TORQUE = ",W,"NEWTON
400 PRINT #2"GAS FLOW RATE:",Q,"CU.M./SEC. (",Q1,"VVM)"
410 PRINT #2"**** OVERALL HOLD-UP : ",H0,"% ****"
420 PRINT #2
430 PRINT #2"PROBE SIZE :",D4, "MM. DIA"
440 PRINT #2"PROBE LENGTH BELOW WATER LEVEL :",D," CM."
450 PRINT #2" ATMOSPHERIC PRESSURE :",C," MM. HG."
460 PRINT #2
470 PRINT #2"-------------------------------------------------------
480 PRINT #2
490 PRINT #2
500 PRINT #2"-------------------------------------------------------
510 PRINT #2
520 REM SETTING UP PROCEDURE
530 GOSUB 1410
590 REM SAMPLE DRAWN-UP
600 WAIT 2
610 DOT(4,0,3)=1
620 WAIT 2
630 DOT(4,0,3)=0
640 GOSUB 1200
650 D0=D0+1
660 IF D0=5 GOTO 750
710 GOSUB 1410
720 GOTO 600
750 GOSUB 1410
760 REM SAMPLE ANALYSIS
780 H1=C1+AVG(0,4,1,3000)*6.88
790 P1'=((AVG(0,0,7,5000)*8412-0.413)*1E2)
800 DOT(4,0,3)=1
810 WAIT 2
820 DOT(4,0,3)=0
830 WAIT 2
840 P2'=((AVG(0,0,7,5000)*8412-0.413)*1E2)
860 H2=C1+AVG(0,4,1,3000)*6.88
870 REM HOLD-UP CALCULATIONS
880 V1'=(117.848-((H1-1.5)*5.314))*1E2
890 V1=V1'/1E2
900 V2'=(117.848-((H2-1.5)*5.314))*1E2
910 V2=V2'/1E2
920 P1=P1'/1E2
930 P2=P2'/1E2
940 J=P1+V1
950 K=P2+V2
960 IF K<J THEN  A=J
970 VG=(K-J)/(J-L)
980 V4=V1-V2
990 H'=1E2*100*VG/(VG-V4)
1000 PRINT H'/1E2, P1,P2,H1,H2
```

```
1010 Z(O)=H*/1E2
1020 S=S+Z(O)
1040 IF O=30 THEN GOTO 1080
1050 O=O+1 GOSUB 1200
1052 GOSUB 1420
1058 GOTO 780
1080 M=S/O
1070 PRINT :2
1090 PRINT :2"  POINT HOLD-UP % "
1090 PRINT :2
1100 FOR O=1 TO 30
1110   PRINT :2 Z(O),
1120 NEXT O
1130 PRINT :2
1140 PRINT :2"=========================================================
1150 PRINT :2
1160 PRINT :2 "PROBE POSITION :",PO,"AVERAGE POINT HOLD-UP % :",M
1170 PRINT :2
1180 PRINT :2"---------------------------------------------------------
1190 GOTO 100
1195 REM SUBROUTINE CHAMBER LEVEL
1200 DOT(4,0,1)=2
1210 WAIT 1
1220 DOT(4,0,2)=10
1240 WAIT 0.1
1250 DOT(4,3)=0
1260 H7=C1+AVG(0,4,1,500)*6.89
1270 IF H7<=10.05 THEN  DOT(4,1)=0 RETURN
1290 GOTO 1230
1400 REM SUBROUTINE FIP CHAMBER PRESSURE
1410 GOTO 1430
1420 DOT(4,0,2)=4
1430 P=AVG(0,0,7,500)*8412+0.418
1440 IF P<=50 THEN  DOT(4,0,2)=0 RETURN
1450 GOTO 1420
```

APPENDIX III
TABLES

The following Tables refer to the selection of the probe used, with the ADA technique to measure the local gas holdup in stirred vessels.

Table A1 Point gas hold-up at position A in T_{20} (see Fig A1)

Test	Point gas hold-up %			
	$P_{1.5}$	$P_{2.5}$	$P_{3.0}$	$P_{4.0}$
1	8.58	8.1	8.2	10.5
2	7.5	8.8	7.5	10.6
3	8.2	7.6	8.7	10.1
4	7.5	7.6	7.5	10.8
5	8.1	7.5	7.8	10.5
Mean	7.98	7.92	7.94	10.5
Standard Deviation	0.45	0.54	0.51	0.25

Probe length: 25cm N = 420 r.p.m.
Sample time: 2 seconds Q = 2.07×10^{-4} m^3/s
Sample size: 30 D = 0.076 m

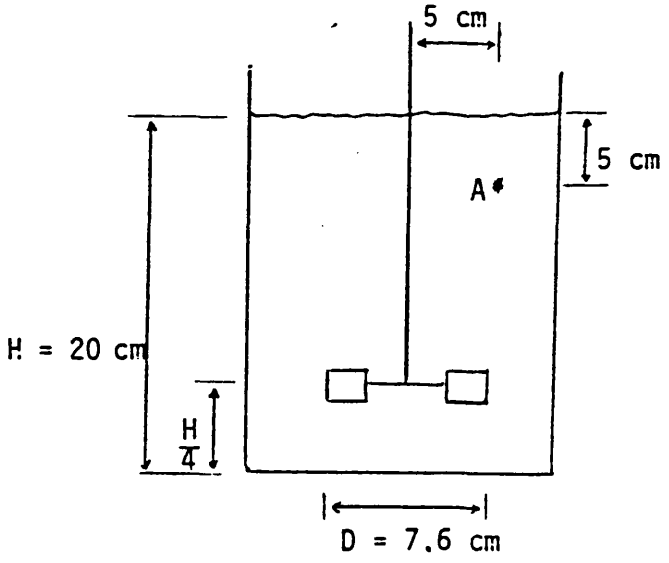

Fig. A1 Sampling position in 0.2 m tank (not to scale)

Table A2 Effect of sample time on measured gas hold-up at position 11.4 (see Fig.6.4)

Sample time(s)	Test	Point gas hold-up %		
		$P_{1.5}$	$P_{2.5}$	$P_{3.0}$
2.0	1	3.63	3.53	3.1
	2	5.04	4.53	5.2
	3	3.8	4.34	3.71
	4	4.5	4.6	3.46
Mean		4.24	4.25	3.87
Standard deviation		0.65	0.49	0.92
4.0	1	5.57	4.83	4.67
	2	4.44	5.42	4.16
	3	5.0	5.32	4.07
Mean		5.0	5.19	4.3
Standard deviation		0.56	0.32	0.32
6.0	1	4.16	5.13	4.09
	2	4.4	4.93	4.09
	3	4.17	4.76	4.42
	4	4.41	5.19	4.83
Mean		4.29	5.00	4.36
Standard deviation		0.14	0.2	0.35
8.0	1	4.29	4.75	4.05
	2	4.41	4.88	4.4
	3	4.22	4.66	4.28
Mean		4.31	4.76	4.24
Standard deviation		0.10	0.11	0.18
10.0	1	4.47	4.43	3.63

Sample size: 30

D = 0.25 m

N = 147 r.p.m.

Q = 1.76×10^{-3} m^3/s

Table A3 Point gas hold-up at position 11.4 (see Fig.6.4) in T_{75}

Test	Point gas hold-up %			
	$P_{1.5}$	$P_{2.5}$	$P_{3.0}$	$P_{4.0}$
1	3.63	3.53	3.1	4.77
2	5.04	4.53	5.2	6.68
3	3.8	4.34	3.71	5.95
4	4.5	4.6	3.46	4.66
Mean	4.24	4.25	3.87	5.51
Standard Deviation	0.65	0.49	0.92	0.97

Probe length: 1.43 m N = 147 r.p.m.
Sample time: 2 seconds Q = 1.76×10^{-3} m^3/s
Sample size: 30 D = 0.25 m

(Notation used: $P_{1.5}$, $P_{2.5}$, $P_{3.0}$ & $P_{4.0}$ subscripts indicate the internal diameter, mm, of probes)

Table A4 Reproducibility of point hold-up values

Sample time (s)	Reproducibility (±) %					
	Sample size					
	20	25	30	40	45	50
4	-	-	12	5.1	5.8	4.3
5	-	-	6.7	-	-	4.4
6	8.0	8.3	3.8	2.0	1.7	-
6a	-	-	3.6	1.8	-	-
7	-	-	7.0	2.3	1.8	-

Degassing Effect:

$$H_A = P_A / X_A$$

where,

H_A = Henry's constant

P_A = partial pressure of the solute in the gas phase

X_A = mole fraction of the solute in the liquid phase

For air at 20 °C, $H_A = 6.64 * 10^4$ atm./unit concentration of the solute in the liquid phase.

From the above equation:

[A] $X_A = 1.5 * 10^{-5}$ at atmospheric pressure (1 atm.)
[B] $X_A = 9.9 * 10^{-7}$ at 50 mm. Hg. (0.0658 atm.)

The following formulation may be used to convert from a molar to a volume basis:

$$\left[\frac{X_A}{1-X_A}\right]\left[\frac{m_A}{m_s}\right]\left[\frac{\rho_s}{\rho_A}\right] 100$$

The volume of air that will be degassed from a sample of water subjected to a pressure of 50 mm.Hg. is given by [A] - [B]. Thus, 1.73 % (volume basis) of air is degassed from a sample of water.

The introduction of a sample of water alone into the sampling chamber at 50 mm.Hg. should therefore show a 1.73 % air but 0% air was measured, i.e the degassed air does not affect the pressure in the collecting chamber. Correction for degassing is therefore not required.

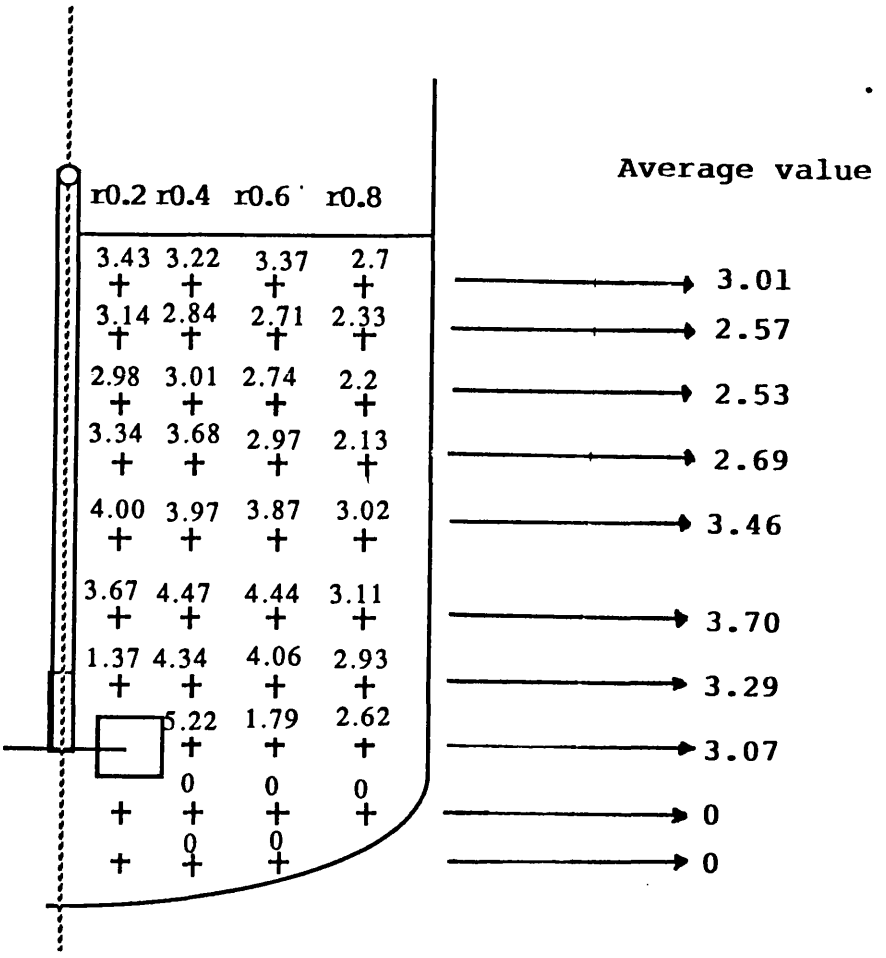

Integral Mean value : 2.43

Average value based on r = 0.2 holdup value being applicable upto r = 0.3; the r = 0.4 holdup value applying for the annulus r = 0.3 to r = 0.5; the r = 0.6 holdup value applying for the annulus r = 0.5 to r = 0.7; and the r = 0.8 holdup value applying for the outermost annulus from r = 0.7 to the wall. Thus the integral mean is given by :

$$(9\, hp_{r=0.2} + 16 hp_{r=0.4} + 24 hp_{r=0.6} + 51 hp_{r=0.8}) / 100$$

Amendment

The integral mean holdup values in Table 6.1 (page 130) should read as follows:

Experimental Conditions		Integral Mean
Q vvm	Ns^{-1}	
0.1	1.75	0.08
	2.17	0.06
	3.73	1.19
	5.18	1.8
0.2	2.43	1.22
	3.37	2.2
	5.18	4.12
0.336	2.43	2.43
	3.37	4.42
	5.18	6.1

The integral means are the weighted values based on radial position of the sampling point. This is demonstrated below for Q = 1.76 x 10^{-3} m^3 s^{-1} (0.336 vvm.) and N = 2.43 s^{-1}